Integration of New Eco-Friendly Armour Units into Coastal Structures

Serim Dogac Sayar

Thesis submitted to the University of Ottawa

in partial Fulfillment of the requirements for the

Doctorate in Philosophy Civil Engineering

Academic advisor: Prof. Ioan Nistor

University of Ottawa
Ottawa, Ontario, Canada

Abstract

Growing demands for resilient and sustainable shoreline protection have led to the development of a new generation of armour systems that combine hydraulic efficiency with ecological performance. This thesis addresses this need by providing an empirical-based framework for the Coastalock armour unit, an eco-engineered alternative to traditional single-layer armour units. Through large-scale experiments, numerical modelling, and design guidelines, the study defines hydraulic performance and bio-enhancing design parameters that facilitate reliable, environmentally enhanced coastal defence solutions.

The large-scale experiments examined the hydraulic performance of Coastalock armour units on low-crested and emergent rubble mound breakwaters under irregular wave conditions, quantifying wave transmission, overtopping, and breakwater stability. Numerical modelling was conducted using the IH2VOF CFD tool to reproduce some of the experimental conditions and investigate detailed hydrodynamic processes for the tested configurations. Sensitivity analyses of grid resolution, boundary conditions, and varying wave and structural configurations assisted the model's accuracy and guided optimal parameter selection for Coastalock units in future simulations. The model simulated wave–structure interaction by providing free-surface elevations, wave transmission coefficients, and overtopping rates observed in laboratory tests, demonstrating its capability to capture complex wave–structure interactions.

The final stage of the research consolidated 417 test runs from four multi-institutional experimental testing campaigns to develop the first comprehensive design recommendations for the Coastalock armour unit. Statistical and deterministic analyses were performed to quantify the effects of Coastalock-specific design parameters on armour stability. Armour unit spacing and underlayer size ratio emerged as the critical parameters for hydraulic stability. Design stability constants of $N_s \approx 2.8$ and $K_D \approx 15$, determined for a 1V:1.5H slope, demonstrating that Coastalock performs comparably to well-established single-layer armour units.

The design framework integrates biological performance by correlating ecological outcomes from ECOncrete's monitoring of Coastalock installations with structural configuration variables, including unit orientation and spacing. Integrating these outcomes into the design process allows engineers to consider ecological functionality as a design objective alongside traditional hydraulic design. The research, therefore, establishes a data-driven foundation for designing dual-purpose coastal structures that satisfy both engineering and environmental targets, offering a practical pathway toward sustainable and resilient coastal infrastructure.

Acknowledgements

First and foremost, I would like to thank my wife, Gozde Yilmaz Sayar, for her patience, understanding, and incredible support throughout this PhD journey, especially during the most demanding periods. She consistently provided encouragement, stability, and perspective when deadlines, long workdays, and uncertainty made the process difficult. Her compassion and resilience helped me stay focused and motivated, and her belief in me gave me the confidence to keep moving forward during challenging moments. I am deeply grateful for the sacrifices she made and the understanding she showed. In many ways, she has been an unseen contributor of this work through her constant encouragement, patience, and the countless unseen contributions that made it possible for me to sustain the effort required to complete this research.

I am deeply grateful to my family for their constant support. I am thankful to my mother, Durdane Sayar, for her belief in me and her encouragement. I am grateful to my brother, Mutlu Sayar, for his support and understanding throughout this process. I respectfully and lovingly remember my father, Yucel Sayar, whose values and guidance inspire me and remain a lasting source of motivation in my personal and professional life. I am also deeply grateful for the continuous support of my extended family: Emrullah and Fatma Yilmaz, and Onur, Fatma, and Baris Efe Yilmaz.

I am grateful to my supervisor, Dr. Ioan Nistor, for his continuous guidance, technical insight, and encouragement throughout my PhD studies. His expertise, constructive feedback, and high academic standards were instrumental in shaping both the direction and the quality of this research. His ability to challenge ideas while providing clear guidance significantly contributed to my development as a researcher and engineer. I also acknowledge his leadership in creating a collaborative and intellectually stimulating research environment. His openness to discussion and willingness to provide guidance at all stages of the research process made a significant difference in the overall experience of this doctoral study. Dr. Nistor's guidance has played a key role in shaping my research mindset and professional development.

I would also like to sincerely thank Scott Baker from the National Research Council of Canada for his continuous and invaluable technical support, practical insight, and mentorship throughout all components of my research. His hands-on expertise, thoughtful discussions, and deep understanding of experimental work were essential to the successful execution of this study. I am especially grateful for his careful reviews and constructive comments on multiple manuscripts, as well as his consistently supportive and encouraging attitude throughout this process.

I would like to thank Jorge Gutiérrez Martínez for his collaboration, technical discussions, and support during my research internship at ECOncrete. His feedback and industry perspective strengthened the practical relevance of this work and contributed significantly to the development of design-oriented outcomes.

I am particularly grateful to Dr. Ahmet Cevdet Yalciner for his continued support and trust in me. I would also like to express my sincere appreciation to my professors during my MSc studies. I am especially grateful to my MSc supervisor, Dr. Gulizar Ozyurt Tarakcıoğlu, for her mentorship and academic guidance during my formative years as a researcher.

I sincerely acknowledge my colleagues at the National Research Council of Canada, Ocean, Coastal and River Engineering, for their collaboration, support, and contributions to the experimental work. I am grateful to Alistair Rayner, Anthony D'Avignon, Justin Hof-Macneil, Kyle Lambert, Maradona Laborde, Michael Achtereekte, Mitchel Provan, Stefano Kerr for their assistance during laboratory activities. Their professionalism, practical expertise, commitment to high-quality work and support to me were essential to the successful execution of the laboratory studies presented in this thesis.

I would also like to sincerely acknowledge Dr. Bas Hofland, Dr. Maria Maza and Dr. Yaeli Rosenberg for their valuable contributions and technical discussions related to this PhD project. Their insights and feedback strengthened the scientific depth of this research and supported the broader interpretation and synthesis of the results.

Finally, I would like to thank my close friends for their friendship, encouragement, and continued support throughout my doctoral studies. I am grateful to Ali Yurekli, Ana Rodriguez, Burak Kuyumcu, Ege Talu, Elizaveta Gerdt, Emre Insel, Eren Koluacik, Isil Servetoglu, Melisa Sayar, Muhammet Sakir Er, Serhat Unlu, and Zeynep Yilmaz Unlu for their understanding, motivation, and companionship during both challenging and rewarding periods of this journey. Their presence, thoughtful conversations, and support provided balance and perspective throughout my PhD.

This thesis would not have been possible without the contributions, support, and collaboration of all the individuals acknowledged above.

Table of Contents

List of Figures

List of Tables

List of Acronyms

2D	Two-Dimensional
3D	Three-Dimensional
APD	Average Percentage Deviation
ASCE	American Society of Civil Engineers
ASTM	American Society for Testing and Materials
AUC	Area Under the ROC Curve
AUS	Australian Standards
BS	British Standards
CFD	Computational Fluid Dynamics
CIRIA	Construction Industry Research and Information Association
CLI	Concrete Layer Innovations
CL	Coastalock
CJCE	Canadian Journal of Civil Engineering
CSCE	Canadian Society for Civil Engineering
DMC	Delta Marine Consultants
DEM	Discrete Elements Method
ECOncrete	ECOncrete Tech Ltd.
EN	European Standards
EU	European Union
EurOtop	Manual on wave overtopping of sea defences and related structures
FUNWAVE	Fully Nonlinear Boussinesq Wave model
GPU	Graphics Processing Unit
GROWTH	Graduate Research on Water Technology and Hydraulics Symposium
IC	Impermeable Core
IHCantabria	Environmental Hydraulics Institute of Cantabria
JONSWAP	Joint North Sea Wave Project
LWF	Large Wave Flume
MPD	Months Post-Deployment
NRC	National Research Council of Canada
NSERC	Natural Sciences and Engineering Research Council of Canada
OCRE	Ocean, Coastal and River Engineering Research Centre
PC	Permeable Core
PoSD	Port of San Diego
PT	(Coastalock Units with) Protrusions
RANS	Reynolds-Averaged Navier–Stokes equations
RMBW	Rubble Mound Breakwater
ROC	Receiver Operating Characteristic

SD	Standard Deviation
SWAN	Simulating WAves Nearshore model
SWL	Still Water Level
TS	Test Series
TU Delft	Delft University of Technology
UNSW	University of New South Wales
USACE	United States Army Corps of Engineers
VARANS	Volume-Averaged Reynolds-Averaged Navier–Stokes equations
VIF	Variance Inflation Factor
VOF	Volume of Fluid method
WL	Water Level

List of Symbols

α	Wave attack or slope angle (°)
β	Non-linear friction coefficient (–)
B_c	Crest width (m)
$\cot\theta$	Slope tangent (horizontal/vertical) (–)
d	Water depth (m)
d_{15}	The particle diameter for which 15% of the material is finer
d_{85}	The particle diameter for which 85% of the material is finer
Δ	Relative submerged density (–)
D_n	Nominal diameter of armour unit (m)
D_{n50}	Median nominal diameter of underlayer material (m)
f_q	Overtopping adjustment factor (–)
g	Gravitational acceleration (m/s²)
γ	Peak enhancement factor (–)
γ_β	influence factor for oblique wave attack
γ_f	Overtopping roughness factor (–)
γ_r	Density of rock (g/cm^3)
H	Wave height (m)
H_b	Breaking wave height (m)
H_{m0}	Spectral (zeroth moment) significant wave height (m)
H_s	Significant wave height (m)
K_D	Hudson stability coefficient (–)
K_t	Wave transmission coefficient (–)
$L_{m-1,0}$	Spectral wave length (m)
n	Porosity (–)
N	Number of incident waves during test (–)
N_s	Stability number (–)
$P_{instability}$	Probability of armour instability (–)
q	Mean overtopping discharge per unit width (m³/s/m)
R_c	Crest freeboard (m)
S	Unit spacing (%)
s_o	Deep-water wave steepness (–)
T	Wave period (s)
T_m	Mean wave period (s)
T_p	Peak wave period (s)
V	Volume of armour unit (m³)
ξ_{op}	Surf similarity parameter (–)
η	Water surface elevation (m)
θ	Front slope angle (°)
φ	Porosity of armour layer (–)
ψ	Obliquity angle of wave incidence (°)
ρ	Density of water (kg/m³)
ρ_r	Density of armour unit (kg/m³)
σ	Standard deviation (–)

Chapter 1. Introduction

1.1 Background

Numerous marine organisms can survive in deep and turbulent environments due to their natural toughness and resilience. The habitat requirements of marine creatures can occasionally be accommodated by coastal infrastructure such as seawalls and breakwaters that use durable, rigid, and solid materials to protect coasts (Hindle, 2018). However, these artificial systems typically support lower biodiversity and often exhibit higher concentrations of opportunistic or invasive species compared to natural shorelines (Dafforn et al., 2009). To address these environmental concerns, there is growing interest in ecological engineering, combining ecosystems with engineering concepts to create coastal structures that serve both people and nature, to lessen the detrimental environmental effects of coastal structures (Mitsch and Jorgensen, 2003).

This thesis focuses on the integration of eco-engineered armour units, specifically the Coastalock unit developed by ECOncrete, into rubble mound breakwaters (RMBWs). The research involves large-scale physical experiments to evaluate the hydraulic performance of these units, including hydraulic stability, wave transmission, reflection, and overtopping characteristics.

The numerical modelling in this study employs computational fluid dynamics (CFD) techniques to simulate the wave–structure interaction. This modelling approach assesses hydraulic interpretation and comparative assessment, supporting the adaptation of eco-friendly breakwater configurations to varying wave climates and site-specific conditions.

The outcomes of multi-institutional experiments contribute to the development of design recommendations for breakwaters with eco-friendly armour units. The guidelines are designed to connect experimental findings to practical solutions for sustainable real-world coastal engineering projects.

1.2 Problem Statement and Motivation

Artificial coastal defence systems, such as concrete armour units, often support less diverse aquatic populations and higher concentrations of invasive species (Dafforn et al., 2009). Therefore, there is a growing need to design or retrofit coastal structures to achieve sustainability targets through ecological engineering interventions that enhance marine habitat complexity and biodiversity. This approach aligns with the broader ecological engineering paradigm, which seeks to minimize the environmental footprint of traditional coastal infrastructure (Mitsch & Jørgensen, 2003). Thus, creating new eco-friendly breakwater design guidelines is critical and will benefit from the multidisciplinary involvement of coastal engineers, marine biologists, and ecologists. Particularly, uncertainties remain regarding how eco-engineered armour unit geometry, placement density, and

underlying layer configuration influence hydraulic stability, wave transmission, and overtopping behaviour.

Baker et al. (2018) conducted physical modelling experiments for the Living Breakwaters to assess the structural stability and design of the breakwaters under wave action and varying water levels and to verify the wave attenuation performance of the system. This included evaluating the size and gradation of the stone used for the breakwater trunk and reef ridges and evaluating non-traditional features such as the reef ridges and reef ridge connection to the breakwater and the crenulated crest (see also Marrone et al. 2019). Molenkamp (2022) and Lawniczak (2024) conducted physical model tests on Coastalock units. Several data sets were collected on various parameters to provide a preliminary understanding of the hydraulic performance of Coastalock armour units.

While many physical and numerical studies have focused on the hydraulic performance of nature-based solutions (Paxton et al., 2024), research on eco-friendly armour units remains limited, and no standardized design guidelines for these structures currently exist. Existing design approaches are widely used for conventional coastal structures but do not explicitly account for the geometric complexity and porosity of eco-engineered armour units. This limitation introduces uncertainty in predicting hydraulic stability and performance, highlighting the need for systematic investigation and design-oriented evaluation.

1.3 Objectives of the Study

This study aims to advance the understanding and practical application of eco-engineered coastal protection systems by establishing a robust hydraulic design basis for eco-friendly armour units integrated into rubble mound breakwaters.

The specific objectives of the thesis are to:

1- Critical review of the literature

Examine existing studies on ecological integration in coastal structures to identify knowledge gaps, research trends, and design challenges related to eco-friendly breakwaters.

2- Large-scale flume experimental program

Conduct an extensive physical modelling program in the NRC-OCRE Large Wave Flume (LWF) to evaluate the hydraulic performance of low-crested and emergent RMBWs with eco-friendly armour units.

3- CFD-based numerical simulations

Apply and evaluate a CFD-based numerical model to reproduce wave–structure interaction processes observed in laboratory experiments and to assess its applicability for simulating the hydraulic performance of eco-engineered breakwater configurations.

4- Design recommendations development

Synthesize multi-institutional experimental findings to establish comprehensive design recommendations for eco-friendly armour units, offering practical recommendations for sustainable coastal engineering applications.

1.4 Scope of the Study

The methodological, geometric, and hydraulic boundaries of the studies conducted define the scope of this thesis as follows:

This literature review focuses on nature-inclusive coastal structures and eco-engineered armour unit systems, concentrating on their hydraulic function and design implications. It reviews ecological enhancement approaches only to that extent as they influence engineering design decisions, and it compiles prior findings on transmission, overtopping, reflection, and stability from both laboratory experiments and numerical modelling studies. Field observations are included selectively to contextualize design intent and practical applicability, while comprehensive ecological assessment and policy evaluation are outside the scope.

The physical modelling is limited to two-dimensional trunk sections of low-crested and emergent rubble mound breakwaters armoured with eco-engineered single-layer Coastalock units. Hydraulic performance is investigated through large-scale physical modelling in the NRC-OCRE Large Wave Flume under irregular wave conditions representative of exposed coastal environments. The experimental analysis is confined to the evaluation of armour stability, wave transmission, wave reflection, and wave overtopping for permeable breakwater configurations. The physical experiments were focused on trunk-section response, and wave setup was not treated as a separate response variable in the present analysis.

Complementary two-dimensional CFD simulations are performed using a RANS–VOF modelling framework (IH2VOF) to reproduce selected experimental conditions and to support the interpretation of observed hydraulic processes. The numerical component is restricted to validation against laboratory data and parametric assessment within the tested configuration space and it is not intended to resolve detailed three-dimensional effects or armour unit failure mechanisms.

The design recommendations developed in this thesis are empirical and apply only to the range of structural geometries, hydraulic conditions, and armour configurations investigated. Three-dimensional effects, oblique wave attack, breakwater heads, long-term morphological evolution, sediment transport, life-cycle performance, and field-scale validation are outside the scope of this research. Ecological performance is addressed in terms of design intent and existing observations reported in the literature but is not experimentally quantified within this study.

1.5 Novelty of the Study

Eco-engineered armour units are increasingly adopted to support nature-inclusive coastal protection, yet their hydraulic design basis remains comparatively underdeveloped. The novelty of this thesis lies in addressing this gap through a coordinated program of large-scale physical modelling and CFD-based numerical simulations, concluding in performance-based design recommendations that support reliable engineering application.

This thesis presents the first large-scale physical experiments designed to quantify the hydraulic performance of eco-engineered single-layer armour units integrated into low-crested and emergent rubble mound breakwaters. The work provides an integrated dataset that characterizes wave transmission, reflection, overtopping, and armour stability under controlled irregular wave conditions, supporting direct performance comparisons across configurations.

A further novel contribution is the first dedicated application and validation of a RANS–VOF numerical modelling framework (IH2VOF) for reproducing wave–structure interaction processes associated with eco-engineered armour units. The numerical model is used not only for comparison with experimental measurements but also to support the interpretation of flow processes and to assess its applicability as a research and design-support tool for eco-friendly armour units.

Finally, this thesis introduces the first consolidated, performance-based design recommendations for single-layer eco-engineered armour units derived from multi-institutional experimental datasets. These recommendations provide a practical bridge between laboratory-scale research and prototype-size engineering applications, allowing the integration of eco-friendly armour units into conventional coastal engineering design.

1.6 Scientific Contributions

1.6.1 Journal Articles

1) **Sayar, S.D., Nistor, I., Baker, S., Gutiérrez, J., Rosenberg, Y. (2025).** Hydraulic Performance of Low-Crested and Emergent Breakwaters with Ecologically Designed Armour Units. *Journal of Waterway, Port, Coastal, and Ocean Engineering*, American Society of Civil Engineers. https://doi.org/10.1061/JWPED5.COASTALOCK.2025

    • The first author (Serim Dogac Sayar) was responsible for conceptualization, methodology, investigation, data curation, formal analysis, visualization, and writing (original draft, review, and editing). A preprint of the published version of this manuscript is included in **Chapter 3** of this thesis.

2) **Sayar, S.D., Baker, S., Nistor, I., Gutiérrez, J. (2026).** Experimental and Numerical Assessment of Low-Crested and Emergent Breakwaters with Eco-Engineered Armour Units. *Canadian Journal of Civil Engineering*. https://dx.doi.org/10.1139/cjce-2025-0373.

   • The first author (Serim Dogac Sayar) was responsible for conceptualization, methodology, investigation, data curation, formal analysis, visualization, and writing (original draft, review, and editing). A preprint of the published manuscript is included in **Chapter 4** of this thesis.

3) **Sayar, S.D., Gutiérrez, J., Nistor, I., Baker, S., Rosenberg, Y., Hofland, B., Van den Bos, J., Colom Jover, F., Kerr, S., Molenkamp, A., & Lawniczak, A. (2026).** *Design Recommendations for Eco-Engineered Coastalock Armour Units: Hydraulic Stability, Performance, and Ecological Functionality.* (manuscript under review).

   • The first author (Serim Dogac Sayar) was responsible for conceptualization, methodology, investigation, data curation, formal analysis, visualization, and writing (original draft, review, and editing). A modified preprint of this manuscript is included in **Chapter 5** of this thesis.

1.6.2 Conference and Symposium Proceedings

1) **Sayar, S.D., Baker, S., Nistor, I. (2023)**. Integration of Eco-Friendly Habitats into Coastal Structures at the 10th Short Course / Conference on Applied Coastal Research (SCACR 2023), Istanbul, Turkiye.

   - The first author (Serim Dogac Sayar) was responsible for conceptualization, experimental setup, data analysis, visualization, and writing (original draft and editing) and delivery of the oral presentation at the conference. The extended abstract is not included in this thesis.

2) **Sayar, S.D., Nistor, I., Baker, S., Gutiérrez Martínez, J. (2024).** Low-crested and Emergent Breakwaters with Eco-Friendly Armour Units. *Proceedings of the 9th International Conference on Physical Modelling in Coastal Engineering (Coastlab24)*, Delft, The Netherlands, May 13–16, 2024. TU Delft OPEN Publishing. DOI: 10.59490/coastlab.2024.775

   - The first author (Serim Dogac Sayar) was responsible for conceptualization, experimental setup, data analysis, visualization, and writing (original draft and editing) and delivery of the oral presentation at the conference. The extended abstract is not included in this thesis.

3) Sayar, S.D., Nistor, I., Baker, S. (2024). Integration of Ecofriendly Armour units into Breakwaters at *Graduate Research on Water Technology and Hydraulics Symposium (GROWTH 2024)*, *Kitchener, ON, Canada.*

• The first author (Serim Dogac Sayar) was responsible for conceptualization, experimental setup, data analysis, visualization, and writing (original draft and editing) and delivery of the oral presentation at the symposium. The extended abstract is not included in this thesis.

4) **Sayar, S.D., Baker, S., Nistor, I., Gutiérrez, J. (2024)** Hydraulic Stability of Coastalock Armour Units. 8*th International Conference on Estuaries and Coasts (ICEC 2024), 2024*, *Quebec, QC, Canada*.

• The first author (Serim Dogac Sayar) was responsible for conceptualization, experimental setup, data analysis, visualization, and writing (original draft and editing) and delivery of the oral presentation at the conference. The extended abstract is not included in this thesis.

5) **Sayar, S.D., Baker, S., Nistor, I., Gutiérrez Martínez, J. (2025).** Hydraulic Performance of Eco-Friendly Breakwater Armour Units. *Coastal Engineering Proceedings (ICCE 2024),* Rome, Italy, 38, 52–52.

- The first author (Serim Dogac Sayar) was responsible for conceptualization, experimental setup, data analysis, visualization, and writing (original draft and editing) and delivery of the oral presentation at the conference. The extended abstract is not included in this thesis.

6) **Sayar, S.D., Nistor, I., Baker, S., Gutiérrez, J. (2025).** *Physical and Numerical Modelling of Eco-Engineered Armour Units on Low-Crested and Emergent Breakwaters. Proceedings of the CSCE 2025 Hydrotechnical Specialty Conference, Winnipeg, MB, Canada.*

• The first author (Serim Dogac Sayar) was responsible for conceptualization, experimental setup, data analysis, visualization, and writing (original draft and editing). The extended abstract is not included in this thesis.

7) **Sayar, S.D., Gutiérrez, J., Nistor, I., Baker, S., Rosenberg, Y., Hofland, B., Van den Bos, J., Kerr, S., Molenkamp, A., Lawniczak, A. (2026).** Hydraulic Design Guidelines for Ecologically Engineered Coastalock Armour Units. *Coastal Engineering Proceedings (ICCE 2026), Galveston, TX, USA*.

• The first author (Serim Dogac Sayar) was responsible for conceptualization, experimental setup, data analysis, visualization, and writing (original draft and editing) and delivery of the oral presentation at the conference. The extended abstract is not included in this thesis.

1.6.3 Invited Lectures

1) **Sayar, S.D., Nistor, I., Baker, S., Gutiérrez, J. (2025).** Integration Of Eco-Friendly Armour Units into Coastal Structures. Oral presentation at *Delft University of Technology (TU Delft)*, Delft, the Netherlands.

    • The first author (Serim Dogac Sayar) was responsible for the delivery of the oral presentation as the invited lecturer.

2) **Sayar, S.D., Baker, S., Nistor, I., Gutiérrez, J. (2025).** Integration of Eco-Friendly Armour Units into Coastal Structures Oral presentation at *the Environmental Hydraulics Institute of Cantabria (IHCantabria), Santander, Spain.*

    • The first author (Serim Dogac Sayar) was responsible for the delivery of the oral presentation as the invited lecturer.

1.7 Awards and Scholarships

The following awards and scholarships recognize the author's (Serim Dogac Sayar) research excellence and scholarly contributions arising from the work presented in this thesis.

1.7.1 Awards

1) **uOGRADFlix Video Competition Award (2023)** — University of Ottawa

    • Awarded for an engaging presentation of the author's graduate research on eco-engineered coastal protection systems.

2) **Sayar, S.D., Baker, S., Nistor, I., Gutiérrez, J., Rosenberg, Y. (2025).** *Hydraulic Performance of Low-Crested and Emergent Breakwaters with Ecologically Designed Armour Units. Journal of Waterway, Port, Coastal, and Ocean Engineering*, American Society of Civil Engineers. https://doi.org/10.1061/JWPED5.COASTALOCK.2025

    • This journal paper, representing a major component of the thesis, was selected as **Editor's Choice** by the Journal of Waterway, Port, Coastal, and Ocean Engineering of the American Society of Civil Engineers (ASCE).

1.7.2 Scholarships

The author (Serim Dogac Sayar) received several competitive scholarships in recognition of academic excellence and research achievement throughout the doctoral program:

• **Geoff Peach Scholarship (2023)** – Lake Huron Coastal Centre
Granted in recognition of contributions to sustainable coastal engineering research promoting the integration of ecological principles into shoreline protection design.

• **Special Merit Scholarship (2023)** – University of Ottawa
Awarded for academic performance during the first year of doctoral studies.

• **International Experience Scholarship (2024)** – University of Ottawa
Awarded to support international research collaboration and experiential learning during the author's research internship in Barcelona, Spain

• **International Doctoral Scholarship (2022–2026)** – University of Ottawa
Provided to international PhD students demonstrating high academic standing and research potential.

• **Doctorate Admission Scholarship (2022–2026)** – University of Ottawa
Offered as part of the University's funding package to support doctoral studies in civil engineering.

1.8 Outline of the Thesis

The goal of this thesis is to synthesize the literature, present the results of physical and numerical experiments, and to provide design recommendations on breakwaters with eco-friendly single-layer armour units. This thesis is organized as follows:

Chapter 1. Introduction
Provides the context, research needs, objectives, novelty, and structure of the thesis, along with a summary of publications, awards, and scholarships associated with this research.

Chapter 2. Literature Review
Reviews existing studies on eco-friendly coastal structures, including oyster reefs, brushwood dams, living breakwaters, and eco-engineered armour units, highlighting key knowledge gaps in their hydraulic and ecological performance.

Chapter 3. Physical Modelling
Describes the experimental program conducted in the Large Wave Flume, focusing on the hydraulic performance of Coastalock armour units under varying wave and structural conditions.

Chapter 4. Numerical Modelling
Presents the application, and validation of a CFD-based numerical model simulating wave–structure interaction and hydrodynamics processes around breakwaters with eco-friendly armour units.

Chapter 5. Design Recommendations for Coastalock Armour Units
Synthesizes findings from the physical investigations and multi-institutional experimental datasets to establish design recommendations for eco-friendly armour units, including hydraulic stability, wave reflection, transmission, overtopping, and ecological integration.

Chapter 6. Conclusions
Summarizes the principal findings of the research, discusses limitations, and proposes directions for future work on eco-engineered coastal infrastructure.

Chapter 2. Literature Review

Since prehistoric times, coastal areas have been vital and the most popular places for human accommodation, and half of the world's population now lives closer than 200 km to the shore. Within 20 to 30 years, it is anticipated that the coastal region's population will almost double (Immanuel et al., 2009). Global demographic trends highlight the increasing pressure on coastal zones. This pressure has increased the need for coastal protection solutions that not only reduce hydraulic risk but also minimize ecological degradation associated with conventional hard infrastructure.

At least 70% of coasts globally are exposed to erosion, leading to shoreline retreat and inland displacement of coastal communities, and up to 4.6% of the world's population might experience yearly floods by 2100 (IPCC, 2022). Coastal defence is nowadays accomplished mostly through armouring with hard structures like seawalls and breakwaters (Hinkel et al., 2014).

Offshore breakwaters are typically constructed parallel to the shoreline and are intended to either enhance recreational conditions or protect the shore (Pilarczyk and Zeidler, 1996). They are made of materials such as concrete, rocks, and geotextiles and are intended to enable some wave transmission by overtopping or flow through the porous structure. A portion of the incident wave energy is reflected seaward, while additional energy is dissipated through frictional losses within the structure and wave breaking on the slope (Pilarczyk, 2003). While providing storm protection, breakwaters can affect the morphodynamics of the shore. The existence of the structure causes changes in hydrodynamics that modify sediment transport patterns, resulting in morphological alterations (Van Rijn, 2013).

The quantity, biomass, and size of macroinvertebrates in the higher intertidal zone, as well as the species diversity and abundance of shorebirds, may significantly reduce as a result of seawalls, according to research by Dugan et al. (2008). Structures with slopes steeper than the natural beach offer less habitat, which causes a loss of regional biodiversity and, ultimately, results in a decline in the number of the region's overall population (Chapman and Underwood, 2011). A steeper slope in intertidal regions brings species that formerly lived in distinct vertical zones considerably closer together, changing the way that biological interactions occur there (Dugan et al., 2011; Nordstrom, 2014).

Likewise, more than 80% of soft-sedimentary coastline degradation has been attributed to artificial constructions (Brown and McLachlan, 2002). Artificial environments, which frequently contain massive numbers of young fish, attract fish species (Clynick, 2006). However, the effects of artificial structures have been identified as harmful to the environment when invasive species colonize them and beneficial when native species are attracted to the region, even if the native species would not have lived there without the infrastructure (Bulleri and Chapman, 2010).

Moreover, although certain species may obtain shelter in artificial structures, this depends on the environment. For instance, seawalls appear to be less favourable for low shore and sub-tidal species (Bulleri et al., 2005) than for mid and high intertidal assemblages (Chapman, 2003).

Over the last decades, there has been a significant increase in interest in the idea of integrating ecological enhancements and ecosystem services into coastal protection (Borsje et al., 2011). This integration can be explained by two main factors. First, there is an urgent need for unique, long-lasting, and affordable solutions for coastal protection that address concerns caused by climate change and sea level rise. Second, there is a growing emphasis on mitigating the adverse ecological impacts of coastal defence structures and may even provide opportunities to improve ecosystem functioning (Day et al., 2000).

Cheong et al. (2013) define ecological engineering as a methodology that takes social values and functions into account in addition to emphasizing ecological solutions. As opposed to a single approach, such as building a seawall, the coordinated methods of coastal adaptation are preferable for preparing for the highly unpredictable and dynamic coastal environment. The authors conclude that relatively limited research on actual implementations has investigated the interactions and co-benefits of combining adaptation strategies.

Implementing ecosystem-based coastal protection may be challenging to utilize due to technical design requirements and regional morphological or hydrodynamical constraints. The ecological value of artificial hard substrate coastal protection structures can be increased by incorporating ecology into coastal protection. This can be achieved by modifying structural elements to increase habitat complexity and by introducing relatively simple adjustments to conventional engineering designs. Although this strategy would not necessarily result in cost savings, it is valuable since it might lessen the environmental effect of the development, which would make it easier to obtain the necessary permissions and gain the local stakeholder support (Borsje et al., 2011). Nevertheless, the adoption of eco-engineered modifications does not eliminate the need for structurally reliable coastal protection in energetic environments, and therefore the hydraulic implications of such modifications must be understood within engineering design frameworks.

Incorporating ecological engineering into coastal protection requires explicit consideration of different temporal and spatial scales. Breakwaters defend the hinterland against floods and erosion on the smallest possible scale. At this scale, the hydrodynamic forces may inhibit the establishment of habitat-building organisms. Without compromising the degree of safety, better settlement and growth conditions might be generated by making minor adjustments to the texture and structure of these breakwaters. Groins and revetments are employed on a larger scale to lessen the impact of waves on dikes while also preventing coastline erosion. It is also known that oyster reefs may stabilize the bed and moderate waves (Borsje et al., 2011). Such measures have proven effective in increasing habitat heterogeneity on coastal structures, thereby enhancing species richness and/or altering community composition (Hall et al., 2018).

In this thesis, the term eco-friendly coastal structures includes coastal defence systems involving natural materials, such as oyster reefs and brushwood breakwaters, in addition to ecologically designed armour units and living breakwaters that benefit from eco-enhancing modifications.

2.1 Eco-friendly Coastal Structures

2.1.1 Classification of Eco-Friendly Coastal Structures

This chapter reviews site observations, physical modelling, and numerical modelling studies focused on the principal types of eco-friendly coastal structures. This review includes an evaluation of coastal structures and investigates the effectiveness and ecological impact of using natural material solutions, such as brushwood dams and oyster reefs, in addition to eco-friendly armour units, as environmentally-friendly alternatives for protecting shorelines. However, their hydraulic roles, material behaviour, and ranges of practical applicability differ significantly, and these differences must be considered when assessing their relevance to breakwater design. Oyster reefs offer an environmentally beneficial method of enhancing coastal resilience because of their capacity to reduce wave energy and promote marine biodiversity. Brushwood dams provide a balance between sustainability and structural stability when multi-purpose breakwaters with ecologically designed elements are intended to serve multiple functions.

Oyster reefs are frequently found seaward of salt marshes in their natural environment, where they may attenuate erosive wave energy, stabilize sediments, and slow marsh retreat (Dame et al., 1981; Meyer et al., 1997; Piazza et al., 2015). As a result, they make an appealing living shoreline approach. Beyond physical protection, oyster reefs deliver diverse ecosystem services, including sediment filtration, predator refuge, and enhanced prey availability (Coen et al., 2018).

Coastal protection by oyster shell bags (see Figure 2-1 and Figure 2-2) provide many advantages over those made of conventional hard-armour designs. Juvenile bivalves have been demonstrated to settle more readily in oyster shell substrate, a natural, renewable, inert substance (Henderson and O'Neil, 2003). Using discarded oyster shells in living shorelines diverts waste material from the disposal stream. Oyster shells are frequently packed into mesh bags to replicate a composite breakwater. Their primary advantage lies in sustainability, as oyster shells are a recycled by-product that would otherwise be discarded (Allen and Webb, 2011).

Figure 2-1. Bagged shells as an oyster reef in Virginia (Morris et al., 2019)

Though few studies have investigated the concept of restoration by facilitation (Bruno et al., 2003; Safak et al., 2020), oyster reefs may be self-sustaining shoreline protection features that improve other ecosystems in the natural landscape if recruitment and survival are appropriate (Meyer et al., 1997; Piazza et al., 2015). Comparative studies evaluating the performance and sustainability of different oyster reef configurations under varying environmental settings remain limited (Walles et al. 2016; Salvador de Paiva et al. 2018). However, their hydraulic roles, material behaviour, and ranges of practical applicability differ significantly, and these differences must be considered when assessing their relevance to breakwater design.

Figure 2-2. Oyster shell gabions and breakwalls (Safak et al. 2020)

The use of locally available, low-cost, and easily handled materials is preferable for local communities in constructing coastal defence structures (Takagi, 2019). Community-based wooden pile structures are commonly implemented along eroding shorelines, particularly in developing countries such as Thailand and Vietnam (Schmitt and Albers, 2014; Rasmeemasmuang and Sasaki, 2015).

In addition to being inexpensive and simple to build, wooden piles positioned with intervals may not considerably restrict sediment transport or seawater exchange. They are, therefore, integrated with the coastal habitat as an environmentally enhancing solution. Circular hardwood piles offer structural advantages, as cylindrical members experience reduced hydrodynamic forces relative to flat or angular elements (Takagi, 2020).

A range of timber types has been employed in the construction of coastal protection structures, depending on local availability and durability. Material selection is typically controlled by the regional availability and construction-related physical properties of the wood. Silva et al. (2016) documented a pile groyne constructed from coconut timber, where the breakwater made of locally available material succeeded in decelerating coastal erosion according to the field observations.

Safak et al. (2020) evaluated the efficiency and suitability of bundled and unbundled wooden breakwalls (Figure 2-3a and 2-3b) for mitigating coastal erosion. The results show that living shoreline breakwalls with proper design may serve as barriers against waves and boat traffic, and their capacity to dissipate wave energy and maintain coastal ecosystems is mainly influenced by water depth and structural porosity.

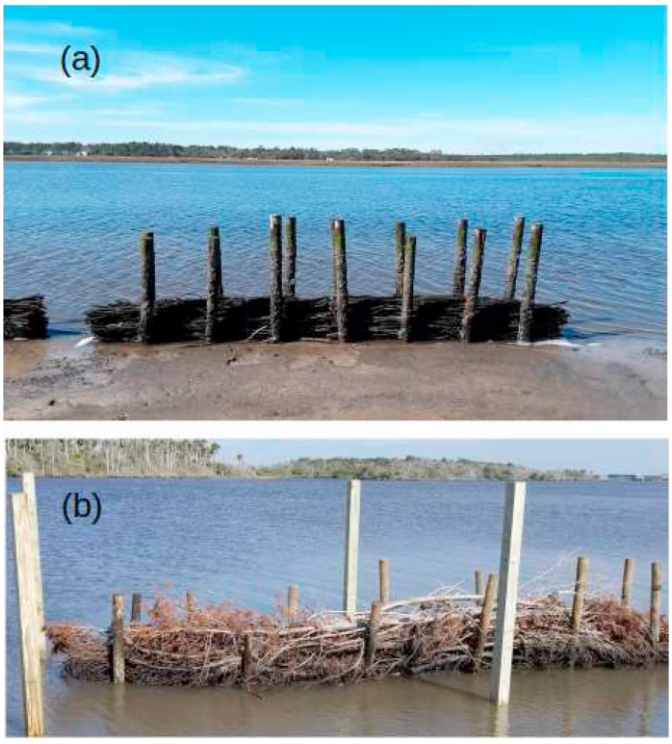

Figure 2-3. Wooden breakwalls at (a) Guana Tolomato Matanzas National Estuarine Research Reserve and (b) North Peninsula State Park in Florida, USA (Safak et al., 2020)

Multi-purpose breakwaters, or living breakwaters, provide structural protection while offering additional environmental and social benefits (Manson et al., 2017). As illustrated in Figure 2-4, the Living Breakwaters project integrates multiple habitat-enhancing elements that improve ecosystem performance without diminishing wave attenuation or sediment control capacity. Reef ridges and reef streets are two key features creating spatial diversity and ecological niches within the structure. In the multi-purpose breakwater design, as stated in Baker et al. (2018), the main body of the breakwater incorporates closely spaced rocky protrusions known as reef ridges extending seaward. The resultant narrow gaps between them, known as reef streets, serve as a semi-sheltered ecosystem. Together, they significantly expand the breakwaters' intertidal and subtidal zones, which act as a productive edge habitat and improve their ecological performance (Baker et al., 2018).

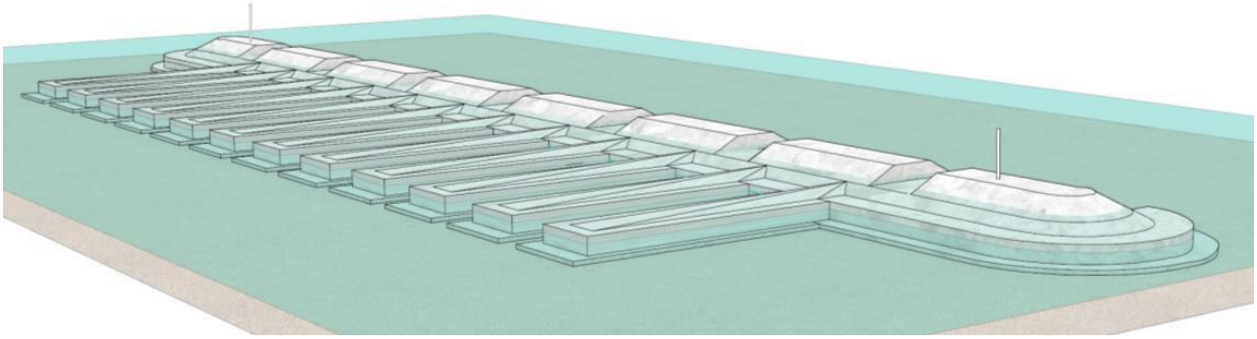

Figure 2-4. Low-crested Living Breakwaters design (Baker et al., 2018)

Marrone et al. (2019) conducted numerical and physical experiments to investigate the sediment transport and the effects of the Living Breakwaters designs on sediment transport, deposition, and erosion. Their results emphasized the importance of balancing storm wave attenuation with the maintenance of longshore sediment transport to avoid long-term beach recession and downdrift erosion (Marrone et al., 2019).

Another eco-enhancing hybrid system is the Oyster Castle pod, shown in Figure 2-5, which is a patented structure consisting of interlocking concrete blocks specifically designed to facilitate oyster settlement. The initiative employs living shoreline approaches, such as oyster habitat restoration, to reduce coastal habitat loss and degradation. The project's objective is to develop a creative and economical living shoreline that enhances shoreline stability while promoting oyster reef development in Delaware Bay (Manson et al., 2017).

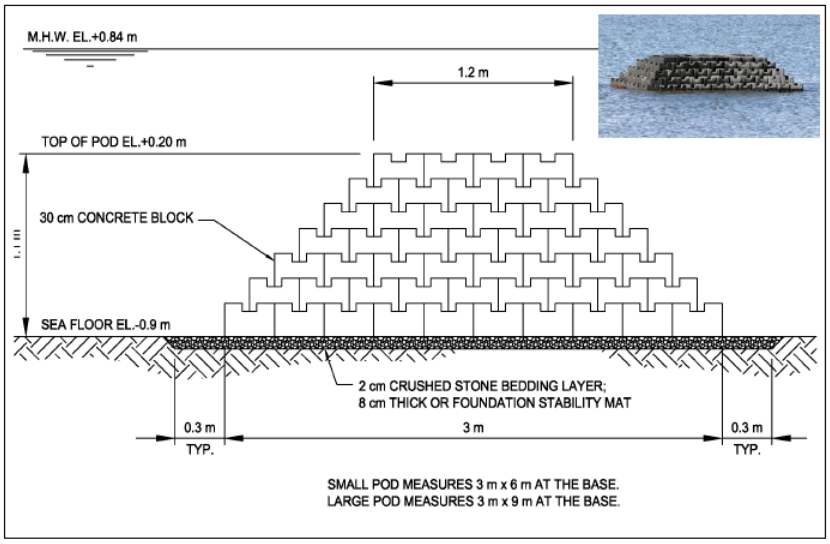

Figure 2-5. Oyster castle cross-section in Gandy's Beach (Manson et al., 2017)

2.1.2 Eco-friendly Coastal Structure Modifications

The implementation of environmentally-friendly technologies such as rock pools, micro-scale modifications, and eco-friendly concrete units in coastal structures represents a significant advancement in sustainable coastal engineering. Artificial rock pools not only provide habitats for marine life but also contribute to wave energy dissipation, offering a sustainable approach to coastal protection. Micro-scale adaptations, such as bio-engineering techniques and ecologically informed design, enhance coastal resilience by integrating natural processes into structural elements. Eco-friendly concrete elements, which incorporate ecologically compatible materials, provide more sustainable alternatives to conventional coastal structures.

Naturally formed rock pools along rural coasts support diverse marine assemblages by providing refuge from predation and environmental stress. In contrast, such complex habitat features are typically absent from engineered urban coastlines. Integrating artificial rock pools into seawalls and breakwaters can enhance species diversity and habitat value.

Studies demonstrate that rock pools offer protection from temperature changes, desiccation stress, and predators by retaining water. Water-retaining units have been attached to seawalls to create artificial tide pools (Chapman and Blockley, 2009; Browne & Chapman, 2011; Hall et al., 2018; Morris et al., 2018), and holes have been drilled into rock armour to artificially create rock pools (Firth et al., 2014b; Evans et al., 2016). These eco-engineered pools demonstrated measurable ecological benefits, though they did not fully replicate the complexity of natural environments (Evans et al., 2016).

Browne and Chapman (2011) described the use of concrete "flowerpot" units to incorporate large artificial rock pools into existing vertical intertidal structures. These flowerpot units, installed at varying tidal elevations (Figure 2-6), emulate the depth variability of natural rock pools, thereby supporting distinct biological assemblages.

Figure 2-6. Flowerpots type artificial rock pools (Browne and Chapman, 2011)

Micro-scale modifications can be applied to coastal defence structures to increase the colonization and survival of intertidal species. Several studies have explored fine-scale (millimetre-level) surface texture adjustments to promote biological colonization on artificial substrates.

The experiments show the significance of fine-scale texture for the formation of marine biofilms, the establishment of invertebrate larvae and spores, the recruitment of juveniles, and the nature of community interactions on rocky substrata (Chabot and Bourget, 1988; Walters and Wethey, 1996; Decho, 2000; Menge, 2000; Hutchinson et al., 2006). On artificial structures, fine-scale topography significantly influences the abundance of dominant species (Moschella et al., 2005), yet deliberate texture design at this scale remains uncommon.

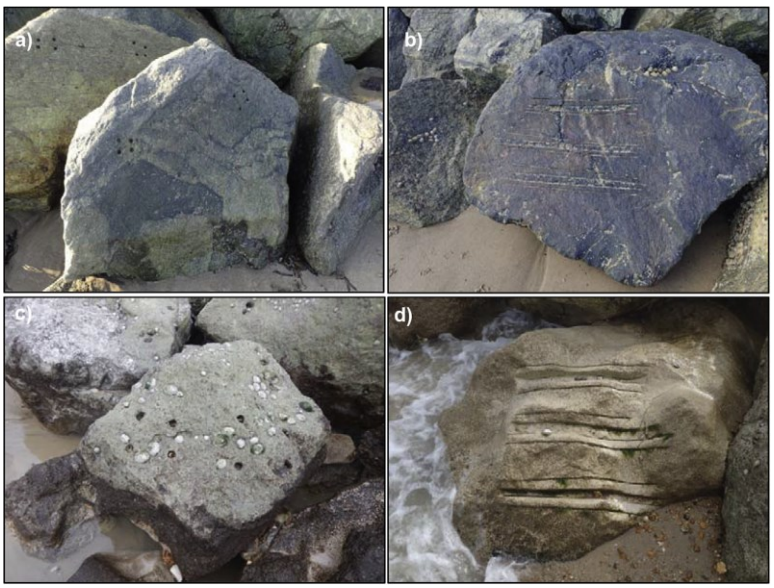

Figure 2-7. Fine-scale rock modifications: a) Holes at Runswick Bay, b) Grooves at Runswick Bay, c) Holes at Boscombe, d) Grooves at Boscombe (Hall et al., 2018)

Fine-scale habitat variability on naturally occurring rocky coastlines (Figure 2-7) is produced by weathering, which includes wetting and drying of rocks, salt crystallization, chemical breakdown, biological weathering, and erosion (Coombes, 2014). Although the rate of surface roughness development depends primarily on rock type, the duration remains a crucial factor absent from most engineered shorelines. According to Coombes et al. (2011), engineering materials are susceptible to the same weathering processes as in situ rock, but they are invariably newer and less physically complex than the rocks of rocky shorelines. Artificial structures generally lack fine-scale complexity unless pre-weathered rock or synthetic texturing is used (Coombes et al., 2015).

Eco-friendly Concrete Units

The engineering firm ECOncrete has recently developed habitat-enhancing technologies through an innovative concrete mix that reduces CO_2 emissions over its lifespan while improving biodiversity and water quality (Perkol-Finkel & Sella, 2014, 2015). Using this ecologically-enhanced concrete, ECOncrete has produced a range of bio-inclusive coastal and marine elements, including quay walls, pile encasements, bottom protections, and tidal-pool modifications to riprap armour.

Among ECOncrete's key innovations is the Coastalock armour unit, an environmentally-friendly block designed for breakwaters and coastal slopes that simultaneously fulfils hydraulic and ecological objectives. The unit has an octahedral geometry featuring an internal cavity that provides multiple ecological functions (Figure 2-8). Each face of the Coastalock unit fosters distinct micro-habitats, including water-retaining pools, crevices, and overhangs that support diverse marine organisms (ECOncrete, 2021). From a hydraulic perspective, this geometry also distinguishes Coastalock from conventional single-layer armour units by combining interlocking capacity with intentionally created voids and cavity features that influence permeability, flow resistance, and localized energy dissipation. The design ensures ease of installation, and effective interlocking between adjacent units. Coastalock units are often cast in situ using steel moulds, which improves manufacturing efficiency and reduces transportation-related environmental impacts. A pilot installation at the Port of San Diego is currently evaluating Coastalock's performance, while previous studies using ECOncrete's admixture demonstrated enhanced marine colonization and biodiversity around similar eco-engineered units (Perkol-Finkel & Sella, 2014, 2015, 2019). Nevertheless, data on the hydraulic performance of Coastalock remains limited (Molenkamp, 2022).

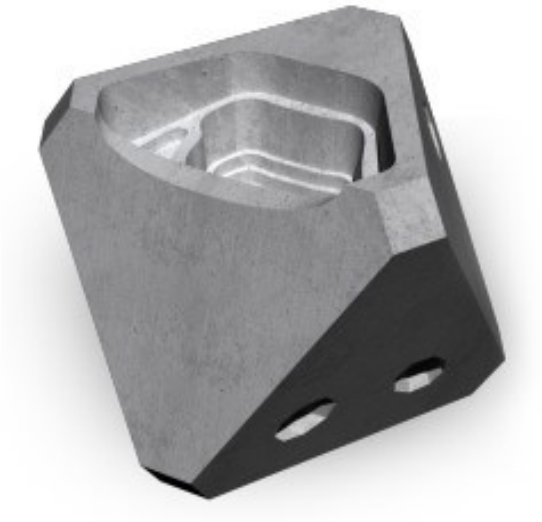

Figure 2-8. Schematic representation of the Coastalock armour unit (ECOncrete Tech Ltd. 2021)

Another ECOncrete product, the bio-enhancing Antifer unit, is employed on breakwaters (Figure 2-9). Their design integrates environmental, biological, and engineering considerations. Three aspects of the ecologically-friendly design vary from conventional concrete armouring units: concrete mixture, surface complexity, and macro-design (ECOncrete, 2018).

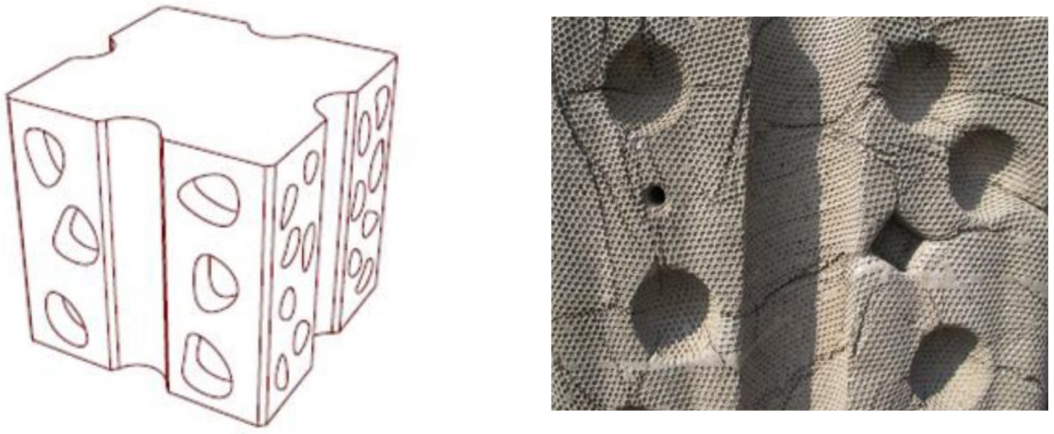

Figure 2-9. Schematic representation (left) and photograph (right) of bio-enhancing holes and crevices on the concrete surface of the ECOncrete Antifers (Ido et al., 2015)

The ecological performance of environmentally-modified Antifer units used to build a breakwater section in the eastern Mediterranean is being tested as part of an experimental pilot study in Haifa, Israel. The current research focused on how concrete complexity (Figures 2-9 and 2-10) and composition impacted the ecological performance of these Antifers units (Ido et al., 2015).

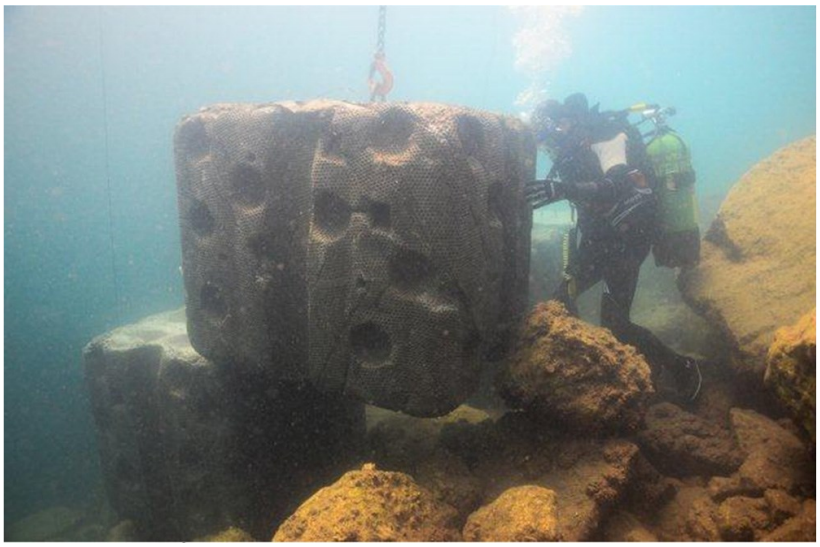

Figure 2-10. ECOncrete Antifers during construction in Polinom Port, Haifa (Ido et al., 2015)

Recent innovations include biomimicry-based artificial coral units that have demonstrated promising hydraulic performance in flume tests, offering potential alternatives to traditional armour shapes with improved wave dissipation and reduced ecological impact (Safa et al., 2024).

ECOncrete has also developed modular seawall components (Figure 2-11) designed to integrate with existing coastal infrastructure or function as load-bearing elements in new construction. These panels can also be retrofitted onto existing seawalls to enhance ecological value. Concrete seawalls improve the structure's capacity to be colonized by different species, and they may be customized for certain species with high conservation value without affecting their structural or functional qualities. Ecologically-enhanced seawalls differ from conventional concrete walls on three levels: concrete chemistry, surface complexity, and macro-design. These combine three components that replicate authentic aquatic habitats and reduce the detrimental impacts of coastal development based on concrete (ECOncrete, 2018).

Figure 2-11. ECOncrete Seawall Panel before and after deployment (Rella et al., 2017)

ECOncrete's articulated marine mattresses (Figure 2-12) are designed to enhance shoreline stability, prevent erosion, and provide anchoring and protective cover for exposed underwater pipelines. The special chemical and physical characteristics of the mattress promote the development of marine flora and fauna, raise species richness, lessen the dominance of invasive species, and promote biodiversity (Moore Concrete, 2021).

Figure 2-12. Ecological Articulated Concrete Marine Mattress (ECOncrete, 2021)

Ecological mattresses consist of interlocking concrete blocks connected by polyester cables, enabling ease of installation, transportation, and modular sizing. The Articulated Concrete Marine Mattress system, produced using dry-cast technology, is one such example. Concrete composition with bio-enhancing properties, combined with scientifically developed designs featuring water-retention elements and complex textures, was applied to improve biological efficiency (Rella et al., 2017).

Another habitat-supporting armour unit, the BIOBLOCK, has been developed to enhance marine biodiversity on breakwaters (Figure 2-13). This large precast unit incorporates a range of habitat features that are typically absent from conventional coastal armour surfaces. Each unit contains a combination of holes and depressions designed to replicate the microhabitats of natural rocky intertidal zones. In riprap structures, individual boulders can be replaced with BIOBLOCK units to enhance ecological function (Firth et al., 2014).

Figure 2-13. The BIOBLOCK unit (Firth et al. 2016)

2.2 Ecological Assessment and Bio-Enhancement Approaches

The main goal of eco-friendly coastal structure applications is to enhance the habitat while providing coastal protection. Recent research and design approaches increasingly prioritize ecological considerations in the development of such structures.

A wide range of marine flora and fauna can colonize artificial coastal structures such as breakwaters, seawalls, and bulkheads. Their capacity to encourage marine development, offer refuge, and provide other ecosystem services depends on their chemical and physical characteristics, such as chemical composition, surface roughness, and design. In contrast, natural rocky substrates possess roughened surfaces, crevices, depressions, water-retaining features, and overhangs, whereas conventional coastal structures offer relatively few microhabitats (Rella et al., 2017). Eco-enhancing coastal structures aim to increase biological abundance and diversity, improve water quality, and provide sheltered habitats for colonization. The type and scale of modifications, as well as the materials used in coastal structures, play a crucial role in determining the species that will colonize them.

Oyster reefs exemplify eco-friendly coastal structures, serving as shelters, nurseries, and feeding grounds for diverse marine species. Integrating engineering and ecological principles into the design of oyster reef living shorelines enables the creation of durable, effective systems that provide both coastal defence and ecosystem restoration benefits (Morris et al., 2019). For instance, live oysters play a key role in sediment stabilization and hydrodynamic regulation. In situ measurements show that healthy oyster reefs generate and dissipate turbulent energy at much higher rates than damaged reefs without living oysters, under identical flow conditions (Kitskoudis et al., 2020).

Oyster reefs enhance the deposition of organic particles both directly and indirectly. Direct bio-deposition occurs through the accumulation of faeces and pseudofaeces, while the reef structure itself traps suspended organic matter, increasing sediment organic content and providing additional food resources for benthic organisms such as polychaetes (Chowdhury et al., 2020). The ecosystem benefits of oyster reefs are illustrated in Figure 2-14.

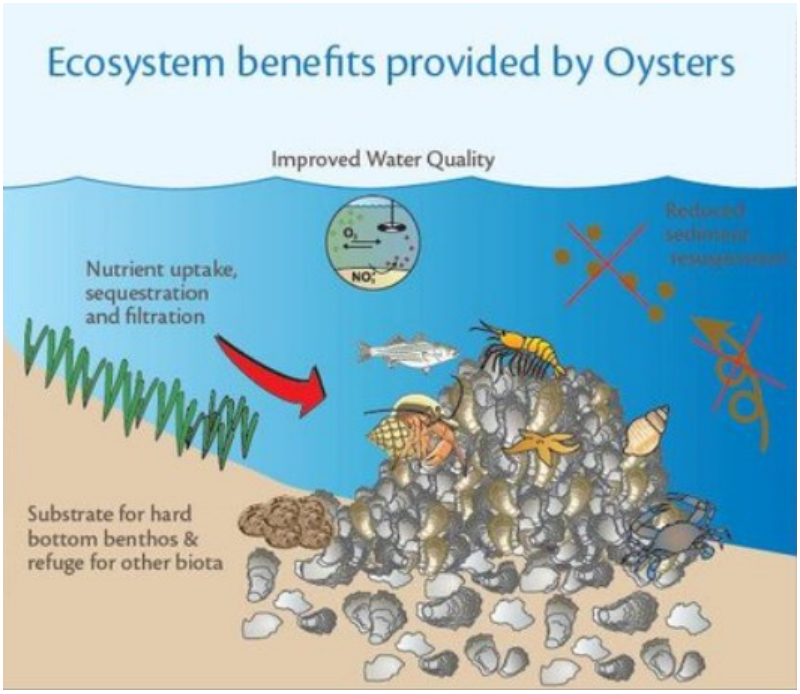

Figure 2-14. Schematic representation of the oyster reefs' benefits on the ecosystem (Ozbay et al., 2014)

Despite their benefits, oyster reef installations have notable environmental constraints. Longer submergence periods lessen the stress caused by desiccation while improving feeding and thereby oyster development. However, excessive immersion increases vulnerability to subtidal predation. Thus, there is an ideal inundation time that varies significantly over the geographical range but appears to be between 5 and 40% (Morris et al., 2018).

Brushwood dams represent another form of eco-enhancing coastal structure. However, the environmental effects of wooden breakwaters remain a recent research topic that deserves further investigation.

The Living Breakwaters project represents an engineered integration of multiple ecologically-supportive design features. Its design aims to enhance aquatic habitat diversity and promote habitat-forming species such as oysters, tube worms, and barnacles, which contribute to biogenic buildup through calcium carbonate deposition (Jones et al., 1994).

The Living Breakwaters were designed to maximize habitat production and ecological services while avoiding or minimizing negative effects. Accordingly, the project incorporates macro- and micro-scale ecological enhancements, including rock pools, surface roughening, pits, crevices, and concrete mix modifications (Figure 2-15). The project includes several active restoration techniques for the eastern oyster (Crassostrea Virginica), an oyster nursery system, and the placement of "spat" (young oysters connected to shells) on the bottom.

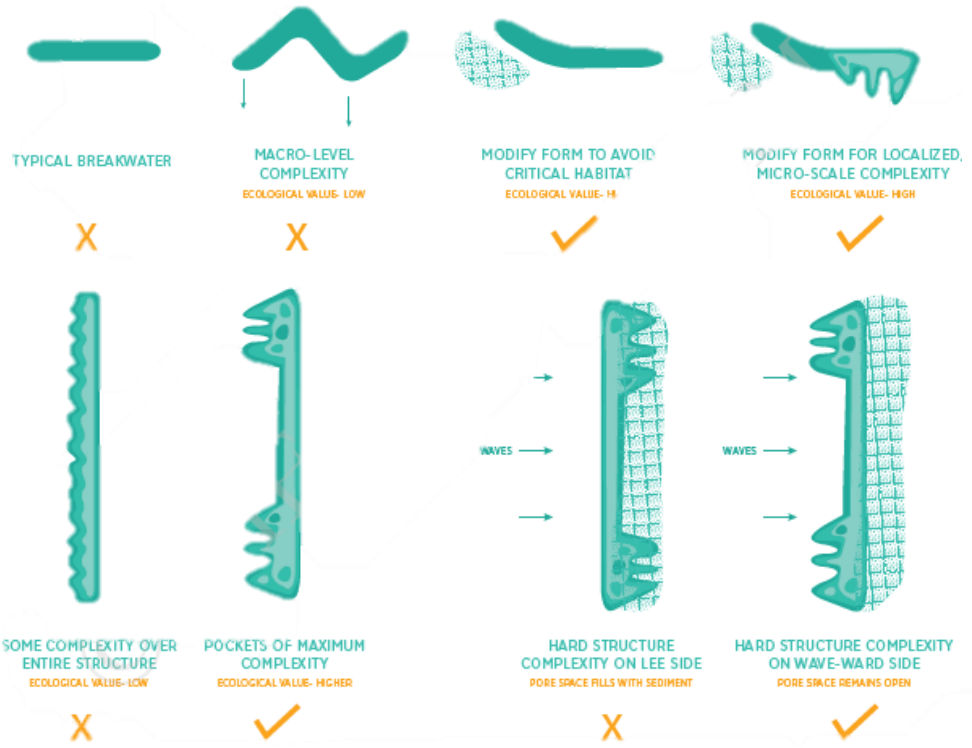

Figure 2-15. Habitat-enhancing modifications used in living breakwaters design (Living Breakwaters, 2013)

Rock pools further enhance habitat complexity and increase species abundance (Firth et al., 2014b; Evans et al., 2016; Chee et al., 2020) (Figure 2-16). However, the effective design of rock pools must account for tidal elevation. Units positioned too high in the intertidal zone will accumulate freshwater and support lower biodiversity due to infrequent tidal inundation. Conversely, pools positioned too low, below the lowest tidal level, may provide limited ecological value.

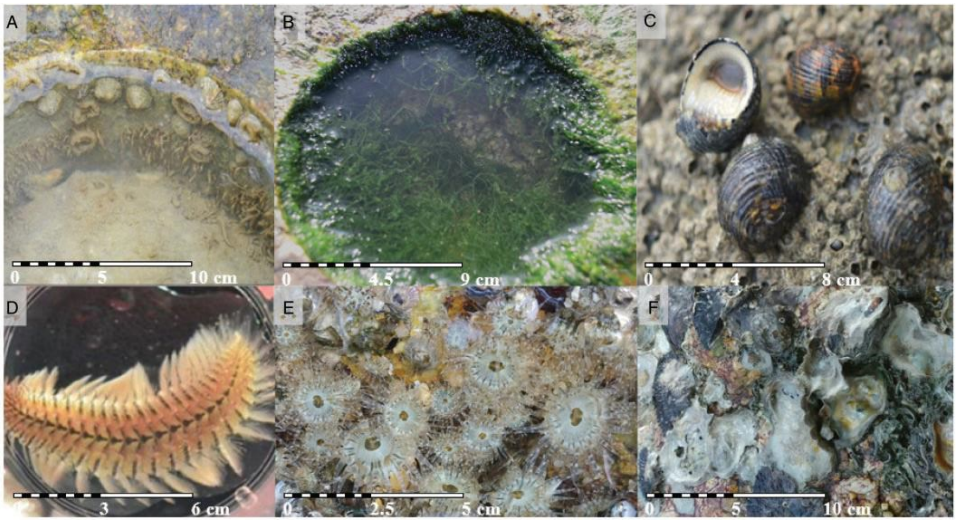

Figure 2-16. Colonized organisms observed in rock pools (A) Limpets, polychaetes, and algae, (B) Penaeus merguiensis and green algae with Nerita sp. egg capsules on the fronds, (C) Nerita chamaeleon, (D) polychaete, (E) Anthopleura nigrescens, and (F) Saccostrea cucullata (Chee et al., 2020)

The type of rock used also significantly influences biological community composition. Sandstone and limestone tend to support greater biodiversity than fine-grained rocks such as granite and basalt (Hall et al., 2018). For smaller-bodied organisms, such as barnacles and bivalves, fine-scale improvements, such as adding roughness, pits, and fissures as depicted in Figure 2-17, have been shown to be most beneficial (Borsje et al. 2011).

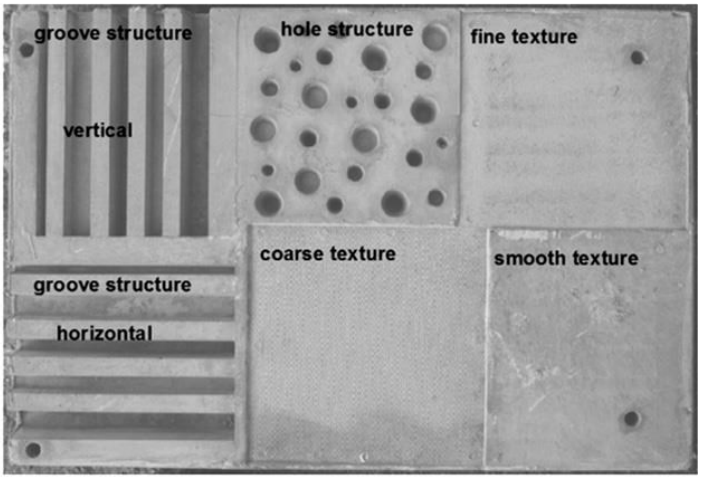

Figure 2-17. A slab composed of different ecological modifications (Borsje et al. 2011)

On the other hand, larger-scale interventions, such as rock pools, can support larger species like branching coralline, canopy-forming algae, and fish (Strain et al., 2017). The relationship between the modification scale and species size is illustrated in Figure 2-18.

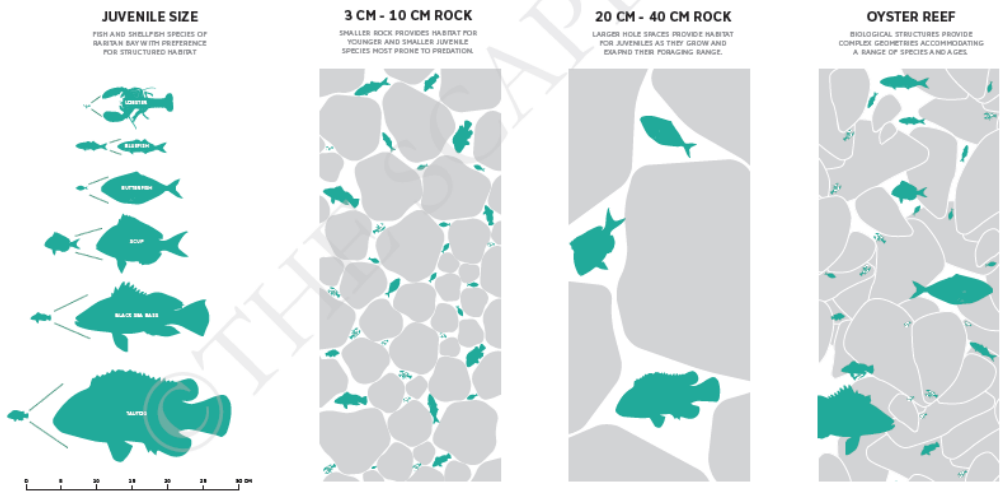

Figure 2-18. Animal abundance on the several sizes of spacings on breakwaters (Living Breakwaters, 2013)

Coombes et al. (2018) highlight that the effectiveness of ecological improvements depends on site-specific factors, such as tidal height and the availability of local larval resources, which often dominate community growth dynamics.

Eco-engineered concrete units with modified chemical compositions have been extensively investigated over the past two decades. Such units often combine eco-friendly concrete formulations with small-scale surface modifications to further enhance colonization potential. Many of these formulations provide ecological benefits by substantially reducing the overall carbon footprint of coastal infrastructure. As the concrete contains different ingredients, the amount of Portland cement, which is known for having a large carbon footprint, in the mixture may be greatly reduced (Matthews et al., 2008). Previous studies have also demonstrated that surface texture can affect micro-scale flow behaviour, possibly increasing the likelihood that larvae will come into contact with the surface and enabling the colonization by a variety of benthic organisms (Mullineaux and Butman, 1990; Walters and Wethey, 1996).

2.3 Site Observations and Field Monitoring of Eco-Engineered Structures

Oyster Reefs

Field monitoring and site-specific observations provide valuable insights into the ecological and hydraulic performance of eco-engineered coastal structures. These studies assess how eco-friendly materials, structural forms, and design modifications influence species abundance and diversity.

Oyster reefs are increasingly popular as a component of coastal protection. Over recent decades, large-scale restoration initiatives have sought to counteract the global decline of oyster populations (Beck et al., 2011). More recently, attention has expanded toward optimizing secondary benefits

such as shoreline protection and water-quality improvement (Grabowski et al., 2012). Oyster reefs and living shorelines in general have the tremendous ability to adapt to environmental change, providing both erosion mitigation and long-term resilience (Taylor and Bushek, 2008; Bible and Sanford, 2015).

Oyster reefs provide two principal benefits: ecological enhancement of flora and fauna, and coastal protection. Several studies show that when oyster reefs are constructed on coasts, they support a wide variety of living animals and organisms (Scyphers et al., 2011; Scyphers et al., 2015; Chowdhury et al., 2020).

Scyphers et al. (2011) found that oyster-shell breakwater reefs supported greater diversity of fish and mobile invertebrates than control sites. In a subsequent study, Scyphers et al. (2015) compared concrete-dome and oyster-shell breakwaters along an eroding shoreline in Alabama. Monitoring showed both configurations increased species richness of juvenile and small fishes relative to controls, while larger fish populations remained unaffected.

Another key function of oyster reefs is erosion mitigation through the dissipation of wave energy. The hydraulic performance of oyster reefs has been studied in several articles (Scyphers et al., 2011; Spiering et al., 2018; Morris et al., 2021). Hydraulic performance, particularly wave attenuation, has been extensively investigated (Scyphers et al., 2011; Spiering et al., 2018; Morris et al., 2021), quantifying the reduction in wave energy attributable to reef structures.

Field evidence from living shorelines indicates that restored oyster reefs can dramatically attenuate wave energy in front of intertidal marshes, even in relatively high-energy environments (Roney et al., 2025). Thus, biologically active reef structures can serve as effective natural breakwaters while enhancing ecosystems.

Wave damping is most effective when the reef crest lies at or slightly above the still-water level (Morris et al., 2021; Stanley et al., 2024). Scyphers et al. (2011) reported that constructed oyster reef treatments reduced coastal erosion by more than 40% compared with the control regions. Furthermore, the wave attenuation was comparable between the oyster reef living shorelines and the natural reefs in Florida (75% and 84%, respectively), and double that of the control (35%).

Reefs exposed less than 50 % of the tidal cycle were significantly more effective at reducing wave height than those submerged for longer durations (Morris et al., 2021). While oyster reefs provide substantial ecological and protective benefits, growth and recruitment are constrained by inundation duration.

Numerous studies examine the ecological effects of oyster reefs on marine habitats. However, the success of design interventions in enhancing species abundance and diversity depends on site-specific factors such as tidal height and local larval availability (Coombes et al., 2015).

Rock Pools

Rock pools provide shelter and habitat for diverse marine species. Browne and Chapman (2011) evaluated the ecological benefits of pot-shaped water-retaining units attached to seawalls. After seven months, 25 species, representing a 64 % increase, had colonized the artificial pools, including a 118 % rise in mobile fauna and a 39 % increase in sessile organisms.

Pool elevation strongly influences biodiversity patterns in artificial rock pools. Firth et al. (2016) found that lower pools supported greater functional richness and more variable community composition than upper pools, largely due to numerous low-occurrence species. After one year, 19 species had colonized the pools, with lower and exposed pools showing higher taxonomic and functional richness than upper or sheltered ones. By 24 months, sheltered pools had filled with sediment, forming muddy habitats that created new ecological niches, while exposed shores hosted 72 taxa, nearly four times more than both exposures combined. Some typically subtidal species also settled in the upper pools.

Chee et al. (2020) found that mid-tidal artificial pools supported both low-intertidal species (e.g., anemones) and subtidal taxa (e.g., shrimp, crabs, and red algae), indicating that they created environmental conditions similar to low-tide or shallow-subtidal habitats. Mobile species rarely present on emergent rock surfaces were also sustained within these pools. After 36 months, mean species richness in the drill-cored pools remained significantly higher than on adjacent emergent surfaces. Evans et al. (2015) tested the ecological potential of two artificial pools, 12 cm and 5 cm deep, drilled into an intertidal granite breakwater. After 18 months, species richness in the artificial pools exceeded that of surrounding granite surfaces and was comparable to natural pools on nearby coasts. However, community composition did not differ significantly between artificial and natural pools, and pool depth had no measurable effect on richness or community structure.

Small-Scale Modifications

Small-scale surface modifications such as pits, cracks, grooves, holes, and textural adjustments are designed to enhance habitat complexity on artificial coastal structures. Multiple studies have explored the combined effects of various small-scale modifications, including grooves, pits, and surface textures (Moschella et al., 2005; Borsje et al., 2011; Coombes et al., 2015; Strain et al., 2018). A key finding from these studies is that minor textural and structural modifications to concrete surfaces in the intertidal zone promote improved settlement and growth of algae and macrobenthic organisms (Borsje et al., 2011). Similarly, adding small pits or cracks to existing walls has been shown to enhance biodiversity. Martins et al. (2010) tested this approach by introducing two densities of differently sized pits into a basalt seawall in the Azores. The presence of pits led to an increase in the population of limpets due to both immigration and recruitment, with more adults living in areas with larger pits and more recruitment occurring in places with smaller pits (Martins et al., 2010).

In another site-observation study, Chapman and Blockley (2009) created cavities at three intertidal elevations within a sandstone seawall overlaying a concrete wall. These were constructed by

removing blocks and placing a shallow lip across the cavity's entrance, which kept water in during low tide. Compared to the adjacent seawall surfaces, these cavities hosted a greater diversity of sessile and mobile fauna and flora. Some of these species inhabited the pools themselves, while others lived on the shady walls of the caverns.

Coombes et al. (2015) investigated barnacle colonization by placing concrete tiles in the intertidal zone with four reproducible fine-scale textures: control, smoothed, grooved, and exposed aggregate, and compared them to natural rock. Concrete texture considerably affected colonization; after one settlement season, smoother tiles supported significantly fewer barnacles, whereas those with intermediate roughness (grooved concrete) supported significantly more.

Moschella et al. (2005) observed that barnacles preferentially settled in small fissures on rougher surfaces compared to adjacent smooth areas, with differences apparent at sub-centimetre scales. Species diversity also increased markedly with greater surface complexity at scales of around 10 cm. For instance, after a year, panels with small pits (16 mm in diameter) typically had more species than smooth panels (Moschella et al., 2005). The abundance and diversity differences of modified and control surfaces are shown in Figure 2-19.

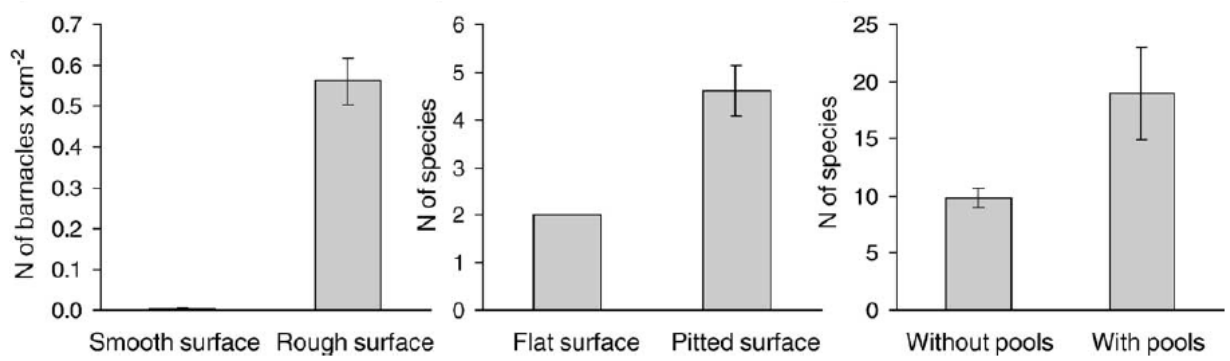

Figure 2-19. Several-sized surface complexity effect on epibiota on low-crested structures at Elmer (Moschella et al. 2005)

Borsje et al. (2011) observed that mussels settled exclusively in the grooved and perforated sections of experimental panels. Panels installed lower in the intertidal zone exhibited faster and more diverse colonization, likely due to longer submergence periods. Strain et al. (2018) found that features providing shade and moisture, such as crevices, pits, and water-retaining depressions, most strongly influenced the diversity of mobile and sessile organisms. These benefits were greatest for species whose body sizes corresponded closely to the dimensions of the surface modifications.

Modifications based on Material Composition

Concrete, which accounts for more than half of global coastal infrastructure, is generally regarded as a poor substrate for biological recruitment due to its potential to leach harmful compounds. However, increasing surface roughness and edge complexity enhances available settlement area, facilitating colonization and growth of benthic organisms. Furthermore, compared to smooth

surfaces, complex surface textures might thicken the boundary layer close to the surface, increasing the chance of larval settling (Sella and Perkol-Finkel, 2015).

In Perkol-Finkel et al. (2018), four 1.5 m × 0.8 m seawall panels constructed of bio-enhancing concrete with a complex structural design were installed in a busy marina in Herzliya, Israel. The panels were surveyed 2, 7, 12, 18, and 22 months after deployment. After two years, monitoring showed that the ECO panels supported significantly higher biodiversity and distinct community assemblages compared with the existing concrete seawall. Species assemblages on the ECO panels diverged markedly from those on control plots of standard marina concrete.

Sella et al. (2017) compared bio-enhanced and standard concrete in terms of structural performance, environmental impact, and cost-effectiveness (Figure 2-20), reporting that bio-enhanced concrete improves structural durability while promoting ecosystem services through increased development of marine flora and fauna. The biological layer formed on bio-enhanced concrete mitigates weathering processes such as thermal fatigue and chloride-ion penetration. This layer can extend service life, reduce maintenance needs, and enhance structural stability and hydrodynamic energy absorption.

		Standard	Bio-Enhanced
Structure	Stability and Durability	Norm	High
	Resistance to Chloride Penetration	Norm	High
	Absorption of Wave Energy	Norm	High
Environment	Ecosystem Services	None	High
	Biodiversity	Low	High
	Invasive/Nuisance Species	High	Low
	Carbon Footprint	High	Low
Cost Effectiveness	Maintenace Fees	Norm	Low
	Financial Incentives	None	High
	Environmental Penalties	High	Low
	Advantages in Project Biddings	None	High
	Out-Greening	None	High

Figure 2-20. Evaluation and comparison of standard concrete and eco-friendly concrete coastal structures (Sella et al., 2017)

Beyond concrete composition, the lithology of natural rock materials also influences habitat quality. Hall et al. (2018) demonstrated that sandstone and limestone structures support more diverse biological communities than hard, fine-grained rocks such as granite and basalt.

Design Recommendations for Ecological Enhancement of Coastal Structures

Numerous studies have examined the design of eco-friendly concrete coastal structures; however, experimental research on brushwood dams remains limited. While the hydraulic performance of oyster reefs has been explored in several investigations, additional experimental research is required to establish comprehensive design guidelines for their implementation.

Eco-enhancing modifications, such as water-retaining units, pit-type features, and surface texture optimization, are integral not only to individual eco-designs but also to the overall configuration of multi-purpose breakwaters. Table 2-1 summarizes key design recommendations from the literature that aim to enhance species abundance and biodiversity through the strategic design and placement of eco-enhancing features.

Table 2-1. Design recommendations for ecological enhancement of coastal structures

Ecological Modifications	Design Recommendations	Working Mechanism	References
Water Retaining Units	-Constructing rock pools lower in the intertidal zone - Using eco-enhancing armour units on breakwaters	Provide shelter for intertidal organisms	Browne and Chapman, 2011 Firth et al., 2013 Firth et al., 2014 Evans et al., 2015 Firth et al., 2016 Naylor et al., 2016 Strain et al., 2017 Chee et al., 2020
Pits, crevices, holes	-Drilling holes, pits, and crevices of different sizes into rocks or concrete units	Provide shelter for intertidal organisms	Martins et al., 2010 Borsje et al., 2011 Firth et al., 2013 Firth et al., 2014 Naylor et al., 2016 Strain et al., 2017 Hall et al., 2018
Surface Texture	-Soft rock use (e.g., limestone) -Roughening rock and concrete surfaces	Creates complex microsurfaces for easier attachment of organisms	Chapman et al., 2006 Borsje et al., 2011 Firth et al., 2013 Firth et al., 2014 Coombes et al., 2015 Naylor et al., 2016 Strain et al., 2017
Concrete Composition	-Eco-friendly concrete compositions use	Supports enhancements of fauna and flora and reduces the CO_2 footprint	Firth et al., 2013 Firth et al., 2014 Sella and Perkol-Finkel, 2015 Perkol-Finkel et al., 2017 Rella et al., 2017 Sella et al., 2017 Molenkamp, 2022

2.4 Physical Modelling

Numerous physical experiments have investigated the hydraulic performance of eco-friendly coastal structures. These investigations encompass various habitat-enhancing structures and modifications, including oyster reefs, wooden and living breakwaters, and ecologically-enhanced

armour units. While numerous experiments have focused on oyster reefs and wooden breakwaters, only a few studies on living breakwaters and eco-enhancing modifications exist in the literature.

As demonstrated by site observation studies (Section 2.3), these coastal structure types are well-established as habitat-enhancing. Consequently, their structural performance is a critical design consideration, particularly since eco-friendly systems incorporate unconventional materials, geometries, and unit configurations compared to traditional breakwaters. Even in the design stage of the majority of conventional coastal structures, physical experiments are needed to understand the behaviour of the structure under extreme wave conditions. Accordingly, such experiments are essential for evaluating the hydraulic performance and stability of innovative eco-friendly structures under varying wave conditions.

Oyster Reef

Oyster reefs function as porous, low-crested breakwaters where wave transmission is governed primarily by submergence depth, incident wave height, and crest width. According to van der Meer et al. (2005), wave transmission increases with increasing submergence depth, increasing incident wave height, and decreasing crest width for low-crested breakwaters. Physical model studies of oyster reefs are compatible with the results of low-crested breakwater studies, which indicate that the freeboard, crest width, and incident wave height are key parameters for wave transmission (Allen and Webb, 2011; Webb and Allen, 2015).

Wave transmission, a key indicator of energy dissipation, is the most frequently examined hydraulic parameter of submerged eco-friendly breakwaters. The shape of the reef section is another major factor that determines the specific parameters of wave dynamics when waves propagate through reefs. Rectangular submerged breakwaters are superior to semi-cylindrical ones in absorbing wave energy (Stamos et al., 2003). The porosity of oyster reefs is often between 0.6 and 0.8 (Hitzegrad et al., 2022). Experimental findings by Morris et al. (2021) indicate that oyster reefs can reduce wave heights by up to 68%.

The experimental findings show a significant impact of the non-dimensional height of the structure on wave transmission for the oyster reef structures (Webb and Allen, 2015; Morris et al., 2019; Yang et al., 2022). The wave attenuation might decrease to 0 – 20% when reefs are submerged (Wiberg et al., 2018). In another test series, oyster bags are used to construct an oyster reef. Although the oyster bags were closely packed, fewer shells remained at the joints due to bag geometry, resulting in reduced wave energy dissipation at those points. Greater displacement of the underlying filter occurred at bag joints compared to central sections (Provan et al., 2024).

Brushwood Dams

In physical model tests of brushwood breakwaters, the most significant parameters are considered as porosity and the shape of the wooden structure. Safak et al. (2020) tested two brushwood breakwater configurations and found that bundled structures achieved higher wave attenuation than unbundled ones. Provan et al. (2024) conducted complementary large-scale flume

experiments on brushwood dams composed of vertically fixed round posts and showed that wave attenuation decreases with increasing water levels

Across studies, higher structural permeability consistently reduced wave attenuation capacity. However, the porosity of brushwood breakwaters changes over a wide range. Moreover, the wave attenuation rates of brushwood breakwaters vary significantly, ranging from 16% to 91% depending on design and wave conditions (Safak et al., 2020).

The Living Breakwaters

In contrast to simpler eco-friendly designs, Living Breakwaters incorporate diverse structural elements such as tidal pools, reef streets and ridges, crenulations, and graded stone arrangements (Tschirky et al., 2018). Designers must balance storm-wave mitigation with the preservation of longshore sediment transport to avoid long-term erosion. Understanding wave conditions, sediment transport, and the shoreline reaction to the project are key factors for the design and advantages of the Living Breakwaters. Baker et al. (2018) conducted physical modelling tests to evaluate the structural stability of the Living Breakwaters under various wave conditions and different water levels.

Structures with Coastalock Armour Units

Eco-enhancing armour units have been developed as environmentally sustainable alternatives to conventional designs. Coastalock is a bio-enhanced concrete armour unit whose hydraulic characteristics are still under investigation. The first physical model testing on Coastalock units was carried out by Molenkamp (2022), where several sets of data on different parameters were gathered to obtain initial knowledge of the hydraulic performance of Coastalock armour units. Layer porosity, defined by unit spacing, is a critical factor influencing Coastalock stability. Compared with other armour types, Coastalock units on an impermeable 2V:3H slope exhibited lower hydraulic stability at spacings below 10%, whereas high stability numbers were recorded for spacings of 10% and above. However, higher stability numbers ($N_s > 3$) are obtained for spacings of 10% and above. No failure of the armour units was seen in the experiment for spacings of 15% and higher. The wave reflection from Coastalock units is primarily influenced by the steepness of the incident waves, with reflection coefficients (K_r) reaching up to 0.78 for waves with a steepness of 1.6% and as low as 0.48 for waves with a steepness of 4.6%. Additionally, in all tests where armour unit spacing exceeds 10%, the overtopping discharge remained below 0.01 L/m/s. Thus, overtopping had a negligible influence on the hydraulic stability of the armour layer, as tested under structural and wave conditions by Molenkamp (2022).

Following the preliminary impermeable-slope tests, Lawniczak (2024) extended the investigation of Coastalock armour performance to permeable rubble mound structures, incorporating toe-supported conditions and modified armour geometries. The study confirmed that the pressure-induced “breathing’’ mechanism reported by Molenkamp (2022) also governs failure on permeable cores, with upward and downward oscillations of the armour layer preceding extraction. As in the impermeable-core tests, larger inter-unit voids significantly enhanced stability: for simple

10% spacing, breathing and extraction thresholds increased to Ns ≈ 3.6, and no breathing or extraction occurred for spacings of 20% or for protrusion-enforced spacings of 22.5%. The introduction of protrusions, designed to guarantee minimum armour spacing and reduce pressure gradients, further improved performance. Long protrusions (22.5% spacing) prevented breathing and extraction up to Ns ≈ 4.2, representing the highest stability levels recorded to date for Coastalock units.

The study also assessed the influence of wave steepness, core permeability, unit orientation, and toe-berm conditions. For long-wave tests (s_{op} = 0.02), stability thresholds increased relative to steeper waves, possibly due to a "reservoir effect'' that reduces pressure gradients during extended run-down phases. Modified unit orientations introduced to accommodate protrusions resulted in measurable differences in armour behaviour; downward-facing cavities reduced stability due to increased buoyancy and altered flow patterns, narrowing the safe orientation envelope.

For overtopping, Lawniczak (2024) found that, similar to Molenkamp (2022), no meaningful overtopping occurred for 0% spacing due to early armour failure. For spacings ≥10%, overtopping became measurable and potentially design-relevant; protruded designs slightly reduced overtopping discharge compared to non-protruded configurations, while reflection coefficients remained comparable across geometries.

Overall, Lawniczak (2024) demonstrated that increased permeability substantially improves stability on permeable core structures, while also offering material-efficient configurations with fewer armour units per square metre of slope. The findings confirm and extend Molenkamp's observations, establishing that Coastalock performance is strongly dependent on armour porosity, unit spacing, and the pressure dissipation within the core.

2.5 Numerical Modelling

Numerical Modelling Methods and Software

The Boussinesq equations, Reynolds-Averaged Navier–Stokes (RANS) equations, and wave-action balance equations are the principal formulations used for simulating wave–structure interactions in eco-engineered coastal systems (Marrone et al., 2019; Takagi et al., 2020; Yang et al., 2022). In general, Boussinesq-type models are more suitable for efficient wave transformation analysis at larger scales, whereas RANS-based approaches are more appropriate when detailed free-surface deformation, porous-media interaction, and overtopping processes must be resolved.

Boussinesq-type models are widely applied to simulate wave propagation and transformation in coastal and harbour environments. Commercial implementations include MIKE 21 and SMS, while open-source alternatives such as Celeris, COULWAVE, and FUNWAVE are commonly used for research purposes. Most models employ finite-difference, finite-volume, or finite-element discretization methods (Kirby, 2003).

RANS models describe fluid motion through time-averaged forms of the Navier–Stokes equations. They approximate mean flow fields by incorporating turbulence models that represent the fluctuating components of the flow and remain the most widely used approach for engineering and industrial applications. Examples include OpenFOAM and Ansys which implement various RANS-based turbulence closures (Menter et al., 2021). At larger spatial scales, spectral models such as WAVEWATCH III, TOMAWAC, and SWAN employ the wave-action balance equation to predict wave transformation and energy dissipation.

Among tools applied to eco-engineered structures, FLOW-3D and OpenFOAM are most frequently used to model wave–structure interaction. FLOW-3D is a commercial finite-volume solver employing the Volume of Fluid (VOF) method within a one-fluid framework to represent free-surface flows (Bayon et al., 2016). OpenFOAM, an open-source C++ platform, provides extensive libraries for continuum-mechanics simulations and utilizes finite-volume and object-oriented programming techniques with tensor-based formulations (Weller et al., 1998).

Wave transformation processes are often simulated using SWAN and FUNWAVE (Marrone et al., 2019; Takagi et al., 2020). SWAN (Simulating WAves Nearshore) solves the wave-action balance equation, incorporating nonlinear quadruplet interactions, wind-wave generation, white-capping, and bottom friction (Rogers et al., 2003). FUNWAVE, a Boussinesq-based model, accounts for shoaling, reflection, transmission, bottom friction, wave breaking, and run-up (Kirby et al., 1998).

Delft3D is a comprehensive three-dimensional suite for modelling hydrodynamics, sediment transport, morphology, and water quality in coastal and estuarine systems. The FLOW module simulates wind- and tide-driven circulation, while the WAVE module (coupled with SWAN) computes wave-induced radiation stresses that drive additional water-level setup. The MOR module calculates sediment resuspension, deposition, and morphological evolution due to combined wave–current interactions (Marrone et al., 2019).

Oyster Reef

Various numerical approaches have been applied to simulate the hydraulic behaviour of eco-engineered coastal structures. In the case of oyster reefs, numerical analyses typically focus on wave attenuation across porous, submerged reef formations. While numerous field observations have assessed the hydraulic performance of oyster reefs, only Yang et al. (2022) have developed a dedicated numerical model to evaluate their wave-attenuation performance.

Yang et al. (2022) investigated the attenuation of shallow-water waves across porous, reef-like terrains using a numerical wave flume built within the OpenFOAM framework. The model solved the Volume-Averaged Reynolds-Averaged Navier–Stokes (VARANS) equations for two-phase incompressible flow, applying the Volume of Fluid (VOF) method to track the free surface. It was then used to examine the influence of wave and morphological parameters on attenuation over porous oyster-reef structures. An empirical equation for predicting wave transmission coefficients was also proposed based on the simulation results. The study showed that increasing porosity,

height, and cluster length reduced wave transmission, whereas larger structure spacing and relative water depth led to higher transmission values (Yang et al., 2022).

Brushwood Dams

The use of timber as a primary material in coastal protection structures remains at an early stage of development. Brushwood dams, typically composed of bundled branches, are designed to dissipate wave energy and mitigate shoreline erosion (Maynord et al., 2006; Safak et al., 2020; Provan et al., 2024). Takagi et al. (2020) numerically investigated an eco-friendly breakwater composed of vertically spaced wooden piles, inspired by community-built defences in Phan Thiet City, Vietnam, where local residents employ timber piles to counter severe coastal erosion.

A three-dimensional hydrodynamic model with irregular waves was used to simulate flow behaviour and wave interactions around the piles. A 3D approach was necessary because conventional 2D models cannot accurately capture the complex interference between incident and reflected waves. OpenFOAM was employed to simulate wave propagation across the shallow nearshore zone at Duc Long Beach, focusing on wave run-up and bending stress as the main performance indicators (Takagi et al., 2020). The results indicated an average of 12.9% and a maximum of 37.2% reduction in wave height relative to control conditions, demonstrating the potential effectiveness of timber piles for wave-energy mitigation.

The Living Breakwaters

Marrone et al. (2019) conducted a comprehensive numerical modelling study for the Living Breakwaters project at Tottenville, Staten Island. Although the general configuration resembled a conventional rubble mound breakwater, the design incorporated several habitat-enhancing features, including ECOncrete armour units, tidal pools, reef streets, and reef ridges that promote ecological functionality while maintaining hydraulic stability.

At the regional scale, the SWAN spectral wave model was applied to evaluate nearshore wave conditions and design parameters along the project shoreline. A nested computational grid was generated, with offshore cell sizes of approximately 300 m refined to 50–100 m in the nearshore region. Thirty years of hourly wave data were processed to establish representative return-period and design-storm conditions for subsequent modelling stages.

During the final design phase, the Fully Nonlinear Boussinesq Wave Model (FUNWAVE) was used to analyze detailed wave transformation and structure interaction under both baseline (no-structure) and proposed (with-structure) scenarios. FUNWAVE accounts for wave-induced currents, shoaling, reflection, transmission, bottom friction, breaking, and run-up, thereby providing a robust representation of nearshore hydrodynamics. Sensitivity analyses were conducted to evaluate the effects of water-level variation and wave-approach orientation on predicted wave heights and durations along the shore.

To assess sediment dynamics, the Delft3D modelling suite was employed for simulating the interaction of tides, winds, currents, waves, and sediments. The model quantified transport

pathways, deposition, and erosion patterns induced by the breakwater system within the project area.

Finally, the near-field hydrodynamics within and around the breakwaters were resolved using the FLOW-3D computational fluid dynamics model. These simulations tested alternative reef-street and reef-ridge configurations, predicted local sediment mobility, and evaluated circulation behaviour inside the reef streets to optimize habitat connectivity and hydraulic performance.

2.6 Critical Review and Research Needs

The reviewed literature indicates a growing interest in eco-engineered and nature-inclusive coastal protection as sustainable alternatives to conventional hard infrastructure. While many studies report promising ecological outcomes and qualitative performance benefits, the hydraulic design basis for eco-engineered armour units remains comparatively underdeveloped, limiting confident application in breakwater design.

Most research on eco-friendly coastal structures has focused primarily on ecological outcomes or structural stability, often at reduced laboratory scales and under limited hydraulic conditions. Comprehensive assessments that simultaneously examine wave transmission, reflection, overtopping, and stability for eco-engineered armour units are lacking, particularly for low-crested and emergent rubble mound breakwaters. As a result, the interaction between hydraulic performance and eco-engineered designs is not yet fully understood.

Numerical modelling studies addressing eco-engineered armour units are also limited. While CFD tools have been successfully applied to conventional rubble mound breakwaters, their application to eco-engineered single-layer systems remains unexplored and unvalidated against experimental data. This gap restricts the use of numerical models as reliable research and design-support tools for eco-engineered breakwaters.

Furthermore, the absence of consolidated, performance-based design guidelines represents a significant barrier to practical implementation. Existing design frameworks and empirical formulations are primarily for conventional armour units and do not explicitly account for the geometric complexity, interlocking and porosity characteristics of eco-engineered units. As a result, practitioners lack reliable guidance to assess hydraulic performance metrics when implementing eco-friendly armour systems in breakwater design.

These limitations highlight the need for large-scale physical modelling, validated numerical simulation, and systematic design synthesis focused specifically on eco-engineered armour units. Addressing these research needs is essential to establish a reliable hydraulic design basis and to facilitate the broader implementation of eco-friendly armour systems in sustainable and climate-resilient coastal protection projects. The present thesis directly responds to these needs through integrated experimental, numerical, and design-oriented investigations.

Chapter 3. Physical Modelling of Eco-Engineered Emergent and Low-Crested Breakwaters

This chapter presents a revised preprint version of the following published article.

Sayar, S.D., Nistor, I., Baker, S., Gutiérrez, J., Rosenberg, Y. (2025). Hydraulic Performance of Low-Crested and Emergent Breakwaters with Ecologically Designed Armour Units. *Journal of Waterway, Port, Coastal, and Ocean Engineering*, American Society of Civil Engineers.

Abstract:

Eco-friendly armour units and coastal structures provide a sustainable alternative to traditional design by incorporating eco-enhancing aspects into the design process to enhance biodiversity in their vicinity. ECOncrete®'s Coastalock™ armour units feature a nature-inclusive design utilizing a bio-enhancing concrete mix, and biological surveys from a pilot deployment have already shown their positive impact in this sense. A comprehensive research program was initiated by the University of Ottawa and the Ocean, Coastal, and River Engineering Research Center of the National Research Council of Canada (NRC-OCRE), in collaboration with ECOncrete, a science-based bio-enhancing concrete technology company. Two-dimensional physical model tests of a low-crested and emergent rubble mound breakwater (RMBW), each armoured with Coastalock units, were conducted in the Large Wave Flume (LWF) of NRC-OCRE. Testing was conducted at a 1/15 scale. Both models were constructed as permeable structures with uniform 2V:3H front and back slopes and exposed to irregular waves with significant wave heights ranging between 0.08 m and 0.38 m (1.2 m and 5.7 m at prototype scale) while the wave steepness ranged between 0.03 and 0.07. This study focused on Coastalock armour unit placement, spacing, and underlayer rock size to understand their impact on hydraulic stability. The hydraulic performance of Coastalock armour units was analyzed by investigating wave transmission using existing formulas in the literature. Overall, the Coastalock armour units exhibited commendable stability against diverse wave conditions.

Keywords: Eco-enhancing design, breakwater stability, eco-friendly armour unit, Coastalock, physical model, emergent and submerged crest, rubble mound breakwater

3.1 Introduction

The concept of integrating ecological enhancements into coastal protection works has received considerable attention in recent decades. In the face of climate change and associated sea level rise, resilient, cost-effective, and sustainable coastal protection solutions are urgently needed. Additionally, it is essential to minimize the harmful effects of traditional coastal structures on the ecosystem and improve habitats in the vicinity of such structures (Chapman and Underwood, 2006). As the idea of an environmentally friendly breakwater is still in its early stages and has

gained increasing interest, several prototype breakwaters are undergoing testing to evaluate their ecological and hydraulic performance (such as Baker et al., 2018; Molenkamp, 2022).

This study endeavours to collect data on the hydraulic performance of low-crested and emergent RMBW under various wave conditions utilizing ecologically engineered armour units known as Coastalock (ECOncrete, 2021). The main objectives of this experimental modelling program were collecting information to develop guidelines for designing innovative and environmentally friendly breakwaters, which would encourage accommodating the presence of an eco-friendly habitat around such coastal structures and the retrofitting of classical breakwaters with ecological armour units. As an initial step in this research conducted to provide data on the hydraulic performance of these armour units, two-dimensional physical model tests were conducted using a low-crested and an emergent rubble mound breakwater (RMBW) armoured with Coastalock units in the Large Wave Flume at NRC-OCRE, scaled at 1/15. The study investigated the hydraulic performance of the units under a variety of wave conditions and water levels, with different wave heights, wave steepness, armour unit spacing, and underlayer rock sizes, in order to assess their impact on stability.

The structure of this paper is as follows: Section 3.2 provides a literature review and outlines the current research needs. Section 3.3 details the experimental program and setup. Section 3.4 presents the results and analysis, followed by a discussion presented in Section 3.5. Finally, Section 3.6 concludes the study, with recommendations presented in Section 3.7.

3.2 Literature Review and Research Needs

3.2.1 Eco-friendly Coastal Structures

Eco-friendly coastal structures serve not only to protect coastal regions against storms but also to enhance natural habitats in their vicinity. These structures involve the use of natural materials such as oyster reefs and brushwood (Safak et al., 2020) in combination with multi-purpose breakwaters (Manson et al., 2017), benefiting from several eco-enhancing modifications (Firth et al., 2013).

While research on the use of natural materials such as oysters and brushwood for the design of coastal structures is increasing (Allen and Webb 2011; Safak et al., 2020; Takagi et al., 2020; Morris et al., 2021; Provan et al., 2023; Provan et al. 2024), the use of coastal defence structures made using such materials is limited in regions with significant wave climate due to their lower strength and durability compared to rock and concrete.

Traditional concrete coastal structures can also be modified to allow for eco-friendly features by incorporating tide pools (as in Browne and Chapman, 2011; Evans et al., 2015; Morris et al., 2018) or micro-scale modifications such as pits, crevices, and texture roughening, thus converting them into structures that improve habitats (such as in Moschella et al., 2005; Martins et al., 2010; Borsje et al., 2011; Coombes et al., 2015; Hall et al., 2018). Multi-purpose breakwaters benefit from these environmentally friendly modified elements such as tidal pools, eco-friendly armour units, reef

ridges and reef streets (see Baker et al., 2018) to maximize ecological enhancement in addition to optimal hydraulic performance.

3.2.2. Coastalock Armour Units

The innovation of Coastalock (CL) armour units includes a biologically enhancing concrete mix, detailed surface textures and increased roughness, as well as a nature-inspired design (as shown in Figure 3-1) which, together, serve to enhance the environmental benefits of coastal structures (Gutiérrez Martínez et al., 2023). Ecologically designed Coastalock armour units support biological recruitment, create a natural carbon sink and improve water quality and biodiversity with ECOncrete's patented bio-enhancing admixture complying with industrial concrete standards (e.g. ASTM, EN, BS, AUS) (Perkol-Finkel and Sella, 2014).

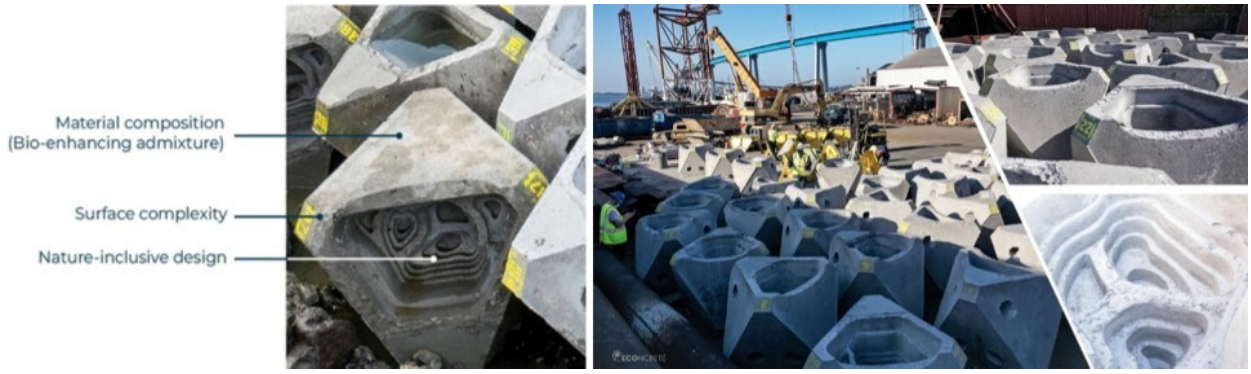

Figure 3-1. Coastalock unit features (ECOncrete, 2023)

3.2.2.1 Ecological Properties of the Armour Unit

The primary goals of the Coastalock armour unit are habitat creation and fostering biodiversity, supported by biological data collected from projects involving the ECOncrete Tide Pool Unit (Perkol-Finkel and Sella, 2015b). Coastalock units fulfill multiple ecological roles, depending on their post-placement orientation (Gutiérrez et al., 2022).

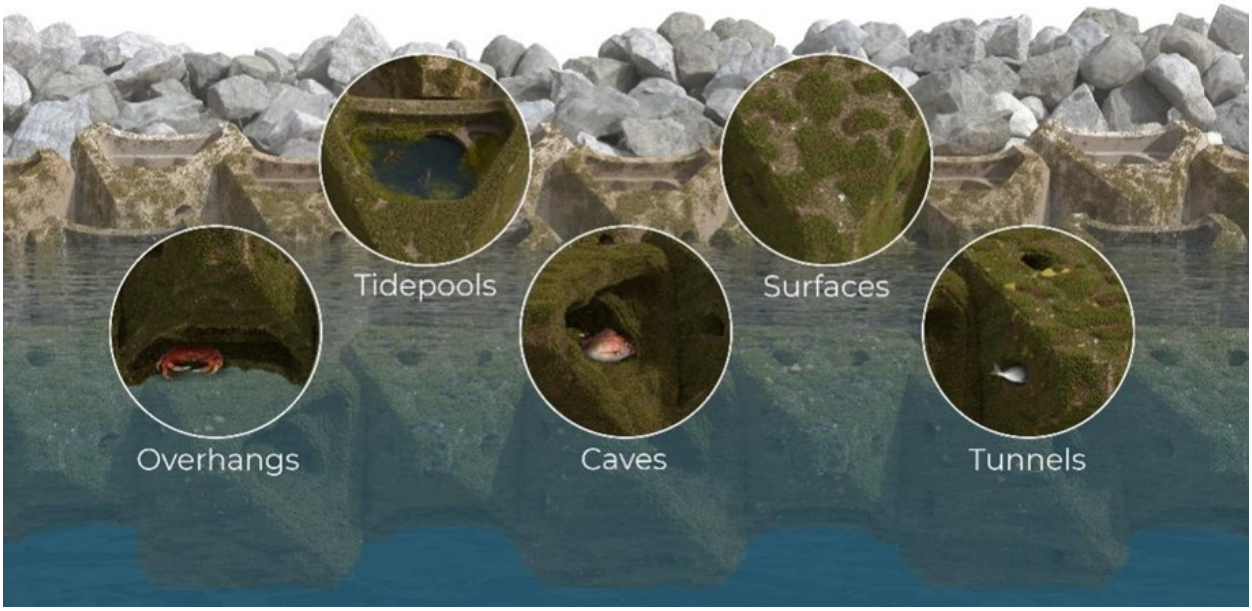

Figure 3-2.Ecological enhancement variation of Coastalock (ECOncrete, 2023)

The different sides of the Coastalock unit, as depicted in Figure 3-2, create distinct positive ecosystem features such as water-retaining tidal pools, caves, and overhangs, providing habitats essential to a variety of marine organisms (Gutiérrez et al., 2022). Additionally, to mitigate the colonization by invasive species, the unit's surface incorporates micro-textures at a scale of a few millimetres, creating micro-turbulence that assists in the settlement of larvae (Rella et al., 2023). Coastalock units, by design, are aimed at mimicking natural habitats that are missing in artificial marine infrastructures (Gutiérrez et al., 2022). These newly introduced habitats enable the recruitment of multiple species of algae and invertebrates, resulting in the establishment of a diverse marine community. Each Coastalock unit presents several ecological niches; when clustered together, they allow for higher connectivity within the ecosystem, creating a synergistic effect on biodiversity which expands further than the project boundaries.

A biological monitoring of a prototype Coastalock pilot project in the Port of San Diego (PoSD) (USA) and previous studies using ECOncrete's technology (Perkol-Finkel and Sella 2014, 2015a, 2019) have shown encouraging results for improving marine life and habitat creation around these armour units.

3.2.2.1.1 Community structure

After two years of monitoring in San Diego, the species richness of Coastalock units demonstrated a diverse community compared to the control rocks, including 15 algae species, 19 sessile invertebrates, and 11 mobile invertebrates (see Figure 3-3).

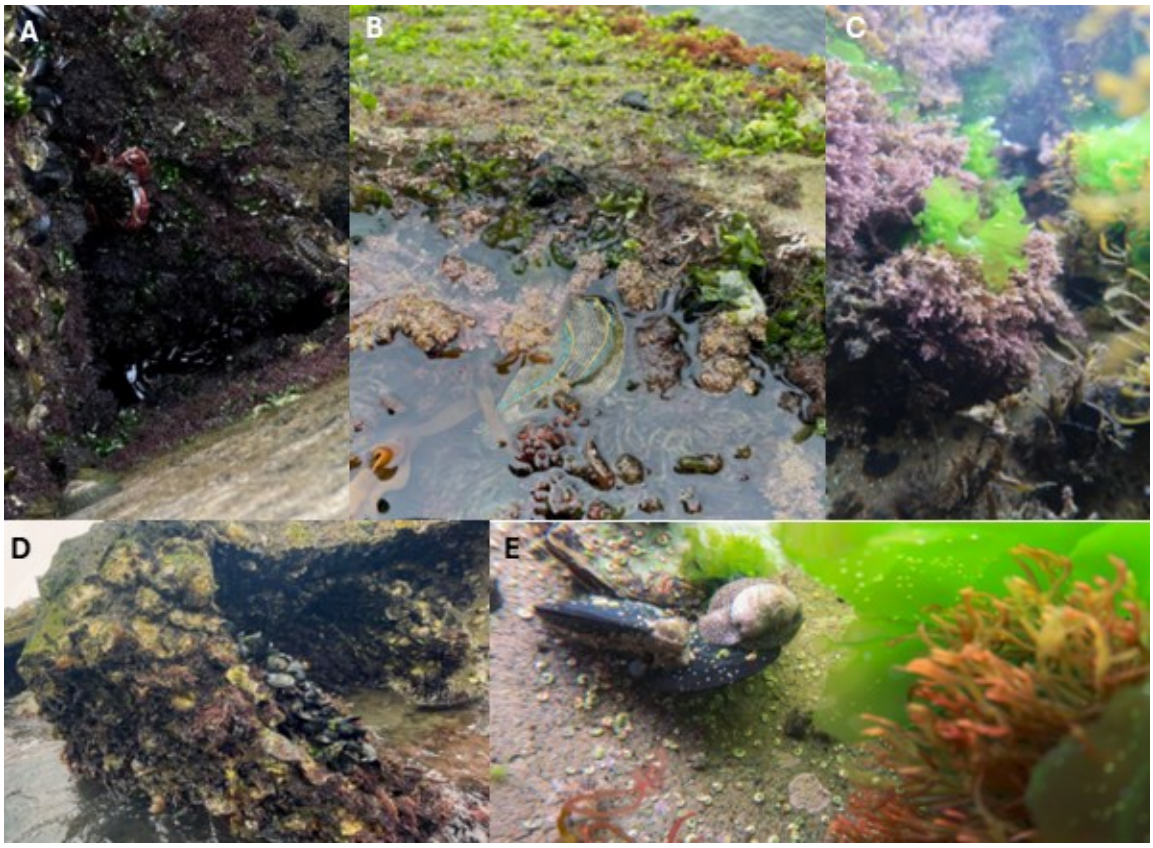

Figure 3-3. Biological development on the CL armour units 26 Months Post-Deployment (MPD); (A) Pachygrapsus crassipes crab between the Coastalock units, surrounded by Mollusks (oysters, mussels, limpets, chitons) and Algae. (B) A Navanax inermis sea slug swimming in the Coastalock cavity, inhabited by different algae species. (C) The brown algae Sargassum muticum, green algae Ulva sp., and coralline algae Corallina sp. within the Coastalock cavity. (D) A Coastalock unit covered by Bivalves (Mytilus sp., Crassostrea gigas, Ostrea lurida), different Algae species, and smaller-scaled species (barnacles and gastropods). (E) A Coastalock cavity populated by green algae Ulva sp. and red algae Amphiroa sp. Mytilus sp. bivalves, Haminoea virescens, and Spirobis sp. (ECOncrete, 2023)

After two years, the average species richness was higher on Coastalock units compared to control rocks that have been there since the construction of the structure in the 1950s. A similar trend was observed in the average biodiversity, showing an increase in counted species and an increase in covering species on the Coastalock units, as shown in Figure 3-4.

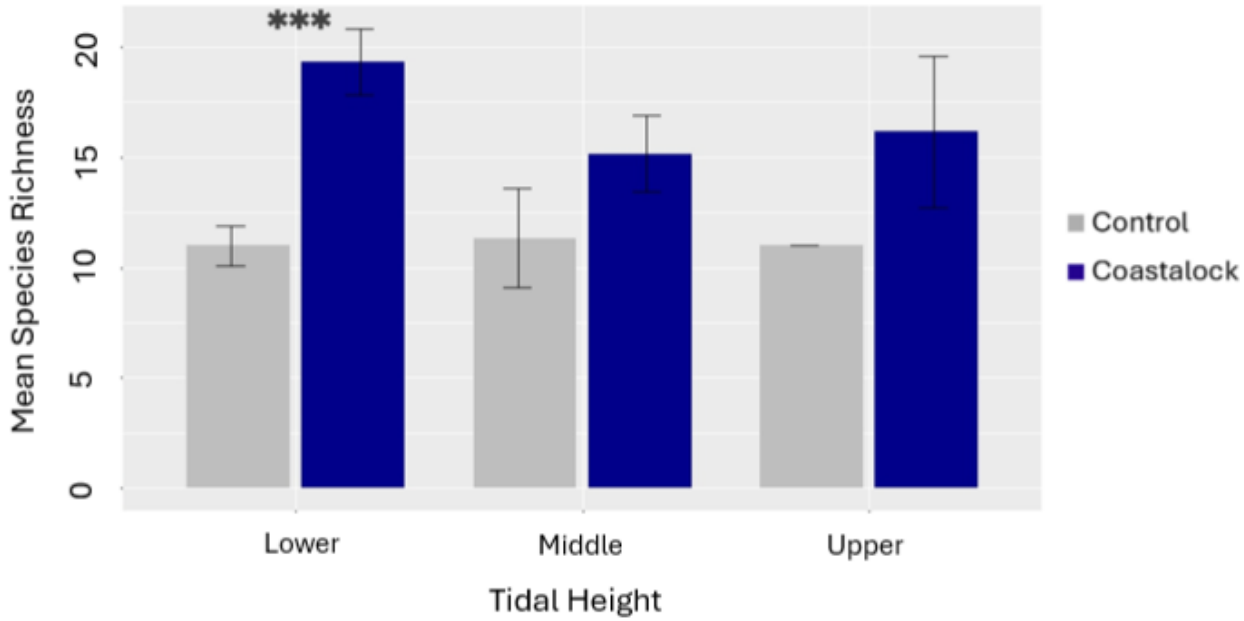

Figure 3-4. Species richness between ECOncrete CL and the control rocks, at three different tidal heights, 26 MPD. Error bars represent the standard deviation of less than 0.001 (ECOncrete, 2023)

3.2.2.1.2 Biomass analysis

The two-year post-deployment monitoring event included sampling for biogenic buildup to assess the organic and inorganic matter to compare the accumulation of calcium carbonate ($CaCO_3$) on the Coastalock units and control rocks. Results show significantly higher biomass on ECOncrete Coastalock units compared to the control rocks, both for organic and inorganic matter accumulation. Significant differences were found between Coastalock and control rocks for organic and inorganic biomass accumulation, as depicted in Table 3-1.

Table 3-1. Differences in the accumulation of organic and inorganic weight between Coastalock and control rocks

Average Accumulated Weight (gr/m^2)	**Inorganic**		**Organic**	
	Coastalock	**Control**	**Coastalock**	**Control**
Upper	1464	844	440	124
Middle	4157	3062	827	430
Lower	8338	2672	971	486
Average	4653	2193	746	346

3.3.2.2.2 Structural Properties and Placement of the Armour Unit

The octahedral hollow block shape of Coastalock allows for interlocking with surrounding units, stability, and easy installation. The units are suitable for installation on steep slopes (e.g., 2V:3H and 3V:4H) to improve their interlocking capacity and stability. The pilot project located near the San Diego International Airport involved the installation of seventy-four Coastalock units, each weighing 3.4 tons, with 0% armour unit spacing (indicating the horizontal placement density of the armour units), at two sheltered locations of the rip-rap armouring surrounding Harbour Island between February and March 2021. In the configuration of armour units referred to as "San Diego configuration", the lower units (typically positioned below mean or mean-low water levels) are oriented cavity-sideways, while the higher units are oriented cavity-forwards, resembling tide pools, as illustrated in Figure 3-5.

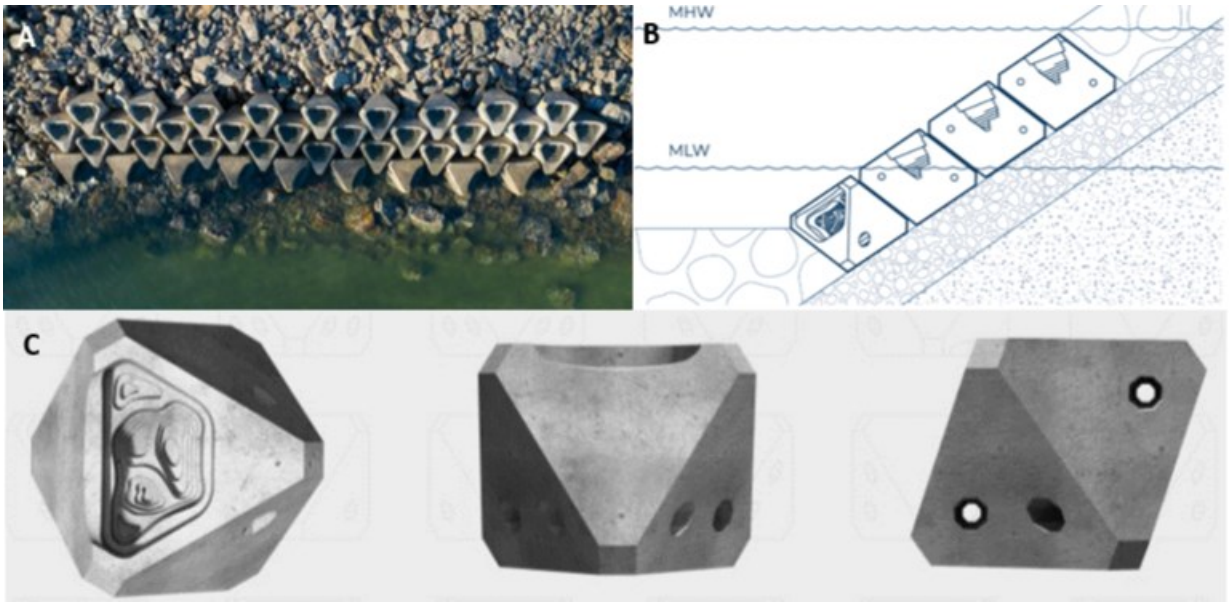

Figure 3-5. Coastalock armour units deployed at PoSD (A), sketch of placement of Coastalock units on revetment/breakwater slopes (B), and Coastalock armour unit drawing (C) (ECOncrete, 2021)

3.2.2.3 Hydraulic Stability of the Armour Unit

Previous studies on Coastalock armour units included tests on a revetment slope with an impermeable core at a smaller scale (Molenkamp, 2022) and tests with clusters of Coastalock units placed on an armour layer revetment (UNSW, 2023). Notably, studies, such as Reedijk et al. (2008), have indicated that the presence of an impermeable core can significantly influence the damage and failure mechanisms exhibited by the armour units. Consequently, given the innovative design and approach of the Coastalock armour units, there is limited knowledge in the literature regarding the hydraulic performance of Coastalock armour units, which has underlined the need for testing the units on low-crested and emergent RMBW with a permeable core.

3.3. Experimental Program

3.3.1 Test Facility and Test Setup

Physical modelling experiments were conducted in the Large Wave Flume (LWF) at the Ocean, Coastal and River Engineering Research Center of the National Research Council of Canada (NRC-OCRE) between March and August 2023. The flume, as shown in Figures 3-6 and 3-7, is 97.0 m in length, 2.0 m in width, and 2.9 m in height. The LWF features a sub-floor current-generation system (which was not used in the present study). The model structures were built in the middle section of the LWF, where the model could be observed through large side-viewing windows. A model foreshore bathymetry was designed and constructed on top of the sub-floor to simulate realistic wave transformation for incoming waves, as shown in Figure 3-7. The foreshore included a 1:16 slope further offshore and a gentle 1:100 slope leading up to the model structure. A steeper 1:8 slope was incorporated in the lee of the model structure.

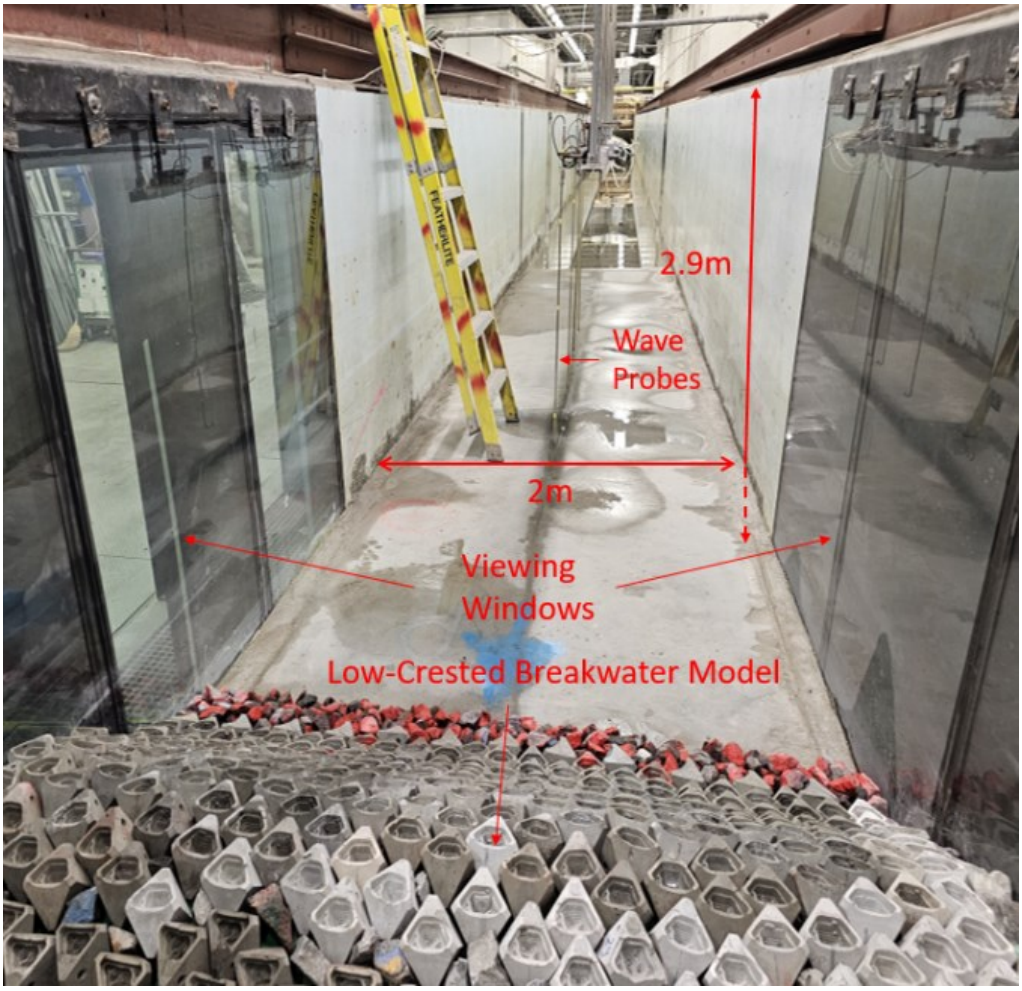

Figure 3-6. Breakwater model built in the NRC-OCRE's LWF

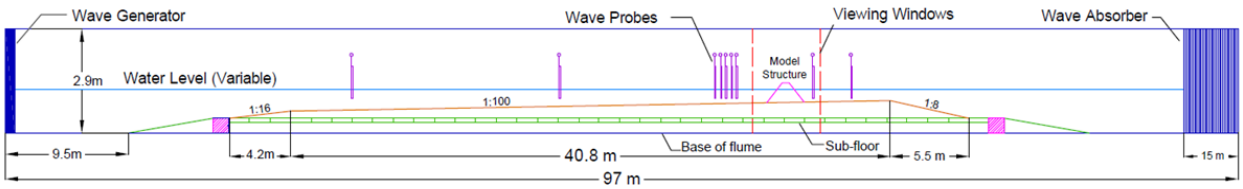

Figure 3-7. Sketch of the experimental setup in the NRC-OCRE's LWF (Scale 1V:3H)

A piston-type wave generator was used to generate irregular waves, while a series of porous-type vertical wave absorbers were positioned at the downstream end of the flume to absorb incoming waves (featuring reflection coefficients below 5% over a wide range of wave conditions). The JONSWAP spectrum was used to define sea states with a peak enhancement factor (γ) of 3.3.

Selection of an appropriate model scale involved consideration of several key factors, including the flume dimensions, capabilities of the wave generator, and practicalities relating to armour unit production. Based on these considerations, the model scale was set as 1/15. This relatively large scale ensured that wave-driven flows around the model armour units remained rough-turbulent at all times, as in nature. Preserving rough-turbulent flow in the model was essential to minimizing scale effects and preserving the realism of the wave–structure interactions in the physical model.

3.3.2 Model Characteristics

Two breakwater models were designed to assess the hydraulic performance of the Coastalock armour units under different wave conditions. The present experiments are the first Coastalock armour unit tests on two different traditional breakwater models (low-crested and emergent) having their front slope, crest, and back slope armoured with Coastalock units. In Test Series 3, 4 and 5, the crest was armoured half with rocks and half with Coastalock units (see Figure 3-9).

3.3.2.1 Low-crested Breakwater Model

The first set of tests involved the design and evaluation of a low-crested breakwater model. The objective was to evaluate the hydraulic performance of a low-crested breakwater with an armour layer of Coastalock units under several sets of irregular waves with five different water levels, with the breakwater crest being either emergent or submerged. Model components included a permeable core material, an underlayer stone, a toe armour stone, and the integration of Coastalock armour units as a concrete single armour layer. The single armour layer configuration involved placing 13 staggered rows of units on each of the front and back slopes, with five rows of units positioned in a horizontal line along the crest, as shown in the sketch and the picture of the constructed breakwater model in Figure 3-8. All the Coastalock units (front slope, crest, and back slope) had the same height of 8.33cm and side length of 7.7cm.

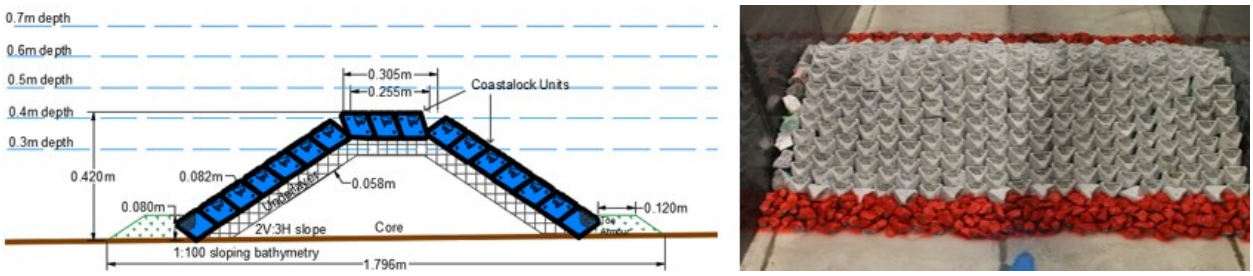

Figure 3-8. Low-crested breakwater model cross-section and the physical model (front slope view) in Test Series 1

The low-crested breakwater model cross-section was designed considering the practical capabilities of the LWF. The model height of 0.42 m enabled the investigation of the hydraulic performance of the model under a total of five different relative freeboard conditions: three submerged and two (emergent) low-crested cases.

The typical geometrical parameters of the low-crested breakwater model are presented in Table 3-2. Model dimensions and shape were kept constant throughout all test series, while the armour unit spacing and underlayer rock size were varied between each test series. Two different underlayer rock sizes and armour unit spacing were tested for the low-crested model to observe the effect of underlayer size on the hydraulic performance of the model (see Tables 3-4 and 3-5). Each structure was tested under a range of significant wave heights and wave steepness with the San Diego orientation (refer to Section 3.2.2.2), which was used as the sole armour unit orientation on the same 2V:3H front and back slope for all tests.

Table 3-2. Typical geometrical parameters for the low-crested breakwater model

Armour unit orientation	San Diego
Front and rear breakwater slope	2V:3H
Model crest height	0.42 m
Model crest width	0.30 m

3.3.2.2 Emergent rubble mound breakwater model

The hydraulic performance of an emergent RMBW with an armour layer of Coastalock units was similarly evaluated under a wide range of irregular wave conditions. The breakwater cross-section was tested as an emergent structure under five water level conditions, as shown in Figure 3-9. The model consisted of the same components as the low-crested model; however, it also incorporated a crest type that included Coastalock units and rocks for each transversal half-width of the model (as shown in Figure 3-9).

The model comprised five staggered rows of units placed on the crest, 31 staggered rows of units placed along the front slope and 23 staggered rows placed along the back slope, as illustrated in Figure 3-9.

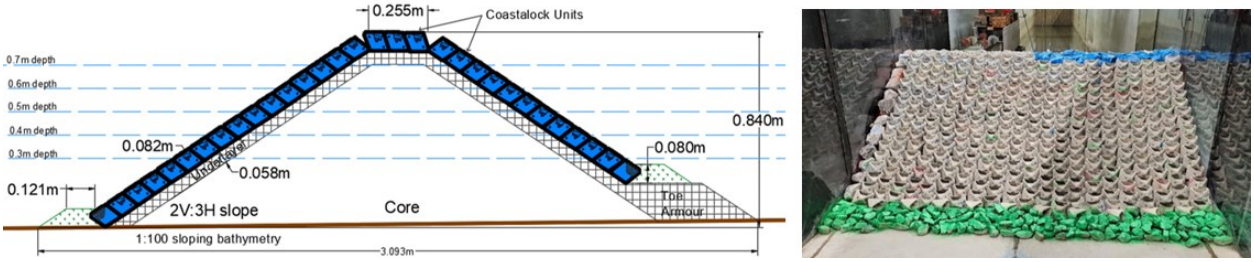

Figure 3-9. Emergent RMBW cross-section and the physical model in Test Series 5

The typical geometrical parameters of the emergent RMBW model are shown in Table 3-3, where dimensions, spacing and orientation of the armour units, as well as the crest type of the model, were kept constant throughout the tests. The rear slope design was modified between TS4 and TS5, which is explained under section 3.4.1.

Table 3-3. Typical geometrical parameters of the model used for the emergent RMBW model

Orientation	San Diego
Armour unit spacing	10%
Front and rear slope	2V:3H
Crest height	0.84 m
Crest width	0.30 m

The breakwater models were designed and built using different-sized rocks and Coastalock armour units as presented in Table 3-4. The Coastalock armour units installed in the PoSD and used in the physical model are the same size at the prototype scale: 3,415 kg (1,012 g at model scale) with around 2400 kg/m^3 density. Underlayer, core, and toe rock sizes were designed and built considering the size and weight of the armour unit size to provide sufficient stability for the armour units. Two different underlayer rock sizes were tested for the low-crested model to observe the effect of underlayer size on the hydraulic performance of the model.

Table 3-4. Grading and nominal diameters (Dn_{50}) of the rocks used for low-crested and emergent RMBW

Layer type	Low-crested RMBW (Model Scale, g)	Emergent RMBW (Model Scale, g)	Low-crested RMBW (Prototype Scale, kg)	Emergent RMBW (Prototype Scale, kg)
Coastalock armour layer	1,012 g 0.073 m	1,012 g 0.073 m	3,415 kg 1.095 m	3,415 1.095 m
Underlayer rocks grading	50-100 g / 25-60 g 0.026 m / 0.024 m	25-60 g 0.024 m	168–338 kg /85–203 kg 0.39 m / 0.36 m	85–203 kg 0.36 m
Core rocks grading	1-10 g 0.003 m	1-10 g 0.003 m	3.4-34 kg 0.045 m	3.4-34 kg 0.045 m
Toe armour rocks grading	100-200 g 0.038 m	100-200 g 0.038 m	340-680 kg 0.57 m	340-680 kg 0.57 m

3.3.3 Armour Unit Production

In San Diego, 3.4-tonne Coastalocks were locally manufactured as precast mass concrete with supplied Coastalock moulds and patented bio-enhancing admixture. Production took place at a designated yard in the port area of Harbor Island. In total, 74 prototype units of 3.4 tons each were produced and then transported and installed by barge.

Four model-scaled Coastalock units were 3D-printed at NRC-OCRE. The 3D-printed Coastalock units were placed in individual wooden boxes. Silicone with a shore hardness of 20A was mixed and poured into the boxes as shown in Figure 3-10. Because the Coastalock units have detailed surfaces, the moulds were vibrated to prevent air bubble formation. A total of 21 silicone moulds were manufactured using this same process.

Each day for a period of 72 days, model armour units were then cast in concrete using the silicone moulds. Lead shot was evenly distributed during production to achieve the desired unit weight at model scale and satisfy the density scaling conditions of mass concrete Coastalock armour units in PoSD. Following 24 hours of concrete curing, the wooden boxes were opened, and the concrete armour units were removed from the silicone by cutting the silicone mould into two parts. The silicone mould's design prompted the formation of neck stems on the upper surface of the concrete units, as depicted in Figure 3-10(C). This configuration facilitated the pouring of concrete into the moulds. Subsequently, these stems were removed to attain the ultimate form of the units. A total of 634 model concrete units were cast with an average weight of 1,012 g, resulting in less than 1% error compared to the target weight of 1,007 g.

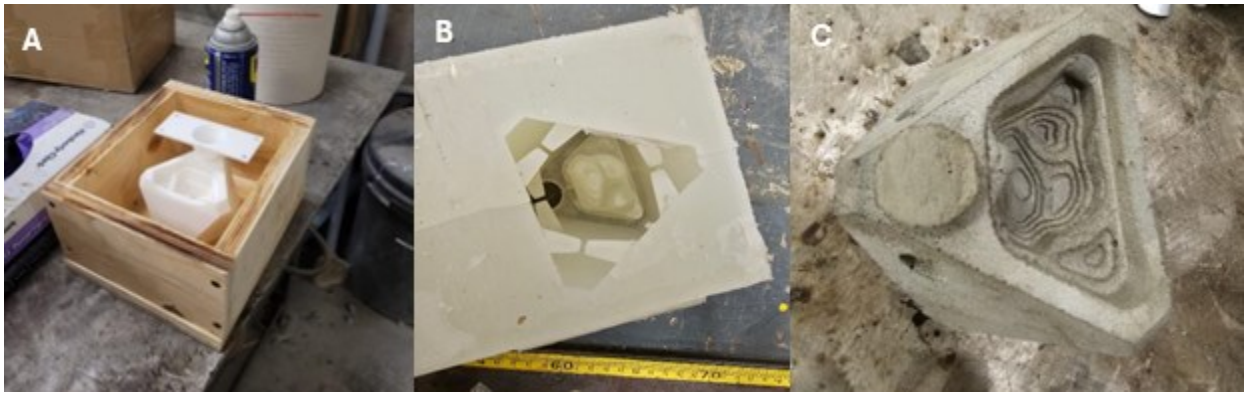

Figure 3-10. (A) 3D-printed Coastalock armour unit, (B) silicone mould and (C) cast concrete Coastalock armour unit (the neck stem shown in (C) was later removed to match the CL design)

3.3.4 Instrumentation and Measurement Techniques

Nine capacitance-wire wave gauges were used to measure the time-history of the water free surface elevation during the tests. The wave gauges were calibrated before starting the tests, and each test series was followed by a calibration check. Wave probes were placed at specific locations in the LWF as shown in Figure 3-7. Two deep-water probes were placed to measure the time-history of the wave train in the section with deeper water depth and negligible bathymetry effect, while five wave probes were placed close together in the front of the model as a wave reflection array to measure both incoming and reflected waves, as presented in Figure 3-7 and Figure 3-11(A). Two probes were also positioned behind the structure for wave transmission measurements.

NRC-OCRE's GEDAP (Miles, 1990, 1997) software is a general-purpose software system for the synthesis, analysis, and management of laboratory data that also includes modules for real-time experiment control and data acquisition functions. Standard GEDAP time-domain and frequency-domain analysis algorithms were applied to analyze in detail the wave conditions measured in the model. The reflection analysis was performed using the Mansard & Funke (1980) measurement of incident and reflected spectra using a least squares method.

The movement of armour units was recorded and evaluated during the tests using a camera-based damage assessment system consisting of four remotely controlled digital cameras. Front and rear cameras (Sony SNC-ER580, see Figure 3-11) were used to capture still photos of the model structure before and after each test, while Bosch Dinion IP 5000i IR video cameras continuously recorded one oblique overhead view and one side view during the tests. These devices delivered images and videos at a resolution of 1920x1280 pixels and a frame rate of 30 frames per second. Using these images, a "flicker" analysis was performed by processing rapid flickering between two photos to detect the differences between them.

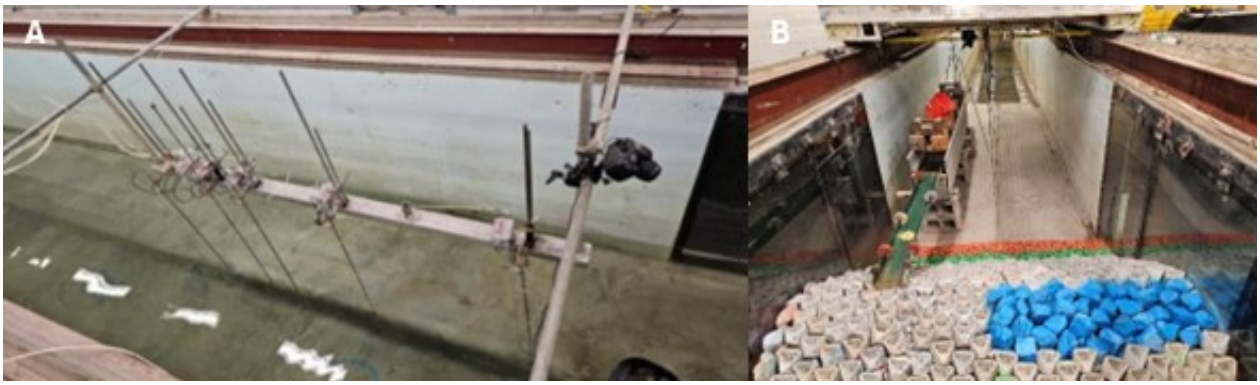

Figure 3-11. (A) Wave probes array and (B) overtopping catchment system in the LWF

3.3.5 Test Program

As a part of this study, 110 individual test runs were performed in five distinct test series (TS). Details of the test parameters are presented in Table 3-5. Each sea state was run for ~1000 waves, while each test series consisted of a sequence of progressively larger sea states (wave heights) combined with increasing water depths. Each test series was terminated after generating the largest possible waves for the given test conditions or after the armour layer failed during a particular test run.

In the first three test series, a low-crested breakwater model was tested over a water depth range of 0.3 m to 0.7 m (yielding both submerged and emergent states). In the final two test series, the emergent RMBW model was tested over the same range of water levels. Wave steepness ranged from 0.030 to 0.055 for the low-crested breakwater tests and between 0.030 to 0.065 for the emergent RMBW model (as shown in Table 3-5). The highest two wave tests of each test series were also conducted with the same significant wave heights but a longer peak wave period. While armour unit spacing and underlayer rock size were varied during the low-crested breakwater tests, typical geometrical parameters consisting of these parameters were unchanged during the emergent RMBW tests (see Table 3-2 and Table 3-3).

Table 3-5. Characteristics of the test series

Test Series ID	Breakwater Type	Number of Tests	Crest Height (m)	Water Depth Range (m)	Significant Wave Height (m)	Wave Steepness Range	Armour Unit Spacing (%)	Underlayer Rock Weight (g)
TS1	Low crested	25	0.42	0.3-0.7	0.08-0.12-0.16-0.20-0.26-0.32-0.38-0.44	0.030-0.055	10	50-100
TS2	Low crested	25	0.42	0.3-0.7	0.08-0.12-0.16-0.20-0.26-0.32-0.38-0.44	0.030-0.055	0	50-100
TS3	Low crested	25	0.42	0.3-0.7	0.08-0.12-0.16-0.20 - 0.26-0.32-0.38-0.44	0.030-0.055	10	25-60
TS4	Emergent RMBW	17	0.84	0.3-0.5	0.08-0.12-0.16-0.20-0.24	0.030-0.045	10	25-60
TS5	Emergent RMBW	18	0.84	0.4-0.7	0.20-0.26-0.32-0.38	0.033-0.065	10	25-60

3.4. Test Results and Analysis

3.4.1 Stability Assessment and Failure Mechanism

The Coastalock armour unit is scalable based on wave and boundary conditions. The size of the underlayer varies with the Coastalock size, like other concrete armour units. The mass of the underlayer should fall within the range of the Coastalock unit mass. Depending on project conditions, such as wave action or quarry production, a finer or coarser underlayer or various armour unit spacing may be preferred. Therefore, the Coastalock unit spacing underwent adjustments between Test Series 1 and 2 for the low-crested breakwater. Although no units were extracted during either series, it was observed that the 0% armour unit spacing in Test Series 2 resulted in a somewhat diminished occurrence of rocking units. Construction posed challenges in both instances, attributed to the relatively large size of the underlayer, occasionally causing units to be perched on a single high point of the layer below. Consequently, the underlayer size was reduced in Test Series 3, enhancing the Coastalock placement process and concurrently reducing the number of rocking units compared to Test Series 1 with the same unit spacing, while remaining hydraulically similar in terms of wave transmission.

The proportion of rocking units for all test series was greater near the crest (as opposed to near the toe). For Test Series 3, half of the structure (across the width of the flume) was built with armour stones on the crest. Comparing the two sections, the armour stone was slightly more stable than the crest Coastalock units. In summary, the structural configuration during Test Series 3 (10% spacing with smaller filter stone) demonstrated optimal performance, with no units extracted from either the seaward or leeward slopes nor from the crest.

Overall, a stability number (N_s) of 4.42 was calculated for the low-crested breakwater tests, based on the maximum wave height of 0.44m (6.6 m in prototype scale) when no failures (i.e. loss of armour units) were observed for the low-crested breakwater.

During test series 4 (emergent RMBW), wave overtopping rates increased significantly as the structure was subjected to larger wave heights and deeper water depths, as expected. These large overtopping events led to substantial plunging waves over the crest of the structure and downrush onto the lee side slope. However, the cross-sectional design assessed during Test Series 4 was deemed to be insufficient to withstand these plunging waves. In the test with a water depth of 50 cm (7.5m in prototype scale), significant wave height of 24 cm (3.6m in prototype scale), and peak wave period of 3.8 s (14.7 s in prototype scale), a complete failure of the leeward armour layer occurred subsequent to the severe damages at rock toe that induced the dislodgement of the bottom row of Coastalock units. This dislodgment resulted in the lack of support for the upper rows, highlighting a critical deficiency in toe support for the armour units on the leeward side.

The cross-sectional configuration evaluated during Test Series 5 demonstrated greater resilience compared to that of Test Series 4, enduring beyond the failure point observed in the latter. In the test with a water depth of 60 cm (9 m in prototype scale), significant wave height of 26 cm (3.9 m in prototype scale), and peak wave period of 3.9 s (15.1 s in prototype scale), although several leeward toe armour stones were displaced, and some settlement of leeward Coastalock units occurred, no substantial gaps emerged. Remarkably, the leeward armour layer remained stable throughout the entirety of Test Series 5.

Like the low-crested breakwater, the proportion of rocking armour units was greater near and at the crest (as opposed to near the toe) for the emergent breakwater. A similar rocking behaviour was also previously observed during the physical experiments of low-crested breakwaters with single-layer armour units conducted by Muttray et al. (2012).

Failure of the armour layer occurred during the test with a water depth of 70 cm (10.5 m in prototype scale), significant wave height of 32 cm (4.8 m in prototype scale), and peak wave period of 3.2 s (12.4 s in prototype scale) when several of the Coastalock units at the crest were displaced, exposing the filter layer beneath as shown in Figure 3-12. Notably, instability among the Coastalock units on the front slope was observed only after the failure of the crest. Moreover, the section of the flume featuring conventional rock armour on the crest exhibited slightly worse performance during the same test, with nearly all the crest armour displaced and significant scouring of the exposed filter layer beneath, as shown in Figure 3-12. A stability number of 3.21 for the armour unit failure was calculated for the emergent RMBW, considering the significant wave height at the time of failure (0.32m in model scale corresponding to 4.8m in prototype scale).

Figure 3-12. Final condition of emergent RMBW after Test Series 5

3.4.2 Wave Transmission

Wave transmission was systematically measured in all tests to observe the wave transmission characteristics of both low-crested and emergent RMBW models. As expected, the low-crested model exhibited higher wave transmission coefficient (K_t, the ratio of transmitted waves to incoming waves) values when the relative freeboard (R_c/H_{m0}, the ratio of crest height to the significant wave height) values were greater since the wave-breaking efficiency of the low-crested model decreases as the water level increases, as shown in Figure 3-13 (where the negative relative freeboard values represent the emergent model cases and the positive relative freeboard values represent the submerged model cases for different water levels). For the low-crested breakwater, the wave transmission results vary in the range of 5% to 58% for emergent cases, and 63% to 92% for submerged cases (as shown in Figure 3-13). On the other hand, wave transmission varied between 3% and 30% for the emergent RMBW (as shown in Figure 3-14).

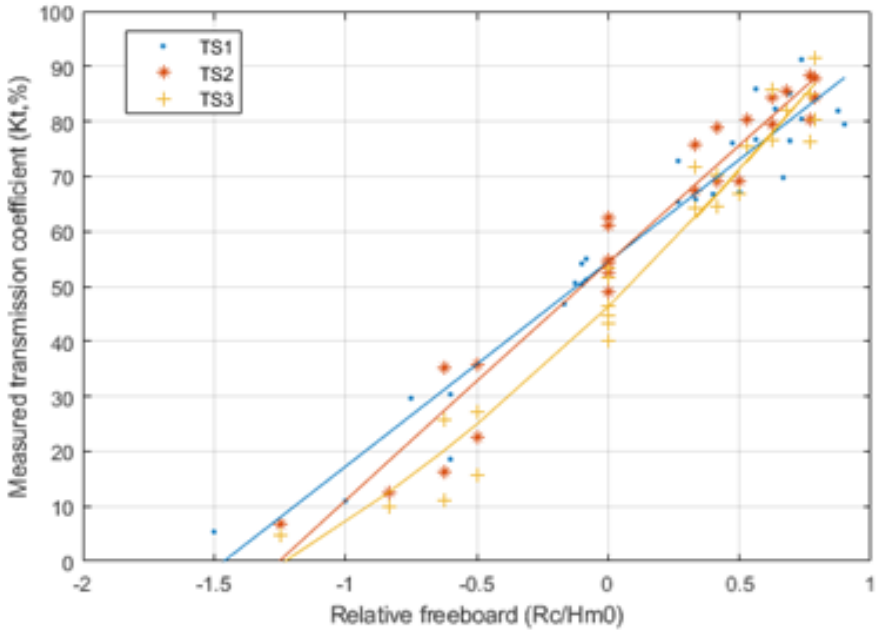

Figure 3-13.Measured wave transmission coefficients against relative freeboard for low-crested breakwater model (TS: Test Series)

The emergent RMBW underwent testing with a broad spectrum of relative freeboard levels, ranging from 0.4 to 6.8. Figure 3-14 highlights a decreasing trend in wave transmission with increasing relative freeboard levels when the maximum wave transmission value achieved during these tests was 36%. While relative freeboard levels exceeded the value of 2, the transmission coefficient was consistently less than 5%.

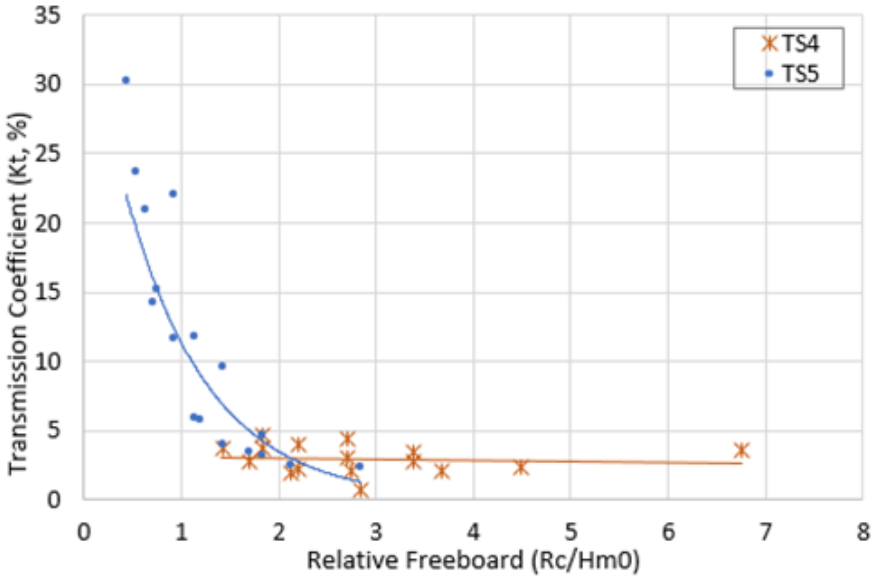

Figure 3-14. Measured wave transmission coefficients against relative freeboard for emergent RMBW model (TS: Test Series)

The wave transmission coefficient results for the low-crested breakwater model were examined by comparing various wave transmission formulas for rubble mound breakwaters from the literature. The selection of these formulas was based on their range of validity for the tested models and wave conditions. Notably, the formula proposed by Van der Meer and Daemen (1994) establishes a connection between the crest height and the nominal diameter of the armour unit and incorporates the crest width.

$$K_t = (0.031\frac{H_{m0}}{D_{n50}} - 0.024)\frac{R_c}{D_{n50}} - 5.42\, s_{op} + 0.0323\frac{H_{m0}}{D_{n50}} - 0.0017(\frac{B_c}{D_{n50}})^{1.84} + 0.51 \qquad \text{Equation 3-1}$$

where H_{m0} represents significant wave height, R_c is crest height, D_{n50} is the nominal diameter of the armour unit, s_{op} is wave steepness, and B_c is the crest width. The formula is applicable for both submerged and emergent structures, specifically for conditions where $1 < H_{m0}/D_{n50} < 6$, $0.01 < s_{op} < 0.05$, and $0.75 > K_t > 0.075$.

The formula introduced by D'Angremond et al. (1996) for both permeable and impermeable structures is used as a second comparison:

$$K_t = -0.4\frac{R_c}{H_{m0}} + C(\frac{B_c}{H_{m0}})^{-0.31}[1 - exp(-0.5\xi op)] \qquad \text{Equation 3-2}$$

where the parameter ξ_{op}, denoting the surf-similarity parameter, relies on H_{m0} (significant wave height) and the peak wave period T_p of incoming waves ($\xi_{op} = tan\alpha/s_{op}^{0.5}$). For permeable structures, the coefficient c is set as 0.8, while for impermeable structures, it is 0.64. The validity range of the formula is the transmission coefficient values of a minimum of 0.075 and a maximum value of 0.8.

A recent formula for wave transmission has been proposed by Van Gent et al. (2023), in which crest height and crest width are non-dimensionally expressed by dividing them by the wavelength ($L_{m-1,0}$). The formula includes different coefficients (c_1, c_2, c_3, c_4, c_5) for impermeable, permeable, and perforated (with screen or perforated screen) structures.

$$K_t = c_1 tanh\left[-(\frac{R_c}{H_{m0}} + c_2(\frac{B_c}{L_{m-1,0}})^{c_3} + c_4)\right] + c_5 \qquad \text{Equation 3-3}$$

The formula proposed by Van Gent et al. (2023) demonstrated the best correlation exhibiting a 3.2% average error value. In comparison, the formulas by Van der Meer and Daemen (1994) and D'Angremond et al. (1996) also provided satisfactory results, with average error values of 22.7% and 12.5%, respectively. The calculated transmission coefficient values, experimental results, and their deviation from the diagonal axis for each formula are depicted in Figure 3-15. Notably, although all three formulas resulted in more accurate outputs for wave transmission data within the range of 60% to 80%, the Van Gent et al. (2023) formula displayed a maximum error of 7% across all data points.

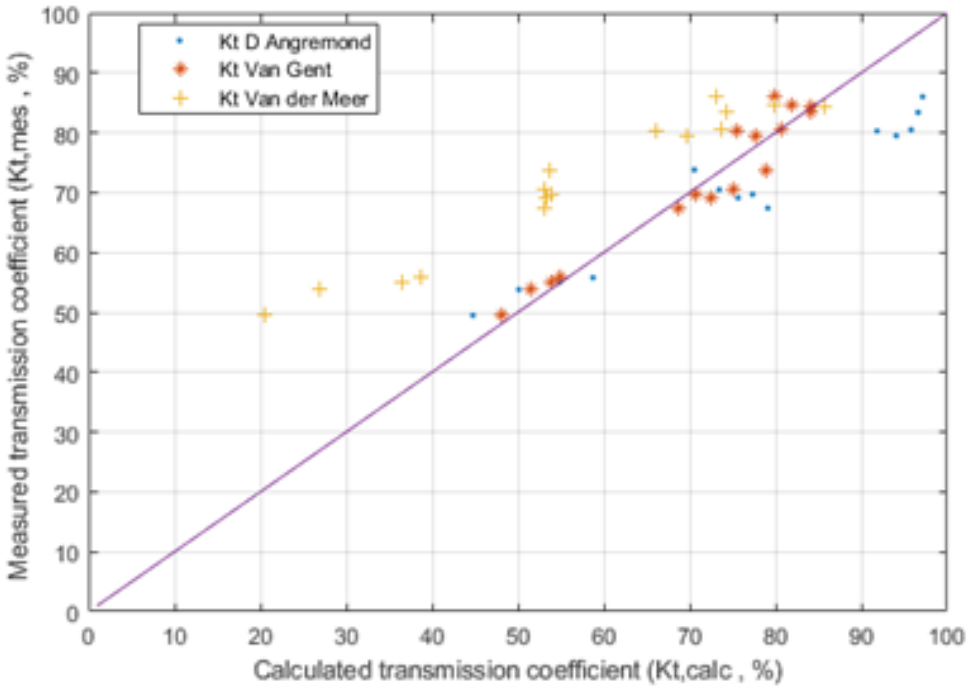

Figure 3-15. Measured and calculated wave transmission coefficient results for low-crested breakwater

3.5 Discussion

3.5.1 The Effect of Armour Unit Spacing and Underlayer Rock Size on Wave Transmission

The low-crested breakwater model underwent testing with three distinct configurations of armour unit spacing and underlayer rock sizes. The testing program of the low-crested breakwater aimed to assess the impact of 0% and 10% armour unit spacing, along with varying underlayer rock sizes (25-60 and 50-100 g), on the hydraulic performance of the armour unit, as detailed in Table 3-6.

Although the differences were minor for wave transmission coefficient results for the submerged cases of low-crested breakwater (refer to Figure 3-13), the configuration of TS3 (10% armour unit spacing and 25-60 g underlayer rock size) demonstrated slightly superior overall performance to reduce the height of incoming waves by resulting in lower wave transmission coefficient values compared to the TS1 (10% armour unit spacing and 50-100 g underlayer rock size) and TS2 (0% armour unit spacing and 50-100 g underlayer rock size).

When the results for only the emergent case of the low-crested model in Figure 3-13 were evaluated, wave transmission coefficients for TS3 were lower than TS2 and TS1, similar to the submerged cases of low-crested breakwater wave transmission results. Therefore, it is concluded that the use of finer rocks for the underlayer led to lower wave transmission coefficient results.

Furthermore, considering both cases, when the TS3 configuration reached the lowest average wave transmission coefficient results (57.5%), the TS2 configuration with 0% spacing of armour units exhibited a lower average wave transmission coefficient (59.7%) than the TS1 configuration (63.3%) with a 10% spacing of armour units. Considering the same underlayer of TS1 and TS2 configurations, this observation suggests that the 0% armour unit spacing was also more effective in reducing the height of transmitted waves when compared to the configuration of TS2 with 10% armour unit spacing.

Table 3-6. Varying parameters and average wave transmission coefficient for the low-crested breakwater

Low-Crested Model	Armour Unit Spacing (%)	Underlayer Rock Weight (g)	Average Wave Transmission Coefficient, Kt (%)
Test Series 1	10	50-100 (168–338 kg in prototype scale)	63.3
Test Series 2	0	50-100 (168–338 kg in prototype scale)	59.7
Test Series 3	10	25-60 (85–203 kg in prototype scale)	57.5

3.5.2 Hydraulic Stability of Coastalock Armour Units

The stability analysis of the low-crested breakwater test results indicated that the armour units positioned at the upper section of the front slope (i.e., at the intersection between the front slope and the crest) were susceptible to rocking due to the lack of interlocking of those armour units. Additionally, it was identified that the presence of larger underlayer rocks resulted in sub-optimal placement of the armour units and consequently increased rocking. Nevertheless, the low-crested model exhibited commendable overall hydraulic stability when subjected to varied wave conditions. Furthermore, no occurrences of armour unit extraction or failure were observed throughout the low-crested model tests (TS1 – TS3).

The tests conducted on the emergent RMBW model (TS4 – TS5) revealed several insights regarding the hydraulic stability of Coastalock armour units. Similar to the observations in the low-crested model, the upper part of the front slope (specifically, the transition zone between the front slope and the crest) and the crest itself were susceptible to rocking units due to reduced interlocking. Therefore, it was concluded that incorporating larger or modified armour units or utilizing rock armour on the crest could be advantageous in mitigating the occurrence of rocking units.

The design of the toe was identified as critical, given the regular pattern single-layer arrangement of the armour units. Additionally, it was noted that displacement of the rear side toe armour could result in the sliding of an entire column of armour units along the slope. Despite significant overtopping recorded during high water level tests, the back slope units demonstrated notable

stability. While two failures occurred during the most challenging wave tests (with one attributed to the failure of the rock toe on the backside slope and the other one attributed to the failure of the units placed on the crest), the overall performance of Coastalock armour units on the emergent RMBW model demonstrated satisfactory results.

3.5.3 Challenges and Limitations

The implementation of Coastalock armour units, characterized by a distinctive design featuring void spaces, holes, and a complex surface, presented a series of challenges to produce high-quality concrete armour model units. First, methods for their production were assessed, leading to the selection of silicone moulds – a less conventional choice in armour unit production but deemed the most suitable. This process involved the meticulous creation and refinement of 3D armour units, application of lubrication prior to silicone mould production, and subsequent removal of each mould. Despite employing silicone with a 20A shore hardness, a few moulds experienced damage during extraction of the 3D printed armour units or later from the concrete armour units due to wear from multiple uses. The occurrence of air bubbles in recessed surfaces and holes during the initial stages resulted in the exclusion of certain concrete armour units due to imperfections. Notably, the weight of the armour units emerged as a critical criterion for usability, requiring careful consideration of concrete density and the incorporation of lead shots. Accordingly, a subset of the produced armour units exceeding a weight tolerance of 5% was excluded from experimentation.

While scaling the experiments at 1/15 ensured rough-turbulent wave-driven flows around the model, it also necessitated the construction of breakwater models utilizing over 1,000 kg of rock (at model scale) for the core and underlayer. This complex construction process required significant labour, overhead cranes, and heavy machinery.

3.6 Conclusions

This comprehensive experimental program focused on assessing the Coastalock armour unit spacing and underlayer rock size on their hydraulic stability, aiming to identify optimal design parameters and breakwater characteristics. The hydraulic performance of Coastalock armour units was further assessed by examining wave transmission results in low-crested and emergent RMBW models. The results of this experimental program provide insights to the coastal engineering community, meeting the increasing interest in the development of environmentally friendly coastal structures. The main findings of this study are presented below:

The finer underlayer rock grading resulted in lower wave transmission coefficients for the low-crested breakwater model. As well, the finer underlayer facilitated the placement of the armour units and reduced the rocking of the armour units.

The rock toe design and stability are shown to be important for the stability of the Coastalock single armour layer. For the low-crested model, the effectiveness of reducing transmitted wave

height was higher in configurations with a 0% armour unit spacing compared to those with 10% spacing. The Coastalock armour units on the slope protection on a permeable core, both for the low-crested model and the emergent model, showed satisfactory hydraulic stability under the test conditions of the study.

The majority of rocking armour units were observed at the transition zone between the front slope and the crest for both models, suggesting that improved stability might be obtained by using larger armour rocks or armour units on the crest.

Concurrently, a biological performance assessment of these armour units, as outlined by Rella et al. (2024), has been completed in the Port of San Diego (USA) and is presently underway for Coastalock armour units installed in the Port of Vigo (Spain).

3.7 Recommendations

In light of the experimental results and the objectives of the current study, several key recommendations are proposed to further advance the understanding of Coastalock units' hydraulic performance on coastal protection structures.

Future research efforts should include an extensive assessment of Coastalock armour units under alternative structure slope conditions and armour unit configurations.

Furthermore, in the analysis of the test results, it was observed that the reduced underlayer rock diameter facilitated the placement of armour units while improving stability in the range of these test parameters. Therefore, a wider range of underlayer rock size use in further studies will contribute to a better understanding of how underlayer size influences the stability of Coastalock units. Consideration should also be given to the utilization of larger or modified Coastalock units or rocks specifically on the structure crest to improve the stability of the armour units at the transition zone between the front slope and the crest.

In addition to these experimental series, implementation of these recommendations will not only enrich the existing knowledge on the hydraulic performance of the Coastalock armour unit but also offer valuable insights for the practical design and implementation of Coastalock units in varying coastal conditions.

Chapter 4. Numerical Modelling of Eco-Engineered Breakwaters

This chapter presents a revised preprint version of the following published article.

Sayar, S.D., Baker, S., Nistor, I., Gutiérrez, J. (2025). Experimental and Numerical Assessment of Low-crested and Emergent Breakwaters with Eco-Engineered Armour Units. *Canadian Journal of Civil Engineering, Canadian Science Publishing.*

Abstract:

This study presents a comprehensive evaluation of the hydraulic performance of low-crested and emergent rubble mound breakwaters (RMBWs) armoured with Coastalock™, an ecologically engineered single-layer armour unit designed to enhance marine biodiversity while providing high hydraulic stability. The study relies on an integrated approach and combines large-scale physical experiments and numerical modelling using the IH2VOF solver to assess wave generation, transformation, transmission, and overtopping under irregular wave conditions. Physical model tests were conducted at the Large Wave Flume (LWF) of the National Research Council of Canada's Ocean, Coastal and River Engineering Research Center (NRC-OCRE), while the numerical simulations recreated the tests to enhance the understanding of overtopping and wave transmission dynamics of eco-engineered breakwaters under varied hydrodynamic conditions, complementing the physical model tests and supporting the evaluation of IH2VOF as a predictive design tool. The numerical model effectively simulated the hydraulic response of the breakwater, showing consistent trends with the physical experiments. A calibrated roughness coefficient (γ_f = 0.48) was identified for EurOtop-based overtopping predictions. The findings confirm the applicability of IH2VOF for simulating wave–structure interactions in RMBWs armoured with Coastalock units.

Keywords: Coastalock, eco-engineering, wave transmission, wave overtopping, hydraulic performance, physical modelling, numerical modelling, IH2VOF

4.1 Introduction

Coastal structures such as seawalls and breakwaters are designed to protect shorelines from erosion and flooding by using durable, rigid, and solid materials (Hindle, 2018). While these structures can sometimes accommodate marine organisms due to their resilience in harsh, turbulent environments, artificial coastal defences typically support lower biodiversity and higher concentrations of invasive species compared to natural habitats (Airoldi and Beck, 2007). Additionally, coastal structures with steeper slopes than natural beaches provide less habitat, resulting in biodiversity loss and an overall decline in regional populations (Firth et al., 2016). Although breakwaters are effective at dissipating wave energy, they often disrupt sediment

transport and coastal hydrodynamics, leading to significant morphological changes along the coast and the propagation of these effects to adjacent downdrift shorelines due to altered sediment transport pathways (Van Rijn, 2013).

To mitigate the environmental impact of conventional coastal defences, ecological-engineering (eco-engineering) approaches have been introduced, integrating ecological principles with traditional engineering to create multi-functional structures that support both human and marine life (Morris et al., 2020). Eco-engineered coastal structures differ from conventional systems by incorporating eco-enhancing modifications that work in synergy, such as biologically engineered armour units, tidal pools, textured surfaces, and bio-enhancing concrete formulations that promote marine life while maintaining hydraulic performance (Sella and Perkol-Finkel, 2015; Hall et al., 2018). Such approaches aim to balance shoreline protection with ecological sustainability, enhancing marine biodiversity while providing structural resilience (Temmerman et al., 2013).

Among these innovations, the Coastalock armour unit has emerged as a promising, eco-engineered solution. Coastalocks are designed to provide both stability under hydrodynamic forces and enhanced ecological functionality, supporting marine colonization through their bio-enhancing properties (Gutiérrez et al., 2023).

This study presents an integrated approach that combines physical experiments with numerical modelling to assess the hydraulic performance of low-crested and emergent RMBWs armoured with Coastalock units. Large-scale wave flume experiments (detailed in Sayar et al., 2025) and numerical simulations were conducted to evaluate key performance-assessment parameters such as wave transmission and overtopping. Alongside new findings from the hydraulic performance tests for Coastalock units, this research examines the effectiveness of volume of fluid (VOF) method-based numerical methods for modelling wave–structure interactions, offering insights into the applicability of numerical approaches for eco-engineered breakwaters.

4.1.1 Relevant Literature

Traditional coastal defence structures such as breakwaters, revetments, and seawalls are designed to reduce wave energy and mitigate coastal erosion. However, these structures often lead to unintended environmental consequences, such as habitat loss, disruption of sediment transport, and localized erosion (Van Rijn, 2013). As a result, there has been a growing shift toward incorporating ecological enhancements into coastal infrastructure to improve biodiversity while maintaining effective coastal protection. Eco-engineering strategies aim to integrate ecological benefits into conventional engineering designs. A combination of biologically engineered concrete, surface complexity, and nature-inclusive designs has been demonstrated to enhance marine biodiversity and support habitat formation (Sella and Perkol-Finkel, 2015).

Earlier physical model tests on low-crested and emergent RMBWs (Sayar et al. 2024a; 2024b; 2025) and revetments (Molenkamp, 2022; Lawniczak, 2024) armoured with Coastalock units evaluated their hydraulic performance under various wave conditions. While these experimental studies provided valuable insights into hydraulic stability, wave transmission, and overtopping,

they also highlighted the need for robust numerical tools capable of representing the complex interactions between waves and eco-engineered coastal structures.

Numerical modelling plays a crucial role in evaluating the hydraulic performance of coastal structures, particularly for optimizing design parameters (Kobayashi, 2003). The IH2VOF model, based on the Reynolds-Averaged Navier-Stokes (RANS) equations, has been extensively used for simulating wave–structure interactions (Lara et al., 2008; Losada et al., 2008). Prior studies have validated IH2VOF for conventional and low-crested RMBWs, demonstrating its ability to accurately capture wave transmission, overtopping, and turbulence effects (Guanche et al., 2009; Torres-Freyermuth et al., 2010; Pilechi et al., 2018).

Studies such as Safa et al. (2024) have begun to apply numerical modelling, specifically OpenFOAM (Weller et al., 1998), to evaluate the hydraulic performance of nature-inspired armour units on a rubble mound slope. While these efforts signal important progress, the integration of numerical modelling for evaluating these novel nature-inclusive armour units remains limited. There is a continued need for research that combines numerical and physical modelling to improve the understanding of wave transmission in low-crested breakwaters and overtopping in emergent RMBWs with eco-engineered armour layers.

Building on previous investigations of hydraulic stability and wave transmission, this study advances the understanding of eco-engineered armour units by analyzing overtopping performance and assessing the numerical model's capability to reproduce wave transmission and overtopping processes. The physical model experiments conducted at a large scale provided the first dataset on the overtopping characteristics of rubble mound breakwaters armoured with Coastalock units. The IH2VOF numerical model was then applied to reproduce these laboratory conditions and assess its predictive capability.

Accordingly, the main objectives of this study are to

- Quantify the overtopping performance of Coastalock-armoured rubble mound breakwaters through large-scale physical modelling, providing new reference data for eco-engineered single-layer armour systems.
- Validate the IH2VOF numerical model by comparing simulated and measured wave propagation, transmission, and overtopping processes under irregular wave conditions.
- Evaluate the numerical configuration that best captures the observed hydrodynamic behaviour of Coastalock units, considering computational accuracy.

Scope of Research Work and Contributions

The main objective of this study is to quantify wave transmission and overtopping characteristics of Coastalock-armoured RMBWs through complementary large-scale experiments and RANS–VOF simulations. The numerical model is employed not only for validation but also to interpret

flow processes, support the overtopping prediction, and assess the applicability of IH2VOF as a design and research tool for eco-engineered armour systems.

The present study builds on the foundational work of Sayar et al. (2025), which focused on the experimental setup, ecological integration, and hydraulic stability of Coastalock units. Expanding on that research, this study introduces new overtopping data and proposes a calibrated friction factor specific to Coastalock units placed on permeable RMBWs. Additionally, it presents the first detailed application of the IH2VOF model for simulating wave overtopping and transmission on low-crested and emergent breakwaters incorporating Coastalock units, offering novel insights into the numerical modelling of eco-engineered coastal structures.

A comparative analysis of physical and numerical data was performed to evaluate the model's performance and identify potential discrepancies in simulating complex wave–structure interactions. The findings enhance the understanding of overtopping and transmission dynamics for eco-engineered breakwaters under varied hydrodynamic conditions and provide a foundation for refining future numerical modelling approaches.

To facilitate a clear understanding of the research framework, the paper is organized as follows. Section 4.2 describes the large-scale physical model experiments conducted to evaluate wave transmission and overtopping of Coastalock-armoured breakwaters. Section 4.3 introduces the numerical modelling framework based on the IH2VOF solver, and Section 4.4 outlines the computational setup and calibration procedure. Section 4.5 presents the comparative analysis between physical and numerical results, followed by the discussion of findings and implications in Section 4.6.

4.2 Experimental Investigations

The physical model experimental program was conducted in the NRC-OCRE Large Wave Flume (LWF) in Ottawa, Canada, to evaluate the hydraulic performance of low-crested and emergent RMBWs with Coastalock armour units (see Figure 4-1B). These physical experiments were designed to systematically investigate the effects of underlayer rock size and armour unit spacing on the hydraulic performance of Coastalock-armoured breakwaters. Specifically, wave transmission, overtopping, and hydraulic stability were analyzed under various wave conditions to assess how these parameters influence the overall hydraulic performance of these breakwater configurations.

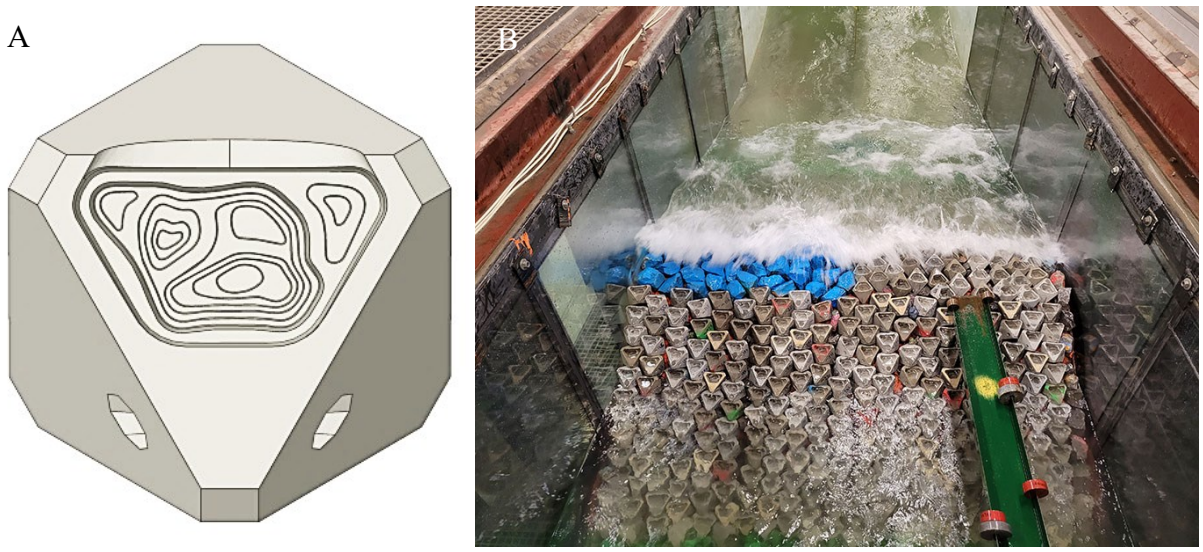

Figure 4-1. (A) Coastalock armour unit; (B) Experimental setup of Coastalock units on the Emergent RMBW under wave action (Photo credit: Scott Baker)

The Coastalock armour unit is a nature-inspired single-layer concrete unit designed to improve hydraulic stability and provide ecological enhancement. The shape (in Figure 4-1A) includes recessed pockets and surface texturing that promote marine colonization while providing high interlocking capacity. Its distinct shape and placement method create a characteristic spacing pattern between adjacent units, which improves interlocking efficiency and flow energy dissipation while promoting localized habitat niches (as described in Gutiérrez Martínez et al., 2023). During testing, the units were arranged in 0 and 10% lateral spacing on 2V:3H front and rear slopes.

The LWF is a 97 m long, 2 m wide, and 2.75 m deep facility equipped with a piston-type wave generator featuring active wave absorption capability, which can generate regular and irregular wave heights up to 1.1 m. The cross-sectional sketch of the flume is shown in Figure 4-2. For these tests, the flume included a 1:100 foreshore slope atop a sub-floor, which could be used for generating currents (currents were not included for these tests). Viewing windows positioned along the flume wall allow visual inspection of the waves and breakwater response.

The model tests were conducted at a 1:15 Froude scale. The selected downscaling refers to typical dimensions of emergent rubble mound breakwaters armoured with Coastalock units rather than a specific prototype project. At prototype scale, this corresponds to structure heights on the order of 6–13 m and a significant wave height range of approximately 1–6 m, which are representative of exposed coastal protection structures. The prototype-to-model length scale was selected based on flume size constraints, armour unit geometry, and wave generation capability. This scale provided a balance between minimizing viscous and surface-tension effects and maintaining sufficiently large armour units for accurate interlocking and overtopping measurements. Froude similitude was adopted to preserve gravitational and inertial forces with fully turbulent flow. Permeability of the

core and underlayer was reproduced using scaled rock gradings consistent with prototype hydraulic conductivity, as mentioned in Sayar et al. (2025).

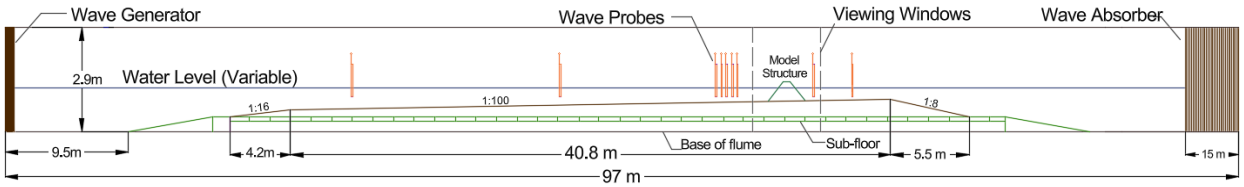

Figure 4-2. Cross-section of the LWF at NRC-OCRE showing the test setup and instrumentation (not at scale)

The model breakwaters in 1:15 scale consisted of a rock core, underlayer, toe protection, and a single layer of Coastalock armour units. More than 600 concrete armour units were cast in mortar using silicone moulds derived from 3D-printed armour units, ensuring high geometric precision and consistency. To satisfy density and mass scaling requirements relative to the prototype Coastalock units (2,400 kg/m³), lead shot was evenly distributed within the moulds during casting, resulting in an average unit weight within 1% of the target value. All physical model experiments were conducted under freshwater conditions. Wave transmission results used for comparison with the numerical model were obtained from low-crested breakwater tests, while overtopping analysis was based on the emergent breakwater tests.

4.2.1 Instrumentation and Data Acquisition

The experimental setup incorporated several wave probes and monitoring tools to record hydrodynamic processes and structural behaviour. Capacitance-type wave probes were placed at multiple locations along the flume to record the free-surface elevation at a sampling frequency of 50 Hz. The incident, reflected, and transmitted wave components were subsequently derived from these measurements using the Mansard and Funke (1980) least-squares method. A five-gauge array was deployed in front of the breakwater and analyzed using the least-squares approach to separate incident and reflected wave components. Data acquisition and wave analysis were conducted using NRC-OCRE's GEDAP software v2.0 (Miles 1990), which provided time-domain and spectral parameters such as significant wave height (H_s) and mean wave period (T_m)

A catchment system installed behind the breakwater was used to collect overtopping volumes, while a wave probe in the overtopping bin recorded water levels that were subsequently converted into discharge rates using calibrated tank measurements. Figure 4-3 presents a sample overtopping time series under the tested conditions (water level 0.50 m, significant wave height 0.30 m, peak wave period 2.2 s), with instantaneous high-discharge events shown in the lower plot and the corresponding cumulative overtopping volume in the upper plot over a 1220 s analysis duration.

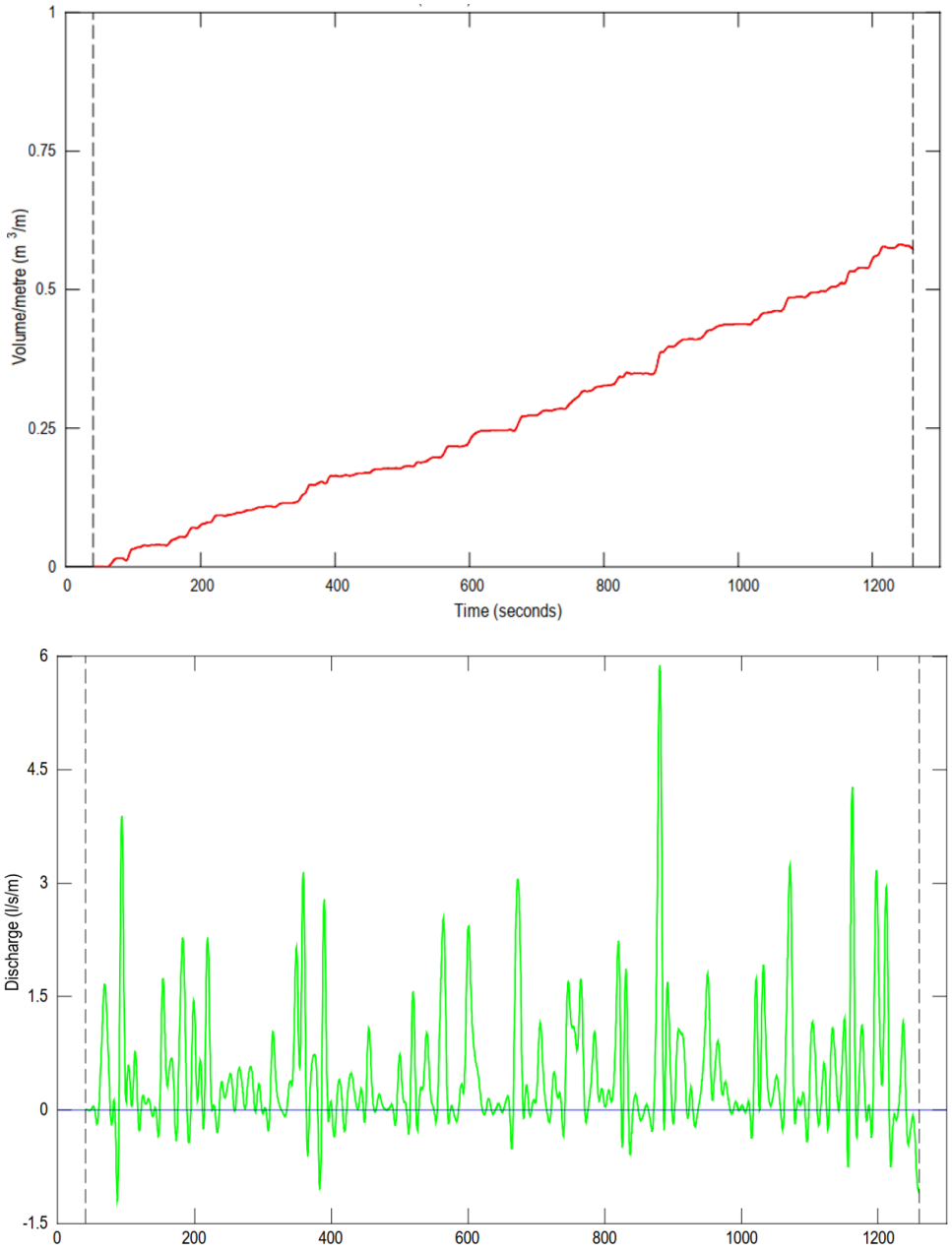

Figure 4-3. Measured cumulative overtopping volume (top) and overtopping time-series (bottom) for test with d: 0.50 m; Hs: 0.30 m; Tp: 2.2 s; analysis interval: 40–1260 s.

High-resolution video monitoring from side and overhead views (1920×1280 resolution at 30 fps) was used to capture wave transformation, overtopping, and transmission during each test. Images were taken before and after each run to support post-processing of wave–structure interaction.

4.2.2 Experimental Test Program

A total of 110 physical tests were conducted across five test series to evaluate the hydraulic performance of Coastalock-armoured rubble mound breakwaters. Three test series focused on low-crested configurations, while two series examined emergent structures. The experiments

systematically varied water depth, wave height, armour unit spacing, and underlayer rock size to investigate their influence on wave transmission, overtopping, and hydraulic stability.

The low-crested model with 0.42 m structure height (6.3 m in prototype scale) was tested under five water levels ranging from 0.3 to 0.7 m (4.5 m to 10.5 m in prototype scale), representing both submerged and emergent conditions. Wave steepness values ranged from 0.030 to 0.055, and significant wave heights up to 0.44 m (6.6 m in prototype scale) were tested. Armour unit spacing was set at either 0% or 10%, and two underlayer gradings (25–60 g and 50–100 g correspond to Dn_{50} values of approximately 0.024 m and 0.026 m) were used.

For the emergent breakwater tests with 0.84 m structure height (12.6 m in prototype scale), wave heights up to 0.38 m (5.7 m in prototype scale) and water levels up to 0.7 m were applied when the overtopping volumes and discharges were recorded for each case. Dimensional analysis and the derivation of relevant non-dimensional parameters for these tests are presented in Sayar et al. (2025).

4.3 Description of the Numerical Model

The numerical model used in this study is IH2VOF (Lara et al., 2011), a RANS-based solver that utilizes the VOF method to simulate free surface evolution. The model incorporates the k-ε turbulence model to resolve energy dissipation within the flow field.

The model solves the incompressible RANS equations using the finite volume method, with the VOF technique employed to capture the interface between air and water. This approach enables the high-accuracy simulation of complex free surface phenomena such as wave breaking, splashing, and overtopping.

The governing equations consist of the continuity equation (Equation 4-1), the momentum equation (Equation 4-2), and the volume fraction transport equation (Equation 4-3), which are described below:

Continuity equation:

$$\nabla \cdot u = 0 \qquad \text{Equation 4-1}$$

Momentum equation:

$$\frac{\partial u}{\partial t} + (u \cdot \nabla)u = -\frac{1}{\rho}\nabla p + \nu \nabla^2 u + g + F_{VOF} \qquad \text{Equation 4-2}$$

Volume fraction transport equation:

$$\frac{\partial \alpha}{\partial t} + u \cdot \nabla \alpha = 0 \qquad \text{Equation 4-3}$$

where u is the velocity vector, p is pressure, ρ is fluid density, ν is the kinematic viscosity, g is gravitational acceleration, and F_{VOF} is the surface tension force across the air-water interface.

Flow within the porous layers of the structure was resolved using the Volume-Averaged Reynolds-Averaged Navier–Stokes (VARANS) equations (Losada et al., 2008; Lara et al., 2011). The

VARANS formulation extends the conventional RANS equations by applying a volume averaging procedure over a representative elementary volume of porous media, allowing simultaneous computation of clear-fluid and seepage velocities. The interfacial momentum exchange between the fluid and the solid matrix is represented through the extended Forchheimer relationship, which includes linear and nonlinear resistance terms expressed as functions of porosity, nominal diameter, and empirical linear and nonlinear friction coefficients. An added-mass coefficient is introduced to account for local acceleration effects within the porous matrix. When porosity approaches unity, the VARANS formulation naturally reduces to the classical RANS equations. This implementation enables IH2VOF to capture both energy dissipation and momentum attenuation processes occurring within the permeable armour, underlayer, and core of the breakwater.

In this framework, the free-surface evolution is captured through the VOF method, which introduces a phase volume fraction (α) to track the air–water interface, where $\alpha = 1$ represents water, $\alpha = 0$ represents air, and intermediate values denote the interface. This coupled VARANS–VOF implementation enables IH2VOF to resolve both energy dissipation within the porous media and surface-wave dynamics above the armour layer, providing a representation of flow throughout the entire structure.

4.4 Numerical Model Setup

To complement the physical experiments conducted on emergent RMBWs armoured with Coastalock units, a series of two-dimensional numerical simulations was conducted using the IH2VOF model. The objective was to simulate wave interaction processes under a range of structural and hydrodynamic conditions tested experimentally and to assess the performance of IH2VOF to represent wave generation, propagation, transmission, and overtopping for this type of armour units. By using the same geometric and hydraulic conditions as in the laboratory setup, the numerical model enabled direct comparison of wave transmission coefficients and mean overtopping discharges. This section outlines the model setup, including the computational domain, boundary conditions, structural geometry, and sensitivity analysis.

4.4.1 Computational Domain

The numerical model simulated the wave interaction with a low-crested breakwater and an emergent RMBW armoured with Coastalock units, at a 1:15 model scale, consistent with the physical experiments.

The computational domain was generated in two dimensions and extended 36 m in the horizontal direction and 1.5 m in the vertical direction. The left boundary of the domain coincided with the location of the first wave gauge in the physical experiments, while the right boundary was defined 3 m beyond the last wave probe on the leeside of the structure. The vertical distance between the top and bottom boundaries was limited to 1.5 m to reduce computational cost while maintaining sufficient freeboard above the maximum wave crest elevation. The layout of the numerical domain

is presented in Figure 4-4. The red markers indicate the location of the wave probes in the numerical model, replicating their placement in the physical experiments.

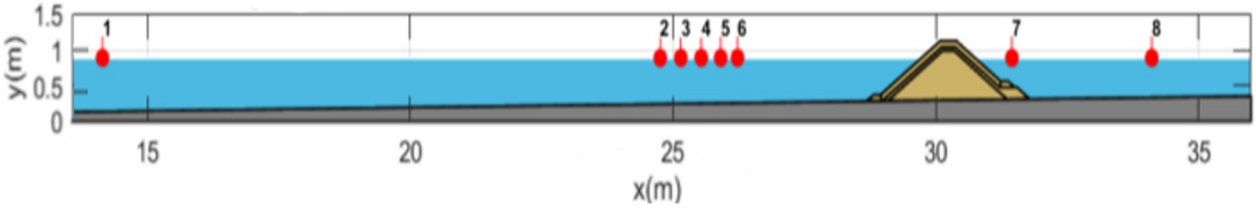

Figure 4-4. Computational domain of the experimental setup

The breakwaters were placed on top of a sloped section of the computational domain, representing the foreshore bathymetry in the physical flume setup. They included the underlying slope, toe, and crest configurations used in the low-crested breakwater and emergent RMBW tests. The geometry was generated based on actual dimensions and bathymetric features observed in the flume tests to maintain consistency in model representation.

Wave probes and overtopping measurement points were positioned to match those in the physical tests for a direct comparison between measured and simulated free-surface flows and overtopping discharges. The initial water levels were set to correspond to the various water depths at the breakwater toe tested in the physical experiments, ranging from 0.3 m to 0.7 m at model scale.

4.4.2 Boundary Conditions

The IH2VOF model uses a single-phase free surface flow approach, separating air and water layers through the VOF method. The left, right, and bottom boundaries of the computational domain were defined as impermeable wall boundaries. These walls were necessary to contain the fluid within the flume environment and to reflect the physical constraints of the laboratory setup. While wave generation in the experimental flume was performed using piston-type wave makers on the left-hand side, the numerical model imposed waves directly using the time series of water surface elevations recorded during the physical tests. At the left-side (offshore) boundary, waves were generated using a Dirichlet boundary condition (Ferziger & Perić, 2002), where the free-surface elevation and velocity components were prescribed at each time step according to the experimental time series. This approach allows the reproduction of wave generation without explicitly modelling the motion of the experimental wave paddle.

A passive wave absorption zone (sponge layer) was implemented adjacent to the offshore boundary to prevent reflections. This region applies a dissipation function that gradually damps wave energy as it propagates toward the boundary, following the methodology of Israeli and Orszag (1981). The passive absorption approach was selected for its confirmed stability and compatibility with the Dirichlet-type wave generation method (as mentioned in Losada et al, 2008; Guanche et al, 2009).

This allowed for the reproduction of irregular wave conditions while avoiding complications associated with numerical wave generation and absorption boundaries. Although IH2VOF includes both active and passive wave absorption capabilities at the boundaries, it does not

explicitly separate or process reflections generated by the structure. Therefore, the total experimental wave signal, including both incident and reflected components, was used as the numerical wave input and corresponding output to ensure an accurate and consistent comparison with the physical model results.

The top boundary of the domain was defined as an atmospheric pressure boundary, allowing free motion of the air phase and the VOF scheme to capture free surface fluctuations, overtopping and wave splashes above the crest level. The air clearance above the highest crest elevation was verified through sensitivity tests to ensure no artificial damping. The initial conditions for the water surface were defined according to the measured still-water depth at the breakwater toe, corresponding to the water depth used in each physical test scenario. The numerical wave probes (as shown in red in Figure 4-4) were placed at the same horizontal locations as those used in the physical experiments. This facilitated direct comparison of free surface elevations at key positions throughout the wave flume, including on the seaside of the structure (incident waves), at the structure (breaking and overtopping), and on the leeside of the structure (transmitted waves). The overtopping discharges were recorded over the measurement location positioned on the crest, matching the location of the physical overtopping catchment system.

4.4.3 Low-Crested and Emergent RMBW Models

The structural configuration of the low-crested breakwater and the emergent RMBW used in the numerical model was designed to match the geometry and material properties of the physical models tested in the wave flume. Both breakwaters consisted of four permeable layers: toe armour, core, underlayer, and the armour layer representing the Coastalock units' configuration with 10% unit spacing, and the structures had a 2V:3H front and back slope.

The low-crested breakwater model employed in the numerical simulations focused on wave transmission performance, whereas the emergent breakwater model simulations were used in the overtopping analysis. The geometry of each breakwater computational model was developed in the IH2VOF Graphical User Interface based on the flume setup. The final geometry of the emergent breakwater model used in the simulations is shown in Figure 4-5.

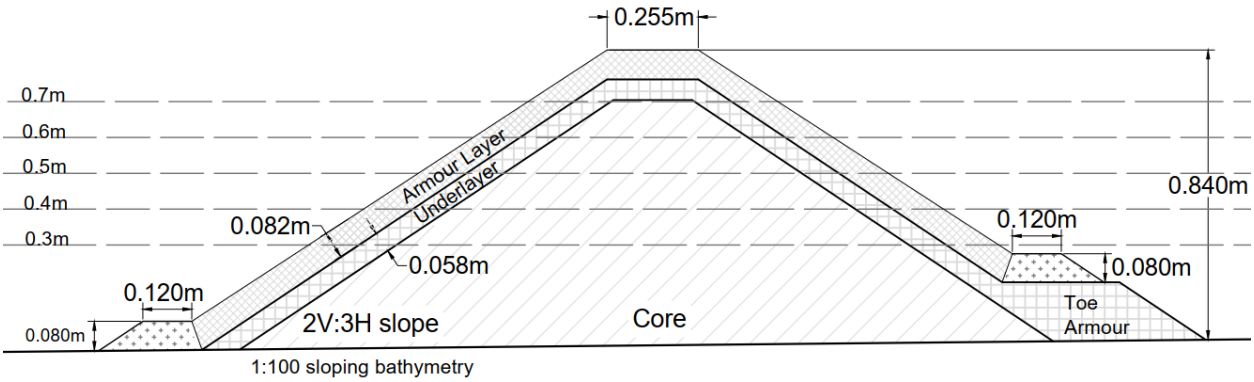

Figure 4-5. Emergent RMBW model generated in IH2VOF (not at scale)

The properties of each permeable layer, including nominal diameter and porosity, were assigned according to values measured during the physical experiments and are summarized in Table 4-1. Nominal diameters and porosity of the layers were selected to accurately represent the permeability and hydraulic behaviour of the breakwater structure under hydrodynamic effects. The simulations were conducted under fixed-bed conditions to focus on the hydrodynamic response of the structure.

Table 4-1. Nominal diameters (D_{n50}), porosity and non-linear friction coefficient of the layers of emergent RMBW

Layer type	**Nominal diameters (D_{n50})**	**Porosity (n)**	**Non-linear friction coefficient (β)**
Coastalock armour	0.073 m	0.48	1.1
Underlayer	0.024 m	0.50	1.0
Core	0.003 m	0.46	0.8
Toe armour	0.038 m	0.53	1.0

The effects of varying linear and non-linear friction coefficients on wave–structure interactions were examined to determine the optimal hydraulic characterization of each permeable layer. Both friction coefficients were assessed to investigate their influence on wave transmission and overtopping performance. It was observed that the linear friction coefficient had minimal impact, consistent with findings reported by Pilechi et al. (2018). In contrast, the non-linear friction coefficient of the armour layer and core had a significant effect on overtopping discharge and wave transmission compared with the non-linear friction coefficient of the other layers. Multiple non-linear friction coefficient configurations were tested, and the final values, shown in Table 4-1, were chosen for their superior agreement with the hydraulic behaviour observed in the physical experiments. These values also align with the observations of Guanche et al. (2009), further supporting their suitability for modelling porous layers in RMBWs.

4.4.4 Sensitivity Analysis

The computational mesh was structured using three horizontal and two vertical subzones, with horizontal cell sizes ranging from 0.8 to 1.5 cm and vertical cell sizes ranging from 0.3 to 0.8 cm. This configuration resulted in approximately 3,300 cells in the horizontal direction and 330 cells in the vertical direction. Finer resolution was applied near the water surface and the breakwater, where wave breaking, run-up, and overtopping processes are more sensitive to numerical accuracy.

The mesh sensitivity analysis was conducted to determine the optimal resolution required to accurately simulate wave processes without excessive computational cost. To assess mesh independence, additional simulations were carried out with refined grids. Five mesh configurations were tested by progressively increasing their resolution. A mesh insensitivity criterion was set such

that further mesh refinement should result in less than 5% change (refer to Ferziger and Perić, 2002 and Celik et al., 2008) in key output parameters, specifically resultant significant wave height (H_s) after wave transformation and mean overtopping discharge (q) after wave–structure interaction. The results showed minimal variation in free surface fluctuations and overtopping discharges between the mesh configurations when the cell sizes were reduced further than 1 cm in the horizontal direction, and the selected mesh structure provided sufficient resolution to capture the key hydrodynamic features of interest.

The numerical simulations were designed to reproduce short-term, high-intensity overtopping events with high spatial and temporal resolution. A fine mesh and small time step were selected to accurately resolve free-surface deformation and water volume transfer during overtopping. Although the simulated durations were limited to short test windows, these intervals correspond to the most energetic and hydraulically representative periods of the highest experimental waves, testing the model with the dominant wave breaking and overtopping dynamics.

4.5 Comparative Results and Analysis

4.5.1 Wave Generation

The wave generation process in the numerical model was carried out using a static wave paddle at the left side boundary of the computational domain. Instead of synthesizing input waves from theoretical spectra, the paddle motion in IH2VOF was defined to reconstruct the wave series that reflected the actual experimental time histories.

These reconstructions allowed for accurate input of wave conditions corresponding to test cases 1, 2, and 3 used in the numerical simulations, ensuring that the generated wave trains in the numerical model matched the wave characteristics observed in the laboratory measurements.

Figures 4-6 and 4-7 show the surface elevation time series recorded at an additional numerical wave gauge positioned 3 metres from the seaward boundary of the numerical domain, alongside measurements from the first wave probe in the physical experiments. The time series shown in Figures 4-6 and 4-7 start at 30 s and extend to 130 s, corresponding to the period after wave generation has fully established but before any boundary effects influence the recorded signals. This additional numerical wave gauge was included solely to evaluate the generated wave conditions before they were affected by wave shoaling, enabling a direct comparison with the incident waves measured by the first probe in the physical model. The results correspond to two representative test cases, where d is the water depth at the breakwater toe (m), H_s is the significant wave height (m), and T_p is the peak wave period (s).

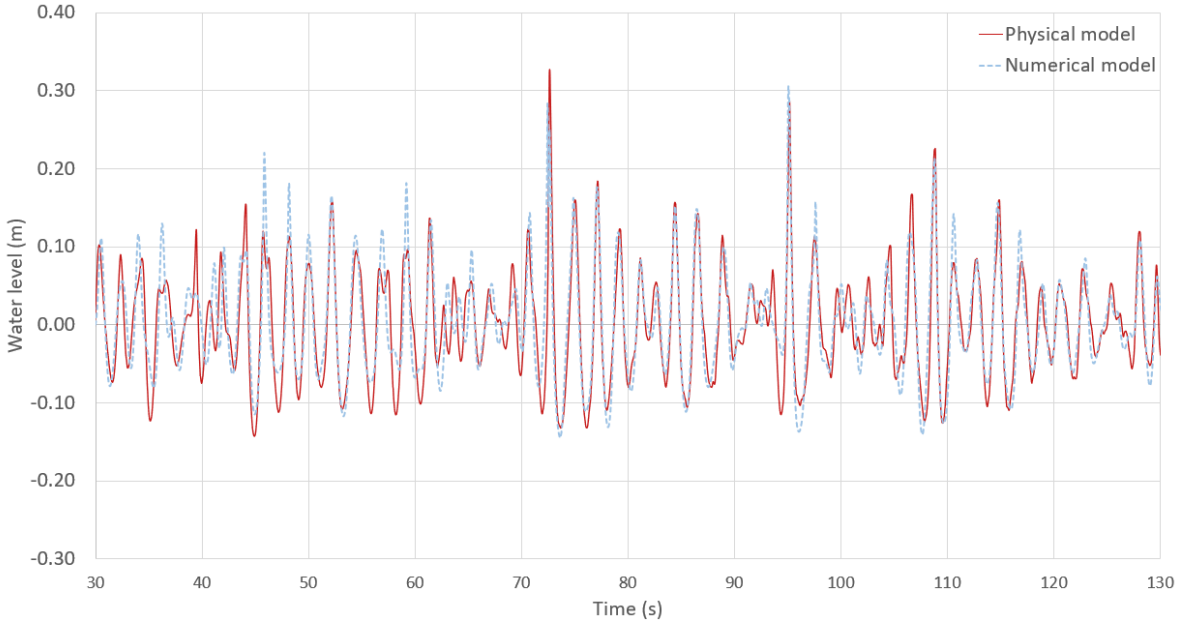

Figure 4-6. Generated wave series in Test Case 1 (d=60 cm, H_s=26 cm, T_p=2.2 s)

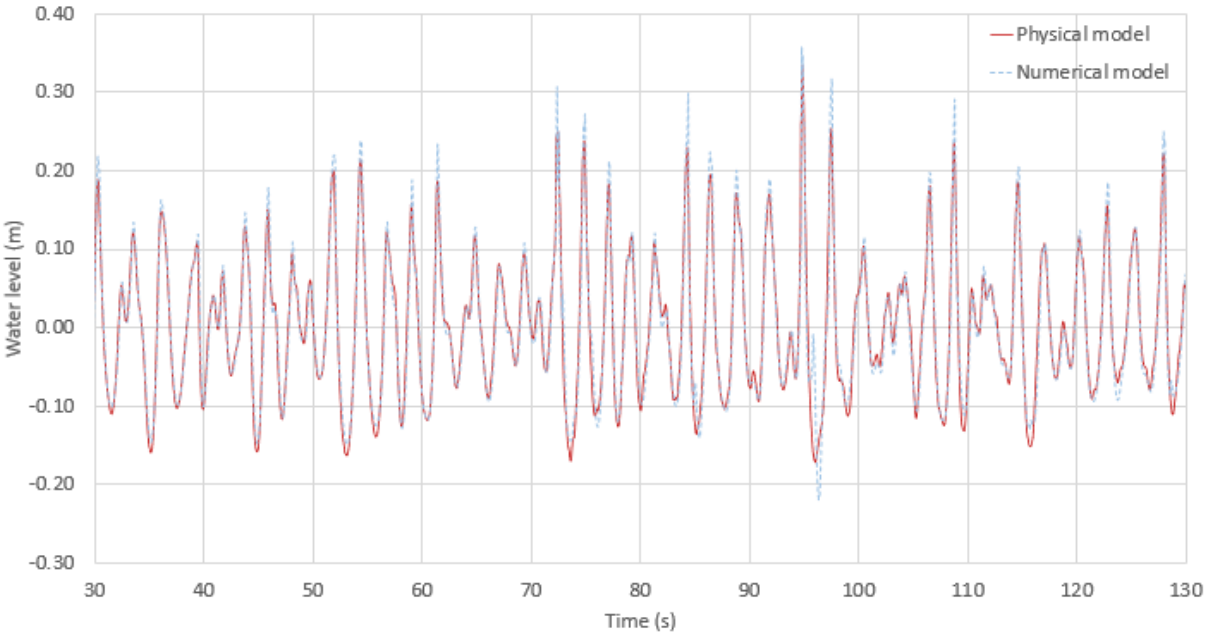

Figure 4-7. Generated wave series in Test Case 2 (d=70 cm, H_s=32 cm, T_p=2.5 s)

To quantitatively evaluate the agreement between the generated wave series in the physical and numerical models, Table 4-2 summarizes the significant wave heights (H_s) and mean wave periods (T_m) for both Test Case 1 and Test Case 2. The results indicate strong consistency in wave characteristics, with average percentage deviations (APDs) below 9% for all parameters. These findings confirm the reliability of the wave generation approach in IH2VOF using physical wave probe inputs as boundary conditions.

Minor differences were observed in wave crest sharpness. These discrepancies can be attributed to numerical dissipation, mesh discretization effects, and the idealized boundary conditions used in the numerical model, as opposed to the physical irregularities and fine-scale energy losses present in the laboratory environment.

Table 4-2. *Wave generation results for Test Cases 1 and 2*

Wave Probes	**Test Case 1 - Generated waves** *(d=60 cm, H_s=26 cm, T_p=2.2 s)*		**Test Case 2 - Generated waves** *(d=70 cm, H_s=32 cm, T_p=2.5 s)*	
Wave Parameters	**H_s (m)**	**T_m (s)**	**H_s (m)**	**T_m (s)**
Physical Model	0.268	1.870	0.341	2.082
Numerical Model	0.290	1.960	0.365	2.186
APD (%)	8.36%	4.81%	7.32%	5.10%

4.5.2 Wave Propagation

Wave propagation over the foreshore in the numerical model was evaluated by comparing the changes in H_s and T_m between the physical and numerical results at wave probes (WP) 1 and 6 (as shown in Figure 4-4). The bathymetry featured a constant 1:100 foreshore slope, which induced depth-related wave shoaling before wave–structure interaction.

As the waves propagate across the foreshore, a decrease in wave height was observed due to depth-induced shoaling, where partial energy dissipation reduced the amplitude of incoming waves. As expected, this behaviour was consistently observed in both the physical and numerical models.

Figures 4-8 and 4-9 show the surface elevation time series from both models measured at the same location for the two cases:

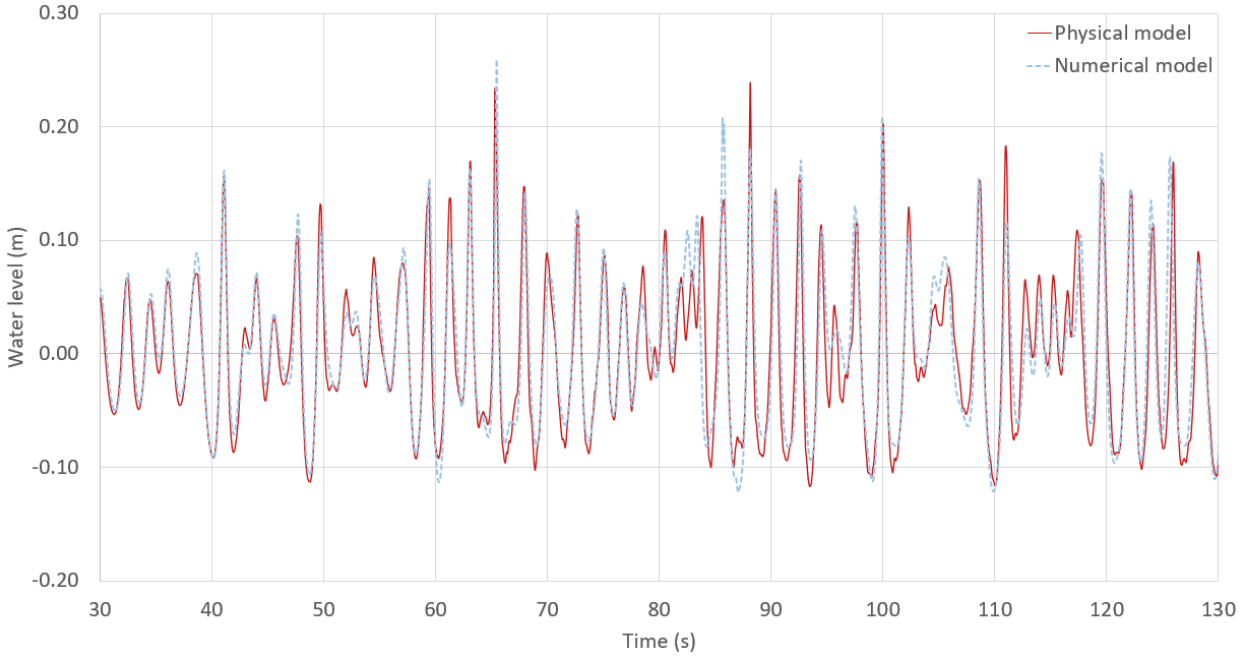

Figure 4-8. Wave series measured at WP6 in Test Case 1 (d=60 cm, Hs=26 cm, Tp=2.2 s)

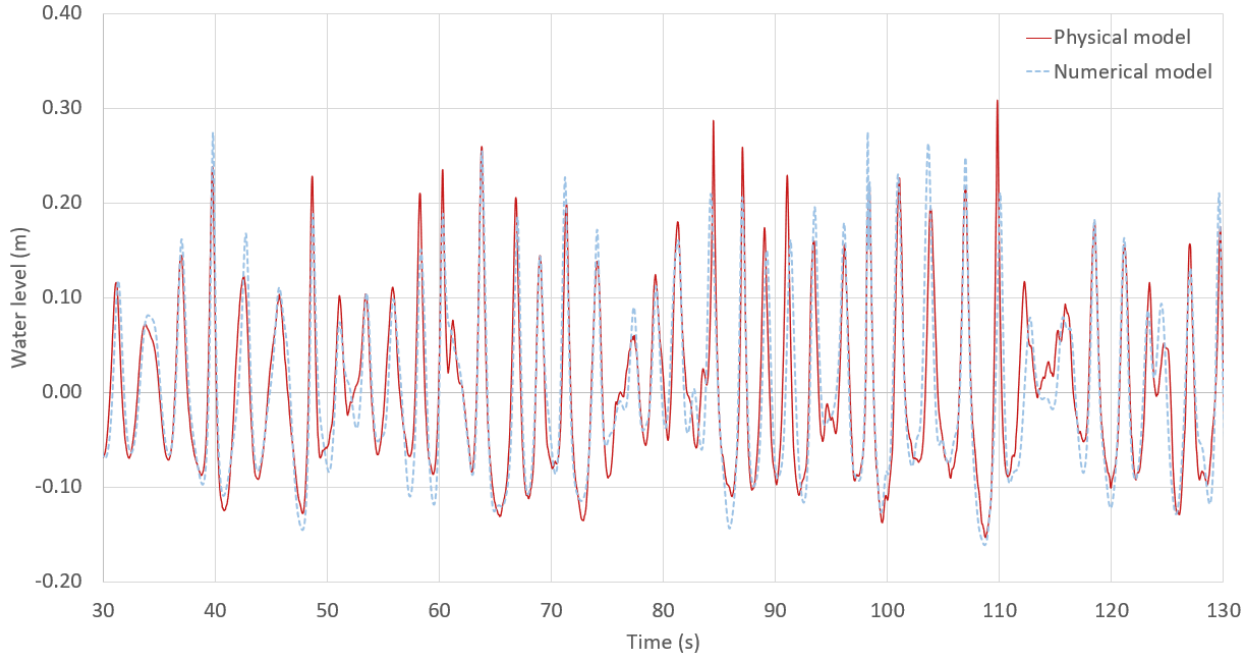

Figure 4-9. Wave series measured at WP6 in Test Case 2 (d= 70 cm, Hs=32 cm, Tp=2.5 s)

The comparison indicates that the reduction in significant wave height along the sloping foreshore was reasonably well processed by the IH2VOF model. However, some slight over- and underestimations in wave height were observed at certain locations. These findings confirm that the numerical model appropriately simulated wave shoaling over the 1:100 slope and provided consistent nearshore wave conditions for the analysis of wave transmission and overtopping.

Table 4-3 presents the numerical and physical results for H_s and T_m after wave propagation over the 1:100 foreshore slope. These values were measured at wave probe WP6, which is the closest wave probe to the breakwater on the seaside. While H_s values between the numerical model and experimental results aligned quite well (APD below 3%), the numerical model slightly overestimated $T_{m,}$ likely due to resolution effects during wave transformation. Nevertheless, the numerical model effectively captured the depth-induced shoaling behaviour and provided valid input for wave–structure interaction analysis.

Table 4-3. Wave propagation results for Test Cases 1 and 2

Wave Probes	**Test Case 1 - Propagated waves** *(d=60 cm, H_s=26 cm, T_p=2.2 s)*		**Test Case 2 - Propagated waves** *(d=70 cm, H_s=32 cm, T_p=2.5 s)*	
Wave Parameters	**H_s (m)**	**T_m (s)**	**H_s (m)**	**T_m (s)**
Physical Model	0.257	1.972	0.328	2.295
Numerical Model	0.251	2.208	0.337	2.572
APD (%)	2.49%	12.10%	2.68%	12.33%

4.5.3 Wave Transmission

Wave transmission through the low-crested breakwater was evaluated by comparing the transmitted wave heights in both the physical and the numerical models. The comparison was performed for test cases 1 and 3 (in Figures 4-10 and 4-11), representing different water depths and wave conditions.

Wave transmission coefficients (K_t) were calculated as the ratio of transmitted to incident significant wave heights as shown in Equation 4-4:

$$K_t = \frac{H_{s,t}}{H_{s,i}} \qquad \text{Equation 4-4}$$

where $H_{s,i}$ is the significant wave height on the seaside of the breakwater, and $H_{s,t}$ is the transmitted significant wave height measured on the leeside. The transmitted waves obtained from the numerical model were compared to the experimental results to evaluate model performance under two specific test cases characterized by intense wave breaking. These cases were selected due to their wave characteristics and water depths, which promoted strong turbulence and presented the most challenging conditions for the numerical model.

Figures 4-10 and 4-11 present the time series of free surface elevation measured on the leeside, showing reasonable alignment in transmitted waves between the numerical and physical models.

Importantly, the experimental setup provided a hydraulic connection between the seaside and leeside domains through the current-generation tunnel beneath the bathymetry (as detailed in Sayar et al., 2025), which would limit persistent water accumulation by allowing slow water exchange. In addition, the tested structure was porous, enabling seepage and pressure equalization through the armour and core, where the numerical simulations reproduced the same boundary conditions as the physical model.

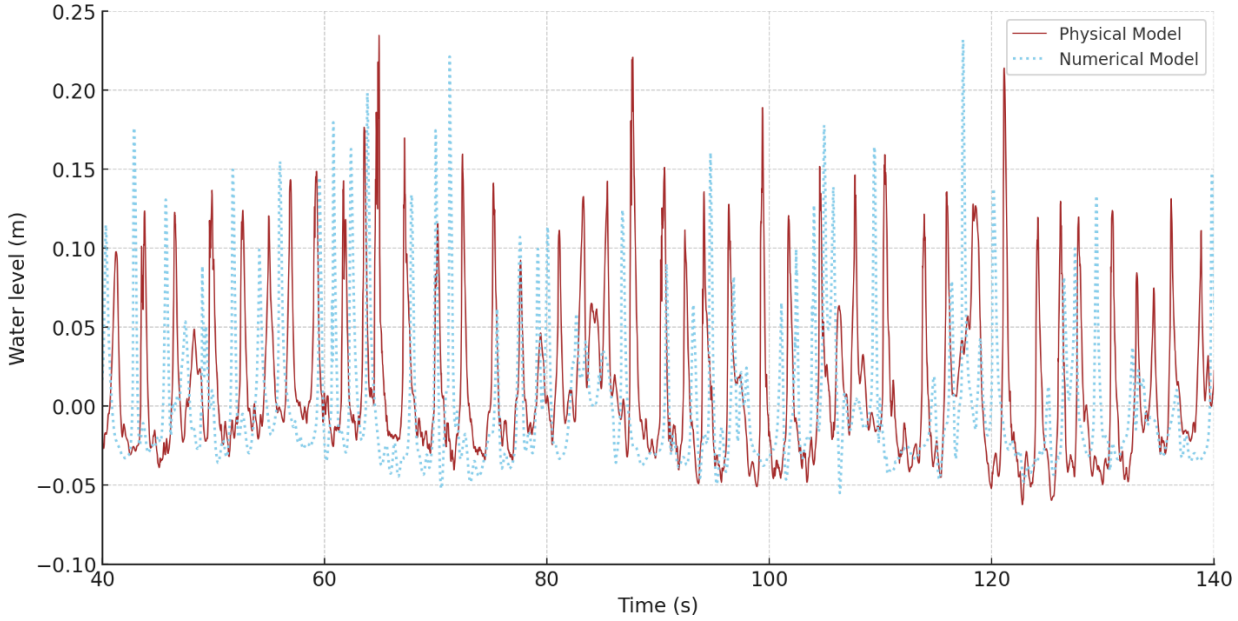

Figure 4-10. Comparison of transmitted waves for Test Case 3 (d=50 cm, H_s=30cm, T_p=2.2s)

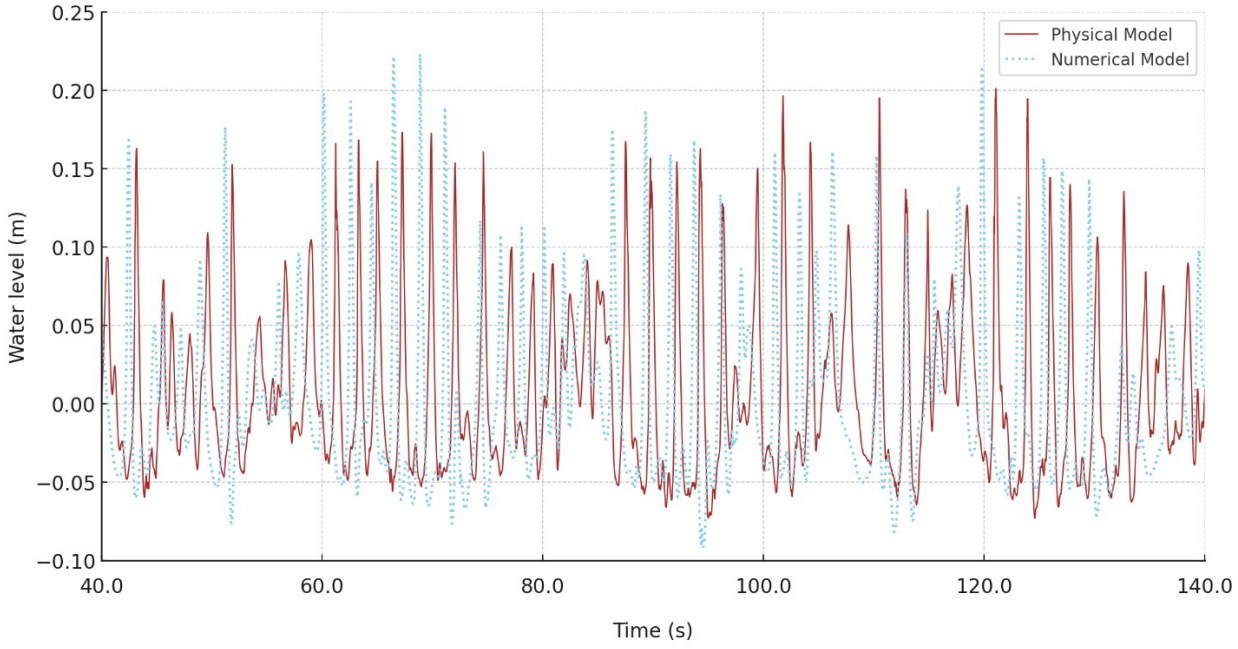

Figure 4-11. Comparison of transmitted waves for Test Case 1 (d=60 cm, H_s=26cm, T_p=2.2s)

Table 4-4 summarizes the comparison of incident and transmitted wave heights, transmission coefficients, and absolute percentage differences (APD) for the following test cases:

Table 4-4. Physical (Exp) and numerical model (Num) wave transmission results for Test Case 1 (d=60 cm, H_s=26cm, T_p=2.2s) and Test Case 3 (d= 50cm, H_s=30cm, T_p=2.2s)

Test Case	Wave Probe	$H_{s,\,Exp}$ (m)	$H_{s,\,Num}$ (m)	APD-H_s (%)	$T_{m,\,Exp}$ (s)	$T_{m,\,Num}$ (s)	APD-T_m (%)	$K_{t,\,Exp}$ (%)	$K_{t,\,Num}$ (%)	APD-K_t (%)
Test Case 1	WP4 (Incident)	0.263	0.285	8.6	1.90	2.24	17.7	—	—	—
Test Case 1	WP7 (Transmitted)	0.214	0.224	4.6	1.81	2.04	12.5	81.4	78.4	3.7
Test Case 3	WP4 (Incident)	0.293	0.269	8.1	2.02	2.34	15.7	—	—	—
Test Case 3	WP7 (Transmitted)	0.196	0.189	3.6	1.92	1.97	2.5	66.9	70.2	4.9

The numerical model demonstrated strong agreement with the experimental data, providing APD values below 5% for transmitted wave heights and transmission coefficients in both cases. The magnitude of the errors in wave transmission may be due to limitations in resolving detailed flow processes and energy dissipation within the porous structure and idealized representations in the numerical domain.

In addition to these minor discrepancies, a consistent phase shift can be observed between the physical and numerical time series of the transmitted wave signals, with the numerical model exhibiting a slight lead in wave crest and trough positions relative to the physical model. This phase lag was not observed in the seaside wave gauge data, suggesting that the shift originates from wave transmission while passing over the structure. While mesh size and time-step refinement primarily affected high-frequency content and therefore zero-crossing T_m at the offshore gauge, their influence on H_s and K_t was minor within the selected grid and time-step. Potential causes also include numerical dispersion and simplified internal flow representation with given core porosity. Despite this phase discrepancy, the model accurately captures the transmitted wave heights and periods.

4.5.4 Overtopping

The overtopping performance of the emergent breakwater was evaluated by comparing cumulative overtopping volumes and discharges between the physical and numerical models. The analysis was conducted under various incident wave heights, water depths, and relative freeboard conditions to assess the model's ability to simulate overtopping dynamics.

In the physical model, a 10 cm-wide overtopping tray was installed along the breakwater centerline to collect the overtopped water, ensuring representative sampling of the flow. The collected

overtopping volume was measured using a wave probe installed in the overtopping tank, with data recorded at a sampling frequency of 50 Hz. The recorded water-level fluctuations were converted into discharge rates based on the area of the overtopping tank. The resulting overtopping discharges were normalized by the flume width and reported as volumetric rates (m^3/s per meter width of structure).

Cumulative overtopping volumes in the numerical model were computed at the crest of the breakwater, using a virtual measurement zone aligned with the catchment point used in the physical experiments. This setup ensured consistency between the two models for evaluating overtopping rates. The measurement approach in both the physical and numerical models is illustrated in Figure 4-12.

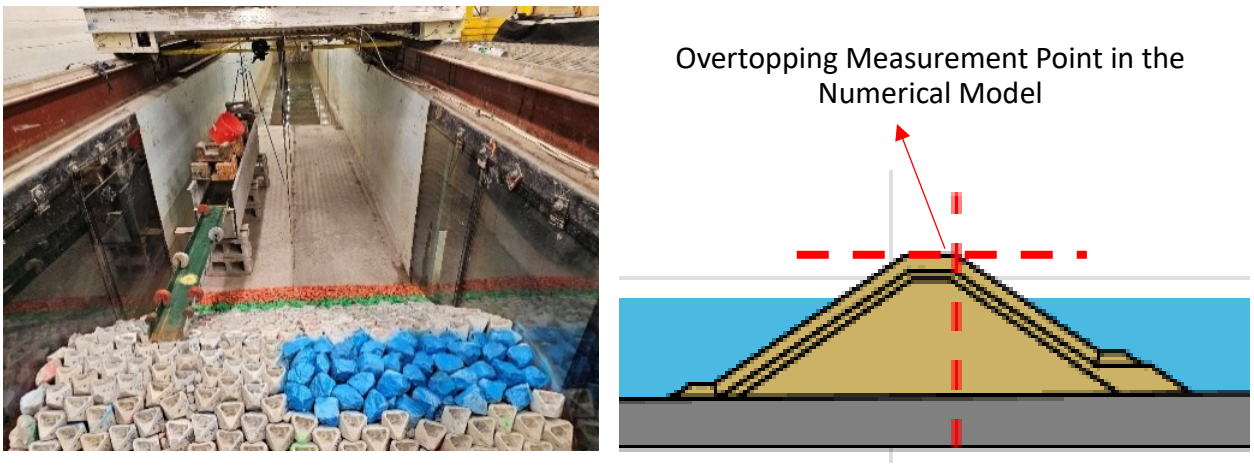

Figure 4-12. Overtopping measurement setup in the physical model (left) and corresponding measurement location in the numerical model (right) (Photo credit: Serim Dogac Sayar)

Test cases 1 and 2, characterized by highly energetic wave conditions, were selected for comparison. As shown in Figures 4-13 and 4-14, the cumulative overtopping volumes are plotted over time to evaluate model performance.

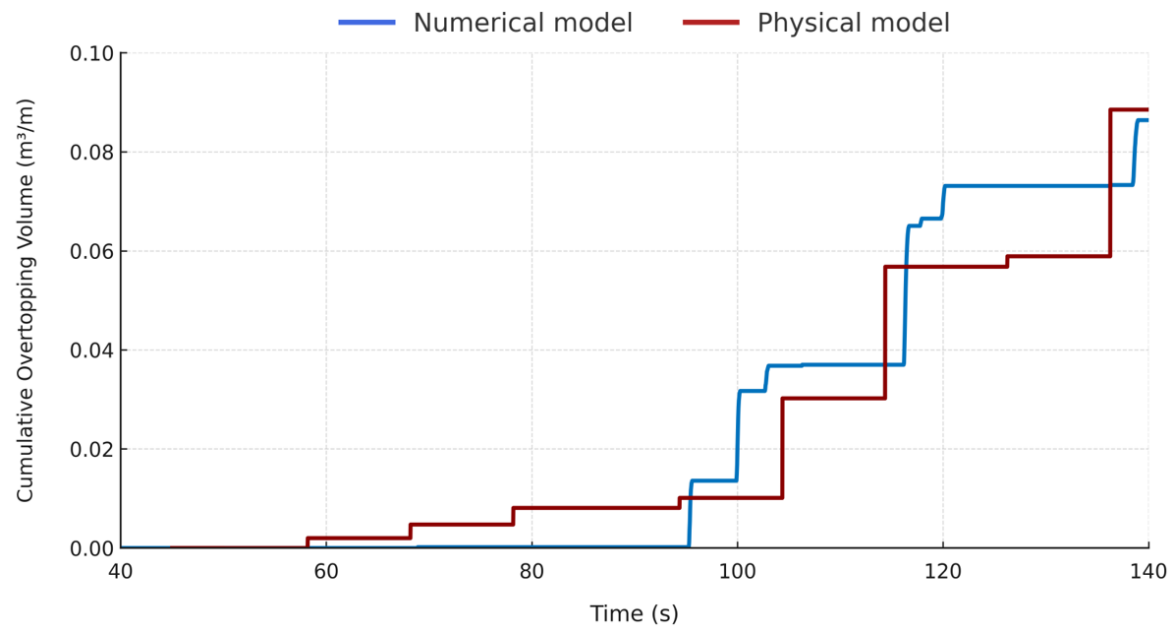

Figure 4-13. Cumulative Overtopping Volume Measurement in Test Case 1 (d=60 cm, H_s=26 cm, T_p=2.2 s)

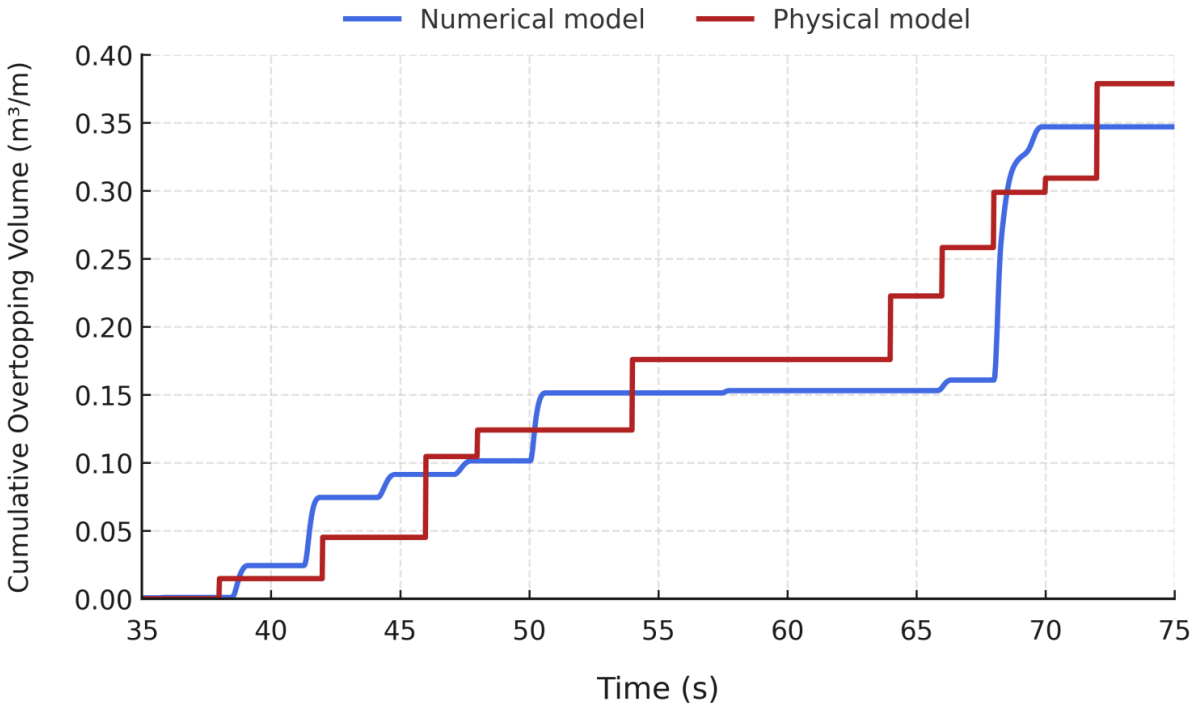

Figure 4-14. Cumulative Overtopping Volume Measurement in Test Case 2 (d=70 cm, H_s=32 cm, T_p=2.5 s)

The recorded overtopping signals were processed using the GEDAP software, applying a low-pass filtering procedure to reduce physical noise in the wave-probe measurements. The filtering method typically tends to attenuate short-period fluctuations when this step was necessary to mitigate the

influence of short-period waves forming within the overtopping catchment reservoir, which introduced fluctuations in the raw measurements.

Some differences were noted in peak flow events and early overtopping onset, which may be attributed to small discrepancies in wave impact timing or turbulence resolution. Although the short-term variability of individual overtopping peaks (Figures 4-13 and 4-14) was not fully captured, the numerical model successfully reproduced the magnitude of overtopping events, cumulative trend and total overtopping volumes.

The temporal span in the numerical simulations begins at 30 and 40 seconds because the initial portion of the laboratory recordings includes the propagation delay between wave generation and the arrival of the first waves at the measurement array; thus, only the portion representing fully developed irregular waves is shown. The comparison was performed for the full duration of each numerical simulation (40 s and 100 s), while the corresponding physical tests lasted over 1000s (as mentioned in Sayar et al., 2025). The relatively short numerical duration was intentionally chosen to capture high-intensity overtopping events with fine temporal and spatial resolution, consistent with the cell sizes required to resolve breaking and run-up processes. This approach follows the rationale of Pilechi et al. (2018), which implied that longer-duration simulations may accumulate numerical errors in overtopping predictions with the use of a turbulence model under highly energetic wave conditions.

The numerical and physical model results for overtopping performance are further detailed in Table 4-5, corresponding to the two test cases presented in Figures 4-13 and 4-14. Table 4-5 compares cumulative overtopping volumes and mean overtopping discharges over the full analysis duration for each scenario.

Table 4-5. Overtopping Results for Test Case 1 (d= 60 cm, H_s=26 cm, T_p=2.2 s) and Test Case 2 (d= 70 cm, H_s=32 cm, T_p=2.5 s)

Test Case	Model	Analysis duration (s)	Cumulative overtopping volume (m^3/m)	Mean overtopping discharge (L/s/m)
Test Case 1	Numerical	100	0.086	0.86
Test Case 1	Physical	100	0.084	0.84
Test Case 2	Numerical	40	0.346	8.65
Test Case 2	Physical	40	0.379	9.48

Each simulated time window corresponded to a physically observed period of peak overtopping activity identified from the experimental records. This approach allowed high-resolution modelling of wave structure interaction. The focus on these short-term windows provided a test of the model's predictive capability under the most demanding flow conditions.

The consistency in cumulative volume and mean discharge values indicates that the numerical model is capable of accurately capturing the time-integrated overtopping response of the breakwater. Minor deviations observed in the results are within acceptable limits and are likely due to slight differences in wave impact timing and the complexity of simulating turbulent overtopping flows. Overall, the results support the reliability of the numerical approach for predicting overtopping under varying wave conditions.

4.6. Discussions and Conclusions

This section discusses the outcomes of the numerical model and its ability to simulate wave interaction with low-crested and emergent breakwaters under irregular wave conditions. The model's agreement with experimental results is interpreted in terms of prediction accuracy and consistency across different structural and wave scenarios. In addition, the friction factor for Coastalock armour units on permeable RMBWs was determined, and the overtopping predictions obtained using empirical formulations from EurOtop were evaluated through comparison.

4.6.1 Performance Assessment of the Numerical Model

The IH2VOF numerical model demonstrated good agreement with the physical model results across multiple hydrodynamic processes, including wave generation, propagation, transmission, and overtopping. The comparisons in Section 4.5 show that the model reliably captured both temporal trends and the magnitude of key parameters such as wave height and period, supporting its suitability for simulating wave–structure interaction for low-crested breakwaters and emergent RMBWs.

For wave propagation (Section 4.5.2), the model accurately reproduced the decreasing wave height trend associated with depth-induced shoaling over the 1:100 foreshore slope. The consistency in mean wave period confirmed the model's ability to reproduce the characteristics of wave trains during wave transformation.

The wave transmission analysis (Section 4.5.3) showed that the model reproduced transmitted wave heights on the lee side with reasonable accuracy, with an absolute percentage difference below 5%. Slight overestimations observed in Test Case 1 are likely due to the simplified treatment of internal flow through the porous structure and the inherent constraints of two-dimensional modelling.

For the overtopping simulations (Section 4.5.4), the simulated wave breaking phenomenon provided overtopping volumes and discharges closely aligned with those observed in the physical experiments. The model showed sensitivity to wave steepness and freeboard, reflecting the key parameters influencing overtopping on emergent RMBWs.

The adopted mesh configuration (Section 4.4.4) provided sufficient resolution in critical zones such as the crest and wave impact regions, while maintaining computational efficiency. The results were stable across all selected test cases, indicating the reliability of the grid structure for

simulating wave transformation and wave–structure interaction. Overall, the IH2VOF model is considered a reliable tool for evaluating the hydraulic performance of low-crested and emergent RMBWs under irregular wave loading conditions.

4.6.2 Friction Factor Determination for Coastalock Units

Measured overtopping discharges for the emergent RMBW in the physical model were evaluated based on the relative freeboard of the structure for five different water levels. An overtopping adjustment factor (f_q, Equation 6.13 in the EurOtop Manual (2018)) was applied to account for scale effects in the measured data. The overtopping results were compared with the overtopping formula (Equation 4-5) in the EurOtop Manual (2018). This comparison involved assessing the average overtopping discharge results from the experimental tests and comparing them with the average overtopping discharge for 1:1.5 smooth and rubble mound slopes, considering various armour units and rocks tested in the CLASH project (van der Meer et al., 2009).

$$\frac{q}{\sqrt{g \times H_{m0}^3}} = 0.09 \times \exp\left(-\left(1.5 \frac{R_c}{H_{m0} \times \gamma_f \times \gamma_\beta}\right)^{1.3}\right) \qquad \text{Equation 4-5}$$

where q represents average overtopping discharge, H_{m0} denotes significant wave height, R_c denotes crest height, γ_f is the influence factor for roughness elements, and γ_β is the influence factor for oblique wave attack. The coefficient γ_β was set to unity, following the recommendation of the EurOtop Manual (2018). The γ_f coefficient was optimized for use in Equation 4-5 with Coastalock armour units, providing a numerical result with the minimum error when compared to measured data. The optimized γ_f coefficient was determined to be 0.48.

The experimental overtopping tests used to derive the roughness factor (γ_f) were based on time series exceeding 1000 s in duration. This test length is consistent with established laboratory practice for overtopping studies (compiled in EurOtop Manual (2018)) and is considered sufficient to obtain statistically representative estimates of mean overtopping discharge. While individual overtopping events exhibit natural variability, the γ_f parameter is derived from time-averaged discharge values and is therefore less sensitive to short-term fluctuations. The numerical simulations were used to reproduce the most energetic overtopping events and to support interpretation, rather than to derive γ_f directly.

Despite the seemingly high percent error values in Table 4-6, averaging 82.7%, the correlation between the results obtained from Equation 4-5 (calculated with γ_f=0.48) and the experimental results is remarkable. This positive correlation is visually presented in Figure 4-15, illustrating the relationship between the relative overtopping rate and the relative freeboard of the structure.

Molenkamp (2022) determined γ_f as 0.73 for the 10% Coastalock armour unit spacing on an impermeable slope. Considering the permeability differences between the slopes in Molenkamp's study and the current research, a permeable slope is expected to provide lower overtopping values, resulting in a reduced γ_f value. According to the EurOtop Manual (2018), permeable structures

such as RMBWs exhibit reduced overtopping rates due to wave energy dissipation through internal flow and infiltration within the porous layers.

The γ_f value determined in this study for the permeable slope is notably lower than the value reported by Molenkamp (2022) and aligns more closely with those typically assigned to highly rough and permeable armour units. EurOtop suggests γ_f values in the range of 0.40–0.55 for rock armour and conventional armour units on permeable structures. Therefore, the result indicates that Coastalock units on permeable slopes provide comparable hydraulic roughness relative to these conventional armour types.

Table 4-6. Measured overtopping and EurOtop (2018) overtopping formula results for emergent RMBW (For TS4-X or TS5-X, the test identifier X represents the number of tests in the corresponding test series)

Test ID / Test Parameters	TS4-1	TS4-2	TS4-3	TS5-1	TS5-2	TS5-3	TS5-4	TS5-5	TS5-6	TS5-7	TS5-8	TS5-9
H_{m0} (m, model scale)	0.24	0.23	0.24	0.19	0.24	0.30	0.23	0.32	0.40	0.44	0.22	0.41
H_{m0} (m, prototype scale)	3.65	3.50	3.6	2.79	3.56	4.41	3.435	4.77	5.91	6.60	3.33	6.21
$Q_{overtop}$ (l/s/m, experiment results in prototype scale)	0. 58	2.90	19.75	1.74	2.90	20.33	21.50	66.81	159.18	366.58	74.36	646.59
$Q_{overtop}$ (l/s/m, EurOtop Equation 6.5)	0. 16	1.53	2.09	10.00	1.83	13.77	17.78	144.57	414.63	663.68	157.87	510.64
Error (%) (for γ_f=0.48)	71.9	47.5	89.4	94.4	37.0	32.3	17.3	116.4	160.5	81.1	112.3	133.6

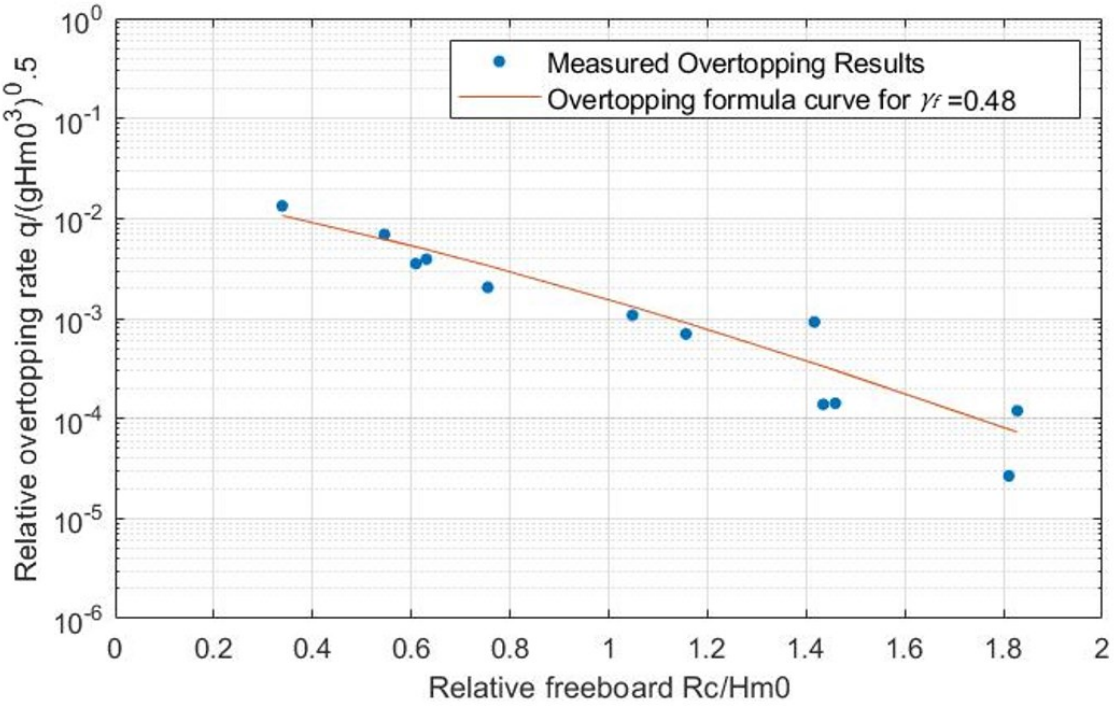

Figure 4-15. Measured and calculated relative overtopping rates

4.6.3- Key Findings and Recommendations

This study presents a comprehensive assessment of the hydraulic performance of eco-friendly rubble mound breakwaters (RMBWs) using Coastalock armour units, through a combined approach of physical and numerical modelling. The following key conclusions can be drawn:

The IH2VOF numerical model was successfully applied for the first time to simulate the characteristics of RMBWs with Coastalock armour units. Following calibration with experimental data, the model accurately reproduced wave generation, propagation, transmission, and overtopping processes. Despite minor deviations, the IH2VOF solver exhibited high reliability and robustness in simulating complex wave–structure interactions relevant to environmentally enhanced breakwater systems.

This study presents, in premiere, overtopping performance data for emergent rubble mound breakwaters armoured with Coastalock units. Both physical and numerical results, after calibrating structure-specific friction coefficients (γ_f=0.48), showed good agreement with the EurOtop (2018) formula (Equation 4-5). Coastalock units exhibited comparable overtopping performance compared to rock armouring and traditional armour units, highlighting their potential not only as a sustainable alternative but also as a reliable solution. These results underscore that eco-engineered single-layer armour systems are a rapidly emerging technology capable of meeting modern hydraulic and structural demands, while simultaneously advancing ecological functionality in coastal infrastructure.

This research also demonstrates the successful adaptation of numerical modelling techniques for evaluating eco-engineered single-layer armour units. It has provided the first numerical study for reproducing wave transmission and overtopping processes of rubble mound breakwaters with eco-engineered armour units using IH2VOF. Based on the outcomes of this integrated physical and numerical investigation on Coastalock-armoured rubble mound breakwaters, the following recommendations are proposed to guide future research and practical applications

Given the observed overtopping and wave transmission performance of Coastalock units relative to conventional armour systems reported in the literature (e.g., EurOtop 2018), design guidelines should begin incorporating provisions for eco-engineered single-layer armour systems. These should account for their unique geometrical and hydraulic characteristics, including porosity, surface texture, and bio-enhancing features.

Although the overtopping rates aligned reasonably well with EurOtop predictions after calibration, current empirical formulas are primarily developed for conventional armour units. It is recommended to develop adjusted coefficients or additional correction factors specifically for uniquely shaped armour units to improve predictive accuracy in empirical formulas.

While the IH2VOF model provided meaningful insights, certain limitations remain. These include the exclusion of dynamic armour unit motion and ecological factors such as biofilm growth or colonization impact on flow dynamics. Additionally, dynamic mesh refinement could not be utilized due to software limitations, and future work should consider models capable of dynamic mesh refinement to capture local turbulence and overtopping details more precisely. Incorporating dynamic modelling to account for potential armour unit displacement would help to assess hydraulic stability, particularly under extreme wave conditions. Extending the analysis to 3D simulations could provide more detailed insights into hydraulic performance.

Chapter 5. Design Guidelines for Coastalock Armour Units

This chapter presents a revised preprint version of the following article under review.

Sayar, S.D., Gutiérrez Martínez, J., Baker, Nistor, I., Rosenberg, Y., Hofland, B., Van den Bos, J., Colom Jover, F., Kerr, S., Lawniczak, A., Molenkamp, A., (2025). Design Recommendations for Eco-Engineered Coastalock Armour Units.

Abstract:

This paper presents the first consolidated hydraulic design recommendations for the Coastalock™ armour unit, an eco-engineered single-layer armour system. Based on 417 test runs from four independent physical modelling campaigns conducted at the National Research Council of Canada (NRC) (Baker et al., 2023; Sayar et al., 2025, 2026), and at the Delft University of Technology (TU Delft) (Molenkamp, 2022; Lawniczak, 2024), this study establishes a robust analytical basis for design. Hydraulic performance was expressed in terms of the stability number (N_s) and the Hudson coefficient (K_D) for both permeable and impermeable core with 2V:3H and 1V:2H slopes. The 2V:3H slope achieved design values of $N_s \approx 2.8$ and $K_D \approx 15$, which are comparable to other single layer systems such as Core-Loc™, Xbloc™, Accropode II™, and Cubipod®. Armour unit spacing (defined as the percentage of exposed underlayer area relative to the total armour layer area) and underlayer sizing were identified as the main effective parameters for hydraulic stability, with optimal performance achieved at a spacing of 22.5% and underlayer-to-armour layer nominal diameter ratios between 0.25 and 0.34. Overtopping analysis, calibrated against EurOtop formulas, produced γ_f values primarily between 0.65 and 0.70, reflecting the overtopping characteristics of Coastalock. Beyond hydraulic criteria, ecological monitoring indicates that Coastalock purposedly designed cavities function as water-retaining tidal pools and shaded refuges. Larger pool dimensions have been shown in independent eco-engineering studies (such as Browne and Chapman, 2011; Hall et al., 2018) to enhance intertidal refuge potential and species richness relative to flat armoured surfaces. The Coastalock cavity geometry was optimized to maximize pool volume within the constraints of armour unit stability. These findings indicate that Coastalock is a single-layer armour unit with optimized dual-purpose functionality: ensuring its hydraulic/structural functions and advancing, at the same time, the eco-engineering practice by embedding ecological enhancement into the design process. While the current recommendations are limited to the structural configurations and hydraulic conditions that were tested, they provide a solid and extensive research-based framework for preliminary design and a foundation for expanding the guidelines through future large-scale and long-term studies.

Keywords: Coastalock, single-layer armour units, design guidelines, hydraulic stability, overtopping, underlayer design, eco-engineering, biodiversity enhancement

5.1. Introduction

The design of coastal protection structures has traditionally focused on providing reliable resistance against wave attack and storm surge, with rubble mound breakwaters and revetments forming the basis of modern shoreline defence systems. These structures are effective in dissipating incident wave energy and maintaining stability under extreme loading conditions. However, the escalating pressures of climate change, environmental standards and coastal urbanization have amplified the demand for resilient and adaptable coastal defence systems, requiring innovative approaches that balance hydraulic stability, constructability, and long-term sustainability (Hinkel et al., 2014; Morris et al., 2020).

Concrete armour units are a cornerstone of rubble mound breakwater design, valued for their ability to provide high hydraulic stability while minimizing material use. Modern single-layer units are engineered to combine interlocking capacity with ease of placement, offering significant advantages like minimizing concrete consumption over traditional double-layer systems such as Tetrapods and Dolosse (Reedijk and Muttray, 2009; Park et al., 2019). Over the past decades, proprietary armour units including Core-Loc™, Xbloc®, XblocPlus®, Accropode II™, and Cubipod® have been widely adopted, each accompanied by dedicated design manuals that define geometric placement rules, stability coefficients, hydraulic performance parameters, and construction tolerances (Medina and Gómez-Martín, 2016; USACE, 2002; CLI, 2023; DMC, 2023). These guidelines provide standardized methodologies for armour layer sizing and stability assessment under wave loading, enabling reliable worldwide applications of these units in large-scale coastal infrastructure.

While armour units have been optimized primarily for hydraulic stability, their environmental footprint has raised concerns, as they typically provide limited habitat heterogeneity and may promote invasive species colonization (Chapman and Bulleri, 2003; Bulleri and Chapman, 2010; Dafforn et al., 2015; Strain et al., 2018). Recent eco-engineering innovations have targeted the limitations of conventional armour units by introducing geometric modifications, surface texturing, and bio-enhancing concrete mixes that promote native species settlement while maintaining hydraulic stability (Browne and Chapman, 2011; Sella and Perkol-Finkel, 2015; Sella et al., 2022). Nature-inclusive features such as tidal pools, ecological cavities, and bio-enhancing materials have proven effective in satisfying coastal protection objectives while incorporating biodiversity enhancement (Hall et al., 2018; Sella et al., 2022).

The Coastalock armour unit was developed in 2021 as part of this eco-engineering transition, aiming to combine the hydraulic performance of modern single-layer units with features that enhance marine biodiversity. Its geometry includes interlocking elements that ensure stability under wave impact, while integrated cavities and textured surfaces create shaded, moisture-retaining microhabitats that support species recruitment and survival across tidal zones (Sella and Perkol-Finkel, 2015; Gutiérrez et al., 2023). By integrating ecological functionality into

conventional engineering design, Coastalock establishes a dual-purpose coastal defence solution that provides reliable coastal defence and measurable ecological benefits.

Since its development, Coastalock has been evaluated in a series of physical modelling campaigns that progressively advanced the understanding of its hydraulic performance. Molenkamp (2022) first investigated revetments with impermeable cores at deeper water, showing unit stability and the onset of uplift-driven instability mechanisms. Lawniczak (2024) extended this work to permeable rubble mound slopes, testing variations in unit spacing, underlayer configurations, and toe armour. Sayar et al. (2024, 2025) conducted systematic physical modelling of low-crested and emergent rubble mound breakwaters (RMBWs), providing detailed insights into hydraulic stability behaviour, failure mechanisms, and hydraulic performance, including wave transmission and reflection. These studies also introduced the integration of ecological design considerations within the hydraulic assessment framework. Subsequently, Sayar et al. (2026) extended this work through combined physical and numerical modelling with overtopping data, validating the hydraulic response of Coastalock-armoured structures and enabling broader interpretation of the experimental results under a wider range of wave conditions. Baker et al. (2023) evaluated revetments with milder slopes over an impermeable core, further expanding the dataset under diverse wave conditions.

Unlike established proprietary systems such as Core-Loc, Xbloc, Accropode II, and Cubipod, which are supported by detailed design manuals defining stability numbers, Hudson coefficients, and overtopping roughness factors, Coastalock currently lacks consolidated design recommendations for engineering applications. The absence of such guidance creates uncertainty for designers, as results from existing experimental studies remain scattered across different configurations and test conditions. Developing a unified design framework is therefore essential to support the use of Coastalock in practical projects.

This thesis aims to develop the first comprehensive design recommendations for the ecologically engineered (eco-engineered) Coastalock single-layer armour unit, integrating findings from multi-institutional physical modelling campaigns. By systematically analyzing hydraulic stability numbers (N_s), Hudson coefficients (K_D), overtopping roughness factors (γ_f), and underlayer-to-armour size ratios, this thesis derives design recommendations that extend existing rubble mound design practice to Coastalock configurations. Beyond hydraulic considerations, the framework also incorporates ecological functionality by evaluating multiple orientations with regular placement, positioning Coastalock as a dual-purpose unit that addresses both engineering and environmental objectives.

5.2. Literature Review

5.2.1 Coastalock Development and Prior Studies

The Coastalock armour unit (Figure 5-1A) was specifically developed to combine hydraulic efficiency with ecological functionality and regular placement by integrating geometric and

material innovations into a single-layer armour element. Its interlocking form (Figure 5-1B) enables stable, regular placement at controlled lateral spacings, a key design variable in Coastalock applications. Unit spacing refers to the intentional lateral gap between adjacent Coastalock units, expressed as the percentage of exposed underlayer area relative to the total plan area of the armour layer. This spacing governs the porosity of the armour layer, influencing internal flow penetration, uplift pressures, and interlocking performance. Although placement density can vary for many single-layer armour units within recommended limits, spacing was treated as primary and systematically varied design parameter in the Coastalock experimental program. While the cavity volume of individual Coastalock units is fixed and independent of spacing, increasing spacing enhances the overall availability of habitat spaces within the armour layer. In addition, larger spacing reduces the total number of units required, thereby decreasing concrete consumption for a given design condition.

Distinct from conventional systems, Coastalock incorporates a cavity in the center of the unit that can be placed with different orientations (cavity upward, sideways, and downward), creating multiple habitat features: water-retaining niches, caves, overhangs, and shaded refuges across tidal elevations, promoting colonization by multiple and different marine organisms at different life stages (Figure 5-1C). In addition, the unit is cast using a bio-enhancing concrete formulation and incorporates micro-textured surfaces that improve larval settlement and long-term adhesion (Sella and Perkol-Finkel, 2015; Gutiérrez et al., 2023). These combined features position Coastalock as an eco-engineered alternative capable of achieving both hydraulic and ecological performance objectives.

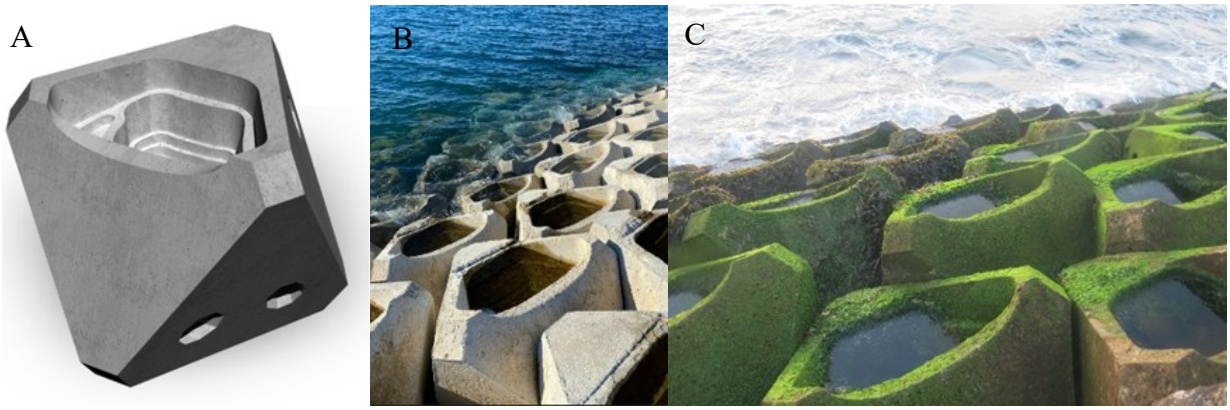

Figure 5-1. Design and field application of Coastalock units. (A) unit geometry highlighting ecological cavities; (B) Port of Vigo (Spain) installation at completion; (C) the same installation after one year, demonstrating rapid biological growth on the units

Experimental campaigns have examined Coastalock performance across a wide range of structural and hydraulic conditions, including impermeable-core revetments (Molenkamp, 2022), permeable revetments with unit spacing and orientation variations (Lawniczak, 2024), emergent rubble mound breakwaters (RMBW) with hydraulic stability and performance outcomes (Sayar et al., 2025), and milder-slope revetments under diverse waves (Baker et al., 2023). The scope of these

studies is summarized in Section 5.3.1, which consolidates regular placement features and structural parameters such as slope geometry, core permeability, spacing, underlayer size, and toe configuration.

5.2.2 Eco-Engineering in Coastal Structures

Eco-engineering strategies for coastal infrastructure have been increasingly adopted to address biodiversity loss caused by conventional hard coastal protection systems (Moschella et al., 2005; Firth et al., 2016; Strain et al., 2018). Field and laboratory studies show that modifications such as bio-enhancing concrete mixes, micro-textured surfaces, and tidal pool modules can significantly increase species richness and habitat heterogeneity compared to smooth concrete or armour rock (Sella and Perkol-Finkel, 2015; Hall et al., 2018; Morris et al., 2020).

Bio-enhancing concrete formulations enriched with mineral admixtures and surface micro textures improve larval settlement and survival of native species, while cavity-forming designs such as tidal pools or overhangs increase habitat complexity across tidal zones (Browne and Chapman, 2011; Morris et al., 2020). For example, bio-enhancing concrete panels installed on seawalls in the Mediterranean supported up to 50% greater colonization by sessile invertebrates compared to standard panels (Sella and Perkol-Finkel, 2015). Similarly, tidal pool features integrated into armour units have been shown to sustain intertidal communities during low tide exposure, providing refuges that enhance persistence of canopy algae and grazing invertebrates (Evans et al., 2016; Hall et al., 2018).

Reviews and recent experimental studies suggest that, under certain conditions, habitat enhancements (e.g., surface texture, crevices, small protrusions) can be integrated into or retrofitted onto coastal structures without adverse hydraulic effects. Surface protrusions on revetments are a well-established means of reducing overtopping on dike revetments, as reflected in the roughness reduction factors presented in the EurOtop Manual (2018). In a flume experiment on vertical walls, surface protrusions reduced mean overtopping rates by increasing roughness (Salauddin et al., 2021). However, most trials do not strongly document stability impacts on rubble mound or armour units placed on steep slopes, and many authors mention that any hydraulic benefit depends heavily on geometry, wave regime, and placement configuration (such as Salauddin et al., 2021; Perricone et al., 2023). In essence, while surface enhancements are hydraulically promising, their influence must be evaluated case by case rather than assumed to be universally beneficial.

5.2.3 Design Parameters in Established Armour Unit Guidelines

Design manuals for proprietary armour units provide engineers with explicit stability numbers (N_s), Hudson coefficients (K_D) (defined in Section 5.3.2.1), and overtopping roughness factors (γ_f) (defined in Section 5.3.2.3) derived from systematic physical model studies.

The hydraulic stability of armour layers is generally described in terms of either K_D or N_s (USACE, 1984; USACE, 2002). Historically, Hudson's formula (Hudson, 1959), which assumes regular wave conditions, provided a simple way to determine the required armour unit weight without

incorporating the effects of parameters such as wave steepness, storm duration or structure permeability. As a result, its direct applicability to interlocking single-layer armour systems is limited and it is not recommended for their design. Reported Hudson coefficients (K_D) for such systems are often presented for comparison purposes only. Recommended Hudson coefficients vary widely by unit type, placement, and slope steepness application. For quarried rock in non-breaking waves, typical values are $K_D \approx 3–4$, whereas double-layer concrete shapes such as cubes or Tetrapods achieve K_D values around 6–8 (USACE, 1984; CIRIA, 2007).

Van der Meer (1988) extended these approaches to irregular wave conditions and variable damage levels, showing that stability of rock slopes decreases with wave steepness and storm duration, while a limited degree of damage may be acceptable for double-layer armours. For single-layer interlocking units (such as Accropode, Core-Loc, and Xbloc), the recommended design practice allows no damage (i.e., no large unit displacements or extractions) at the design wave height, in consequence of the brittle damage behaviour where an initial unit extraction more quickly leads to progressive damage development. In physical model testing of such interlocking systems, stability criteria typically distinguish between acceptable rocking motion and unacceptable unit displacement or extraction. Manufacturers commonly impose limits on allowable rocking during testing to prevent unit breakage, as excessive rocking may precede structural damage of the unit itself or progressive layer destabilization. Thus, the “no damage” condition refers to the absence of significant displacement or extraction of armour units, while limited rocking may still occur. Consequently, the design N_s for single-layer systems are typically in the range of N_s=2.4–2.8, corresponding to K_D of 12–16 (for the 2:3 or 3:4 slopes applied), depending on slope steepness and placement density (Melby and Turk, 1997; Bakker et al., 2003; Reedijk and Muttray, 2009).

Another important parameter for design is the roughness factor γ_f used in overtopping assessments (EurOtop, 2018). Rough, porous armour layers reduce wave run-up and overtopping by increasing turbulence and energy dissipation. Typical γ_f values are about 0.40 for rock armour in a double layer and 0.44–0.47 for most single-layer armour units (Bruce et al., 2009).

Table 5-1 summarizes representative design parameters for conventional and proprietary armour units. The N_s and K_D values correspond to preliminary design conditions for breakwater trunk sections under breaking waves (USACE, 1984; van der Meer, 1988; USACE, 2002; CIRIA, 2007; Bruce et al., 2009; Reedijk and Muttray, 2009; Medina and Gómez-Martín, 2014; CLI, 2023; DMC, 2023), and the γ_f values are roughness factors from the EurOtop Manual (2018).

Table 5-1. Typical hydraulic design constants for rock slopes and established armour units

Armour Unit	Design Stability Number (N_s)	Hudson Coefficient (K_D)	Overtopping Roughness Factor (γ_f)
Accropode II (single layer)	2.5 [1,3]	12	0.46
Core-Loc (single layer)	2.8 [1,3]	16	0.44
Cube (single layer)	2,2 [2,3]	7	0.47
Cubipod (single layer)	2.5 [2,4]	12	0.47
Dolos (double layer)	2.5 [2,3]	12	0.43
Tetrapod (double layer)	2.2 [2,4]	7	0.38
Xbloc (single layer)	2.8 [1,3]	13	0.44
XblocPlus (single layer)	2.5 [1,3]	12	0.45

[1] Design N_s, corresponding K_D and γ_f for a 3V:4H slope. [2] Design N_s, corresponding K_D and γ_f for a 2V:3H slope. [3] no damage condition. [4] initial damage condition.

5.2.4 Research Gaps

The available literature on Coastalock has provided important insights into hydraulic stability, unit spacing effects, underlayer requirements, and overtopping performance across different structural configurations. However, these findings are dispersed among separate studies and have not yet been unified into a comprehensive basis for design. Conventional single-layer units such as Accropode II, Xbloc and XblocPlus, Cubipod, and Core-Loc are supported by well-established guidelines that provide explicit stability numbers, design equations for armour sizing, and clear recommendations on underlayer size and overtopping protection (USACE, 2002; Medina and Gómez-Martín, 2016; CLI, 2023; DMC, 2023).

For Coastalock, no comparable set of design-oriented recommendations exists, leaving practitioners uncertain about how to transform experimental results into engineering guidelines. Currently, several Coastalock applications (European Commission, 2023; ECOncrete, 2023, 2024) have been implemented at the Port of San Diego (USA), the Port of Vigo (Spain), the Port of Bilbao (Spain), and the Port of Prince Rupert (Canada), with a standard unit size (1.42 m^3), while a bigger unit size (2 m^3) was used for more challenging climatic conditions in Monaco. The lack of engineering design guidelines constrains its broader and more systematic application.

Addressing this gap requires consolidating available experimental outputs into a unified framework that can inform the preliminary design of Coastalock-armoured coastal structures.

5.3. Materials and Methods

5.3.1. Summary of Coastalock Experiment Datasets

This study relies on the synthesis of experimental results collected across multiple institutions to establish a robust foundation for the Coastalock design guidelines. Four experimental campaigns conducted at Delft University of Technology (TU Delft) (Molenkamp, 2022; Lawniczak, 2024) and the National Research Council of Canada (NRC) (Baker et al., 2023; Sayar et al., 2025), provide the most comprehensive dataset currently available and serve as the empirical basis for the hydraulic performance and analyses presented in this paper. The structural layouts tested in these campaigns are illustrated in Figure 5-2, while the corresponding hydraulic and geometric parameters are summarised in Table 5-2.

A

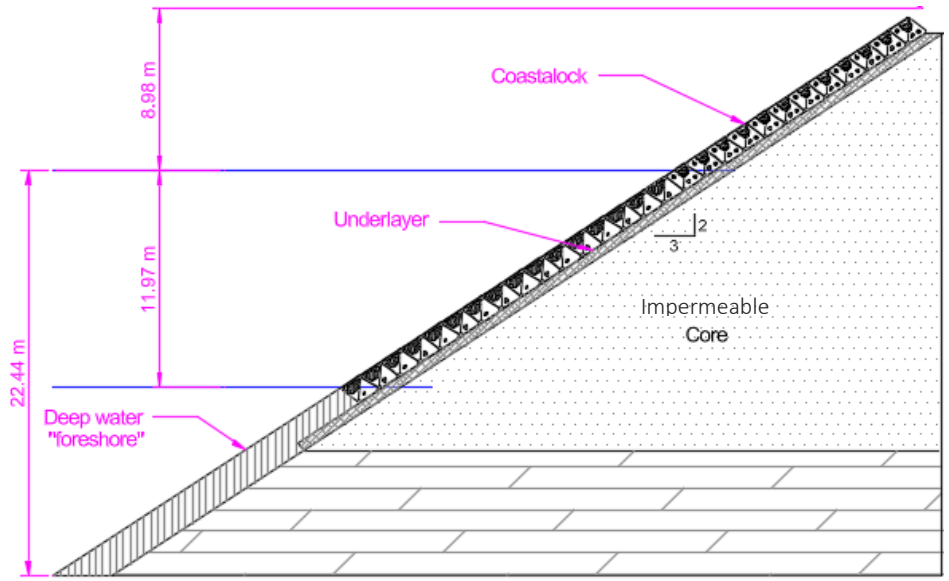

B

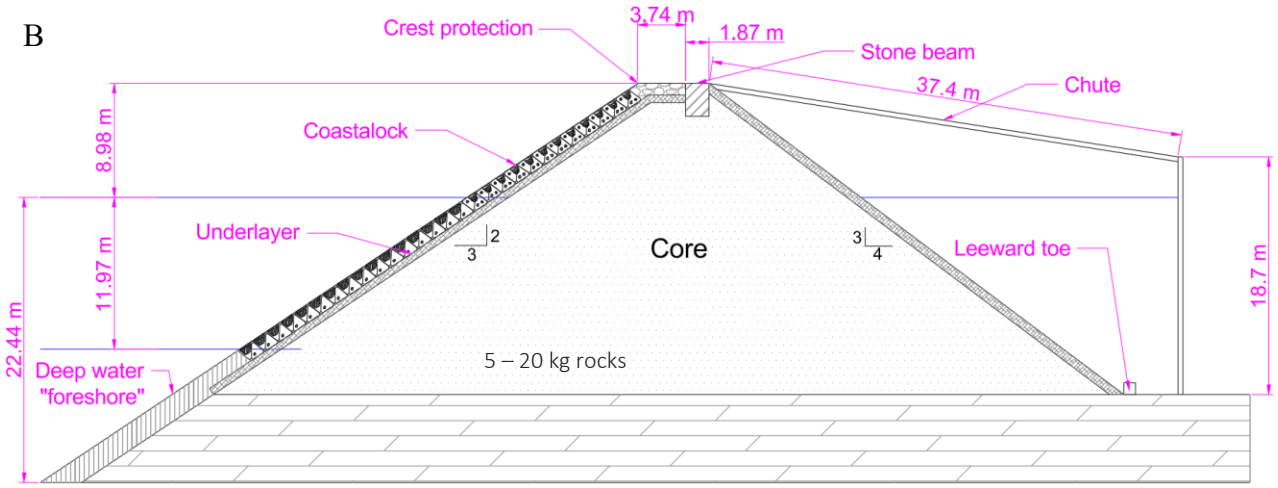

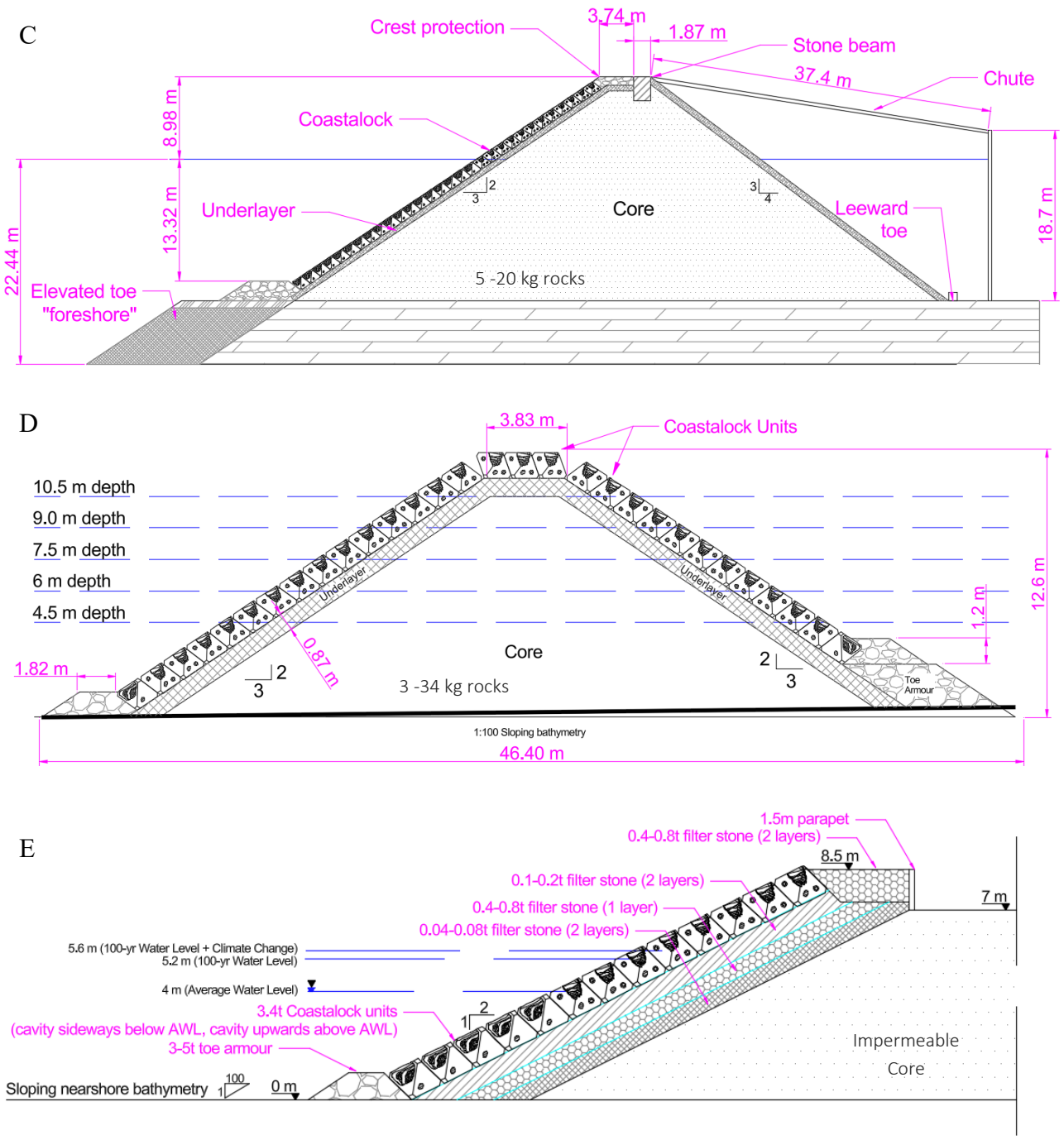

Figure 5-2. Structural configurations (in prototype scale) tested in Coastalock studies: (A) Molenkamp (2022), (B) structure without toe in Lawniczak (2024), (C) structure with toe in Lawniczak (2024), (D) Sayar et al. (2025) and (E) Baker et al. (2023)

The experimental campaigns tested a variety of structural configurations representative of conventional rubble mound coastal structures. These included revetment slopes of 2V:3H (as shown in Figure 5-2A, 5-2B and 5-2C) and 1V:2H (in Figure 5-2E), as well as a conventional RMBW (in Figure 5-2D) with a 2V:3H front and rear slope. The test sections differed in the

presence or absence of a foreshore, water depth, slope steepness, toe configuration, underlayer grading and thickness, core permeability, crest elevation and material, and armour unit spacing and orientation, which provide a diverse basis for assessing the hydraulic stability and performance of Coastalock units under multiple design conditions. Although additional experiments on submerged breakwater configurations were performed as part of Sayar et al. (2025), these are intentionally excluded from the present synthesis, which focuses on emergent structures. Nevertheless, those low-crested datasets contribute valuable insight into Coastalock performance under reduced freeboard conditions and are acknowledged in the broader interpretation of the unit's hydraulic behaviour.

Different Coastalock unit orientations were adopted across the experimental programs to investigate how the cavity position might influence hydraulic stability performance. Figure 5-3 illustrates the Coastalock configurations tested by Lawniczak (2024). The San Diego orientation, first applied for the Port of San Diego prototype project and subsequently used in the TU Delft experiments, refers to a mixed configuration in which rows below the mean low water level are placed with the cavity sideways, creating a cave, while upper rows are placed cavity forwards, forming water-retaining tide pools to promote ecological enhancement. In contrast, the cavity sideways and cavity forwards orientations isolate each of these configurations to examine their individual hydraulic responses. The cavity forwards orientation positions the main cavity facing vertically forward, creating a tide pool at low tide.

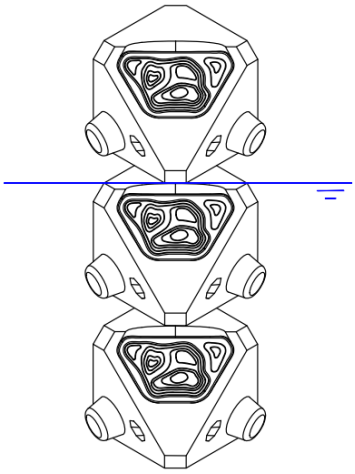

Figure 5-3. Vertical arrangement of Coastalock armour units on a slope in a cavity-forward orientation relative to the still water level (SWL)

Additional orientations, including the cavity downwards from design water level to the bottom, were introduced by Lawniczak (2024) and were designed to align the cavity openings at specific elevations relative to the still-water level or the vertical midpoint of the armour layer, respectively, enabling targeted evaluation of water-retention and flow-through characteristics under varying tidal conditions.

Armour unit spacing was defined as the horizontal centre-to-centre distance between adjacent units within the same row, measured parallel to the slope surface. The spacing percentage, *S*, was calculated relative to the nominal armour diameter D_{n50} in Equation 5-1 as:

$$S(\%) = \frac{d_{cc} - D_{n50}}{D_{n50}} \times 100 \qquad \text{Equation 5-1}$$

where d_{cc} denotes the centre-to-centre distance between neighbouring units. A spacing of 0% corresponds to units placed in direct contact without intentional gaps.

Meanwhile, an important feature in Lawniczak (2024) was the inclusion of protrusions (refer to Figure 5-4) in the armour units tested to provide the same spacing as for 10% and 22.5% spacing. These protrusions are small extensions integrated into the Coastalock geometry, designed to ensure the porosity of the Coastalock armour while maintaining hydraulic stability and the interlocking between units, and contribute to keep the underlayer material in place under significant wave loading.

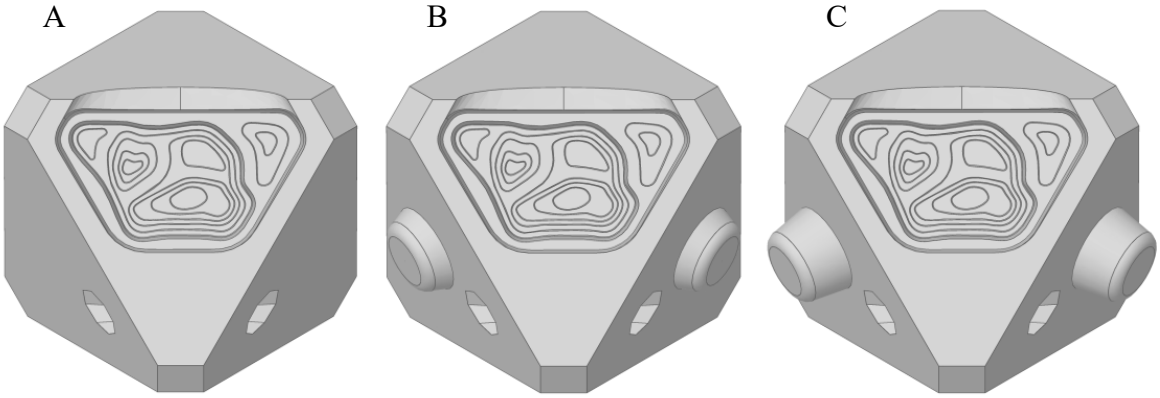

Figure 5-4. Coastalock armour units: (A) standard design, (B) design with protrusions for 10% spacing and (C) design with protrusions for 22.5% spacing

As summarised in Table 5-2, the dataset covers stability numbers approximately within the range $N_s \approx 0.49$–4.66 and relative wave heights (H_s/h) ≈ 0.03–0.90, indicating coverage from low loading to design-level conditions with a range of wave steepness (S_{op}) values (2.0%–6.5%), variable crest geometries, and different underlayer and toe arrangements. The four campaigns differed in scale, flume facilities, and structural details, which is needed to obtain generally applicable robust conclusions. Still their designs were based on the same Coastalock unit design and comparable rubble mound geometries and followed similar hydraulic modelling protocols. The merged dataset, consisting of 417 individual test runs, demonstrates that the dataset is well-distributed in terms of tested wave heights, wave steepness, underlayer sizes, and unit spacings, which enables direct comparison across tested configurations. This common base justifies consolidating the results into a single database to support the analyses presented in Section 6.3.2 and the design recommendations developed in Section 6.6.

Table 5-2. Summary of key structural and hydraulic parameters for Coastalock physical model studies in the literature (PT: Coastalock units with protrusions)

Parameter / Study	Molenkamp (2022)	Lawniczak (2024)	Sayar et al. (2025)	Baker et al. (2023)
Scale	1/37.5	1/37.5	1/15	1/15
Breakwater type	Revetment	Revetment	Emergent RMBW	Revetment
Front slope	2V:3H	2V:3H	2V:3H	1V:2H
Significant wave height (H_s)	0.71 – 6.39m	2.44 – 6.14m	1.31 – 6.58m	1.79 – 4.18m
Corresponding stability number (N_s)	0.49 – 4.42	1.68 – 4.19	0.93 – 4.66	0.98 – 2.30
Wave steepness (s_{op})	2% – 6%	2% – 4%	3.3% – 6.5%	3.5% – 6%
Armour unit size	1.42 m^3	1.42 m^3	1.42 m^3	1.42 m^3
Armour layer thickness	1.25 m	1.25 m	1.25 m	1.25 m
Armour unit spacing	0%, 5%, 10%, 15%, 20%, 25%	0%, 10% (PT), 20%, 22.5% (PT)	10%	10%
Underlayer material diameter (d_{n50})	0.25 m	0.30 m	0.36 m	0.46 m
Underlayer thickness	0.50 m (2 layers), 0.85 m (~3 layers)	0.60 m (2 layers)	0.87 m (~2 layers)	0.77 m (~2 layers)
Structure height	31.5m	31.5 m	12.6 m	8.5m
Crest width	0 m	5.61 m	4.5 m	4.0 m
Water depth at toe	18.0 m	22.4 m	4.5 m, 6.0 m, 7.5 m, 9.0 m, 10.5 m	4.0 m, 5.2 m, 5.5 m
Core type	Impermeable	Permeable	Permeable	Impermeable
Unit orientation	San Diego, Cavity Sideways, Cavity Forwards	San Diego, PO-SWL, Forwards, PO-Midpoint	Cavity Forwards	Cavity Forwards
CL unit design	Standard	Standard and CL with protrusions	Standard	Standard
Toe height	No toe	No toe / 2.21 m	0.75 m	1.15 m

5.3.2. Data Analysis

5.3.2.1. Hydraulic Stability Analysis

The hydraulic stability of single-layer armour units was evaluated using the stability number (N_s), a non-dimensional index originally introduced by Hudson (1959) and widely applied in rubble mound armour design. N_s is defined in Equation 5-2 as

$$N_S = \frac{H_S}{\Delta\, D_n}$$ Equation 5-2

where H_s is the incident significant wave height, D_n is the nominal diameter of the armour unit, and Δ is the relative submerged density ($\Delta = \frac{\rho_r}{\rho_w} - 1$). The N_s expresses the ratio between the applied wave loading and the resisting weight of the unit. This formulation provides a direct comparison of armour performance across scales and configurations and serves as the reference parameter for subsequent design recommendations.

To establish design-relevant stability limits, N_s was calculated for each test regardless of the instability occurrence using the measured significant wave height, armour unit size, and relative density. These values were then matched with the observed binary outcome (stable or unstable) to determine the range of $N_s$associated with the onset of failure, defined here as visible armour unit displacement or extraction exceeding the stability criteria adopted in each experimental campaign. Since stability was recorded as a binary outcome, the exact critical condition cannot be observed directly but is constrained between consecutive test conditions. This is consistent with the discrete definition of damage levels in physical modelling, where continuous damage evolution is represented by threshold-based criteria (e.g., Vidal et al., 1991). Following common laboratory practice for threshold-type phenomena, the critical condition was therefore identified by interpolating stability numbers between the highest stable and lowest unstable runs. This provides a single representative threshold consistent with stability limits derived from discrete experimental observations and damage-based design approaches (Van der Meer, 1988; CIRIA et al., 2007), and comparable to the deterministic stability numbers of Hudson (1959) and Van der Meer (1988).

The stability numbers calculated from the consolidated dataset span a broad range of conditions. To visualize these outcomes, Figure 5-5 presents the distribution of N_s values for tests conducted with permeable cores and varying armour unit spacings, while Figure 5-6 illustrates the corresponding distributions for impermeable core configurations. These figures highlight the transition between stable and unstable outcomes, which formed the basis for identifying critical thresholds. The 10% and 22.5% spacing data from Lawniczak (2024) shown in Figure 5-5 corresponds to tests conducted with Coastalock units with protrusions, whereas the remaining data in Figure 5-5 and all data presented in Figure 5-6 represent tests performed with the standard Coastalock geometry.

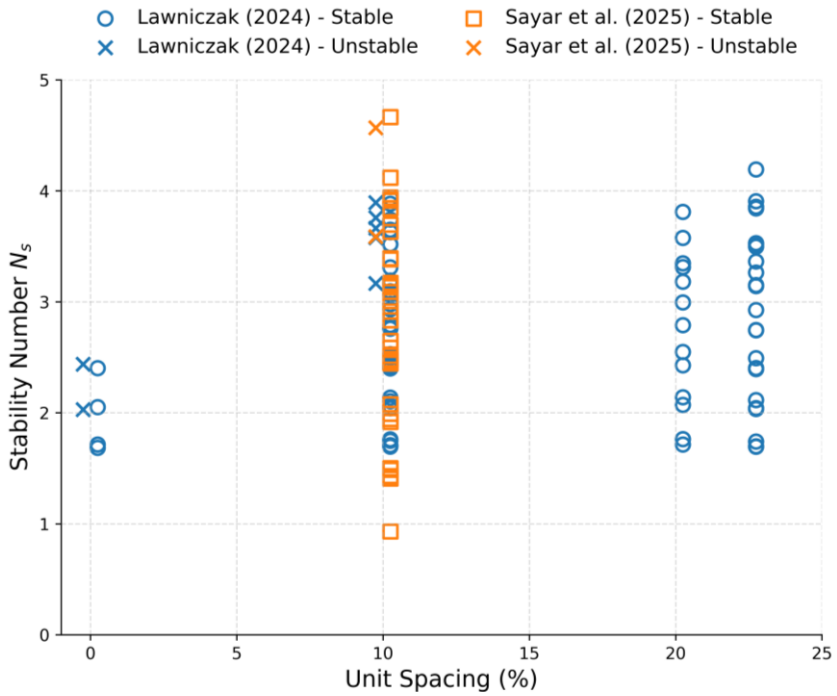

Figure 5-5. Stability number (N_s) distribution for Coastalock units placed on permeable cores with different spacings. Each marker references one test run. Stable test cases are shown with hollow markers, while unstable cases are indicated with "×" markers. Stable and unstable markers are shifted slightly right & left (respectively) for visual clarity.

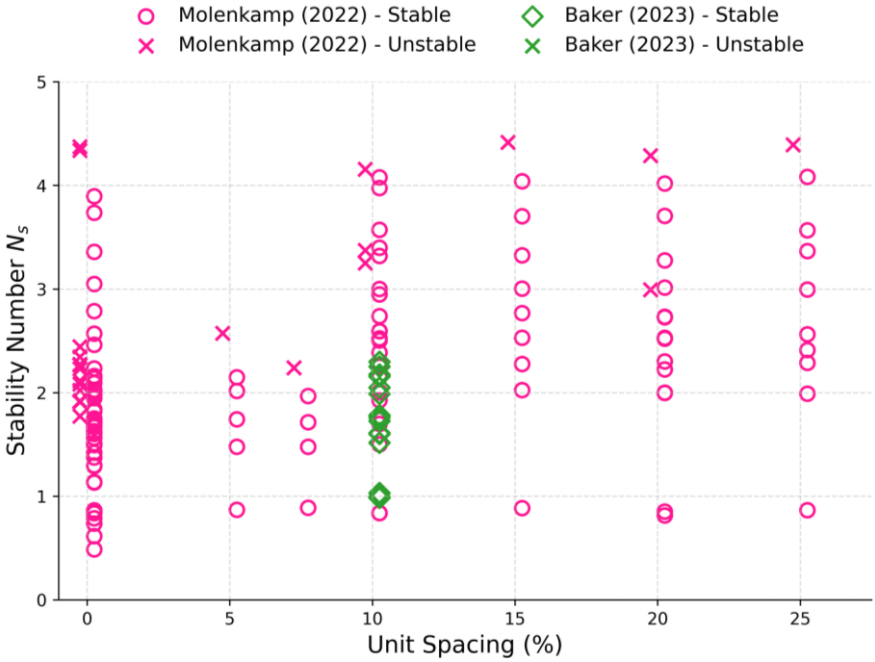

Figure 5-6. Stability number (N_s) distribution for Coastalock units (without protrusions) placed on an impermeable core. Each marker references one test run. Stable test cases are shown with hollow markers, while unstable cases are indicated with "×" markers. Stable and unstable markers are shifted slightly right and left (respectively) for visual clarity.

The plotted results in Figures 5-5 and 5-6 indicate that the datasets converge within comparable ranges of N_s (and corresponding H_s values, since identical prototype unit properties were applied), despite differences in scale and structural configuration. The colour coding of individual studies facilitates direct visual comparison and demonstrates that Coastalock stability trends remain mostly consistent across permeable and impermeable cores. Differences in unit spacing are also evident, with permeable cores generally producing higher N_s values than impermeable sections.

In line with the objective of proposing a baseline design configuration for practical applications, the stability analysis focused on tests of both permeable and impermeable core sections. For each configuration, the critical N_s was used to calculate the corresponding K_D through the classical Hudson (1959) relationship, as shown in Equations 5-3 and 5-4:

$$W = \frac{\gamma_r {H_s}^3}{K_D \Delta^3 cot\theta} \qquad \text{Equation 5-3}$$

$$K_D = \frac{H_s}{N_s\, cot\theta} \qquad \text{Equation 5-4}$$

In line with conventional practice in rubble mound armour design, a safety factor is typically applied to laboratory-derived N_s to account for prototype uncertainties related to wave climate, construction tolerances, and scale effects (USACE, 2002; CIRIA, 2007). Considering these established recommendations and recognizing the distinctive geometry, placement precision, and interlocking mechanism of the Coastalock unit, a global safety factor of 1.5 was applied to the experimentally determined critical N_s values to account for experimental scatter, scale effects, and the limited number of observations. This approach provides conservative design N_s and corresponding K_D values, consistent with the safety margins typically adopted for established single-layer armour systems, as summarized in Tables 5-5 and 5-6.

As an additional conservatism check, a lower-tail statistical estimate was performed on the impermeable core configurations with spacing ≥ 10%. This subset was selected because it represents comparable cases, while also providing multiple independent configurations within a consistent structural configuration. The sample mean and standard deviation are 3.76 and 0.75, respectively. Using a one-sided 5% lower confidence bound based on the Student-t distribution (number of samples is 4, degree of freedom is 3), the conservative estimate of the critical stability number is approximately $N_{s-critical,5\%} \approx 2.0$. This statistical approach was not extended to all configurations due to the limited number of independent cases within other subsets and the heterogeneity in tested configurations arrangements, which would not provide a statistically meaningful estimate. The resulting lower-tail value is consistent with the adopted design stability number obtained by applying the global safety factor of 1.5 to the experimentally observed critical values.

5.3.2.2. Underlayer Assessment

Since the interaction between the armour layer and its supporting filter layer is fundamental to the performance of single-layer armour systems, the experiments were analyzed with respect to the

effect of the underlayer-to-armour nominal diameter ratio (D_{n50}/D_n). This ratio reflects the relative capacity of the underlayer to resist uplift and prevent armour displacement and to prevent wash out of the small material and has been emphasized in several armour unit design guidelines. For the Coastalock dataset, cases were categorized into different D_{n50}/D_n classes, which allowed the effect of underlayer sizing on N_s to be systematically evaluated. The grouping and corresponding stability outcomes are summarized in Figure 5-7. Within each D_{n50}/D_n class, the associated N_s were compared against the binary stability outcomes to identify the transition between stable and unstable results.

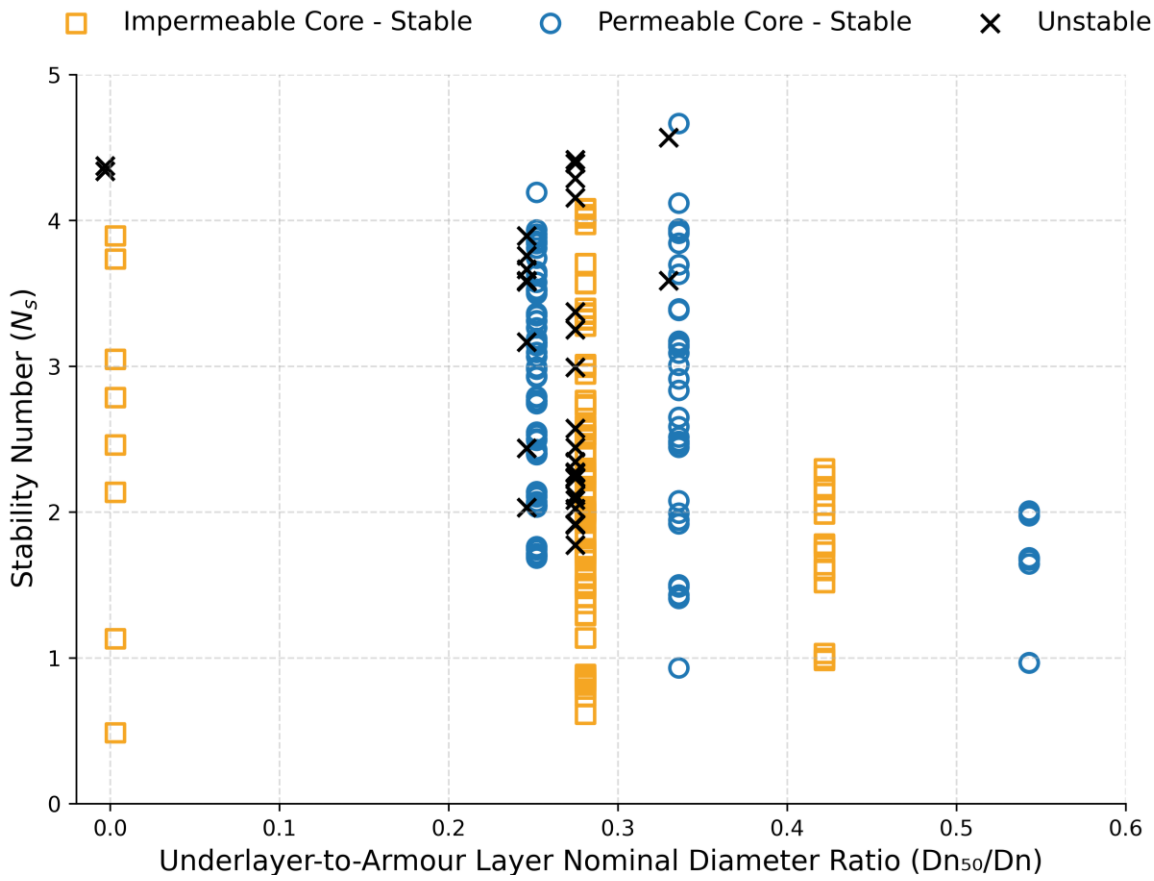

Figure 5-7. Stability number (N_s) versus underlayer-to-armour layer nominal diameter ratio (Dn_{50}/D_n) for Coastalock units placed on permeable and impermeable cores. Stable test cases are shown with hollow markers, while unstable cases are indicated with crosses.

5.3.2.3. Overtopping Analysis

Wave overtopping was analyzed by expressing the mean overtopping discharge in a non-dimensional form (EurOtop 2018). For each test, the overtopping volumes collected behind the crest of the structure were converted into a mean discharge per unit width (q). These values were then normalized as $q/(gH_s^3)^{0.5}$ which allows direct comparison of the Coastalock measurements with the empirical EurOtop prediction curves, providing thus a consistent framework for assessing overtopping performance.

The influence of the armour unit characteristics was incorporated by calibrating the roughness factor (γ_f) against the EurOtop (2018) prediction formula (presented here as Equation 5-5) for mean overtopping discharge:

$$\frac{q}{\sqrt{g \times H_s^3}} = 0.09 \times exp\left(-(1.5 \frac{R_c}{H_s \times \gamma_f \times \gamma_\beta})^{1.3}\right) \quad \text{Equation 5-5}$$

Here, q is the mean overtopping discharge per unit width, R_c is the crest freeboard, H_s is the incident significant wave height, and γ_β represents the obliquity factor, respectively. The calibration employed a best-fit optimization, in which γ_f was varied until the error between the measured and predicted non-dimensional discharges was minimized. This approach provided an objective means of identifying optimum γ_f values for Coastalock-armoured slopes, ensuring that the experimental data could be consistently expressed within the standard EurOtop methodology. The optimized γ_f values derived from this calibration are presented in Section 5.4.4 and provide the empirical basis for the overtopping recommendations outlined in Section 5.6.

5.3.2.4. Toe Stability Assessment

Because the stability of rubble mound armour is strongly related to the design of the toe structure, this element was explicitly included in the Coastalock analysis. Test cases were grouped according to their structure's toe dimensions. The methodology for this classification is provided in Table 5-3, while the corresponding hydraulic conditions for each configuration are summarized in Table 5-4. Since the dataset contained a single case where instability was attributed to toe failure, this condition was analyzed separately to better understand its underlying causes. For the remaining stable cases, the tested toe rock weights and configurations were systematically compared to the values predicted by the Van der Meer (1996) toe stability formula, which has become a standard reference in rubble mound toe design. The most critical case for toe design was used for the formula calculations. The tested toe rock weights spanned a range of configurations, and their differences from the calculated values highlighted the influence of experimental design choices on observed performance.

Table 5-3. Summary of toe berm configurations used in Coastalock physical model studies

Study	Toe rock D_{n50} (m)	Prototype-scale toe rock weight (kg)	Model-scale toe rock weight (kg)	Grading	Geometry	Surface type beneath the toe
Sayar et al. (2025)	0.72	506	0.150	340-680 kg	3 rocks wide, 2 rocks high	Concrete seabed
Lawniczak (2024)	1.09	1817	0.235	d_{85}/d_{15}= 1.19	3 rocks wide, 2 rocks high	Glued rock (rough and smooth)
Baker et al. (2023)	1.42	3973	1.180	3000-5000 kg	2 rocks wide, 1 rock high	Concrete seabed

Table 5-4. Required toe rock size and weight calculated using the Van der Meer (1996) toe stability formula for Coastalock physical model tests with a permeable core. The calculated values correspond to the most critical conditions for toe stability tested in each study (H_s: significant wave height, h_t: vertical distance from the toe berm to the still water level, h: still water level)

Study	H_s (m)	h_t (m)	h (m)	Calculated toe rock D_{n50} (m)	Calculated toe rock weight (kg)	Tested toe rock weight (kg)
Sayar et al. (2025)	6.58	7.80	9.00	0.58	268	506
Lawniczak (2024)	6.14	13.31	22.43	0.95	1206	1817
Baker et al. (2023)	4.19	4.33	5.50	0.44	115	3973

5.4. Hydraulic Performance of Coastalock

5.4.1. Hydraulic Stability Assessment

The consolidated dataset was examined to identify the primary parameters governing Coastalock stability across all tested configurations. Particular attention was given to relative freeboard, armour unit spacing, and underlayer grading, which consistently influenced the onset of instability.

5.4.1.1 Standard Coastalock Design

The stability performance of the Coastalock armour layer was expressed in terms of the stability number (N_s), following the conventional approach used in RMBW design practice. The results revealed a distinct threshold behaviour: stable configurations were maintained up to moderate values of N_s, whereas instability emerged once this limit was exceeded, providing a clear benchmark for performance evaluation.

A consistent trend was observed between core type and hydraulic response. Permeable-core structures exhibited higher N_{sc} (critical stability number) than impermeable-core sections for unit spacing lower than 10%, confirming that increased drainage capacity reduces uplift pressure beneath the armour layer and delays the onset of instability. Impermeable cores, in contrast, showed earlier transitions to instability, with reduced capacity for pore pressure dissipation and greater underlayer deformation under energetic wave run-down.

The influence of armour unit spacing and protrusions was similarly pronounced. 22.5% spacing provided the most stable configuration, achieving the highest critical N_s values, while compact placements (<10%) reduced porosity and favoured uplift-driven displacement. Protruded units (PT) demonstrated enhanced interlocking and resistance against rocking or extraction, especially on permeable cores, where improved porosity and fit between adjacent units minimized vertical motion. These trends in stability, as shown in Table 5-5, confirm that spacing and protrusions exhibit decisive control on Coastalock stability.

Table 5-5. Critical stability numbers (N_s) obtained with the model tests for all tested spacings (PC: Permeable Core, IC: Impermeable Core, PT: Coastalock Units with Protrusions)

Armour unit spacing (%)	**Critical N_s**
0 (PC)	2.83
5 (IC)	2.36
7.5 (IC)	2.10
10 (PC-PT)	3.62
10 (IC)	4.11
10 (PC)	4.12
15 (IC)	4.03
20 (PC)	3.51
20 (IC)	2.86
22.5 (PC-PT)	4.19
25 (IC)	4.08

The stability analysis demonstrated thresholds emerging for the unit spacing effect. To transform these experimental observations into conservative design practice, a safety factor is applied to both stability parameters, as shown in Table 5-6. The Coastal Engineering Manual (USACE, 2002) and the Rock Manual (CIRIA, 2007) recommend such safety factors when using experimental results for armour layer design, reflecting uncertainties associated with hydraulic variability, construction tolerances, and scale effects. In this study, a safety factor of 1.5 was adopted, corresponding to the common practice of designing for approximately 67% of the experimentally observed critical N_s, thereby providing adequate conservatism in Coastalock stability assessment.

Table 5-6. Design stability number (N_s), slope steepness and corresponding Hudson stability coefficient (K_D) for different spacings (PC: Permeable Core, IC: Impermeable Core, PT: Coastalock Units with Protrusions)

Spacing (%)	Design N_s	Corresponding K_D
10 (PC-PT)	2.4	9.33
10 (IC)	2.7	13.71
10 (PC)	2.7	13.86
22.5 (PC-PT)	2.8	14.63

The stability coefficients derived from these results, presented in Table 5-6, indicate that N_s for design values for permeable core configurations typically range between 2.4 and 2.8, corresponding to design K_D values of approximately 9–15 for 2V:3H slopes, consistent with the hydraulic performance of established single-layer systems such as Accropode and Xbloc. Impermeable-core cases showed a slightly lower design N_s value for the same spacing percentage.

Across multiple experimental programs, breathing (defined as the cyclic uplift and settlement of the armour layer induced by pressure differentials during wave run-down and subsequent impact) of the armour layer was identified as a characteristic but not necessarily critical response of Coastalock slopes when the Coastalock armour units were placed together, without spacing (0%) or with minor spacings (<10%). Molenkamp (2022) and Lawniczak (2024) observed cyclic uplift and resettlement of the armour layer under energetic wave run-down, occasionally accompanied by minor underlayer deformation on impermeable and permeable cores, respectively. The breathing effect was only observed for the armour layer of Coastalocks placed altogether, with no or low spacings (<10%) when these effects were linked to pore pressure fluctuations, but remained localized and did not translate into rapid slope-wide instability. Importantly, in the large-scale breakwater tests of Sayar et al. (2025), where hydraulic loading extended up to the prototype significant wave height, $H_s \approx 5.7$ m, no breathing effect nor underlayer deformation was recorded. This indicates that while breathing is an identifiable process in model-scale testing, Coastalock units maintained structural integrity and preserved interlocking without compromising the underlayer under more severe and representative conditions.

Unit extraction was identified as the terminal stage of instability in some model-scale cases with 10% or lower spacing despite its limited occurrence. Molenkamp (2022) recorded extraction once cyclic breathing exceeded interlocking resistance, which happened only for configurations below 10% spacings, while Lawniczak (2024) reported occasional extraction events at 10% or lower spacings under steep waves. Sayar et al. (2025) observed a single case of slope failure with 10% unit spacing due to unit extraction at the transition between the slope and the crest (where there is a lack of interlocking from the crest to the slope) under the tested extreme wave conditions, highlighting that armour instability only developed at the upper bound of tested wave heights. By

contrast, Baker et al. (2023) reported no instability, with Coastalock slopes remaining fully stable under all applied conditions. Collectively, these results underscore the overall robustness of the Coastalock system: breathing and minor rocking were observed only for very densely packed configurations of the armour (<10% spacing), not for the configurations with 10% or higher spacing, but failure of the armour occurred at high stability numbers around test conditions and the N_s shown in Table 5-5.

5.4.1.2 Coastalock with Protrusions

Following the results of the impermeable core tests (Molenkamp, 2022) that resulted in higher stability and reduced overtopping when armour layer spacing was increased, the Coastalock was tested with protrusions of two different lengths that maintained the same spacings tested previously (10% and 22.5%).

The tests with protrusions indicated that a more porous armour layer and enhanced interlocking provided by the protrusions with 22.5% spacing preserved structural integrity with no failure reported throughout the entire set of tests. The structure remained fully stable at the maximum significant wave height that could be produced at the flume, corresponding to a critical N_s= 4.19 (design N_s = 2.80).

5.4.2. Underlayer

The underlayer plays a crucial role in single-layer armours. Similarly, in Coastalock armour stability, serving as the structural bed that maintains unit interlocking and resists deformation under wave-induced forces, its adequacy therefore directly determines whether the armour slope remains stable or becomes vulnerable to progressive damage.

Observed damage mechanisms mostly linked instability to underlayer behaviour, with Molenkamp (2022) and Lawniczak (2024) documenting breathing, sliding, and S-shaped settlements as early signs of total failure when spacings were below 10%. Conversely, large-scale tests by Sayar et al. (2025) showed that relatively larger underlayer rocks with a permeable core can prevent these mechanisms. Both Molenkamp (2022) and Lawniczak (2024) demonstrated that underlayer deformation disappeared once armour spacing is 15% or higher, even when the same underlayer grading was used, indicating that the occurrence of underlayer movement is dependent on the hydraulic porosity of the armour layer. Accordingly, the interpretation of underlayer performance must be made in conjunction with the applied armour spacing.

Importantly, Sayar et al. (2025) further showed that underlayer grading does not always correlate positively with stability: the larger underlayer grading (168–338 kg) resulted in greater armour layer instability than the smaller underlayer grading (85–203 kg). This behaviour reinforces that, for Coastalock units, the hydraulic interaction between armour porosity, uplift pressures, and unit interlocking dominates over simple increases in underlayer stone size. Coarser underlayer gradings create a highly irregular support surface making it more difficult to achieve consistent unit placement, spacing, and orientation.

Results shown in Table 5-7 indicates that, for permeable-core configurations, instability occurrence decreases as the D_{n50} underlayer to D_n armour layer increases within the tested range. Instability was observed in 7.4% of tests at $D_{n50,UL}/D_{n,CL} \approx 0.249$, reduced to 5.6% at $D_{n50,UL}/D_{n,CL} \approx 0.339$, and was not observed for the ratios above 0.419 under the tested hydraulic conditions. These results suggest that larger underlayer ratios improve resistance to breathing and extraction mechanisms when combined with adequate armour spacing and a permeable core, while no single ratio should be interpreted as an absolute stability threshold. Additionally, core permeability was found to be a dominant parameter, as impermeable-core cases exhibited substantially higher instability occurrence even at comparable underlayer ratios, wave and structural conditions.

Table 5-7. Underlayer to Armour Unit Nominal Diameter Ratio and Hydraulic Instability Occurrence (IC: Impermeable Core (presented at the top rows), PC: Permeable Core)

D_{n50} Underlayer / D_n Armour layer	Number of tests resulting in hydraulic instability	Total number of tests	Instability 0ccurrence (%)
0.000 (IC)	2	11	18.2
0.278 (IC)	20	123	16.3
0.419 (IC)	0	30	0
0.249 (PC)	8	108	7.4
0.339 (PC)	2	36	5.6
0.541 (PC)	0	10	0

5.4.3. Overtopping Analysis

The overtopping performance of Coastalock-armoured slopes was assessed using the EurOtop (2018) framework, with measured overtopping volumes converted into dimensionless mean discharges to allow direct comparison with standard prediction curves. Figure 5-8 highlights the influence of unit spacing on the top graph, while demonstrating the distribution of data across the four experimental campaigns on the bottom graph. Previous investigations (Molenkamp, 2022; Lawniczak, 2024; Sayar et al., 2026) of unit spacing and core permeability effects found no significant influence on overtopping rates; therefore, these variables were not re-examined in the present study.

.

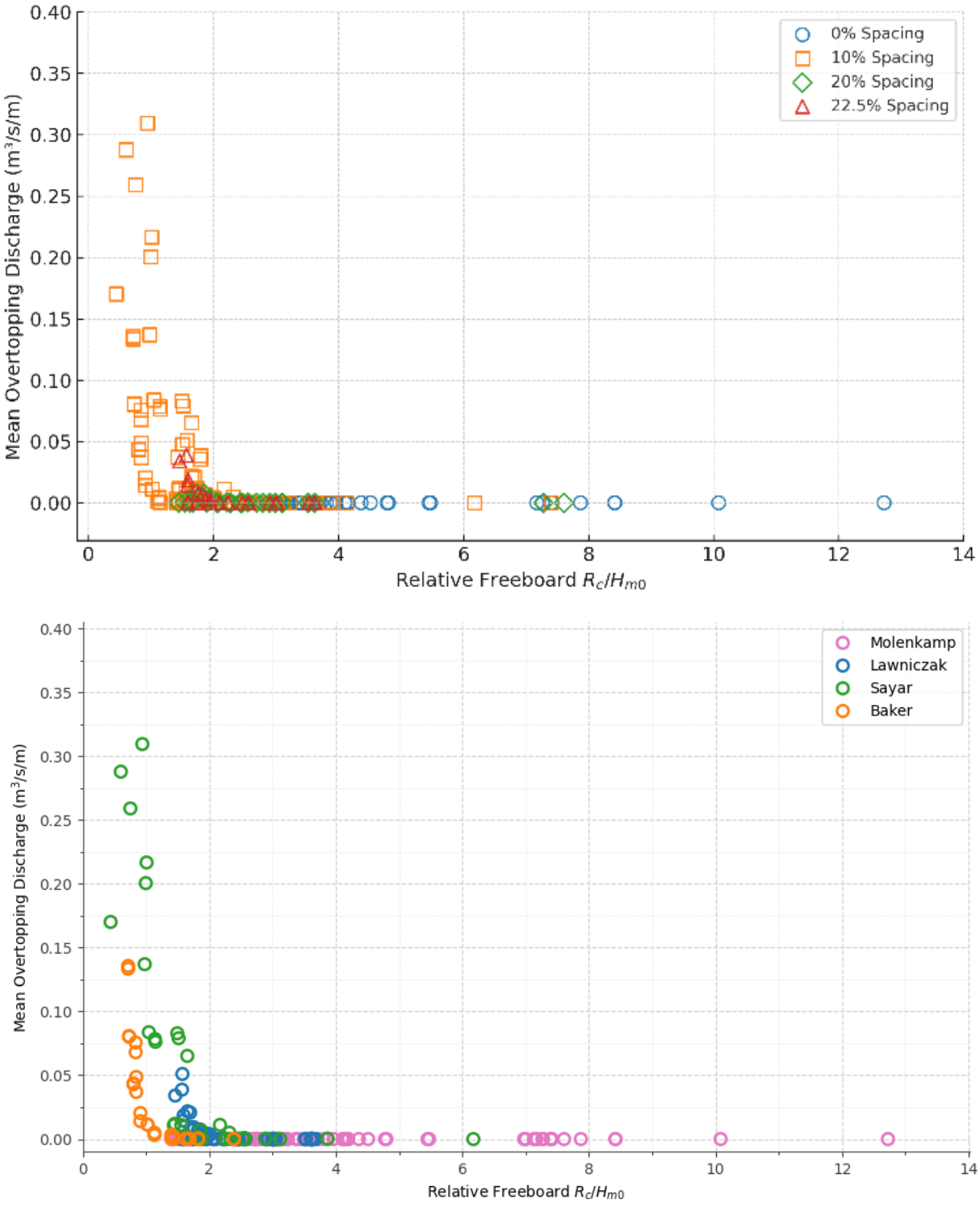

Figure 5-8. Mean wave overtopping discharge for Coastalock-armoured slopes. Each marker represents one test run. Top: comparison of overtopping results for different armour unit spacings as a function of relative freeboard. Bottom: comparison of overtopping results from different experimental studies as a function of relative freeboard (R_c/H_{m0})

Figure 5-9 and 5-10 focus on the 10% spacing configuration, where measured mean overtopping discharges align closely with EurOtop (2018) curves; calibration produced a roughness factor of $\gamma_f \approx 0.67$, consistent with established single-layer armour units.

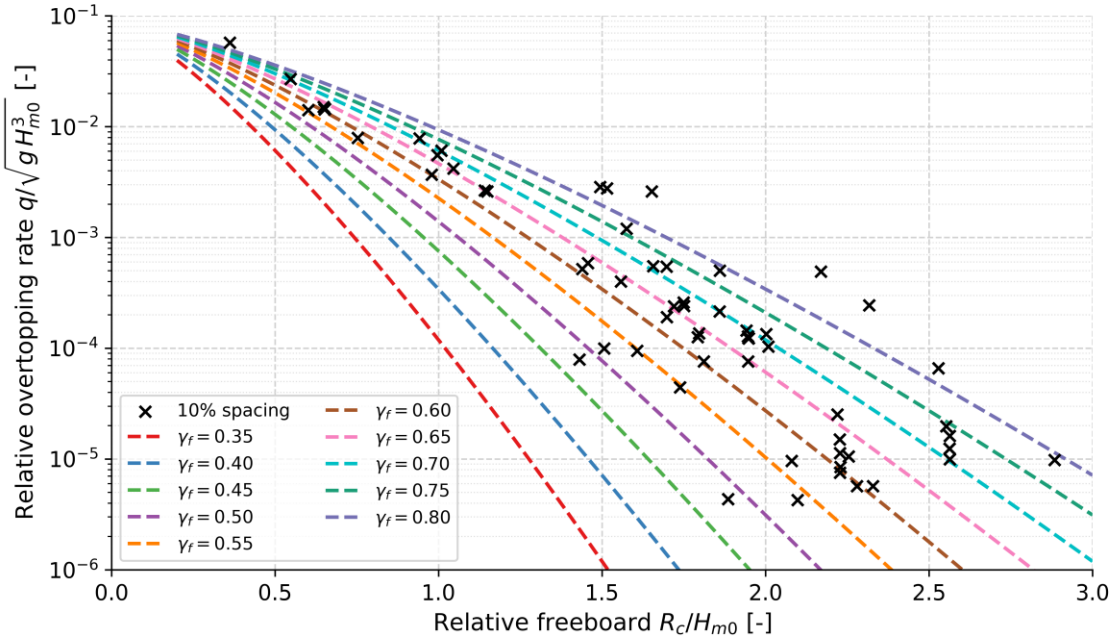

Figure 5-9. Relative overtopping rates ($q/(gH_{m0}^3)^{0.5}$) for 10% armour unit spacing

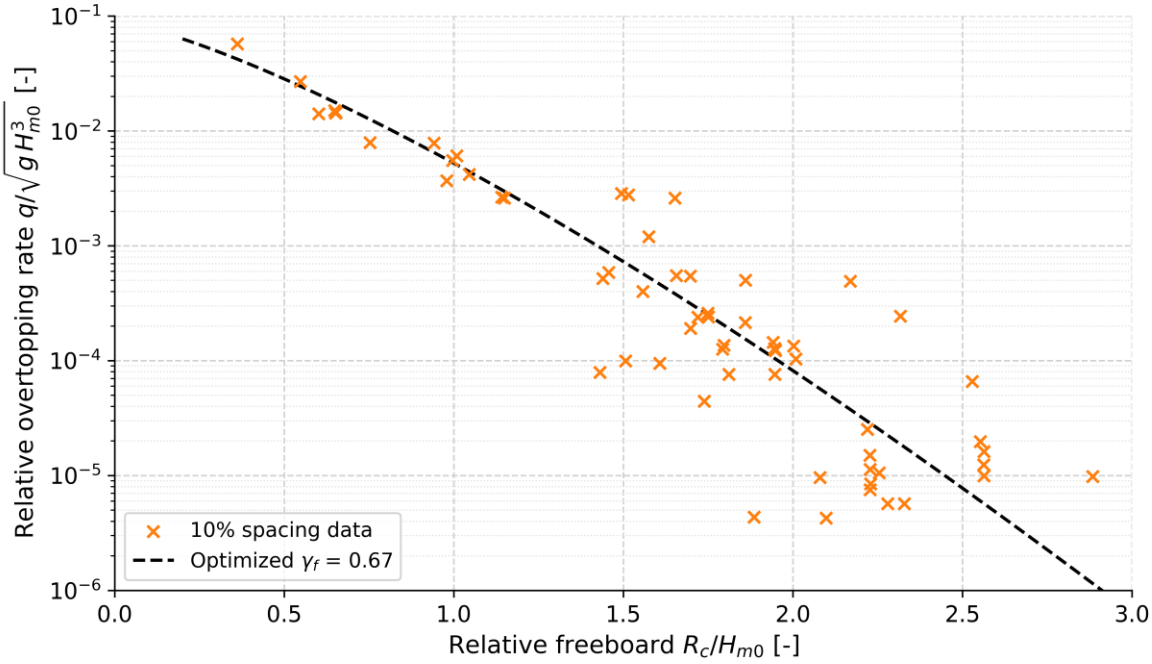

Figure 5-10. A best-fit curve to the 10% spacing data yields an optimized roughness factor of $\gamma_f = 0.67$

As shown in Figure 5-11, the 22.5% spacing tests produced overtopping discharges that align closely with EurOtop (2018) predictions, with calibration indicating γ_f values mostly between 0.65 and 0.70. This range demonstrates that the configuration performs reliably within the expected bounds of single-layer unit behaviour.

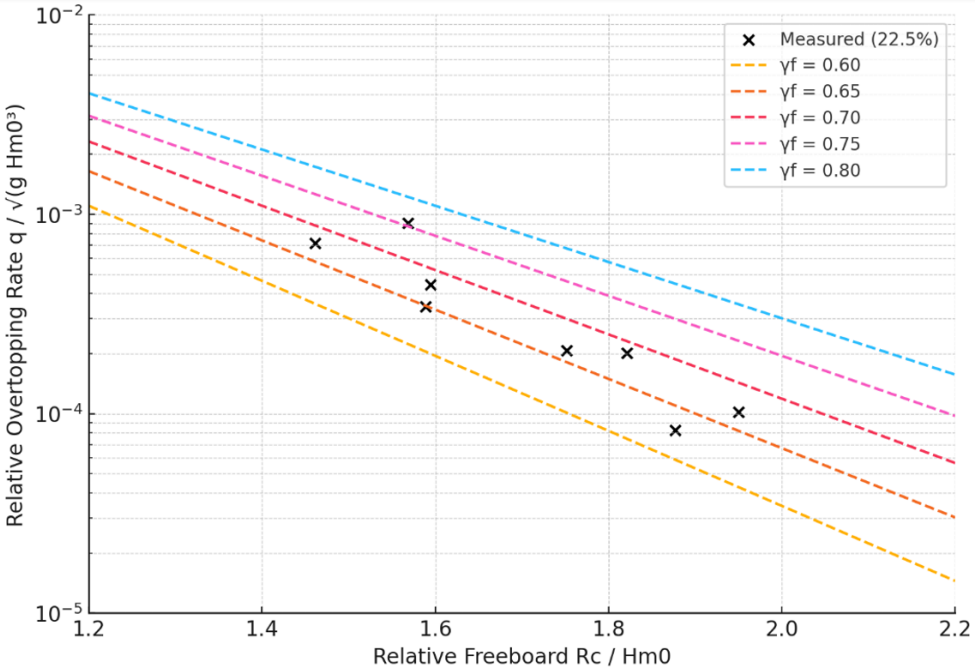

Figure 5-11. Relative overtopping discharge plotted against relative freeboard for 22.5% spacing configuration. Dashed lines represent EurOtop (2018) predictions using different γf ranging from 0.60 to 0.80 (tests with no overtopping rates were excluded)

5.4.4. Toe Design

In Coastalock-armoured slopes, as in other single-layer armour unit systems, the toe plays a critical role in stability by providing support to the first rows of the armour, resisting scour and settlement, and preventing slope failure triggered at the base. Across the experimental series, only one toe-related instability was observed during the large-scale experiments of Sayar et al. (2025), occurring at the lee side of the emergent breakwater structure under severe overtopping volumes that exceeded the suggested limits in EurOtop (2018). The overtopping downrush and localized wave forces damaged the leeward toe, dislodging the bottom toe armour row and triggering subsequent slope failure. Once the leeward toe was reinforced and deepened, no failure of the toe was registered under the same wave and overtopping conditions.

These findings highlight the critical role of toe stability in Coastalock design, as failure initiated at the toe can compromise the entire armour slope; ensuring conservative toe design and sizing remains essential.

5.5. Ecological Performance

5.5.1. Biodiversity Monitoring at Port of Vigo

As part of the Living Ports project, Coastalock units were deployed at the Port of Vigo to test their potential as eco-engineering solutions: from production to placement of the units, including an extensive biological monitoring plan of more than two years, aiming at evaluating the ability of the units to enhance local marine life and biodiversity, contributing to a Nature Positive port infrastructure.

To evaluate biological outcomes, one hundred Coastalock units of 1.42m^3 each were deployed at Bouzas, Vigo (Spain), with sloped protection following a regular placement grid of ten rows positioned at distinct tidal heights, as illustrated in Figures Figure 5-12 and Figure 5-13, providing a living laboratory for biodiversity monitoring. Ecological data were collected from the Coastalock units and adjacent rocks that were treated as the control, following the protocol of Perkol-Finkel et al. (2008), combining percent cover estimates, counts of solitary organisms, and index-based evaluations for taxa not suited to direct quantification. Standardized quadrat surveys were conducted quarterly over 24 months on both Coastalock units and control riprap, with triplicates placed at upper, mid, and lower intertidal zones. Each quadrat was photographed in situ, and the percent cover of major taxonomic groups (macroalgae, barnacles, bivalves, and mobile invertebrates) was later quantified using image analysis techniques. This approach ensured comparability between treatments and provided statistical data on community development.

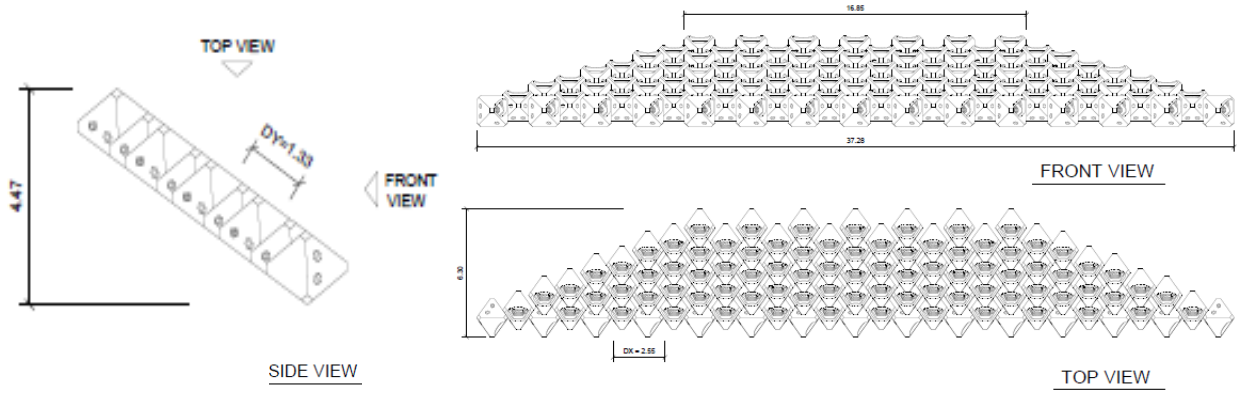

Figure 5-12. The sketch of the installed Coastalock configuration at the Port of Vigo from different views (dimensions in meters, not at scale)

Figure 5-13. Left: Aerial view of the project's locations. Coastalock placement in Bouzas sloped protection; Right: Coastalock units after demoulding (upper) and after installation in Bouzas sloped protection (lower)

Figure 5-14 illustrates the colonization of Coastalock units during the monitoring campaign, showing both exposed underwater surfaces (A) and the protected microhabitats within cavities (B and C). Algae, mussels, and other sessile taxa established across these surfaces, demonstrating how the units provide stable settlement areas as well as sheltered niches that enhance ecological complexity. Clear tidal patterns were observed: brown algae and early colonizers dominated the lower rows, while mid- and upper rows supported more diverse assemblages including red algae, mussels, and barnacles. The cavities also enhanced water retention at low tide, favouring moisture-dependent species and extending habitat availability across tidal cycles.

Figure 5-14. Biological development on Coastalock; (A) Underwater unit, (B and C) inside Coastalock cavities

Beyond sessile communities, the Coastalock revetment supported ten unique species groups (eight marine fish and two invertebrates from six families) within 12 months of deployment, with species richness significantly higher than on adjacent riprap (Figure 5-15). A total of 404 individuals were documented, including particularly strong associations with gobies (Gobiidae spp.) and sea bream (Sparidae spp.). Gobies and shrimps were frequently observed in the tidal pools formed in the upper rows, highlighting the role of Coastalock in generating novel habitats that sustain aquatic life during emersion.

As shown in Figure 5-15, species richness and diversity were consistently higher on Coastalock units than on adjacent control rocks which were placed there at a minimum of two decades ago with the greatest differences occurring in the mid and upper-tidal rows where cavities retained water.

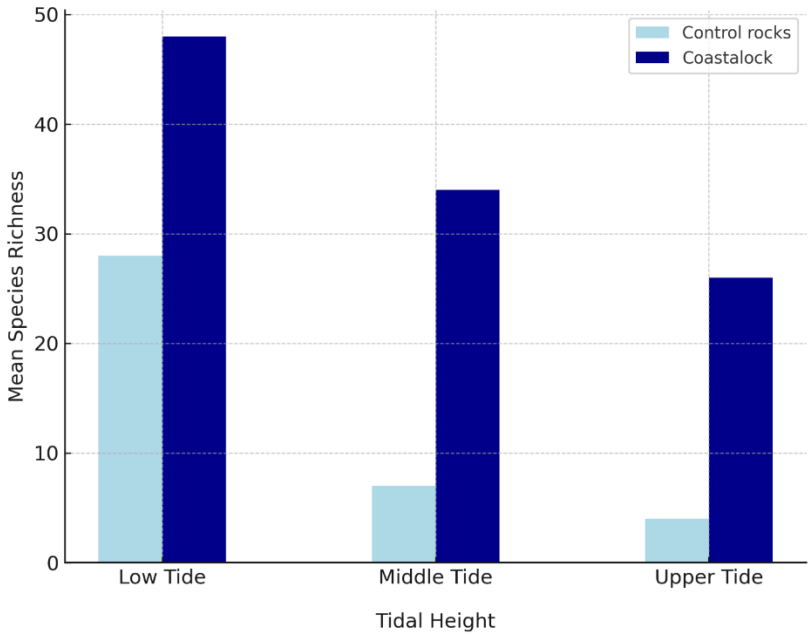

Figure 5-15. Mean species richness on Coastalock units and adjacent control rocks at three tidal heights, measured 12 months after deployment (ECOncrete, 2024)

5.5.2. Design Features for Ecological Enhancement

The ecological outcomes of Coastalock installations were strongly influenced by unit orientation and natural tidal zonation. Surfaces oriented upward tended to accumulate higher algal cover and encrusting organisms, benefiting from direct light and water retention in shallow depressions. In contrast, downward-facing surfaces supported distinct communities dominated by sessile invertebrates such as sponges, bryozoans, and tunicates, reflecting reduced exposure to desiccation and shading effects. These complementary assemblages across orientations enhanced overall

community diversity, confirming that orientation is a key design variable shaping habitat provision.

Sideward-facing cavities created shaded, moisture-retaining refuges that preserved aquatic conditions during low tide and protected organisms from thermal stress and desiccation. Monitoring revealed that such microhabitats sustained gobies, shrimps, and moisture-dependent invertebrates during emersion, highlighting their functional role in extending habitat availability across tidal cycles. By providing persistent refugia, Coastalock units facilitated species survival under fluctuating tidal exposure, a feature absent on conventional riprap.

These findings demonstrate that deliberate inclusion of varied surface orientations and cavity placements enhances the ecological value of armour layers. Unit orientations that combine upward surfaces for algal colonization and downward cavities for invertebrate refuges maximize functional diversity within the same structural footprint.

Lawniczak (2024) tested the Coastalock orientations previously shown in Figure 5-3, indicating that upward-facing orientations enhanced armour stability on a permeable core, with no extraction observed up to $N_s = 3.9$, while or orientation changes reduced thresholds slightly to $N_s = 3.5–3.8$. Separately, ecological monitoring in Vigo indicated that upward cavities retained water and supported greater richness, whereas sidewards orientations provided shaded refugia for invertebrates. Together, these results highlight orientation as a dual-purpose parameter: it governs stability margins in laboratory settings while shaping habitat diversity in the field.

From a design standpoint, distributing orientations in a balanced way allows Coastalock units to deliver ecological enhancement without lowering hydraulic stability. Depending on the site conditions and the intended function of the structure, designers may choose to emphasize either ecological gains, such as tidal pools and shaded refugia, or hydraulic performance. The integration of laboratory and field results thus offers a flexible framework allowing various orientation strategies for specific future applications.

5.6. Design Recommendations

5.6.1. Baseline Design Configuration and Observations

The optimal configuration (provided in Table 5-8) for Coastalock design is defined by tests on a permeable core with a 2V:3H slope, 22.5% unit spacing with protrusions, and an underlayer-to-armour size ratio of 0.34. Under these conditions, the armour remained fully stable under all wave conditions achievable within the laboratory. The maximum tested stability number was $N_s = 4.19$. Since no failure occurred, this value represents a lower bound of the critical stability number ($N_{sc} > 4.19$) rather than an experimentally interpolated failure threshold. Applying a global safety factor of 1.5 to this lower-bound estimate results in a conservative design $N_s \approx 2.8$.

When compared to proprietary single-layer systems, the baseline Coastalock configuration performed within the upper range of reported stability constants, with a design N_s aligning closely

with values established for Accropode II, Xbloc and XblocPlus. The measured stability values for XblocPlus (DMC, 2023) were in the same range, but a larger safety factor was used for these. Under these conditions, the armour layer remained hydraulically stable up to 28 rows of units on the slope, confirming that the interlocking geometry maintained the integrity even at significant slope lengths. It should be emphasized that the observed stability up to 28 rows refers strictly to hydraulic stability under wave loading and does not inherently imply structural stability of the bottom row units under cumulative self-weight loading from the overlying armour. In single-layer interlocking systems, the vertical load transferred through the armour layer increases with the number of rows, potentially inducing elevated compressive stresses in the bottom units. Furthermore, longer armour layers increase the horizontal forces acting at the toe, which may promote toe displacement or push-out if not properly accounted for in detailed design. The experimentally observed maximum number of rows should therefore be interpreted as a hydraulic performance baseline rather than a structural or geotechnical design limit.

It should also be noted that the 22.5% spacing configuration was tested exclusively with Coastalock units with protrusions. No corresponding tests without protrusions were conducted at this spacing. Therefore, the observed performance at 22.5% spacing cannot be directly attributed to spacing alone, nor can the independent contribution of protrusions be isolated. The conclusions for this configuration are thus limited to the tested geometry.

In addition to the optimal configuration with 22.5% spacing with protrusions, Coastalock units without protrusions placed at 10% armour unit spacing on a permeable core require particular consideration, as this represents the most extensively tested configuration to date while exhibiting comparable stability performance. This spacing was investigated across three independent physical modelling campaigns included in this study, encompassing different structure types, laboratory scales, and hydraulic conditions. Although its stability margin was slightly lower than that of the 22.5% spacing configuration, the consistency of the results across studies confirms 10% spacing as a robust and well-validated design alternative within the tested range.

Table 5-8. Optimal Design Case

Parameter	Optimal configuration	Alternative configuration
Spacing (%)	22.5	10
Armour unit type	with Protrusions	Standard
Core type	Permeable	Permeable
Slope	2V:3H	2V:3H
$D_{n50,\ underlayer}$ / $Dn_{\ armour\ unit}$	0.25-0.34	0.25-0.34
Armour unit volume (V) (in m^3)	1.42	1.42
Stability number (N_s)	4.19	4.12
Design N_s (with safety factor, 1.5)	2.80	2.75
Nominal diameter of Coastalock units (D_n in m)	1.11 m	1.11 m
Hudson coefficient (K_D) for 2V:3H slope	14.63	13.71

The baseline tests employed underlayer sizes slightly larger than those typically recommended in conventional rock armour guidelines, a factor that likely contributed to the observed robustness of the Coastalock slope. This finding underscores the importance of conservative underlayer design in ensuring armour layer stability, particularly under energetic wave conditions. In addition, the toe design warrants careful attention, as results indicate that toe armour weights exceeding Van der Meer's (1996) predictions are advisable when significant overtopping is expected, thereby reducing the risk of progressive slope failure initiated by the structure's toe instability.

5.6.2. Underlayer Design

The test results confirm that Coastalock stability is influenced by the underlayer ratio ($D_{n50,UL}/D_{n,CL}$) but also demonstrate that underlayer performance cannot be interpreted independently from armour porosity and core permeability. For permeable core configurations, instability occurrence decreased as the underlayer ratio increased within the tested range. Ratios between 0.25–0.34 were associated with limited instability under specific hydraulic and unit spacing conditions (critical N_s values in the range of 3.5–4), while no instability was observed for ratios ≥0.42 within the tested hydraulic range (up to a critical N_s of 2.34). However, the higher underlayer size ratio cases were not systematically tested under the most severe loading conditions and therefore should not be interpreted as absolute stability guarantees. These findings indicate

that the stabilizing effect of the underlayer becomes effective only when adequate armour spacing (≥10%) and a permeable core are provided to dissipate uplift and pore pressures.

Based on the compiled dataset, a practical design range of $D_{n50,UL}/D_{n,CL}$ between 0.25 and 0.34 is recommended for permeable-core applications. The lower bound corresponds to cases where limited instability was observed and should therefore be combined with appropriate armour spacing and permeability conditions rather than interpreted as a stand-alone stability threshold. It should be noted that excessively large underlayer stones may increase surface roughness and irregularity, potentially reducing placement regularity of the armour layer and locally increasing rocking and damage risk of the armour units. Therefore, increasing underlayer size beyond the validated range does not necessarily provide additional stability benefits.

5.6.3. Toe and Rear Design

Toe stability was identified as a significant factor for the Coastalock armour layer. The only recorded failure in the test campaigns was reported at the lee side of the structure and linked to toe instability under heavy overtopping. Evaluation against Van der Meer's (1996) toe stability formula confirmed that conservative toe rock weights, often greater than the calculated values, contributed to overall slope robustness. On the rear side, armour stability was fully maintained as long as the toe remained intact, but excessive overtopping volumes proved capable of weakening the rear toe stability and initiating slope damage. It is therefore advised that designers apply conservative toe sizing, particularly for rear-side protection with moderate to heavy overtopping rates in highly exposed sites.

5.7. Discussion

This study consolidates results from four independent physical modelling programs, yielding the first unified dataset for the hydraulic stability and performance of Coastalock armour units. By integrating over 417 individual tests, the research establishes a coherent framework for developing practical design recommendations.

The hydraulic stability of Coastalock is broadly comparable to other proprietary armour units such as Core-Loc, Xbloc, Accropode II, and Cubipod. Coastalock achieved a design $N_s = 2.8$ ($K_D \approx 15$) for trunk sections, which falls within the general design range of $N_s = 2.0–3.0$ for single-layer systems. In contrast, Dolos and other traditional double-layer units require more material for similar hydraulic stability (Muttray and Reedjik, 2008; Dupray and Roberts, 2010). For overtopping calculations, Coastalock follows the EurOtop methodology using a friction factor γ_f consistent with values applied to other single-layer concrete armour units. This research also integrated Coastalock unit spacing (0–25%) and orientation effects into these recommendations as specific and ecology-related parameters.

Coastalock armour units incorporate geometric features intended to promote habitat formation. Field observations at the Port of San Diego (Sayar et al., 2025) and the Port of Vigo indicate

measurable biological colonization within the created surface features. The present study evaluates hydraulic stability independently from ecological performance, while acknowledging that ecological functionality introduces additional design considerations. The integration of hydraulic and ecological criteria should therefore be assessed critically, ensuring that stability performance remains the governing requirement under design wave conditions.

Application Limits

The present results apply solely to straight, two-dimensional sections with slopes of 2V:3H and 1V:2H. Since no data are available for other slope geometries or three-dimensional features such as roundheads or curved structures, model testing is recommended for these applications.

The design recommendations are based on tests covering spacings from 0 to 25%, of which 10–22.5% proved effective and 22.5% performed optimally. In terms of orientation, San Diego (without protrusions) and cavity forward arrangements showed reliable results across studies, whereas designs employing cavity-sideways and downward orientations were more limited and therefore additional model testing is suggested.

The stability results are based on test durations roughly between 600 and 1,100 waves per condition, with most of them having a minimum of 1,000. While this provides confidence in short-term behaviour, such as resistance against storm conditions, long-term exposure and lifetime performance of Coastalock armour layers have yet to be demonstrated under prototype sea states. It should be noted, however, that the material durability of the Coastalock units themselves is not a limiting factor: the units are produced in compliance with ASTM and EN 206 concrete standards, ensuring a minimum material lifespan of 50 years. This durability assurance relates to concrete performance and not to long-term hydraulic stability, for which additional monitoring or physical modelling would still be beneficial. Lack of rocking of the tightly placed units would indicate that less wear might be expected than for irregularly placed single layer units.

While the most comprehensive dataset available for Coastalock to date is used for the analyses, the results are constrained by the boundaries of the tested conditions, and caution is required when interpreting the results.

5.8. Conclusions

This work presents the first consolidated recommendations for the design of placement of the Coastalock armour unit, derived from an extensive series of independent physical model investigations. The recommendations establish validated thresholds for hydraulic stability and performance while integrating ecological considerations based on field monitoring. Coastalock thereby extends the tradition of concrete armour units by combining engineering performance with nature-inclusive design and biological restoration and habitat creation objectives. While the present dataset defines clear application limits, it also provides a foundation for future research to expand the guideline scope. The integration of Coastalock into coastal infrastructure offers a pathway toward structures that are both reliable and ecologically beneficial.

In projects with large tidal variability, the elevation at which the armour placement transitions from forward-facing to side/downward orientation should be selected relative to a representative low-water level, since the transition zone may be exposed to recurrent wetting–drying and wave run-up under moderate conditions. However, during storm events the water level may exceed the transition elevation by a large margin due to tide and surge, such that a portion of the slope designed for “low-water orientation” will be subjected to wave loading. Therefore, the transition elevation should be treated as a practical placement guideline rather than a hydraulic stability boundary; stability must be verified for the governing storm water levels and wave conditions regardless of the selected transition elevation.

The intended ecological function may lead to bio-colonization and partial infill of voids, which can temporarily reduce the effective hydraulic porosity of the armour layer. However, marine growth is inherently dynamic, governed by natural cycles of colonization, growth, and decay, meaning that full and permanent clogging is unlikely. Since uplift pressures and pore-pressure dissipation are sensitive to armour porosity, the stability recommendations should be interpreted in terms of a minimum operational spacing/porosity. Designers should therefore consider potential temporal variations in porosity by selecting an initial spacing that maintains hydraulic performance while supporting ecological functionality, and by promoting conditions (e.g., material properties and surface complexity) that sustain continuous biological renewal within the structure.

The experimental database primarily represents straight trunk sections under controlled geometry and predominantly surging-wave conditions. In practice, several site-specific factors can increase hydrodynamic demand or reduce the stability margin, warranting a more conservative design. These include conditions promoting plunging or severely breaking waves (e.g., steep foreshores and shallow toe depths), low-crested/overtopped configurations, curved alignments and transitions with three-dimensional flow, oblique wave attack and currents, mobile beds and scour-prone toes, extended storm duration, construction tolerances affecting placement regularity, and long-term reductions in armour permeability due to bio growth or sediment infill. For such cases, designers should adopt increased stability margin (e.g., lower allowable design Ns and/or heavier units locally), apply more conservative toe and underlayer design, and maintain a minimum operational porosity concept.

The maximum number of armour rows should also be considered as a practical design limitation. Although stable configurations were observed up to approximately 28 rows in the present dataset, this should be interpreted within the tested range, and designers should verify toe and structural stability when applying higher armour layer heights.

This study contributes to the advancement of eco-engineering practices in single-layer armour unit design by demonstrating that hydraulic stability and ecological enhancement can be addressed within a unified framework. Through extensive physical modelling and ecological monitoring, the Coastalock design recommendations introduce unit spacing, orientation, and underlayer thresholds as explicit design variables, while also showing the ecological value of nature-inclusive designs.

By integrating engineering performance with biodiversity outcomes, this research extends the scope of armour unit design beyond purely hydraulic and economical considerations, setting a precedent for nature-inclusive approaches in future coastal infrastructure.

Chapter 6. Conclusions

6.1 Main Findings and Contribution

This thesis has demonstrated that Coastalock armour units successfully integrate hydraulic efficiency, delivering ecological functionality, providing a data-driven, nature-inclusive alternative to conventional single-layer armour systems. Through a combination of large-scale physical modelling, numerical simulations, and comprehensive design synthesis, the research establishes Coastalock as a solution for sustainable coastal protection that meets both engineering and ecological objectives.

The flume experiments captured the wave–structure interactions, while the IH2VOF model enabled the systematic assessment of wave generation, propagation, and energy dissipation processes. The agreement between numerical and experimental results confirmed the reliability of both approaches and strengthened confidence in the derived hydraulic performance parameters.

Among the tested configurations, an armour unit spacing of 22.5% with protrusions proved to be the optimal arrangement, balancing the interlocking effect and layer porosity. This configuration minimized uplift forces by allowing controlled energy dissipation through the armour layer while maintaining structural stability.

The performance of the underlayer emerged as a critical factor influencing the overall stability of the armour layer. Tests indicated that maintaining an underlayer-to-armour nominal diameter ratio ($D_{n50,\ underlayer}/D_{n,\ armour}$) of at least 0.34, and preferably within the range of 0.34–0.41, effectively suppressed failure mechanisms.

Core permeability was found to have a significant influence on the hydraulic stability of Coastalock-armoured slopes. Test results consistently demonstrated that permeable cores dissipated pore pressures more effectively and delayed the onset of uplift or rocking compared to impermeable configurations.

Overtopping analysis demonstrated that the measured discharges for Coastalock-armoured slopes aligned well with predictions from the EurOtop (2018) formulation when appropriate roughness factors were applied. Calibrated values of γ_f between 0.65 and 0.70 captured the influence of the unit's surface texture and interlocking pattern on flow resistance. This consistency confirms that overtopping on Coastalock structures can be reliably estimated using existing empirical tools, facilitating their integration into conventional design practice.

The stability of the toe armour proved to be a decisive factor in the overall performance of Coastalock-armoured slopes. Comparative analyses with Van der Meer's (1996) formulations and visual observations of failure modes indicated that insufficient toe protection initiated progressive

armour displacement. Consequently, conservative toe sizing and adequate placement are recommended, particularly for cases where high overtopping is anticipated.

The experimental and analytical findings collectively revealed that Coastalock performs within the hydraulic stability envelope of established single-layer systems. For slopes of 1V:1.5H with Coastalock units, the resultant design stability constants of $N_s \approx 2.8$ and $K_D \approx 15$ align closely with values reported for units such as Accropode, Xbloc, and Core-Loc.

6.2 Study Limitations

While the results presented in this thesis are based on an extensive and robust program of large-scale physical experiments and complementary numerical simulations, several limitations constrain the applicability and generalization of the findings. The limitations associated with the physical modelling, numerical simulations, and consolidated design analyses conducted in this thesis are examined in detail at the end of Chapter 3, Chapter 4, and Chapter 5, respectively. These chapters outline the constraints related to the experimental setups, modelling assumptions, and structural configurations tested. Building on those discussions, the principal limitations relevant to the applicability and generalization of the findings are synthesized below.

The proposed design recommendations are applicable only to the conditions investigated in this research. The results pertain to two-dimensional trunk sections of rubble mound breakwaters or revetments, slope configurations ranging from 1V:1.5H to 1V:2H, and armour unit spacings between 0% and 25%. Among the tested orientations, San Diego and cavity-upwards configurations demonstrated consistent hydraulic performance, whereas other orientations were not sufficiently explored to support generalization.

The stability assessment is based on test durations of approximately 600 to 1,100 waves per condition, which provides confidence in short-term hydraulic response and resistance under storm-like loading. However, these durations do not allow direct inference of long-term or lifetime performance, particularly under repeated storm exposure, cumulative damage, or evolving seabed and toe conditions. Consequently, extrapolation beyond the tested durations should be undertaken with caution.

The experimental findings also revealed that toe stability is a critical controlling factor for overall armour-layer performance. While existing toe stability formulations were used for comparison, a Coastalock-specific toe stability relationship was not established within the scope of this study.

From a numerical perspective, the CFD simulations were limited by software and computational constraints. The IH2VOF solver does not support dynamic mesh refinement, restricting the resolution of localized turbulence, wave breaking, and overtopping events. Additionally, the numerical model assumed rigid and immobile armour units, thus excluding potential rocking, rearrangement, or displacement under energetic wave loading. Air entrainment and compressibility effects were not explicitly resolved, which may influence overtopping discharge

and free-surface dynamics under highly energetic wave conditions. Simulation durations were also necessarily limited to ensure computational feasibility and numerical stability.

Together, these limitations define clear and empirically validated boundaries for the application of the design recommendations.

6.3 Recommendations for Future Research

Building on the findings and limitations identified in this thesis, several directions for future research are recommended to expand the applicability, robustness, and design maturity of eco-engineered Coastalock armour units.

A primary research need is the extension of investigations to three-dimensional breakwater configurations, including roundheads, curved sections, transitions, and head–trunk interfaces. These regions are subject to complex flow patterns, diffraction effects, and multidirectional wave attack, none of which were addressed in the present two-dimensional study. Dedicated 3D physical model testing is required to verify armour stability and hydraulic performance under these conditions.

Further experimental research is recommended to explore alternative armour unit orientations and spacing configurations beyond those validated in this study. While spacings between 10% and 22.5% performed effectively and 22.5% emerged as optimal within the tested range, configurations such as cavity-sideways and cavity-forward orientations require systematic testing. Additionally, the influence of wave obliquity and multidirectional wave spectra remains unexplored and should be investigated to reflect more realistic offshore wave climates.

Future studies should also focus on a more detailed characterization of internal flow processes, particularly the role of pore pressure transients, core permeability, and filter-layer performance. The present results demonstrate the importance of permeability in delaying instability; however, advanced measurements or numerical techniques could improve quantification of internal hydraulics and refine filter and core design requirements.

The performance of the underlayer and toe structures warrants further investigation. Broader testing across different rock types, shapes, gradations, and densities, including double underlayer systems, would strengthen confidence in the proposed underlayer thresholds. Similarly, future experiments should investigate Coastalock-specific toe stability formulations, incorporating varied toe geometries, reduced crest elevations, and more aggressive overtopping conditions representative of highly exposed sites.

On the numerical modelling side, future research should adopt advanced CFD approaches, including solvers with adaptive mesh refinement and Large Eddy Simulations (LES) or hybrid RANS–LES turbulence modelling, to better resolve small-scale hydrodynamic processes. Coupling CFD with Discrete Element Method (DEM) or block-motion modules would allow

simulation of dynamic armour unit behaviour, enabling a more realistic assessment of hydraulic stability under extreme wave loading. Future numerical work should also include systematic sensitivity analysis of turbulence models and numerical parameters to better quantify uncertainty in CFD-based simulations of wave–structure interaction.

Finally, future studies should explore the interaction between ecological development (e.g., bio-growth) and hydraulic performance, including potential changes in roughness, porosity, and overtopping behaviour over time. Field-scale monitoring and long-term performance studies are strongly recommended to complement laboratory findings. Such studies would enable validation of hydraulic behaviour under natural variability, assessment of cumulative damage mechanisms, and evaluation of performance over realistic service lifetimes. Integration of field data with physical and numerical modelling would represent a critical step toward full-scale validation and broader adoption of eco-engineered armour systems.

References

Airoldi, L., and Beck, M. W. (2007). Loss, status and trends for coastal marine habitats of Europe. In R. N. Gibson, R. J. A. Atkinson, and J. D. M. Gordon (Eds.), Oceanography and Marine Biology: An Annual Review, Vol. 45, 345–405. CRC Press. https://doi.org/10.1201/9781420050943.ch7

Allen, R. J., & Webb, B. M. (2011). Determination of wave transmission coefficients for oyster shell bag breakwaters. Coastal Engineering Practice. https://doi.org/10.1061/41190(422)57

Armono, H. D., Putra, A. R., & Wahyudi. (2021). Analysis of tsunami wave height, run-up, and inundation in the coastal areas of Blitar and Malang regency. IOP Conference Series: Earth and Environmental Science, 936(1), 012013. https://doi.org/10.1088/1755-1315/936/1/012013

Baker, S., Brashear, P., Tschirky, P., Marrone, J., & Larson, M. (2018). Design and physical model studies of innovative living breakwaters. Coastal Engineering Proceedings, 1. https://doi.org/10.9753/icce.v36.papers.59

Baker, S., P. Knox, M. Provan, & E. Murphy. (2023). Retrofitting rock-armoured revetments to combat wave overtopping amidst rising sea levels. Unpublished.

Bakker, P., van den Berge, A., Hakenberg, R., Klabbers, M., Muttray, M., Reedijk, B., & Rovers, I. (2003). Development of concrete breakwater armour units. In Proceedings of the 1st Coastal, Estuary and Offshore Engineering Specialty Conference of the Canadian Society for Civil Engineering (CSCE), Moncton, New Brunswick, Canada, June 4–7, 2003.

Bayon, A., Valero, D., García-Bartual, R., Vallés-Morán, F. J., & López-Jiménez, P. A. (2016). Performance assessment of OpenFOAM and FLOW-3D in the numerical modeling of a low Reynolds number hydraulic jump. Environmental Modelling & Software, 80, 322–335. https://doi.org/10.1016/j.envsoft.2016.02.018

Beck, M. W., Brumbaugh, R. D., Airoldi, L., Carranza, A., Coen, L. D., Crawford, C., Defeo, O., Edgar, G. J., Hancock, B., Kay, M. C., Lenihan, H. S., Luckenbach, M. W., Toropova, C. L., Zhang, G., & Guo, X. (2011). Oyster reefs at risk and recommendations for conservation, restoration, and management. BioScience, 61(2), 107–116. https://doi.org/10.1525/bio.2011.61.2.5

Bible, J. M., & Sanford, E. (2015). Local adaptation in an estuarine foundation species: Implications for restoration. Biological Conservation, 193, 95–102. https://doi.org/10.1016/j.biocon.2015.11.015

Borsje, B. W., van Wesenbeeck, B. K., Dekker, F., Paalvast, P., Bouma, T. J., van Katwijk, M. M., & de Vries, M. B. (2011). How ecological engineering can serve in coastal protection? Ecological Engineering, 37, 113–122. https://doi.org/10.1016/j.ecoleng.2010.11.027

Brackbill, J. U., Kothe, D. B., & Zemach, C. (1992). A continuum method for modeling surface tension. Journal of Computational Physics, 100(2), 335–354. https://doi.org/10.1016/0021-9991(92)90240-Y

Brown, A. C., & McLachlan, A. (2002). Sandy shore ecosystems and the threats facing them: Some predictions for the year 2025. Environmental Conservation, 29(1), 62–77. https://doi.org/10.1017/s037689290200005x

Browne, M. A., & Chapman, M. G. (2011). Ecologically informed engineering reduces loss of intertidal biodiversity on artificial shorelines. Environmental Science & Technology, 45(19), 8204–8207. https://doi.org/10.1021/es201924b

Bruce, T., van der Meer, J.W., Franco, L., Pearson, J.M. (2009). Overtopping performance of different armour units for rubble mound breakwaters. Coastal Eng. 56(2), 166–179. https://doi.org/10.1016/j.coastaleng.2008.03.015

Bruno, J. F., Stachowicz, J. J., & Bertness, M. D. (2003). Inclusion of facilitation into ecological theory. Trends in Ecology & Evolution, 18(3), 119–125. https://doi.org/10.1016/s0169-5347(02)00045-9

Bulleri, F., & Chapman, M. G. (2010). The introduction of coastal infrastructure as a driver of change in marine environments. Journal of Applied Ecology, 47(1), 26–35. https://doi.org/10.1111/j.1365-2664.2009.01751.x

Celik, I. B., Ghia, U., Roache, P. J., Freitas, C. J., Coleman, H., & Raad, P. E. (2008). Procedure for estimation and reporting of uncertainty due to discretization in CFD applications. Journal of Fluids Engineering, 130(7), 078001. https://doi.org/10.1115/1.2960953

Chan, J., L. Blanchard, & F. Flocard (2023). Te Ara Tupua Physical Modelling—PAA Stage. Sydney, Australia: UNSW Water Resources Laboratory.

Chapman, M. G., & Underwood, A. (2011). Evaluation of ecological engineering of "armoured" shorelines to improve their value as habitat. Journal of Experimental Marine Biology and Ecology, 400, 302–313. https://doi.org/10.1016/j.jembe.2011.02.025

Chapman, M.G., Bulleri, F. (2003). Intertidal seawalls: new features of landscape in intertidal environments. Landsc. Urban Plan. 62, 159–172. https://doi.org/10.1016/S0169-2046(02)00148-2

Cho, Y.J. (2021). Level III reliability design of an armor block of rubble mound breakwater using probabilistic model of wave height optimized for the Korean Sea wave conditions and non-Gaussian wave slope distribution. J. Mar. Sci. Eng. 9(2), 223. https://doi.org/10.3390/jmse9020223

CIRIA, CUR, CETMEF (2007). The Rock Manual: The Use of Rock in Hydraulic Engineering (2nd ed.). C683. CIRIA, London.

Concrete Layer Innovations (CLI) (2023). ACCROPODE™ II Design Guidelines (Version V03, February 2023). Concrete Layer Innovations, Woerden, Netherlands, 41 pp.

Coombes, M. A., La Marca, E. C., Naylor, L. A., & Thompson, R. C. (2015). Getting into the groove: Opportunities to enhance the ecological value of hard coastal infrastructure using

fine-scale surface textures. Ecological Engineering, 77, 314–323. https://doi.org/10.1016/j.ecoleng.2015.01.032

d'Angremond, K., Van Der Meer, J. W., & De Jong, R. J. (1996). Wave transmission at low-crested structures. Coastal Engineering Proceedings, 1(25). https://doi.org/10.9753/icce.v25.%p

Dafforn, K.A., Glasby, T.M., Johnston, E.L. (2015). Marine urbanization: an ecological framework for designing multifunctional artificial structures. Front. Ecol. Environ. 13, 82–90. https://doi.org/10.1890/140050

Delta Marine Consultants (DMC) (2023). Xbloc and XblocPlus Design Guidelines 2023. Delta Marine Consultants, Gouda, Netherlands.

Dupray, S., & Roberts, J. (2010). Review of the use of concrete in the manufacture of concrete armour units. In Coasts, Marine Structures and Breakwaters: Adapting to Change – Proceedings of the 9th International Conference on Coasts, Marine Structures and Breakwaters (Vol. 1, pp. 245–259). Thomas Telford, London. https://doi.org/10.1680/cmsb.41301.0021

ECOncrete. (2021). COASTALOCK: Single-layer-armor unit designed for project and planet. Retrieved February 28, 2024, from https://econcretetech.com/blogcat/coastalock-single-layer-armor-designed-for-project-and-planet

ECOncrete. (2023). Tide pool armor in the Port of San Diego: Fourth monitoring report, 26 months post deployment. ECOncrete. 2025. The Living Ports Project: Eco-engineered port infrastructure-Monitoring results and analysis. ECOncrete Tech, Tel Aviv, Israel.

EurOtop (2018). Manual on Wave Overtopping of Sea Defenses and Related Structures: An Overtopping Manual Largely Based on European Research but for Worldwide Application. Van der Meer, J.W., Allsop, N.W.H., Bruce, T., De Rouck, J., Kortenhaus, A., Pullen, T., Schüttrumpf, H., Troch, P., and Zanuttigh, B. Retrieved from www.overtopping-manual.com.

Evans, A. J., Firth, L. B., Hawkins, S. J., Morris, E. S., Goudge, H., & Moore, P. J. (2015). Drill-cored rock pools: An effective method of ecological enhancement on artificial structures. Marine and Freshwater Research, 67(1), 123. https://doi.org/10.1071/mf14244

Evans, A.J., Garrod, B., Firth, L.B., Hawkins, S.J., Morris, E.S., Goudge, H., Moore, P. (2016). Stakeholder priorities for multi-functional coastal defence developments and steps to effective implementation. Mar. Policy 65, 103–111. https://doi.org/10.1016/j.marpol.2015.12.009

Ferziger, J. H., and Perić, M. (2002). Computational Methods for Fluid Dynamics (3rd ed.). Springer, Berlin.

Firth, L. B., Knights, A. M., Bridger, D., Evans, A. J., Mieszkowska, N., Moore, P., O'Connor, N. E., Sheehan, E. V., Thompson, R. C., and Hawkins, S. J. (2016). Ocean sprawl: challenges and opportunities for biodiversity management in a changing world. Oceanography and Marine Biology: An Annual Review, 54, 189–262. https://doi.org/10.1201/9781315368597-9

Firth, L. B., Mieszkowska, N., Thompson, R. C., & Hawkins, S. J. (2013). Climate change and adaptational impacts in coastal systems: The case of sea defences. Environmental Science: Processes & Impacts, 15(9), 1665. https://doi.org/10.1039/c3em00313b

Firth, L. B., Thompson, R. C., Bohn, K., Abbiati, M., Airoldi, L., Bouma, T. J., Bozzeda, F., Ceccherelli, V. U., Colangelo, M. A., Evans, A., Ferrario, F., Hanley, M. E., Hinz, H., Hoggart, S. P. G., Jackson, J. E., Moore, P., Morgan, E. H., Perkol-Finkel, S., Skov, M. W., … Hawkins, S. J. (2014). Between a rock and a hard place: Environmental and engineering considerations when designing coastal defence structures. Coastal Engineering, 87, 122–135. https://doi.org/10.1016/j.coastaleng.2013.10.015

Gómez-Martín, M.E., Medina, J.R., 2014. Heterogeneous packing and hydraulic stability of cube and Cubipod armor units. J. Waterway Port Coastal Ocean Eng. 140(1), 100–108. https://doi.org/10.1061/(ASCE)WW.1943-5460.0000223

Guanche, R., Losada, I. J., and Lara, J. L. (2009). Numerical analysis of wave loads for coastal structure stability. Coastal Engineering, 56(5–6), 543–558. https://doi.org/10.1016/j.coastaleng.2008.11.003

Gutiérrez, J., Bezner, M., Molenkamp, A., van den Bos, J., Hofland, B., LeBlanc, P., Rella, A., Rosenberg, Y., & Sella, I. (2023). Physical evaluation of the hydrodynamic stability of an eco-engineered armouring unit. Coastal Engineering Proceedings, 37, 35–35. https://doi.org/10.9753/icce.v37.papers.35

Gutiérrez, J., Tagar-Hadary, T., Rosenberg, Y., Neder, M., & LeBlanc, P. (2022). Eco-engineering solution for nature-based shoreline protection at the Port of San Diego (USA). 1ères Rencontres de l'Ingénierie Maritime.

Gutiérrez Martínez, J., Bezner, M., Molenkamp, A., van den Bos, J., Hofland, B., Leblanc, P., Rella, A., Rosenberg, Y., Sella, I. (2023). Physical evaluation of the hydrodynamic stability of an eco-engineered armouring unit. Coastal Eng. Proc. 37, Paper 35

Hall, A. E., Herbert, R. J. H., Britton, J. R., & Hull, S. L. (2018). Ecological enhancement techniques to improve habitat heterogeneity on coastal defence structures. Estuarine, Coastal and Shelf Science, 210, 68–78. https://doi.org/10.1016/j.ecss.2018.05.025

Heller, V. (2011). Scale effects in physical hydraulic engineering models. *Journal of Hydraulic Research, 49*(3), 293–306. https://doi.org/10.1080/00221686.2011.578914

Hindle, R. (2018). Sustainable coastal design and planning. In E. Mossop (Ed.), Sustainable Coastal Design and Planning (pp. 387–415). CRC Press. https://doi.org/10.1201/9780429458057

Hinkel, J., Lincke, D., Vafeidis, A.T., Perrette, M., Nicholls, R.J., Tol, R.S.J., Marzeion, B., Fettweis, X., Ionescu, C., Levermann, A. (2014). Coastal flood damage and adaptation costs under 21st-century sea-level rise. Proc. Natl. Acad. Sci. USA 111(9), 3292–3297. https://doi.org/10.1073/pnas.1222469111

Hirt, C. W., & Nichols, B. D. (1981). Volume of fluid (VOF) method for the dynamics of free boundaries. Journal of Computational Physics, 39(1), 201–225. https://doi.org/10.1016/0021-9991(81)90145-5

Hosmer, D.W., Lemeshow, S., Sturdivant, R.X. (2013). Applied Logistic Regression (3rd ed.). Wiley. https://doi.org/10.1002/9781118548387

Hudson, R.Y. (1959). Laboratory investigation of rubble-mound breakwaters. J. Waterways Harbors Div. ASCE 85(4), 93–121

Hughes, S. A. (1993). Physical models and laboratory techniques in coastal engineering (Vol. 7). World Scientific Publishing. https://doi.org/10.1142/2154

Hughes, S. A., & Fowler, J. E. (1995). Estimating wave-induced kinematics at sloping structures. Journal of Waterway, Port, Coastal, and Ocean Engineering, 121(4), 209–215. https://doi.org/10.1061/(ASCE)0733-950X(1995)121:4(209)

Intergovernmental Panel on Climate Change (IPCC). (2022). Climate change 2022: Impacts, adaptation and vulnerability. Cambridge University Press, Cambridge, United Kingdom. https://doi.org/10.1017/9781009325844

Kobayashi, Nobuhisa. (2003). Numerical modeling as a design tool for coastal structures. Advances in Coastal Structure Design. 80-96. https://doi.org/10.1061/9780784406892.ch04.

Lara, J. L., Losada, I. J., and Guanche, R. (2008). Wave interaction with low-mound breakwaters using a RANS model. Ocean Engineering, 35(13), 1388–1400. https://doi.org/10.1016/j.oceaneng.2008.05.006

Lara, J. L., Ruju, A., and Losada, I. J. (2011). Reynolds-averaged Navier–Stokes modelling of long waves induced by a transient wave group on a beach. Proceedings of the Royal Society A: Mathematical, Physical and Engineering Sciences, 467(2129): 1215–1242. https://doi.org/10.1098/rspa.2010.0331

Launder, B. E., & Spalding, D. B. (1974). The numerical computation of turbulent flows. Computer Methods in Applied Mechanics and Engineering, 3(2), 269–289. https://doi.org/10.1016/0045-7825(74)90029-2

Lawniczak, A. D. (2024). Coastalock™ Performance on a Permeable Breakwater Slope (Master's thesis). Delft University of Technology. https://doi.org/10.4121/f9830419-f519-4767-a289-4de2dcb0907c.v1

Ławniczak, A.D., 2024. Coastalock™ Performance on a Permeable Breakwater Slope: Model Tests on the Influence of a Permeable Core, Unit Modifications and Toe Support on the Hydraulic Performance of an Ecological Armour Unit. M.Sc. Thesis, Delft University of Technology, Delft, The Netherlands.

Lee, C.-E., Kim, G., & Kim, S.-U. (2013). Stochastic reliability analysis of armor units of rubble-mound breakwaters under multiple loads. Journal of Coastal Research, 65, 308–313. https://doi.org/10.2112/SI65-053.1

Losada, I. J., Lara, J. L., Guanche, R., and González-Ondina, J. M. (2008). Numerical analysis of wave overtopping of rubble mound breakwaters. Coastal Engineering, 55(1), 47–62. https://doi.org/10.1016/j.coastaleng.2007.06.003

Mansard, E. P. D., & Funke, E. R. (1980). The measurement of incident and reflected spectra using a least-squares method. Coastal Engineering Proceedings, 1(17), 8. https://doi.org/10.9753/icce.v17.8

Manson, T., Gilman, J. F., Perkol-Finkel, S., Sella, I., & Marrone, J. F. (2018). Multi-purpose breakwaters. Coasts, Marine Structures and Breakwaters 2017. https://doi.org/10.1680/cmsb.63174.0449

Martins, G. M., Thompson, R. C., Neto, A. O., Hawkins, S. J., & Jenkins, S. R. (2010). Enhancing stocks of the exploited limpet Patella candei d'Orbingny via modifications in coastal engineering. Biological Conservation, 143, 203–211. https://doi.org/10.1016/j.biocon.2009.10.004

MathWorks Inc. (2023). MATLAB R2023a. The MathWorks, Inc., Natick, Massachusetts, USA.

Medina, J.R., Gómez-Martín, M.E. (2016). Cubipod® Manual 2016. Valencia: Universitat Politècnica de València

Melby, J.A., Turk, G.F. (1997). CORE-LOC™ concrete armor units: final report. U.S. Army Engineer Waterways Experiment Station, Vicksburg, MS (Technical Report CERC-97-1).

Miles, M. D. (1990). The GEDAP data analysis software package. NRC Technical Report TR-HY-030, Ottawa, Canada.

Miles, M. D. (1997). GEDAP user's guide for Windows NT. NRC Technical Report HYD-TR-021, Ottawa, Canada.

Molenkamp, A. (2022). Hydraulic performance of Coastalock armour units. Delft University of Technology Repository. https://repository.tudelft.nl/record/uuid:f45f0aaa-200d-4db9-9738-230ec8c46728 (Accessed January 14, 2023)

Morris, R. L., Boxshall, A., and Swearer, S. E. (2020). Climate-resilient coasts require diverse defence solutions. Nature Climate Change, 10(6), 482–490. https://doi.org/10.1038/s41558-020-0798-9

Morris, R. L., Konlechner, T. M., Ghisalberti, M., & Swearer, S. M. (2018). From grey to green: Efficacy of eco-engineering solutions for nature-based coastal defence. Global Change Biology, 24, 1827–1842. https://doi.org/10.1111/gcb.14063

Morris, R. L., La Peyre, M. K., Webb, B. M., Marshall, D. A., Bilkovic, D. M., Cebrian, J., McClenachan, G., Kibler, K. M., Walters, L. J., Bushek, D., Sparks, E. L., Temple, N. A., Moody, J., Angstadt, K., Goff, J., Boswell, M., Sacks, P., & Swearer, S. E. (2021). Large-scale variation in wave attenuation of oyster-reef living shorelines and the influence of inundation duration. Ecological Applications, 31(6). https://doi.org/10.1002/eap.2382

Moschella, P. S., Abbiati, M., Åberg, P., Airoldi, L., Anderson, J. M., Bacchiocchi, F., Bulleri, F., Dinesen, G. E., Frost, M., Gacia, E., Granhag, L., Jonsson, P. R., Satta, M. P., Sundelöf, A., Thompson, R. C., & Hawkins, S. J. (2005). https://doi.org/10.1016/j.coastaleng.2005.09.014

Moschella, P.S., Abbiati, M., Åberg, P., Airoldi, L., Anderson, J.M., Bacchiocchi, F., Bulleri, F., Dinesen, G.E., Frost, M., Gacia, E., Granhag, L., Jonsson, P.R., Satta, M.P., Sundelöf, A., Thompson, R.C., & Hawkins, S.J. (2005). Low-crested coastal defence structures as

artificial habitats for marine life: Using ecological criteria in design. Coastal Engineering, 52(10–11), 1053–1071. https://doi.org/10.1016/j.coastaleng.2005.09.014

Muttray, M., & Reedijk, J. (2008). “Design of concrete armour layers.” Delta Marine Consultants, Gouda, The Netherlands.

Muttray, M., ten Oever, E., & Reedijk, B. (2012). Stability of low-crested and submerged breakwaters with single-layer armouring. Journal of Shipping and Ocean Engineering, 2(3), 140–152

Park, Y.H., Oh, Y.-M., Ahn, S.M., Han, T.H., Kim, Y.-T., Suh, K.-D., Won, D. (2019). Development of a new concrete armor unit for high waves. J. Coast. Res. 35(3), 719–728. https://doi.org/10.2112/JCOASTRES-D-17-00224.1

Perkol-Finkel, S., & Sella, I. (2014). Ecologically active concrete for coastal and marine infrastructure: Innovative matrices and designs. ICE Publishing, 1139–1149. https://doi.org/10.1680/fsts597571139

Perkol-Finkel, S., & Sella, I. (2015a). Harnessing urban coastal infrastructure for ecological enhancement. Proceedings of the Institution of Civil Engineers. https://doi.org/10.1680/jmaen.15.00017

Perkol-Finkel, S., & Sella, I. (2015b). Blue is the new green: Ecological enhancement of concrete-based coastal and marine infrastructure. Ecological Engineering, 84, 260–272. https://doi.org/10.1016/j.ecoleng.2015.09.016

Perkol-Finkel, S., & Sella, I. (2019). Blue is the new green: Eco-engineering for climate change. Marine Technology Society Journal, 53(4), 7–10. https://doi.org/10.4031/MTSJ.53.4.13

Perkol-Finkel, S., Shashar, N., Benayahu, Y. (2008). Can artificial reefs mimic natural reef communities? The roles of structural complexity and time. Mar. Environ. Res. 65, 1–12. https://doi.org/10.1016/j.marenvres.2005.08.001

Perricone, V., Contestabile, P., Santulli, C., Rendina, F., Langella, C. (2023). Nature-based and bioinspired solutions for coastal protection: an overview among key ecosystems and new sustainable design approaches. ICES J. Mar. Sci. (Advance online publication). https://doi.org/10.1093/icesjms/fsad080

Pilechi, A., Baker, S., and Cornett, A. (2018). Evaluation of a numerical wave modelling tool for studying the overtopping of rubblemound breakwaters. In Proceedings of the 7th International Conference on the Application of Physical Modelling in Coastal and Port Engineering and Science (Coastlab18), Santander, Spain, May 22–26, 2018. Retrieved from https://nrc-publications.canada.ca/eng/view/object/?id=94ba2dba-798a-49ad-adae-8da16d881b9c

Provan, M., Murphy, E., Rahman, A., Morris, E., & Matfin, A. (2023). Experimental study of wave and sediment interactions with edge-treatment features on a living dyke. Coastal Sediments 2023. https://doi.org/10.1142/9789811275135_0199

Provan, M., Rahman, A., & Murphy, E. (2024). Full-scale experiments on wave transmission and stability of oyster shell-filled bag berms. Coastal Engineering, 193, 104578. https://doi.org/10.1016/j.coastaleng.2024.104578

Reedijk, B., Muttray, M. (2009). Design of concrete armour layers. Hansa International Maritime Journal, 6, 111–118

Reedijk, B., Muttray, M., van Berge, A., & Rover, R. D. (2009). Effect of core permeability on armour layer stability. Coastal Engineering, 3358–3367. https://doi.org/10.1142/9789814277426_0278

Rella, A. J., Gutiérrez, J., Tagar-Hadary, T., Rosenberg, Y., Bezner, M., Neder, M., LeBlanc, P., Sella, I., & Perkol-Finkel, S. (2023). The development of a fully constructive ecological unit for coastal armouring. Coasts, Marine Structures and Breakwaters 2023: Resilience and Adaptability in a Changing Climate. https://doi.org/10.1680/cmsb.67042.0953

Rijn, L. C. V., Ribberink, J. S., Werf, J. V. D., and Walstra, D. J. R. (2013). Coastal sediment dynamics: recent advances and future research needs. Journal of Hydraulic Research, 51(5), 475–493. https://doi.org/10.1080/00221686.2013.849297

Roney, S. H., Haas, K., Bliss, T., & Weissburg, M. J. (2025). Restored oyster reefs function as living shorelines to reduce wave energy in intertidal marshes. Ecological Engineering, 221, 107774. https://doi.org/10.1016/j.ecoleng.2025.107774

Safa, E., Mojtahedi, A., Mohammadian, A., and Lotfollahi Yaghin, M. A. (2024). Hydrodynamic assessment of a new nature-based armour unit on rubble mound breakwater for coastal protection. China Ocean Engineering, 38(3), 439–452. https://doi.org/10.1007/s13344-024-0035-9

Safak, I., Angelini, C., Norby, P. L., Dix, N., Roddenberry, A., Herbert, D., Astrom, E., & Sheremet, A. (2020). Wave transmission through living shoreline breakwalls. Continental Shelf Research, 211, 104268. https://doi.org/10.1016/j.csr.2020.104268

Salauddin, M., O'Sullivan, J.J., Abolfathi, S., & Pearson, J.M. (2021). Eco-engineering of seawalls—An opportunity for enhanced climate resilience from increased topographic complexity. Frontiers in Marine Science, 8, 674630. https://doi.org/10.3389/fmars.2021.674630

Sayar, S.D., Gutiérrez, J., Baker, S., Nistor, I., Rosenberg, Y., Hofland, B., van den Bos, J., Colom Jover, F., Kerr, S., Lawniczak, A. & Molenkamp, A. (under review). Design recommendations for eco-engineered single layer armour units. Manuscript under review at Coastal EngineeringSayar, S. D., Baker, S., Nistor, I., & Gutiérrez, J. (2026). Experimental and numerical assessment of low-crested and emergent breakwaters with eco-engineered armour units. Canadian Journal of Civil Engineering, 53, 1–19. https://doi.org/10.1139/cjce-2025-0373

Sayar, S. D., Nistor, I., Baker, S., and Gutiérrez Martínez, J. (2024). Low-crested and emergent breakwaters with eco-friendly armour units. In Proceedings of the 9th International Conference on Physical Modelling in Coastal Engineering (Coastlab24), Delft, Netherlands, May 13–16, 2024. https://doi.org/10.59490/coastlab.2024.775

Sayar, S.D., Nistor, I., Baker, S., and Gutiérrez Martínez, J. (2024). Hydraulic performance of ecofriendly breakwater armour units. In Proceedings of the 38th International Conference

on Coastal Engineering (ICCE 2024), Rome, Italy, 8–14 September 2024. https://doi.org/10.59490/coastlab.2024.775

Sayar, S.D., Nistor, I., Baker, S., Gutiérrez Martínez, J., & Rosenberg, Y. (2025). Hydraulic performance of low-crested and emergent breakwaters with ecologically designed armour units. Journal of Waterway, Port, Coastal, and Ocean Engineering, 151(2), 04024027. https://doi.org/10.1061/JWPED5.WWENG-2158

Scaravaglione, G., Melby, J. A., Tomasicchio, G. R., van Gent, M. R. A., Saponieri, A. (2025). On the uncertainties in stone armor stability. Coastal Engineering, 202, Article 104790. https://doi.org/10.1016/j.coastaleng.2025.104790

Sella, I., and Perkol-Finkel, S. (2015). Blue is the new green—ecological enhancement of concrete-based coastal and marine infrastructure. Ecological Engineering, 84, 260–272. https://doi.org/10.1016/j.ecoleng.2015.09.016

Sella, I., Hadary, T., Rella, A.J., Riegl, B., Swack, D., Perkol-Finkel, S. (2022). The design, production and validation of an ecologically engineered concrete block mattress – a nature-inclusive design for shoreline and offshore construction. Integr. Environ. Assess. Manag. 18(1), 148–162. https://doi.org/10.1002/ieam.4523

Sella, I., Perkol-Finkel, S. (2015). Blue is the new green – ecological enhancement of concrete-based coastal and marine infrastructure. Ecol. Eng. 84, 260–272. https://doi.org/10.1016/j.ecoleng.2015.09.016

Stagnitti, M., Lara, J. L., Musumeci, R. E., & Foti, E. (2023). Numerical modeling of wave overtopping of damaged and upgraded rubble-mound breakwaters. *Ocean Engineering, 280*, 114798. https://doi.org/10.1016/j.oceaneng.2023.114798

Stanley, R. E., Bilskie, M. V., Woodson, C. B., & Byers, J. E. (2024). A model for understanding the effects of flow conditions on oyster reef development and impacts to wave attenuation. Ecological Modelling, 489, 110627 https://doi.org/10.1016/j.ecolmodel.2024.110627

Strain, E.M.A., Olabarria, C., Mayer-Pinto, M., Cumbo, V.R., Morris, R.L., Bugnot, A.B., Dafforn, K.A., Heery, E., Firth, L.B., Brooks, P.R., Bishop, M.J. (2018). Eco-engineering urban infrastructure for marine and coastal biodiversity: which interventions have the greatest ecological benefit? J. Appl. Ecol. 55(1), 426–441 https://doi.org/10.1111/1365-2664.12961

Takagi, H. (2019). Adapted mangrove on hybrid platform: Coupling of ecological and engineering principles against coastal hazards. Results in Engineering, 4, 100067. https://doi.org/10.1016/j.rineng.2019.100067

Temmerman, S., Meire, P., Bouma, T. J., Herman, P. M. J., Ysebaert, T., and De Vriend, H. J. (2013). Ecosystem-based coastal defence in the face of global change. Nature, 504(7478), 79–83. https://doi.org/10.1038/nature12859

Torres-Freyermuth, A., Lara, J. L., and Losada, I. J. (2010). Numerical modelling of short- and long-wave transformation on a barred beach. Coastal Engineering, 57(3), 317–330. https://doi.org/10.1016/j.coastaleng.2009.10.013

U.S. Army Corps of Engineers (USACE) (1984). Shore Protection Manual (4th ed.). U.S. Army Corps of Engineers, Coastal Engineering Research Center, Vicksburg, MS.

U.S. Army Corps of Engineers (USACE) (2002). Coastal Engineering Manual (Engineer Manual 1110-2-1100). U.S. Army Corps of Engineers, Washington, DC (6 vols).

Van der Meer, J. W. (1992). Conceptual design of rubble mound breakwaters. Delft Hydraulics Report No. 483.

Van der Meer, J. W., & Daemen, I. F. R. (1994). Stability and wave transmission at low-crested rubble mound structures. Journal of Waterway, Port, Coastal, and Ocean Engineering (ASCE), 120(1), 1–19. https://doi.org/10.1061/(ASCE)0733-950X(1994)120:1(1)

Van der Meer, J. W., Briganti, R., Zanuttigh, B., & Wang, B. (2005). Wave transmission and reflection at low-crested structures: Design formulae, oblique wave attack and spectral change. Coastal Engineering, 52(10–11), 915–929. https://doi.org/10.1016/j.coastaleng.2005.09.005

Van der Meer, J. W., Verhaeghe, H., & Steendam, G. J. (2009). The new wave overtopping database for coastal structures. Coastal Engineering, 56(2), 108–120. https://doi.org/10.1016/j.coastaleng.2008.03.012

Van der Meer, J.W. (1988). Rock slopes and gravel beaches under wave attack. Ph.D. thesis, Delft University of Technology. Delft Hydraulics Publication No. 396, Delft, Netherlands.

Van der Meer, J.W. (1992). Conceptual design of rubble mound breakwaters. Delft University of Technology, Delft, The Netherlands.

Van der Meer, J.W. (1999). Design of concrete armour layers. Infram BV, Zeewolde, The Netherlands.

Van der Meer, J.W., d'Angremond, K., and Gerding, E. (1996). Toe structure stability of rubble mound breakwaters. In Advances in Coastal Structures and Breakwaters, Thomas Telford, London, United Kingdom, pp. 29–36. https://doi.org/10.1680/aicsab.25097.0029

van Gent, M. R. A., Buis, L., van den Bos, J. P., & Wüthrich, D. (2023). Wave transmission at submerged coastal structures and artificial reefs. Coastal Engineering, 184, 104344. https://doi.org/10.1016/j.coastaleng.2023.104344

Vidal, C., Losada, M.A., Mansard, E.P.D. (1992). Stability criteria for low-crested detached breakwater sections (trunk and slope). J. Waterway Port Coastal Ocean Eng. 118(2), 209–225. https://doi.org/10.1061/(ASCE)0733-950X(1992)118:2(209)

Weller, H. G., Tabor, G., Jasak, H., and Fureby, C. (1998). A tensorial approach to computational continuum mechanics using object-oriented techniques. Computers in Physics, 12(6), 620–631. https://doi.org/10.1063/1.168744

Zanuttigh, B., & van der Meer, J. W. (2007). Wave reflection from coastal structures. International Conference on Coastal Engineering. https://doi.org/10.1142/9789812709554_0364

Appendix A. Comprehensive Experimental Dataset

The tables presented in this appendix compile the complete physical modelling dataset used to assess the hydraulic performance of Coastalock armour units on low-crested and emergent rubble mound breakwaters (RMBW). Tables A1 and A2 summarize the detailed test programs, including water levels, wave steepness, significant wave heights, wave periods, armour unit spacing, and underlayer rock sizes for each test series. Tables A3 to A5 present measured and calculated hydrodynamic parameters derived from these tests. Specifically, Table A3 compares the experimental wave-transmission coefficients with established empirical formulas from the literature, while Tables A4 and A5 contain corresponding wave-reflection coefficients for the low-crested and emergent RMBW models, respectively. Together, these datasets provide the full basis for the analyses and discussions presented in Chapter 3.

Table A-1. The test program of the low-crested breakwater model

Test Series 1	Water Level (m)	Measured wave steepness	Measured significant wave height (m)	Measured wave period (s)	Armour unit spacing (%)	Under layer rock size (g)	Test Series 2	Water Level (m)	Measured wave steepness	Measured significant wave height (m)	Measured wave period (s)	Armour unit spacing (z%)	Under layer rock size (g)	Test Series 3	Water Level (m)	Measured wave steepness	Measured significant wave height (m)	Measured wave period (s)	Armour unit spacing (%)	Under layer rock size (g)
Water Level 30cm							**Water Level 30cm**							**Water Level 30cm**						
TS1_D30_1	0.3	0.030	0.087	1.244	10	50-100	**TS2_D30_1**	0.3	0.030	0.087	1.258	0	50-100	**TS3_D30_1**	0.3	0.030	0.087	1.239	10	25-60
TS1_D30_2	0.3	0.036	0.140	1.609	10	50-100	**TS2_D30_2**	0.3	0.036	0.140	1.610	0	50-100	**TS3_D30_2**	0.3	0.036	0.142	1.571	10	25-60
TS1_D30_3	0.3	0.034	0.207	4.075	10	50-100	**TS2_D30_3**	0.3	0.045	0.178	2.269	0	50-100	**TS3_D30_3**	0.3	0.043	0.177	2.272	10	25-60
TS1_D30_4	0.3	0.054	0.218	3.704	10	50-100	**TS2_D30_4**	0.3	0.035	0.203	4.336	0	50-100	**TS3_D30_4**	0.3	0.034	0.200	4.340	10	25-60
TS1_D30_5	0.3	0.038	0.213	4.310	10	50-100	**TS2_D30_5**	0.3	0.054	0.217	2.213	0	50-100	**TS3_D30_5**	0.3	0.052	0.217	3.604	10	25-60
Water Level 40cm							**TS2_D30_6**	0.3	0.038	0.212	5.888	0	50-100	**TS3_D30_6**	0.3	0.039	0.211	5.989	10	25-60
TS1_D40_1	0.4	0.039	0.133	1.538	10	50-100	**Water Level 40cm**							**Water Level 40cm**						
TS1_D40_2	0.4	0.043	0.173	1.978	10	50-100	**TS2_D40_1**	0.4	0.038	0.133	1.541	0	50-100	**TS3_D40_1**	0.4	0.037	0.134	1.538	10	25-60
TS1_D40_3	0.4	0.046	0.220	2.094	10	50-100	**TS2_D40_2**	0.4	0.042	0.174	1.821	0	50-100	**TS3_D40_2**	0.4	0.041	0.172	1.974	10	25-60
TS1_D40_4	0.4	0.050	0.254	2.962	10	50-100	**TS2_D40_3**	0.4	0.046	0.218	2.094	0	50-100	**TS3_D40_3**	0.4	0.045	0.218	2.094	10	25-60
TS1_D40_5	0.4	0.032	0.227	3.778	10	50-100	**TS2_D40_4**	0.4	0.031	0.228	3.783	0	50-100	**TS3_D40_4**	0.4	0.031	0.227	3.781	10	25-60
TS1_D40_6	0.4	0.035	0.249	3.839	10	50-100	**TS2_D40_5**	0.4	0.049	0.253	2.988	0	50-100	**TS3_D40_5**	0.4	0.049	0.255	2.971	10	25-60
Water Level 50cm							**TS2_D40_6**	0.4	0.035	0.250	3.832	0	50-100	**TS3_D40_6**	0.4	0.035	0.248	3.828		
TS1_D50_1	0.5	0.037	0.123	1.423	10	50-100	**Water Level 50cm**							**Water Level 50cm**						

TS1_D50_2	0.5	0.040	0.162	1.641	10	50-100	**TS2_D50_1**	0.5	0.043	0.198	1.840	0	50-100	**TS3_D50_1**	0.5	0.044	0.198	1.863	10	25-60
TS1_D50_3	0.5	0.043	0.197	1.845	10	50-100	**TS2_D50_2**	0.5	0.046	0.262	2.225	0	50-100	**TS3_D50_2**	0.5	0.047	0.265	2.226	10	25-60
TS1_D50_4	0.5	0.047	0.263	2.225	10	50-100	**TS2_D50_3**	0.5	0.031	0.249	3.824	0	50-100	**TS3_D50_3**	0.5	0.032	0.250	3.829	10	25-60
TS1_D50_5	0.5	0.053	0.317	2.574	10	50-100	**TS2_D50_4**	0.5	0.055	0.316	2.583	0	50-100	**TS3_D50_4**	0.5	0.054	0.316	2.589	10	25-60
TS1_D50_6	0.5	0.036	0.279	3.960	10	50-100	**TS2_D50_5**	0.5	0.037	0.280	3.966	0	50-100	**TS3_D50_5**	0.5	0.036	0.280	3.970	10	25-60
Water Level 60cm							**Water Level 60cm**							**Water Level 60cm**						
TS1_D60_1	0.6	0.044	0.197	1.818	10	50-100	**TS2_D60_1**	0.6	0.047	0.299	2.410	0	50-100	**TS3_D60_1**	0.6	0.048	0.300	2.416	10	25-60
TS1_D60_2	0.6	0.047	0.299	2.410	10	50-100	**TS2_D60_2**	0.6	0.029	0.253	3.769	0	50-100	**TS3_D60_2**	0.6	0.029	0.253	3.772	10	25-60
TS1_D60_3	0.6	0.048	0.348	2.723	10	50-100	**TS2_D60_3**	0.6	0.048	0.348	2.724	0	50-100	**TS3_D60_3**	0.6	0.049	0.347	2.673	10	25-60
TS1_D60_4	0.6	0.056	0.382	2.866	10	50-100	**TS2_D60_4**	0.6	0.034	0.303	4.111	0	50-100	**TS3_D60_4**	0.6	0.034	0.302	3.340	10	25-60
TS1_D60_5	0.6	0.028	0.252	3.769	10	50-100	**TS2_D60_5**	0.6	0.059	0.385	2.869	0	50-100	**TS3_D60_5**	0.6	0.059	0.382	2.878	10	25-60
TS1_D60_6	0.6	0.033	0.302	4.109	10	50-100	**Water Level 70cm**							**Water Level 70cm**						
Water Level 70cm							**TS2_D70_1**	0.7	0.048	0.363	2.842	0	50-100	**TS3_D70_1**	0.7	0.048	0.363	2.840	10	25-60
TS1_D70_7	0.7	0.044	0.335	2.765	10	50-100	**TS2_D70_2**	0.7	0.033	0.345	3.997	0	50-100	**TS3_D70_2**	0.7	0.034	0.346	3.999	10	25-60
TS1_D70_8	0.7	0.049	0.364	2.841	10	50-100	**TS2_D70_3**	0.7	0.050	0.375	2.837	0	50-100	**TS3_D70_3**	0.7	0.050	0.373	2.843	10	25-60
TS1_D70_9	0.7	0.034	0.347	4.000	10	50-100														
TS1_D70_10	0.7	0.049	0.376	2.895	10	50-100														

Table A-2. The test program of the emergent RMBW model

Test Series 4	Water Level (m)	Measured wave steepness	Measured significant wave height (m)	Measured wave period (s)	Armour unit spacing (%)	Under layer rock size (g)	Test Series 5	Water Level (m)	Measured wave steepness	Measured significant wave height (m)	Measured wave period (s)	Armour unit spacing (%)	Under layer rock size (g)
Water Level 30cm							**Water Level 40cm**						
TS4_D30_1	0.3	0.031	0.088	1.217	10	25-60	**TS5_D40_1**	0.4	0.046	0.286	2.160	10	25-60
TS4_D30_2	0.3	0.036	0.144	1.570	10	25-60	**TS5_D40_2**	0.4	0.037	0.280	3.889	10	25-60
TS4_D30_3	0.3	0.041	0.186	2.279	10	25-60	**Water Level 50cm**						
TS4_D30_4	0.3	0.031	0.226	4.091	10	25-60	**TS5_D50_1**	0.5	0.033	0.133	1.473	10	25-60
TS4_D30_5	0.3	0.046	0.229	3.676	10	25-60	**TS5_D50_2**	0.5	0.036	0.186	1.524	10	25-60
TS4_D30_6	0.3	0.034	0.229	4.305	10	25-60	**TS5_D50_3**	0.5	0.040	0.237	1.940	10	25-60
Water Level 40cm							**TS5_D50_4**	0.5	0.046	0.294	2.093	10	25-60
TS4_D40_1	0.4	0.034	0.143	1.537	10	25-60	**TS5_D50_5**	0.5	0.038	0.316	3.851	10	25-60
TS4_D40_2	0.4	0.037	0.193	2.066	10	25-60	**TS5_D50_6**	0.5	0.054	0.364	3.571	10	25-60
TS4_D40_3	0.4	0.042	0.243	2.874	10	25-60	**TS5_D50_7**	0.5	0.043	0.344	4.177	10	25-60
TS4_D40_4	0.4	0.031	0.258	4.449	10	25-60	**Water Level 60cm**						
TS4_D40_5	0.4	0.044	0.277	3.601	10	25-60	**TS5_D60_1**	0.6	0.041	0.229	1.922	10	25-60
TS4_D40_6	0.4	0.036	0.276	3.857	10	25-60	**TS5_D60_2**	0.6	0.049	0.318	2.179	10	25-60
Water Level 50cm							**TS5_D60_3**	0.6	0.036	0.343	5.290	10	25-60
TS4_D50_1	0.5	0.035	0.131	1.463	10	25-60	**TS5_D60_4**	0.6	0.052	0.394	4.409	10	25-60
TS4_D50_2	0.5	0.036	0.183	1.525	10	25-60	**TS5_D60_5**	0.6	0.065	0.440	4.593	10	25-60
TS4_D50_3	0.5	0.039	0.233	2.028	10	25-60	**Water Level 70cm**						
TS4_D50_4	0.5	0.045	0.293	2.867	10	25-60	**TS5_D70_1**	0.7	0.037	0.222	1.981	10	25-60
TS4_D50_5	0.5	0.040	0.319	3.827	10	25-60	**TS5_D70_2**	0.7	0.043	0.323	2.037	10	25-60
							TS5_D70_3	0.7	0.049	0.414	3.913	10	25-60
							TS5_D70_4	0.7	0.040	0.381	3.555	10	25-60

Table A-3. Measured wave transmission coefficient and calculated literature formula results for low-crested breakwater (D: water depth in model scale, cm; for D40-X, X: the number of tests in the corresponding test series)

Test ID / Test Parameters	D40-1	D40-2	D40-3	D40-4	D50-1	D50-2	D50-3	D50-4	D50-5	D60-1	D60-2	D60-3	D60-4	D70-1	D70-2	D70-3
Hm0 (m, prototype scale)	2.00	2.60	3.30	3.81	1.74	2.43	2.96	3.95	4.76	2.96	4.49	5.22	5.73	5.03	5.46	5.64
T_p (s, prototype scale)	5.85	7.05	7.63	8.56	5.27	6.24	7.17	8.60	9.53	7.28	8.68	10.11	10.53	9.76	11.00	11.00
K_t-Experiment Results (%)	46.8	50.6	50.3	51.2	69.8	67.2	66.8	65.8	65.3	79.5	76.5	76.7	76.1	81.9	80.5	82.3
K_t-Van der Meer and Daemen (1994)	20.5	27.0	36.4	38.8	53.6	53.1	53.4	53.9	53.2	74.3	73.7	69.7	66.1	85.6	79.9	73.1
K_t-D'Angremond et al. (1996)	44.8	50.1	54.9	58.8	70.6	73.5	75.6	77.3	79.1	96.6	95.8	94.1	91.8	108.5	103.1	97.1
K_t-Van Gent et al. (2023)	48.2	51.5	53.9	55.0	79.0	75.1	72.5	70.7	68.7	84.1	80.6	77.8	75.6	84.2	81.8	79.8
Error (%)-Van der Meer and Daemen (1994)	58.5	49.9	33.7	30.6	27.4	24.6	22.8	22.7	21.1	10.9	8.4	12.3	17.6	1.7	5.7	15.0
Error (%)-D'Angremond et al. (1996)	9.6	6.9	0.2	5.3	4.4	4.2	9.5	11.0	17.4	15.9	19.0	18.3	14.4	28.9	21.7	13.0
Error (%)-Van Gent et al. (2023)	2.7	4.3	1.9	1.5	7.0	6.5	5.0	1.4	1.9	0.9	0.2	2.2	5.9	0.0	3.4	7.2

Table A-4. Measured wave reflection coefficient and calculated literature formula results for low-crested breakwater (D: water depth in model scale, cm; for D30-X, X: the number of tests in the corresponding test series)

Test ID / Test Parameters	D30-1	D30-2	D30-3	D40-1	D40-2	D40-3	D40-4	D50-1	D50-2	D50-3	D50-4	D60-1	D60-2	D60-3	D60-4	D70-1	D70-2	D70-3
H_{m0} (prototype scale)	1.31	2.10	3.27	2.00	2.60	3.30	3.81	2.43	2.96	3.95	4.76	2.96	4.49	5.22	5.73	5.03	5.46	5.64
T_p (prototype scale)	4.8	6.47	8.33	5.85	7.05	7.63	8.56	6.24	7.17	8.6	9.53	7.28	8.68	10.11	10.53	9.76	11.00	11.00
K_r-Experiment Results (%)	31.1	37.4	54.1	20.2	28.7	31.6	38.6	17.0	21.5	30.3	29.7	21.7	26.5	27.1	30.8	24.7	27.4	27.6
K_r- Van der Meer (1992)	30.3	29.1	27.4	30.2	29.5	28.5	27.8	28.9	28.2	27.7	26.7	28.9	28.7	27.7	27.0	28.8	28.4	27.7
K_r-Hughes and Fowler (1995)	35.9	40.1	45.7	37.3	40.8	42.9	44.7	36.5	38.7	40.7	42.5	37.0	40.8	42.5	44.0	41.8	44.0	45.3
K_r-Zanuttigh and Van der Meer (2005)	28.6	29.2	30.1	29.2	30.3	30.1	30.3	27.0	27.1	27.5	27.1	27.1	29.1	28.6	28.4	29.8	30.6	30.5
K_r - Zanuttigh and Van der Meer (2006)	31.4	29.8	27.7	31.2	30.3	29.1	28.2	29.6	28.7	28.1	26.8	29.5	29.3	28.1	27.2	29.4	28.9	28.1
Error (%) - Van der Meer (1992)	2.4	22.3	49.4	49.4	2.9	9.8	27.9	70.2	31.3	8.6	10.0	33.2	8.3	2.1	12.4	16.5	3.4	0.4
Error (%) - Hughes and Fowler (1995)	15.4	7.2	15.6	84.8	42.3	35.5	15.9	114.6	80.0	34.2	43.5	70.5	53.8	56.5	43.0	69.0	60.3	64.2
Error (%) - Zanuttigh and Van der Meer (2005)	8.0	21.9	44.3	44.5	5.8	4.7	21.6	58.7	26.3	9.2	8.7	25.2	9.7	5.4	7.6	20.6	11.6	10.4
Error (%) - Zanuttigh and Van der Meer (2006)	0.9	20.3	48.9	54.2	5.8	7.9	26.9	74.3	33.7	7.4	9.6	36.3	10.7	3.5	11.7	19.1	5.4	1.8

Table A-5. Measured wave reflection coefficient and calculated literature formula results for emergent RMBW (D: water depth in model scale, cm; for D30-X, X: the number of tests in the corresponding test series)

Test ID / Test Parameters	D30-1	D30-2	D30-3	D30-4	D40-1	D40-2	D40-3	D40-4	D50-1	D50-2	D50-3	D50-4	D50-5	D60-1	D60-2	D60-3	D60-4	D70-1	D70-2	D70-3
H_{m0} (prototype scale)	1.34	2.16	2.79	3.44	2.15	2.9	3.65	4.16	1.97	2.75	3.5	4.4	5.16	3.44	4.77	5.85	6.66	3.33	4.85	6.21
T_p (prototype scale)	4.8	6.47	6.89	7.05	6.24	6.74	7.28	7.82	4.84	6.43	6.66	8.02	9.02	6.78	9.64	10.3	10.92	7.24	8.6	10.53
K_r– Experiment Results (%)	31.7	38.9	44.1	57.1	35.2	42.9	56.6	62.0	29.4	34.9	41.3	50.5	54.5	38.6	51.0	52.5	68.7	38.6	44.7	46.3
K_r– Van der Meer (1992)	30.3	29.1	28.3	27.4	30.2	29.5	28.5	27.8	30.0	28.9	28.2	27.7	26.7	28.9	28.7	27.7	27.0	30.8	27.8	27.2
K_r–Hughes and Fowler (1995)	35.9	40.1	43.6	45.7	37.3	40.8	42.9	44.7	34.0	36.5	38.7	40.7	42.5	37.0	40.8	42.5	44.0	37.5	40.1	41.8
K_r-Zanuttigh and Van der Meer (2005)	28.6	29.2	30.3	30.1	29.2	30.3	30.1	30.3	27.2	27.0	27.1	27.5	27.1	27.1	29.1	28.6	28.4	30.1	27.4	27.3
K_r - Zanuttigh and Van der Meer (2006)	31.4	29.8	28.9	27.7	31.2	30.3	29.1	28.2	30.9	29.6	28.7	28.1	26.8	29.5	29.3	28.1	27.2	31.9	28.3	27.4
Error (%) - Van der Meer (1992)	4.2	25.2	35.8	52.1	14.3	31.3	49.6	55.1	2.0	17.1	31.7	45.1	51.0	25.2	43.7	47.2	60.7	20.2	37.7	41.3
Error (%) - Hughes and Fowler (1995)	13.3	3.1	1.2	20.0	6.0	5.0	24.3	27.9	15.7	4.5	6.4	19.4	22.0	4.3	20.0	19.1	35.9	2.9	10.1	9.7
Error (%) - Zanuttigh and Van der Meer (2005)	9.7	24.9	31.3	47.2	17.1	29.4	46.7	51.2	7.4	22.8	34.3	45.5	50.3	29.7	43.0	45.5	58.6	21.9	38.6	40.9
Error (%) - Zanuttigh and Van der Meer (2006)	1.0	23.4	34.6	51.6	11.5	29.3	48.5	54.5	5.2	15.2	30.5	44.4	50.8	23.5	42.4	46.5	60.5	17.3	36.8	40.8

Appendix B. Formulation of the Numerical Model

This appendix provides supplementary mathematical formulation for the IH2VOF numerical model described in Section 4.3. It expands the compact governing equations used in Chapter 4 and defines the principal variables and model terms relevant to the simulations. The appendix focuses on the clear-fluid RANS formulation, the Volume of Fluid (VOF) free-surface representation, the porous-media resistance formulation used in the VARANS framework, the turbulence closure, and the interpretation of the principal physical parameters used in the numerical model. The formulation follows the established IH2VOF/VARANS-VOF framework for wave interaction with porous coastal structures (Losada et al., 2008; Lara et al., 2011).

B.1 Clear-fluid formulation

Outside the porous structure, the incompressible two-phase flow is represented using the Reynolds-Averaged Navier-Stokes (RANS) equations, consistent with the two-dimensional RANS-VOF formulation implemented in IH2VOF (Lara et al., 2011). The incompressibility condition is expressed in Equation 4-1 where u is the velocity vector. The corresponding momentum equation may be written in expanded form as

$$\frac{\partial \mathrm{u}}{\partial t} + (\mathrm{u}\cdot\nabla)\mathrm{u} = -\frac{1}{\rho}\nabla p + \nabla\cdot[(\nu+\nu_t)(\nabla\mathrm{u}+\nabla\mathrm{u}^T)] + \mathrm{g} + \mathrm{f}_\sigma \qquad \text{Equation B-1}$$

where p is pressure, ρ is the local fluid density, ν is the molecular kinematic viscosity, ν_t is the turbulent or eddy viscosity, g is gravitational acceleration, and f_σ represents the interfacial surface-tension force. This expanded form clarifies the compact momentum equation presented in Chapter 4. In the Reynolds-averaged formulation, diffusion of momentum is governed not only by the molecular viscosity of the fluid, but also by the modelled turbulent viscosity generated through the turbulence closure.

This distinction is important for the wave–structure interaction problem considered in this thesis. Energy dissipation is influenced not only by viscous effects, but also by turbulence associated with wave transformation, run-up, overtopping, and flow through porous layers. The numerical model therefore uses the RANS equations to represent the mean flow field while modelling the contribution of unresolved turbulent fluctuations through ν_t.

For the two-phase formulation, local mixture properties depend on the VOF phase fraction. The VOF approach was originally developed to capture the moving free boundaries by including a phase indicator function (Hirt and Nichols, 1981). In the present formulation, the mixture density and dynamic viscosity may be written as:

$$\rho = \alpha\rho_w + (1-\alpha)\rho_a \qquad \text{Equation B-2}$$

$$\mu = \alpha\mu_w + (1-\alpha)\mu_a \qquad \text{Equation B-3}$$

and the corresponding kinematic viscosity is:

$$\nu = \frac{\mu}{\rho}$$ Equation B-4

where the subscripts w and a denote water and air, respectively, and α is the water volume fraction. These relations clarify how the fluid properties in the momentum equation are evaluated locally. In water-filled cells, the properties approach those of water; in air-filled cells, they approach those of air; and in interface cells, they are blended according to the local value of α.

B.2 Free-surface tracking and VOF variable

The air-water interface is captured using a VOF transport equation of the form (Hirt and Nichols, 1981):

$$\frac{\partial \alpha}{\partial t} + \nabla \cdot (\alpha \mathrm{u}) = 0$$ Equation B-5

where α is the water volume fraction. In this formulation, $\alpha = 1$ corresponds to a cell filled with water, $\alpha = 0$ corresponds to a cell filled with air, and intermediate values $0 < \alpha < 1$ identify cells intersected by the free surface.

The physical role of Equation 4-3 is therefore to transport the free surface through the computational domain. It does not describe the porosity of the breakwater. This distinction is essential because two different quantities are involved in the numerical model:

- α is the phase fraction used to identify water and air and to reconstruct the free surface.
- n is the porosity of the porous medium and is used in the porous-region formulation.

Accordingly, the VOF equation determines the evolution of the water surface elevation, whereas porosity affects the momentum balance inside the armour layer, underlayer, toe, and core through the porous-media resistance terms described below.

B.3 Porous-region formulation and VARANS equations

Inside the breakwater, the flow is not resolved as water passing around every individual armour unit, underlayer stone, or core particle. Instead, the porous layers are represented as equivalent porous media using a volume-averaged Reynolds-Averaged Navier-Stokes (VARANS) formulation, which has been widely applied to wave interaction with permeable and rubble mound coastal structures (Losada et al., 2008; Lara et al., 2008; Lara et al., 2011).

In simplified notation, and for the interpretation of the present simulations, the volume-averaged continuity condition may be expressed in divergence-free form for the velocity variable used by the solver. More generally, porous-media continuity depends on the definition of the velocity variable and the spatial distribution of porosity. The momentum balance in a porous region may be expressed conceptually as:

$$(1 + C_m)\frac{\partial \mathrm{u}}{\partial t} + \frac{1}{n}(\mathrm{u} \cdot \nabla)\mathrm{u} = -\frac{1}{\rho}\nabla p + \nabla \cdot [(\nu + \nu_t)(\nabla \mathrm{u} + \nabla \mathrm{u}^T)] + \mathrm{g} - \mathrm{R}$$ Equation B-6

where n is the porosity of the porous medium, C_m is an added-mass coefficient, and R is the momentum sink representing hydraulic resistance within the porous matrix. The exact implementation in IH2VOF follows the solver formulation, but this expression captures the principal physical meaning relevant to the interpretation of Chapter 4.

The porous-media resistance term is commonly expressed as the sum of a linear component and a nonlinear component:

$$\mathrm{R} = \mathrm{R}_L + \mathrm{R}_N \qquad \text{Equation B-7}$$

A generalized representation of these terms is:

$$\mathrm{R} = a\frac{\nu}{D_{n50}^2}\mathrm{u} + \beta\frac{|\mathrm{u}|}{D_{n50}}\mathrm{u} \qquad \text{Equation B-8}$$

where D_{n50} is the nominal diameter of the porous layer material, a is a linear resistance coefficient, and β is the nonlinear friction coefficient. In the numerical implementation, the final resistance also depends on the porosity assigned to each layer. The linear term represents viscous resistance, while the nonlinear term represents inertial losses associated with form drag, flow contraction, expansion, and separation within the porous structure.

In this formulation, porosity enters through the VARANS momentum balance rather than through the free-surface transport equation. The porous structure is represented by introducing resistance terms into the momentum equation, while pressure is obtained through the incompressible pressure-velocity coupling of the RANS/VARANS solver.

B.4 Interpretation of the linear and nonlinear friction terms

The linear and nonlinear resistance terms have different physical meanings. The linear term is proportional to velocity and is associated with viscous resistance within the porous media. The nonlinear term is proportional to the square of velocity and represents inertial losses caused by form drag, flow separation, and acceleration through the pore spaces. For wave impact on rubble mound structures, nonlinear resistance often becomes particularly important because local velocities during run-up, down-rush, transmission, and overtopping can be large (Losada et al., 2008; Pilechi et al., 2018).

This interpretation is consistent with the numerical observations reported in Chapter 4. The nonlinear friction coefficient had a stronger influence on overtopping discharge and wave transmission than the linear friction coefficient. For this reason, the practical calibration of the numerical model focused primarily on the nonlinear resistance assigned to the porous layers, particularly the armour layer and core.

The friction coefficients should not be interpreted as universal material constants. They are empirical parameters used to represent unresolved energy losses within a porous-continuum model. Their values depend on the structural material, layer arrangement, nominal stone or unit size, porosity, and numerical representation of the structure. In that sense, the calibration process

should be interpreted as a hydraulic characterization of the porous layers for the present model configuration and tested wave range.

B.5 Turbulence closure and role of the k-ε model

The Reynolds-averaged formulation requires a turbulence closure to represent the effects of velocity fluctuations that are not resolved explicitly. In the present model, this closure is provided by the standard k-ε approach, which is commonly used in engineering RANS simulations and forms part of the IH2VOF modelling framework (Launder and Spalding, 1974). The turbulent viscosity is computed as:

$$\nu_t = C_\mu \frac{k^2}{\varepsilon} \qquad \text{Equation B-9}$$

where k is the turbulent kinetic energy, ε is the dissipation rate of turbulent kinetic energy, and C_μ is an empirical coefficient.

The transport equation for turbulent kinetic energy may be written as:

$$\frac{\partial k}{\partial t} + \mathrm{u} \cdot \nabla k = \nabla \cdot \left[\left(\nu + \frac{\nu_t}{\sigma_k}\right) \nabla k\right] + P_k - \varepsilon \qquad \text{Equation B-10}$$

and the corresponding transport equation for the dissipation rate is:

$$\frac{\partial \varepsilon}{\partial t} + \mathrm{u} \cdot \nabla \varepsilon = \nabla \cdot \left[\left(\nu + \frac{\nu_t}{\sigma_\varepsilon}\right) \nabla \varepsilon\right] + C_{\varepsilon 1} \frac{\varepsilon}{k} P_k - C_{\varepsilon 2} \frac{\varepsilon^2}{k} \qquad \text{Equation B-11}$$

where P_k is the production of turbulent kinetic energy due to mean velocity gradients, and σ_k, σ_ε, $C_{\varepsilon 1}$, and $C_{\varepsilon 2}$ are empirical model constants.

The main role of the k-ε model in this thesis is to represent turbulence generated by wave transformation, breaking, overtopping, and seepage-driven flow through the porous layers without resolving the full instantaneous turbulent structure. This approach is commonly adopted for two-dimensional engineering-scale simulations where the objective is to reproduce the main hydraulic response of the structure rather than to resolve all small-scale turbulent eddies explicitly.

At the same time, the k-ε closure introduces an important modelling assumption. Turbulence is represented through an isotropic eddy-viscosity concept, and therefore anisotropic turbulent structures and highly transient local flow features are not reproduced explicitly. This limitation should be considered when interpreting local phase differences and amplitude deviations between physical and numerical signals, particularly in regions with strong wave breaking, transmission through the porous medium, and overtopping.

B.6 Meaning of viscosity and turbulent viscosity in the present model

The distinction between molecular viscosity and turbulent viscosity is important for interpreting the momentum equation used in the numerical model. In the present formulation, the viscosity-related terms can be summarized as follows.

The molecular kinematic viscosity ν is a fluid property that reflects the internal friction of the fluid itself. In the two-phase formulation, this quantity is evaluated locally from the phase fraction, as shown previously. Its direct physical contribution is generally small compared with gravity and inertia for the large-scale and energetic wave conditions investigated in this thesis.

The turbulent viscosity ν_t, by contrast, is a modelled quantity that represents the momentum transfer associated with unresolved turbulent fluctuations. In practical terms, the turbulent viscosity governs much of the Reynolds-averaged dissipation in zones involving breaking, transmission, and overtopping. This is why clarification of the k-ε formulation is important when interpreting the compact momentum equation presented in Chapter 4.

B.7 Surface-tension term

The momentum equation includes an interfacial force term to represent surface tension at the air-water interface. In VOF-type two-phase solvers, this force is commonly represented using a continuum surface-force approach or equivalent numerical treatment to maintain a stable air-water interface (Brackbill et al., 1992). In the large-scale wave conditions considered in this thesis, the dominant balance is between gravity, inertia, turbulent dissipation, and porous-media resistance. Surface tension is therefore not expected to control the bulk hydraulic response of wave transmission or mean overtopping discharge.

Surface-tension effects may nevertheless influence small-scale interface details, such as localized splashing, thin water filaments, and very minor overtopping droplets. These processes are secondary to the engineering-scale quantities emphasized in Chapter 4, but they remain part of the general uncertainty associated with detailed free-surface representation in two-phase numerical modelling.

B.8 Practical calibration of the porous layers in the present study

In the numerical simulations reported in Chapter 4, the geometric characteristics of the porous layers were assigned from the physical model configuration. The nominal diameters and porosity values of the armour layer, underlayer, core, and toe were therefore not treated as arbitrary free parameters. This approach is consistent with the use of VARANS models for porous coastal structures (Losada et al., 2008; Díaz-Carrasco et al., 2024), where geometric and porous-medium properties are assigned from the physical structure and hydraulic resistance parameters are then selected or calibrated to reproduce the measured response.

The hydraulic characterization of the porous layers was then refined by varying the porous-media friction coefficients within physically reasonable bounds and comparing the resulting free-surface elevations, transmitted waves, and overtopping discharges with the experimental measurements. The calibration exercise showed that changing the nonlinear resistance produced a more noticeable effect on the predicted hydraulic response than changing the linear resistance. This behaviour is consistent with previous numerical applications of IH2VOF/VARANS-type models to rubble

mound breakwaters (Losada et al., 2008; Pilechi et al., 2018), where nonlinear porous resistance plays an important role in wave transmission and overtopping processes.

B.9 Concluding remark

This appendix provides the mathematical background supporting the compact numerical-model description presented in Chapter 4. It clarifies that the VOF equation tracks the air-water interface rather than the porosity of the structure, that the porous layers are represented through a VARANS momentum balance with linear and nonlinear resistance terms, and that the k-ε closure supplies the turbulent viscosity used to represent unresolved Reynolds-averaged dissipation. These supplementary details support the interpretation of the IH2VOF simulations without modifying the numerical results presented in Chapter 4.

Appendix C. Mesh Resolution, Time Stepping, and Validation of the Numerical Model

This appendix supplements the mesh-resolution, time-stepping, and validation information presented in Sections 4.4.4 and 4.5. It provides additional methodological context for the numerical discretization strategy adopted in the IH2VOF simulations, the practical interpretation of the mesh-adequacy assessment, and the validation metrics used to compare the numerical and physical model results.

C.1 Mesh strategy adopted for the present simulations

The numerical simulations were performed using a structured mesh with local refinement near the free surface and the breakwater. This approach is consistent with the finite-volume and structured-grid formulation commonly used in IH2VOF applications, where local refinement is applied in regions with strong velocity, pressure, and phase-fraction gradients while coarser resolution is retained in less dynamically active portions of the domain (Ferziger and Perić, 2002).

The principal hydraulic processes of interest in this thesis were wave transformation over the foreshore, wave transmission through the low-crested structure, and overtopping of the emergent structure. These processes occur primarily near the still-water level, around the seaward slope, within and above the porous armour and underlayer, and in the crest and overtopping zones. A uniform fine mesh across the full numerical domain would have substantially increased computational cost without providing equivalent benefit in offshore regions where the flow was comparatively less complex.

Near the still-water level, the mesh resolution corresponded to approximately 10-50 cells per incident wave height and over 100 cells per wavelength, consistent with typical IH2VOF applications. Accordingly, the mesh was refined near the free surface, the front and rear slopes of the breakwater, the crest, and the overtopping region. The offshore part of the domain was represented with comparatively coarser resolution because its main role was to reproduce wave input and shoaling prior to wave–structure interaction. The simulations were performed using a variable time step controlled by the Courant number, which was maintained below a specified threshold ($Co < 1.0$) to ensure numerical stability and accurate free-surface tracking. The practical objective was not to resolve every local geometric feature of the Coastalock units explicitly, but to provide sufficient spatial resolution for predicting the engineering-scale hydraulic response of the porous breakwater representation used in IH2VOF.

C.2 Representation of the breakwater geometry on the mesh

The breakwater was represented through porous zones rather than by direct geometric reconstruction of each individual armour unit and rock. This treatment follows the VARANS-

based representation commonly used for rubble mound and permeable coastal structures, where the structure is characterized through layer properties such as porosity, nominal diameter, and porous resistance coefficients rather than by resolving pore-scale flow paths explicitly.

In the present model, separate porous zones were assigned to the Coastalock armour layer, underlayer, toe, and core. The numerical mesh therefore did not conform to the exact external shape of each Coastalock unit or the detailed inter-unit void network. Instead, the hydraulic influence of the armour and rock layers was represented in an averaged sense through the porous-media formulation described in Chapter 4 and Appendix B.

The numerical model captures the integrated effect of the porous layers on wave transformation, transmission, and overtopping, while local flow pathways, small-scale pressure concentrations, and detailed inter-unit circulation are not resolved explicitly. As a result, mesh adequacy should be assessed primarily in relation to bulk hydraulic quantities such as significant wave height, wave transmission coefficient, cumulative overtopping volume, and mean overtopping discharge.

A second geometric consideration arises from the structured-grid representation of sloping boundaries. IH2VOF uses an orthogonal structured mesh and includes techniques for representing immersed solid boundaries within the computational grid. Nevertheless, any structured-grid representation of a sloping rubble mound section can introduce local geometric approximation. Such effects are expected to influence localized run-up, transmitted wave shape, or phase behaviour more strongly than integrated performance indicators.

C.3 Practical meaning of the mesh-adequacy assessment

The purpose of the mesh assessment in this thesis was to determine whether additional refinement would essentially alter the engineering conclusions drawn from the simulations. The selected comparison quantities were the transformed significant wave height near the structure and the overtopping response following wave–structure interaction. These quantities were selected because they directly reflected the role of the numerical model in Chapter 4.

The adopted criterion was based on the relative stability of those outputs under additional refinement. Once differences between successive mesh levels became less than 5%, the selected grid was considered adequate for the validation and comparison tasks undertaken in this thesis. This approach is common in engineering-oriented CFD studies where the numerical model supports a broader experimental-numerical investigation rather than serving as an independent numerical-methods study (Ferziger and Perić, 2002).

C.4 Near-wall treatment and interpretation of y+

Near-wall treatment is relevant in RANS simulations because the near-wall resolution must be consistent with the wall-treatment strategy used by the turbulence closure. In the present simulations, the flume bed and solid numerical boundaries were handled through the standard wall

treatment associated with the adopted IH2VOF solver configuration. The formulation is therefore consistent with the engineering use of the standard k-ε turbulence closure, which remains widely used for practical Reynolds-averaged modelling of turbulent flows (Launder and Spalding, 1974).

A dedicated y+ assessment was not conducted as an independent component of the present thesis. The absence of a dedicated y+ analysis may remain relevant when interpreting local phase differences, wave crest sharpness, and short-duration overtopping peaks.

C.5 Validation philosophy adopted in the thesis

The validation strategy used in Chapter 4 emphasized physically meaningful engineering quantities rather than exact point-by-point duplication of every instantaneous feature of the measured signals. This distinction is important for irregular-wave, two-phase simulations involving wave breaking, porous-media flow, and overtopping. Prior IH2VOF applications for rubble mound breakwaters have similarly assessed model skill using free-surface elevations, transmission behaviour, and mean overtopping discharge as primary comparison quantities (Losada et al., 2008; Guanche et al., 2009; Pilechi et al., 2018).

For wave generation and propagation, the model was assessed using representative wave parameters such as significant wave height and mean wave period, together with direct inspection of the time histories. For wave transmission, the main comparison quantities were the transmitted free-surface signal and the derived transmission coefficient. For overtopping, the emphasis was placed on cumulative overtopping volume and mean overtopping discharge over the selected analysis interval.

C.6 Interpretation of phase and amplitude differences

Phase and amplitude differences between numerical and physical records can arise from several sources in RANS-VOF simulations of porous coastal structures. Transmission through a porous breakwater is sensitive to the representation of porosity, hydraulic resistance, and internal energy dissipation. Small differences in these representations can affect both the attenuation and timing of transmitted waves. Similar sensitivity to porous-media parameterization has been documented in RANS/VARANS modelling of rubble mound and low-mound breakwaters (Losada et al., 2008; Lara et al., 2008).

Mesh resolution and time stepping also influence the sharpness of the free surface and the local shape of transmitted crests and troughs. In addition, the k-ε turbulence closure represents unresolved turbulence through an eddy-viscosity concept. This approach is suitable for many engineering-scale applications, but it does not reproduce all transient local flow structures associated with wave breaking, splash processes, or pore-scale turbulence.

Accordingly, phase or amplitude deviations should be interpreted as expected consequences of the adopted modelling approximations. In the present thesis, model adequacy is judged from the

combined interpretation of free-surface evolution, representative wave parameters, transmission coefficients, cumulative overtopping volume, and mean overtopping discharge.

C.7 Calibration strategy and parameter selection

It is useful to distinguish between quantities that were selected or adjusted in a practical modelling sense and quantities that were not independently calibrated as part of the thesis. The porous-layer representation required assigning porosity and hydraulic-resistance properties to the armour layer, underlayer, toe, and core. The calibration logic therefore focused on the hydraulic characterization of the porous structure, especially because porous resistance directly affects wave transmission, internal dissipation, and overtopping response (Losada et al., 2008; Lara et al., 2008; Guanche et al., 2009).

The final mesh structure and time-step level were selected through a pragmatic adequacy process intended to provide stable simulations and consistent engineering interpretation. By contrast, the k-ε turbulence closure was adopted as part of the selected IH2VOF modelling framework rather than being tuned against a separate turbulence dataset. The wall treatment associated with solid boundaries was also not independently calibrated, and no separate wall treatment optimization was performed.

Similarly, the offshore boundary was driven by measured experimental input rather than through calibration of a synthetic wavemaker signal. The present modelling strategy should therefore be understood as calibration and selection of practical hydraulic representation and numerical settings for the tested structure and wave range, not as an independent calibration program for every turbulence, wall, or boundary-process parameter in the solver.

Appendix D. Discussion of Model Limitations and Experimental Variability

This appendix supplements the numerical modelling component of the thesis by consolidating technical discussion required for interpreting the physical-numerical comparison presented in Chapter 4. This appendix clarifies the principal assumptions, limitations, and applicability boundaries associated with the use of IH2VOF for the simulation of Coastalock armoured rubble mound breakwaters. The discussion focuses on scale effects, experimental variability, equivalent porous-media representation, turbulence closure, wave absorption, overtopping variability, and the extent to which the findings can be generalized beyond the tested configuration space.

D.1 Limitations associated with the physical model

D.1.1 Scale effects and hydraulic similitude

The experiments were conducted at a 1:15 Froude scale, selected to preserve the dominant balance between gravitational and inertial forces while maintaining sufficiently large armour units and measurable overtopping volumes. In coastal physical modelling, Froude similitude is generally the governing scaling requirement for free-surface gravity-wave processes (Hughes, 1993). However, not all relevant processes scale perfectly. Residual scale effects may remain in local viscous behaviour, turbulence structure, seepage through porous layers, and droplet-scale overtopping processes, as discussed in broader reviews of physical hydraulic model scaling (Heller, 2011).

The adopted scale was considered sufficiently large to support rough-turbulent wave-driven flow around the structure and to provide credible comparison of transmission and overtopping trends. Nevertheless, prototype-scale interpretation should recognize that some local phenomena, including detailed flow separation, small overtopping events, and pressure fluctuations within the armour and underlayer, may remain partially affected by scale effects.

D.1.2 Armour placement variability and structural repeatability

Although the model units were cast carefully and placed systematically, the hydraulic response of a single-layer armour system is inherently sensitive to local placement details. Small differences in seating, interlocking, support from the underlayer, and local void geometry can influence rocking behaviour, local pressure gradients, and the development of transmitted and overtopping flows. Such variability is not unique to Coastalock; it is characteristic of many concrete armour systems and is particularly relevant for units placed in regular patterns on porous slopes.

For this reason, scattering in the experimental data should not automatically be interpreted as measurement error. Part of the variability reflects true physical sensitivity of the system to local geometry, wave grouping, and nonlinear wave–structure interaction. This is especially relevant

when interpreting the spread of transmission coefficients and the occurrence of overtopping fluctuations under similar nominal hydraulic conditions.

D.1.3 Overtopping measurement variability

Overtopping measurements are among the most valuable outputs of the experimental program, but they are also among the most difficult to interpret without uncertainty. Wave overtopping is intermittent and strongly influenced by wave grouping, local crest impact, splash, droplet transport, and shallow flow over the crest. Guidance documents such as EurOtop (2018) emphasize that overtopping predictions are inherently statistical and should be interpreted in relation to both mean discharge and event variability.

For rubble mound structures, numerical and experimental studies using IH2VOF have also shown that overtopping comparisons depend on the accurate reproduction of free-surface elevation, wave transformation, and the local wave sequence (Pilechi et al., 2018; Stagnitti et al., 2023). In the present thesis, agreement in cumulative overtopping trends and representative discharge levels is therefore more meaningful than exact agreement in every instantaneous overtopping peak. This interpretation is particularly important when comparing short-duration physical and numerical overtopping records. These physical-model limitations also influence the interpretation of the numerical simulations, since the numerical model is calibrated and validated against the experimental data and therefore inherits part of the associated uncertainty.

D.2 Limitations associated with the numerical model

D.2.1 Two-dimensional representation

The numerical simulations were performed in two dimensions to reproduce the cross-sectional behaviour of the laboratory tests efficiently and consistently. This assumption is appropriate for trunk-section analysis of a straight breakwater under normal wave attack, where the principal interest is in cross-shore wave transformation, transmission, and overtopping. Two-dimensional RANS/VARANS simulations have been widely used for low-crested and rubble mound breakwater applications (Lara et al., 2006; Lara et al., 2008; Losada et al., 2008).

However, a two-dimensional model cannot capture alongshore circulation, transverse inter-unit flow redistribution, local three-dimensional turbulence structures, or the hydrodynamics of breakwater heads and curved alignments. Accordingly, the numerical results should be interpreted as representative of idealized trunk-section behaviour under normal wave attack. They should not be extended directly to head sections, oblique wave attack, or situations where three-dimensional flow redistribution is expected to be significant.

D.2.2 Geometric idealization of the structure

The porous breakwater layers were represented through equivalent porous media rather than through explicit geometric resolution of every individual rock and Coastalock unit. This approach

is consistent with the VARANS framework used in IH2VOF and with previous RANS/VARANS applications to submerged, low-crested, and rubble mound structures (Lara et al., 2006; Lara et al., 2008; Losada et al., 2008). It provides an efficient way to capture bulk hydraulic behaviour while maintaining feasible computational cost.

The corresponding limitation is that the numerical model smooths the local geometry and does not reproduce exact inter-unit pathways, small contact gaps, or localized pressure concentration zones that may influence the onset of armour movement. The use of a structured rectilinear mesh also introduces a discretized representation of sloping boundaries and transitions. These approximations are acceptable for integrated hydraulic quantities such as wave transmission and mean overtopping discharge, but they may contribute to local phase, amplitude, and dissipation differences when compared with physical measurements.

D.2.3 Turbulence closure and near-wall behaviour

The k-ε turbulence model used in IH2VOF is robust, computationally efficient, and widely used in engineering simulations of free-surface and porous-structure flows. Its use is consistent with the RANS/VARANS modelling approach and reflects the need to simulate irregular wave transformation and overtopping over relatively large spatial and temporal domains within practical computational limits (Launder and Spalding, 1974).

Nevertheless, the k-ε model remains an eddy-viscosity closure based on simplifying assumptions, including an isotropic representation of Reynolds stresses. As a result, the model may not fully resolve anisotropic turbulence, strongly separated local flow structures, or detailed near-wall processes around complex armour geometry. These limitations are not expected to invalidate the global comparisons presented in Chapter 4, but they can contribute to observed discrepancies in local phase behaviour, crest sharpness, and short-duration overtopping peaks.

D.2.4 Boundary conditions and wave absorption

The numerical wave generation approach was based on prescribed boundary input derived from experimental measurements rather than on explicit simulation of a moving paddle. IH2VOF supports multiple wave-generation and absorption methods, including Dirichlet boundary conditions, moving-boundary methods, internal wave makers, active absorption, and passive sponge-layer absorption. The boundary treatment adopted in Chapter 4 was selected to reproduce the measured wave conditions consistently and to maintain a direct basis for comparison with the physical experiments.

Numerical implementations of irregular-wave input and absorption may introduce residual reflection, numerical dissipation, or slight phase distortion. These effects are expected to be limited in the present simulations, but they provide a plausible contribution to small shifts between measured and simulated transmitted-wave series, particularly after wave interaction with the porous structure where multiple sources of model approximation accumulate.

D.2.5 Constant material properties and friction representation

The porous layers in the numerical model were assigned fixed porosity and friction parameters. This assumption is necessary for practical computation and is consistent with equivalent porous-media modelling of rubble mound and permeable breakwater structures. Previous numerical studies have shown that porous-media friction parameters strongly influence reflection, transmission, and overtopping behaviour, and that their selection requires careful calibration or hydraulic characterization (Lara et al., 2006).

In reality, the effective hydraulic resistance of a coastal structure may evolve over time due to local rearrangement, partial clogging, biological growth, ageing, and changes in surface roughness. For the present short-duration laboratory comparisons, constant hydraulic properties are reasonable. However, this assumption limits the long-term interpretation of calibrated friction parameters, which should not be treated as permanent field-scale properties under ecological colonization or long-term maintenance effects.

D.2.6 Surface tension and wave setup

For the bulk hydraulic quantities emphasized in this thesis – wave heights, transmission behaviour, cumulative overtopping, and mean overtopping discharge – gravitational, inertial, and porous-resistance effects dominate the response. Surface tension is therefore not expected to govern the principal engineering conclusions at the model scale used in the experiments. Its influence is more likely to appear in localized small-scale processes such as droplet formation, splash behaviour, and the drainage of very small overtopping events into the physical collection system.

Wave setup was not treated as a separate response variable in present experimental and numerical investigations. The focus of the study was placed on wave transformation, transmission, and overtopping under the tested hydraulic conditions. Mean water-level redistribution may be relevant in broader hydrodynamic interpretations, particularly for longer-duration simulations, stronger overtopping, or more extensive domains. For the present thesis, the absence of a separate setup analysis is best interpreted as a scope limitation rather than a limitation of the principal hydraulic objectives.